



University
of Glasgow

Sadler, Jessica B. A. (2014) *Analysis of VAMP levels and function in 3T3L1 adipocytes*. PhD thesis.

<http://theses.gla.ac.uk/5852/>

Copyright and moral rights for this thesis are retained by the author

A copy can be downloaded for personal non-commercial research or study, without prior permission or charge

This thesis cannot be reproduced or quoted extensively from without first obtaining permission in writing from the Author

The content must not be changed in any way or sold commercially in any format or medium without the formal permission of the Author

When referring to this work, full bibliographic details including the author, title, awarding institution and date of the thesis must be given

Analysis of VAMP levels and function in 3T3 L1 adipocytes

Jessica Betty Arnold Sadler

BSc (Hons)

Thesis submitted in fulfilment of the requirements for the Degree of

Doctor of Philosophy

October 2014

Institute of Molecular, Cell and Systems Biology

College of Medical, Veterinary and Life Sciences

University of Glasgow

Abstract

A major action of the hormone insulin is to increase glucose uptake into muscle and adipose tissues. This occurs through the insulin-regulated translocation of the glucose transporter GLUT4 from intracellular deposits to the cell surface. The dysregulation of this process is a major facet of insulin-resistance and Type-2 diabetes.

In the absence of insulin, GLUT4 is sequestered intracellularly in two interlinked pools. These pools are the endosomal recycling compartment and a specialised insulin-sensitive compartment. GLUT4 vesicles within the specialised insulin-sensitive compartment are termed GSVs. GSVs provide a readily available store of GLUT4 that can be rapidly mobilised to the cell surface in response to insulin stimulation. GLUT4 within the cell is continually recycled through multiple compartments, including the endosomal recycling compartment and GSVs. Perturbation of flux through any of these compartments disrupts GLUT4 traffic and thus disrupts the insulin-response. Consequently, understanding these trafficking steps is an important research goal.

The formation of GSVs and their insulin-stimulated translocation to, and fusion with, the plasma membrane are examples of regulated and specific membrane trafficking events. As such these events require SNARE proteins. This study has examined the functions of each of the members of the post-Golgi vSNAREs that make up the VAMP subfamily in the trafficking of GLUT4 into the insulin-sensitive compartment, as well as examining the contribution each of these vSNAREs plays in the SNARE complex involved in the insulin-stimulated translocation of GLUT4 to the cell surface.

GLUT4 traffics through the endosomal system and the *trans* Golgi network (TGN) *en route* into GSVs in a process known to involve the t-SNARE syntaxin 16. In order to dissect the roles VAMP proteins play in the intracellular recycling and trafficking of GLUT4, the interactions of VAMP proteins with syntaxin 16 and its regulatory Sec-1/Munc-18 protein, mVps45 have been examined. Further, the effects of depletion of these VAMPs in GLUT4 distribution has been examined in HeLa cells expressing HA-GLUT4-GFP as a surrogate for adipose and muscle tissue.

The fusion of GLUT4-containing vesicles with the cell surface in response to insulin stimulation is a key component of the insulin-response. Although there is consensus that tSNAREs involved in this process are syntaxin 4 and SNAP23, there is discord in the literature regarding the role each vSNARE plays in this fusion event. Many studies support a role for VAMP2, however recently it has been suggested that VAMPs 3 and 8 may also be involved. The roles of these VAMPs, as well as the other post-Golgi vSNAREs expressed in adipocytes, in the fusion of GLUT4-containing vesicles with the cell surface have been examined. This has been achieved through the characterisation of the expression level, subcellular distribution of the VAMPs and determination of associations that take place between each VAMP protein and the tSNARE complex made up of syntaxin 4 and SNAP23.

The results from these experiments show that despite all VAMPs being capable of forming SDS-resistant SNARE complexes with either syntaxin 4 and SNAP23 or syntaxin 16 and SNAP23, in the cellular environment only VAMP2 interacts with syntaxin 4 and only VAMP4 interacts with syntaxin 16. This, alongside the finding that each VAMP protein is expressed at varying levels and localises with different pools of GLUT4, suggests that VAMP2, not VAMPs 3 or 8, is the major vSNARE involved in the trafficking of GLUT4 to the cell surface.

The finding that VAMP4 is the only VAMP that interacts with syntaxin 16, alongside the results of VAMP depletion in HeLa cells expressing HA-GLUT4-GFP, support the hypothesis that VAMP4 is involved in sorting GLUT4 out of the endosomal pool and into GSVs.

Table of Contents

Abstract	2
Table of Contents	4
List of Tables.....	9
Table of Figures	10
Acknowledgements.....	12
Author's Declaration	13
Definitions/Abbreviations	14
Chapter 1 - Introduction	17
1.1 Type 2 diabetes mellitus	21
1.2 GLUT4	22
1.2.1 Intracellular pools of GLUT4	23
1.2.2 GLUT4 trafficking.....	24
1.2.3 Targeting motifs within GLUT4	27
1.2.4 Formation of GSVs.....	30
1.2.5 Insulin sensitivity of GSVs	34
1.2.6 Retention of GSVs	34
1.2.7 Insulin response of GLUT4.....	36
1.3 SNAREs and SM Proteins	38
1.3.1 SNARE proteins.....	38
1.3.1.1 Discovery of SNARE proteins	39
1.3.1.2 SNARE protein structure	39
1.3.1.3 SNARE Complex formation.....	42
1.3.1.4 Specificity of Fusion	43
1.4 Tethers.....	44
1.5 SM Proteins	45
1.5.1 Munc18c.....	46
1.5.2 mVps45.....	47
1.6 SNAREs in GLUT4 trafficking	47
1.6.1 SNAREs in GSV fusion with plasma membrane.....	47
1.6.2 SNAREs in sorting	49
1.7 SNAREs in diabetes	50
1.8 Aims of this study.....	52
1.8.1 Aims of Chapter 3	52
1.8.2 Aims of Chapter 4	52
1.8.3 Aims of Chapter 5	52
1.8.4 Aims of Chapter 6	53

Chapter 2 - Materials and Methods	54
2.1 Materials	55
2.1.1 General reagents and enzymes	55
2.1.2 Solutions	57
2.1.3 Plasmids.....	59
2.1.4 Yeast Strains.....	59
2.1.5 Bacterial Strains	60
2.1.6 Mammalian Cell Lines.....	60
2.1.7 Antibodies	61
2.2 Molecular Biology Methods	63
2.2.1 Plasmid DNA purification	63
2.2.2 Agarose gel electrophoresis.....	63
2.2.3 Digestion using restriction endonucleases	63
2.2.4 Transformation of plasmid into bacterial cells.....	63
2.3 Protein Methods	64
2.3.1 Purification of recombinant fusion proteins from <i>E.coli</i>	64
2.3.2 GST tagged proteins.....	64
2.3.3 Protein A tagged proteins	65
2.3.4 SDS-Polyacrylamide gel electrophoresis.....	65
2.3.5 Coomassie staining	65
2.3.6 Immunoblotting	66
2.3.7 Estimation of protein concentrations.....	67
2.3.7.1 Tagged proteins	67
2.3.7.2 Micro BCA	67
2.3.7.3 GST and Protein A pull-down assays with yeast lysate	68
2.3.7.4 GST pull-down assays with recombinant protein.....	68
2.3.7.5 SNARE complex assembly assay (CAA)	69
2.4 Cell Culture Methods.....	69
2.4.1 Yeast cell culture	69
2.4.2 Mammalian cell culture.....	69
2.4.2.1 Growth of 3T3 L1 adipocytes.....	69
2.4.2.2 Passage of 3T3 L1 adipocytes	70
2.4.2.3 Differentiation of 3T3 L1 adipocytes.....	70
2.4.2.4 Freezing of 3T3 L1 adipocytes	70
2.4.2.5 Resurrection of cells	71
2.4.2.6 Growth of HeLa cells	71
2.4.2.7 Passage of HeLa cells.....	71
2.4.2.8 Transfection of HeLa cells with plasmid DNA.....	71
2.5 Production of HeLa cell lysates.....	72

2.6	Protein depletion in cell culture	72
2.6.1	siRNA treatment of HeLa cells.....	72
2.6.2	Generation of inducible shRNA vector for use in 3T3 L1 adipocytes	73
2.6.2.1	shRNA Production	73
2.6.2.2	Shuttling oligonucleotides into pEN vector	73
2.6.2.3	Shuttling pEN vector into pSLIK Vector.....	73
2.7	Subcellular Fractionation Methods.....	74
2.7.1	Preparation of total membrane fractions.....	74
2.7.2	Preparation of subcellular fractions	74
2.7.3	Preparation of iodixanol gradients.....	75
2.8	Immunoprecipitation from 3T3 L1 adipocytes.....	77
2.9	Indirect immunofluorescence	77
Chapter 3	- Interactions between the tSNARE complex syntaxin 4/SNAP23 and VAMP proteins.....	79
3.3	Introduction	80
3.3.1	SNARE complex involvement in GLUT4 fusion with the plasma membrane.....	80
3.3.2	Interactions between syntaxin 4/SNAP23 and VAMPs	82
3.4	Aims of Chapter.....	84
3.5	Results	85
3.5.1	Purification of recombinantly expressed tagged proteins	85
3.5.2	SNARE Complex Assembly Assay (CAA)	87
3.5.3	Interactions between syntaxin 4 and VAMP proteins in 3T3 L1 adipocytes.....	89
3.6	Discussion.....	91
3.6.1	Methodological considerations.....	91
3.6.2	Discussion of findings	92
3.7	Conclusion	97
Chapter 4	- Endogenous Levels and Subcellular Distribution of VAMPs and in 3T3 L1 Adipocytes.	98
4.1	Introduction	99
4.1.1	Current Understanding of Roles and Localisation of VAMPs	99
4.1.2	Identification of VAMPs on GLUT4 containing vesicles	100
4.1.3	Levels of VAMPs in 3T3 L1 adipocytes	101
4.1.4	Mobilisation of VAMPs in response to insulin	102
4.1.5	Roles of VAMPs in insulin response.....	102
4.2	Aims	103
4.3	Results	103
4.3.1	Testing of VAMP antibodies	103

4.3.2	Determination of changes in expression levels upon adipocyte differentiation.....	106
4.3.3	Determination of expression levels in 3T3 L1 adipocytes	109
4.3.4	Subcellular distribution of VAMP proteins in 3T3 L1 adipocytes	112
4.3.5	Iodixanol gradient analysis of LDM fractions.	117
4.4	Discussion	122
4.4.1	Methodological Considerations	122
4.4.2	VAMPs involved in fusion of GLUT4 containing vesicles with the PM. 123	
4.4.3	Plasticity in vSNARE requirements for GLUT4 fusion with the plasma membrane - Possible Mechanisms	125
4.4.4	How many VAMPs per insulin sensitive GLUT4 vesicle?	127
4.5	Conclusions	131
Chapter 5	- Interactions between VAMPs and syntaxin 16 and mVps45.	132
5.1	Introduction	133
5.1.1	tSNAREs involved in recycling of GLUT4.....	133
5.1.2	SM proteins in intracellular sorting of GLUT4	136
5.2	Aims	136
5.3	Results	137
5.3.1	Effect of mVps45 depletion on VAMP protein levels.....	137
5.3.2	Interactions between mVps45 and VAMP proteins	139
5.3.3	Interactions between syntaxin 16 and VAMP proteins.....	140
5.4	Discussion	146
5.5	Conclusion	148
Chapter 6	- Knock down of VAMP proteins in mammalian cells.	150
6.1	Introduction	151
6.1.1	Use of RNAi	153
6.1.2	Studying GLUT4 trafficking using RNAi	153
6.1.3	HeLa cells.....	154
6.1.4	Inducible vector system	154
6.2	Aims	155
6.3	Results	156
6.3.1	VAMP protein knock down in HeLa cells.....	156
6.3.2	Generation of inducible vector system to knock down VAMP proteins in 3T3 L1 adipocytes.....	161
6.4	Discussion	167
6.5	Conclusion	173
Chapter 7	- Discussion	174
7.1	Summary of findings	175
7.2	Findings in the context of existing literature	176

7.3 Wider implications	182
7.4 Conclusions and future directions.....	182
Chapter 8 - Appendicies.....	184
8.1 Immunoprecipitation of syntaxin 4 and syntaxin 16.....	184
List of References	185

List of Tables

Table 2-1: Plasmids used in this study.	59
Table 2-2: Yeast strains used in this study	59
Table 2-3: Bacterial strains used in this study	60
Table 2-4: Mammalian cell lines used in this study	60
Table 2-5: Antibodies used in this study	61
Table 3-1: SNARE proteins that can form SDS-resistant SNARE complexes <i>in vitro</i>	93
Table 4-1: Copies of each VAMP protein in 3T3 L1 adipocytes,	111
Table 6-1: Expected fragment size for each pEN plasmid following digestion with endonucleases.	164

Table of Figures

Figure 1-1: Regulation of blood glucose levels by the action of insulin and glucagon.	19
Figure 1-2: Insulin signalling stimulates the translocation and tethering of GLUT4 containing vesicles with the plasma membrane.	21
Figure 1-3: GLUT4 continuously cycles through two inter-linked pools.	26
Figure 1-4: Targeting motifs in GLUT4 trafficking.	30
Figure 1-5: GSV formation.	33
Figure 1-6 SNARE complex structure.	40
Figure 1-7: Structure of SNAREs discussed in this thesis.	42
Figure 1-8: Different binding modes of SM proteins interacting with syntaxins. .	46
Figure 2-1: Flow chart displaying the subcellular fractionation procedure of 3T3 L1 adipocytes.	76
Figure 3-1: Purification of VAMP proteins.	86
Figure 3-2: Purification and thrombin cleavage of protein A tagged syntaxin 4. .	86
Figure 3-3 Redundancy in the vSNARE requirements for SNARE complex assembly with the tSNARE syntaxin4-SNAP23.	88
Figure 3-4: Immunoprecipitation of syntaxin 4 and co-immunoprecipitation of VAMP proteins in 3T3 L1 adipocytes.	90
Figure 4-1: VAMP antibodies are specific.	105
Figure 4-2: Example of the steps taken to optimise antibodies for use in 3T3 L1 adipocytes.	106
Figure 4-3: Changes in VAMP protein levels upon adipocyte differentiation. ...	108
Figure 4-4: SDS-PAGE analysis of recombinant proteins.	110
Figure 4-5: Representative immunoblot showing the method used to quantify the levels of VAMP protein in 3T3 L1 adipocytes.	110
Figure 4-6: Copy number of each VAMP protein in 3T3 L1 adipocytes.	111
Figure 4-7: Representative immunoblots showing the subcellular distribution of each VAMP protein in 3T3 L1 adipocytes.	114
Figure 4-8: Localisation of marker proteins in basal (A) and insulin-stimulated 3T3 L1 adipocytes (B).	115
Figure 4-9: localisation of the vSNAREs and GLUT4 in basal (A) and insulin-stimulated (B) 3T3 L1 adipocytes.	116
Figure 4-10: Effect of insulin stimulation on the distribution of GLUT4 and VAMP proteins in 3T3 L1 adipocytes.	117
Figure 4-11: Localisation of GLUT4 in GSVs and the endosomal recycling compartment (ERC) fractions of 3T3 L1 adipocytes.	119
Figure 4-12: Localisation of IRAP and TfR in GSVs and ERC fractions of 3T3 L1 adipocytes.	120
Figure 4-13: Localisation of VAMP proteins in GSVs and ERC fractions of 3T3 L1 adipocytes.	121
Figure 5-1: mVps45 Knock-down reduces the levels of VAMPs 2 and 4 in 3T3 L1 adipocytes.	138
Figure 5-2: mVps45 does not directly interact with any of the VAMP proteins but does interact with syntaxin 16.	139
Figure 5-3: Protein A tagged syntaxin 16 can pull GST-VAMPs out of bacterial lysate.	141
Figure 5-4: Interactions between GST-VAMPs and cleaved syntaxin 16	142

Figure 5-5: Purification and thrombin cleavage of protein A tagged syntaxin 16.	143
Figure 5-6: VAMP proteins form SDS-resistant SNARE complexes with the syntaxin 16 and SNAP23	144
Figure 5-7: Immunoprecipitation of syntaxin 16 and co-immunoprecipitation of VAMP proteins from basal and insulin-stimulated 3T3 L1 adipocytes.....	145
Figure 6-1: Insulin-stimulation causes HA-GLUT4-GFP translocation in HeLa cells.	157
Figure 6-2: Knockdown of, VAMP2, VAMP4 and VAMP8 in HeLa cells	158
Figure 6-3: Effect of VAMP2, 4 or 8 Knockdown on GLUT4 distribution under basal and insulin-stimulated conditions.....	159
Figure 6-4: Design of shRNA constructs	163
Figure 6-5: Generation of pEN and pSLIK vectors.....	165
Figure 6-6: Testing of pSLIK_TG_VAMP2 and pSLIK_TG_VAMP4 constructs in HeLa cells.	166
Figure 6-7: GLUT4 recycling:	171

Acknowledgements

First and foremost I would like to thank Diabetes UK for funding me through the Arthur and Sadie Pethybridge studentship.

I would like to offer my sincere gratitude to my supervisors Prof. Gwyn Gould and Prof. Nia Bryant for their guidance and support throughout this project. You have provided not only a platform for me to learn and develop as a scientist but also been there for support and assistance whenever I have needed it. Thank you for believing in me even when I couldn't.

I owe my thanks to Dr Rob Semple and Dr Nuno Rocha at the University of Cambridge for their guidance in the pSLIK cloning platform.

I would like to thank all my family (Arnold-Sadlers and Fahys). You have all helped me in so many ways. Mum and Dad thank you for providing me with an upbringing that made me inquisitive, instilling me with my refusal to give up and my work ethic. Julie and Brendan, thank you for housing me, feeding me and generally looking after me! Dennis, Ewan, Rory, Shona and Leanne I know you guys don't entirely understand why I have put myself through this, but thank you for always being there for a chat when I needed it.

To all the members of Lab 241 - you have been a joy to work with. Helen and Anna, I don't quite know how I would have coped without you guys next to me. Thanks for making sure I ate regularly and actually went home sometimes. Also ta for coming running with me.

Finally, to Eamonn, I would not have been able to even contemplate doing any of this without your unwavering support and love. You have picked me up when I was down and celebrated with me when my experiments worked. You have tolerated numerous weekends and evenings working and have made some truly heroic proofreading efforts.

Thank you to all

Author's Declaration

I declare that the work presented in this thesis is my own, unless otherwise cited or acknowledged. It is entirely of my own composition and has not, in whole or in part, been submitted for any other degree.

Jessica Betty Arnold Sadler

October 2014

Definitions/Abbreviations

Abbreviation

PM	plasma membrane
GLUT4	Glucose Transporter Protein isoform 4
SNARE	soluble N-ethylmaleimide sensitive factor attachment receptor protein
SNAP23	synapse associated protein of 23kDa
vSNARE	vesicle associated SNARE
tSNARE	target associated SNARE
VAMP	vesicle associated membrane protein
IRAP	insulin responsive aminopeptidase
LDM	high density membrane fraction
HDM	low density membrane fraction
Sol	soluble fraction
GSV	insulin -sensitive pool of GLUT4
ERC	endosomal recycling compartment (endosomal pool of GLUT4)
TfR	transferin receptor
GAPDH	Glyceraldehyde 3-phosphate dehydrogenase
CDMPR	cation-dependent mannose 6-phosphate receptor
APS	Ammonium Persulphate
BSA	Bovine Serum Albumin
°C	degrees Celsius
cDNA	complementary DNA
C/EBP	CAAT/ enhancer-binding protein
DMEM	Dulbecco's modified Eagle Medium
DMSO	dimethyl sulfoxide
DNA	deoxyribonucleic acid
DTT	Dithiothreitol
E.coli	Escherichia coli
ECL	enhanced chemiluminescence
EDTA	Ethylenediaminetetraacetic Acid
FCS	Fetal Calf Serum
g	gram

x g	gravitational force
GFP	Green Fluorescent Protein
GLUT4	Glucose Transporter Protein isoform
h	hour
H ₂ O ₂	hydrogen peroxide
HA	Influenza hemagglutinin epitope tag
HCl	hydrochloric acid
HEPES	2-[4-(2-Hydroxyethyl)-1-piperazine]ethanesulfonic Acid
GST	glutathione S-transferase
HRP	Horse Radish Peroxidase
IMBX	Isobutylxanthine
IgG	Immunoglobulin G
IP	immunoprecipitation
IPTG	Isopropyl β-D-1-thiogalactopyranoside
kb	kilobase
kDa	kiloDalton
KCl	potassium chloride
K ₂ HPO ₄	dipotassium hydrogen orthophosphate
KH ₂ PO ₄	potassium dihydrogen orthophosphate
LSB	Laemmli sample buffer
μ	micro
μg	microgram
μl	microliter
μM	micromolar
M	molar
mA	milliamp
mg	milligram
MgCl ₂	magnesium chloride
min	minute, minutes
ml	millilitre
mM	millimolar
nm	nanometers
nm	nanomolar
NaCl	sodium chloride
Na ₂ HPO ₄	disodium hydrogen orthophosphate

NaOH	sodium hydroxide
NCS	Newborn calf serum
NEM	N-ethylmaleimide
NSF	N-ethylmaleimide-sensitive factor
OD600	optical density at 600nm
P/S	Penicillin/Strepomycin
PBS	Phosphate buffered saline
PBST	Phosphate buffered saline supplemented with 0.1% Tween-20
PCR	Polymerase Chain Reaction
PFA	paraformaldehyde
PPAR γ	Peroxisome proliferator activated receptor gamma
PrA	Protein A
rpm	revolutions per minute
<i>S.cerevisiae</i>	<i>Saccharomyce cervisiae</i>
SD	yeast synthetic difined media
SDS	Sodium dodecyl sulphate
SDS-PAGE	Sodium dodecyl sulphate polyacrylamide gel electrophoresis
sec	second
SM	Sec1p/Munc18
SOC	Supoer Optimal Broth
Sx	syntaxin
TAE	Tris acetic acid EDTA
TB	Terrific Broth
TBST	Tris buffered saline supplemented with 0.1% Tween-20
TBS	Triss buffered saline
TCA	Tricholoroacetic acid
TE	Tris EDTA
TEMED	N, N, N', N'-Tetramethylenediamine
TfR	transferin receptor
TGN	trans Golgi network
Tris	2-amino-2-(hydroxymethyl)-1,3-Propanediol
v/v	volume per volume
w/v	weight per volume
DFP	Diisopropylfluorophosphate

Chapter 1 - Introduction

Glucose is a fundamental cellular energy source. In healthy humans blood glucose levels are normally maintained between 4 and 7mM. The maintenance of blood glucose within this narrow range is achieved through the action of two counteracting hormones: insulin and glucagon (Figure 1-1).

Both insulin and glucagon are released from the islets of Langerhans in the pancreas; insulin is released from beta cells in response to an elevation in blood glucose levels and glucagon from the alpha cells in response to a fall in blood glucose levels. Glucagon primarily acts on the liver to increase hepatic glucose output by increasing gluconeogenesis and glucose release. On the other hand, insulin acts on the liver, skeletal muscle, and adipose tissue to increase glucose uptake and glucose storage. Glucose is stored as glycogen in the liver and skeletal muscle or as triglycerides in adipose tissue. Skeletal muscle is responsible for the majority of the glucose clearance (~90%) (Kraegen et al. 1985). The increase in glucose clearance in response to insulin occurs through an increase in the number of facilitative glucose transporters (GLUT4) at the cell surface of peripheral insulin-sensitive tissues. This occurs through the translocation of GLUT4 from intracellular deposits to the cell surface. Although adipose only accounts for a small portion of insulin-stimulated glucose uptake, its importance in the maintenance of whole body insulin-sensitivity is not to be underestimated. Adipose tissue senses the energy status of the body and responds by secreting hormones that regulate the metabolism of other tissues. Furthermore, resistance of adipose tissue to insulin affects whole body glucose homeostasis to a degree higher than that of its individual contribution to glucose uptake (Abel et al. 2001; Leto & Saltiel 2012). Mice with adipose specific GLUT4 knock out show both hepatic and skeletal muscle insulin resistance despite having normal GLUT4 expression levels in these tissues (Abel et al. 2001). Therefore, despite adipose tissue only accounting for <10% of insulin-stimulated glucose uptake (Kraegen et al. 1985), GLUT4 translocation within and glucose uptake into adipose tissue is of high importance.

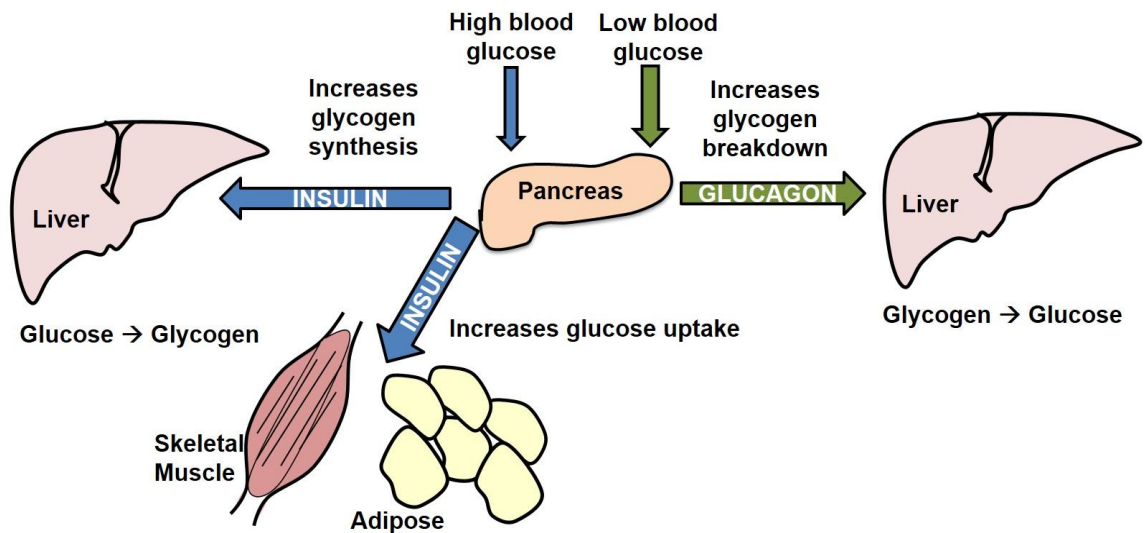


Figure 1-1: Regulation of blood glucose levels by the action of insulin and glucagon.

Fluctuations in blood glucose levels are detected by the pancreas. A fall in blood glucose levels leads to the release of glucagon. Glucagon acts on the liver to increase glycogen breakdown and glucose release. This results in a rise in blood glucose levels. Elevations in blood glucose levels lead to the release of insulin. Insulin acts on the liver to increase glycogen synthesis, and acts on peripheral insulin-sensitive tissues to increase glucose uptake. This results in an increase in glucose clearance out of the blood stream which lowers blood glucose levels.

Insulin is released from the islets of Langerhans in response to a rise in blood glucose levels. It travels in the blood to peripheral insulin-sensitive tissues where it initiates several signalling cascades that regulate a range of processes from glucose and lipid homeostasis to cell growth and protein synthesis. There are two main signalling pathways that induce the translocation of GLUT4 from intracellular deposits to the cell surface and thereby increase glucose uptake. These are the phosphoinositide 3-kinase (PI3K) pathway and the adaptor protein with pleckstrin homology and Src homology domains (APC) pathway (Leto & Saltiel 2012; Figure 1-2). For GLUT4 to be successfully inserted into the plasma membrane in response to insulin-stimulation it must be mobilised from intracellular deposits and targeted to the correct domains of the plasma membrane. Activation of the PI3K and APC pathways affect both the translocation and tethering of GLUT4 vesicles to the plasma membrane. Both pathways are initiated following insulin binding to its receptor in the plasma membrane. This leads to insulin receptor autophosphorylation, which in turn leads to recruitment and phosphorylation of IRS (insulin receptor substrate) and APC to the insulin receptor. At this point the two pathways diverge. IRS acts as a docking site for PI3K, and the interaction between IRS and PI3K activates PI3K. PI3K converts phosphatidylinositol-4,5-bisphosphate (PIP₂) to

phosphatidylinositol-3,4,5-triphosphate (PIP3) at the plasma membrane. PIP3 in turn acts as docking site for both phosphoinositide-dependent kinase 1 (PDK) and Akt. Once they are docked with PIP3, PDK 1 phosphorylates and activates Akt. Akt connects insulin signalling with downstream insulin-stimulated processes. With regard to GLUT4 translocation to the plasma membrane Akt has two major targets; AS160 and RalA. AS160 contains a GTPase Activating Protein (GAP) domain, which means that it promotes GTP hydrolysis, preventing GTP loading and activation of its GTPase effectors. In terms of stimulating GLUT4 mobilisation to the cell surface, the main AS160 effector in adipocytes appears to be Rab10 (Sano et al. 2007; Chen et al. 2012; Chen & Lippincott-Schwartz 2013). Akt phosphorylates and inactivates AS160; when active AS160 prevents the translocation of GLUT4 to the plasma membrane. Once AS160 is inactivated GLUT4 can be mobilised to the cell surface (Karylowski et al. 2004; Sano et al. 2007). Akt also mediates the activity of the GTPase RalA. This occurs through the recently characterised Ral GAP complex (RGC) (Chen & Saltiel 2011). Once GTP loaded, Ral1A interacts with the Myo1c motor to mediate the translocation of GLUT4 vesicles and also with the exocyst complex to mediate tethering (Chen et al. 2007).

The APS pathway has been less intensely studied, and is therefore not as well characterised as the PI3K pathway. Despite this, it is known that APS recruits c-CBL to the plasma membrane via c-CBL associated protein (CAP). c-CBL in turn interacts with CRK, this leads to the recruitment of C3G to the plasma membrane. C3G is a Guanine Nucleotide Exchange Factor (GEF). GEFs promote the exchange of GDP for GTP on GTPases and thus activate the GTPase. The effector for C3G is TC10. C3G converts TC10 from a GDP to a GTP bound state. TC10 in turn interacts with the exocyst mediating vesicle tethering, and also binds to CIP4 (Cdc42-interacting protein 4) which in turn may regulate the translocation of GLUT4 vesicles (Leto & Saltiel 2012).

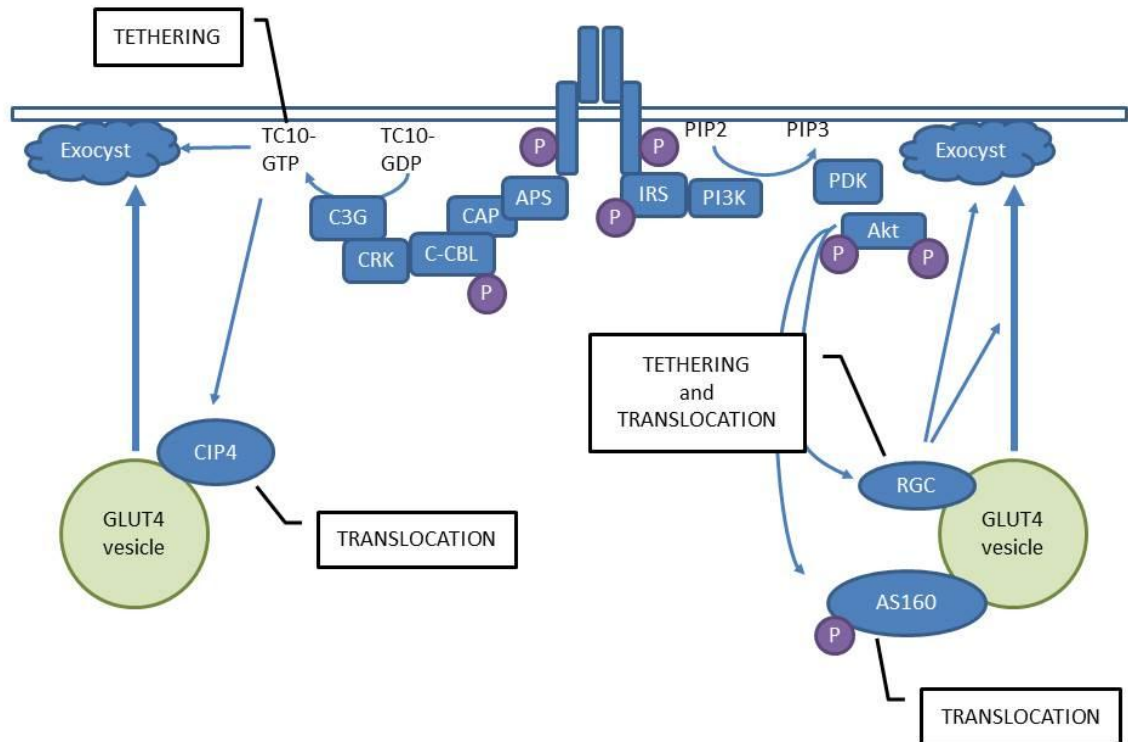


Figure 1-2: Insulin signalling stimulates the translocation and tethering of GLUT4 containing vesicles with the plasma membrane.

Insulin initiates two signalling cascades. The APS signalling cascade is initiated upon recruitment to the insulin receptor. APS recruits CAP-CBL to the plasma membrane, which in turn recruits the adapter protein CRK and its associated protein C3G, C3G activates TC10 by stimulating GTP loading. TC10 interacts with the exocyst and CIP4 to induce GLUT4 containing vesicle translocation and tethering. The PI3K signalling cascade is initiated when IRS-1 is recruited to the insulin receptor and phosphorylated. Phosphorylated IRS-1 recruits PI3K which converts PIP2 to PIP3. PIP3 interacts with PDK and Akt. PDK phosphorylates Akt. Akt interacts with AS160 to induce GLUT4 vesicle translocation and with RGC which induces translocation and vesicle tethering.

1.1 Type 2 diabetes mellitus

In healthy individuals the counteracting actions of the hormones insulin and glucagon maintain blood glucose levels within a tight range. The process by which insulin regulates blood glucose levels can become dysregulated resulting in hyperglycaemia and eventually leading to diabetes mellitus. Broadly speaking diabetes can be divided into two conditions; Type 1 (insulin-dependent) and Type 2 (non-insulin-dependent). Type 2 diabetes is by far the more common, with more than 90% of patients having this form (WHO estimate). In Type 1 diabetes the pancreatic beta cells do not produce insulin, and this condition can be largely treated by the administration of insulin. Type 2 diabetes is a more complex condition and many factors can contribute to its onset and progression (Johnson & Olefsky 2013). A key facet of type 2 diabetes is resistance of peripheral tissues (skeletal muscle and adipose tissue) to the action of insulin.

This insulin-resistance means that the glucose transporter GLUT4 is not mobilised from intracellular deposits to the cell surface in response to insulin. This in turn prevents insulin-induced glucose clearance and leads to hyperglycaemia. For insulin to mobilise GLUT4 from intracellular deposits a number of key criteria must be met, one of which is the sorting of GLUT4 into an insulin-sensitive GLUT4 storage site. This storage site is made up of GLUT4 storage vesicles (GSVs), see below.

Although there seems to be a reduction in the expression of GLUT4 in adipose tissue in insulin-resistant obese patients (Garvey et al. 1988), this cannot solely account for the impaired insulin-stimulated translocation of GLUT4. There also seem to be defects in intracellular trafficking of GLUT4. Compared to healthy patients, patients with insulin resistance show reduced GLUT4 mobilisation from intracellular deposits to the plasma membrane in response to insulin (Garvey et al. 1988). They also display abnormal trafficking of IRAP, a component of insulin-sensitive GLUT4 containing vesicles in adipose tissue (Maianu et al. 2001). As previously mentioned, adipose-specific impairments in insulin-stimulated glucose uptake have implications for whole body glucose uptake (Abel et al. 2001). Therefore understanding the mechanisms underlying the trafficking of GLUT4 into insulin sensitive vesicles in adipose tissue is of vital importance in order to increase our understanding of the molecular defect(s) which underlie diabetes mellitus.

1.2 GLUT4

GLUT4 is one of 14 hexose transporters expressed in humans and is part of the Major-Facilitator Superfamily of transporter proteins. It is an integral membrane protein with 12 transmembrane domains. Each member of the GLUT family has a distinct affinity for its hexose substrate and shows differential tissue and cellular distribution patterns which relates to its function in the maintenance of hexose homeostasis. For example, GLUT2 seems to have a role in glucose sensing and is expressed in the intestine, liver, pancreas, kidney and brain. On the other hand GLUT5 is primarily a fructose transporter and is expressed in the intestine and kidney. GLUT4 is the only member of the GLUT family that is regulated by insulin. It is a glucose transporter and is expressed solely in insulin sensitive tissues; adipose tissue, skeletal and cardiac muscle. Its presence at the cell

surface is altered by the level of insulin in the blood (Pessin & Bell 1992; Huang & Czech 2007; Mueckler 1994). When blood insulin levels are high, it is found at the cell surface where it transports glucose into the cell via facilitated diffusion. Conversely under basal (no insulin) conditions, GLUT4 is effectively sequestered away from the plasma membrane within intracellular deposits. It is present at the *trans* Golgi network and in cytoplasmic vesicular structures (Slot et al. 1991).

1.2.1 Intracellular pools of GLUT4

GLUT4 is present within vesicular structures localised at the *trans* Golgi network and throughout the cytoplasm, notably at the cell periphery (Slot et al. 1991). These vesicular structures do not represent a homogenous pool of GLUT4, but GLUT4 in two major pools: the endosomal recycling compartment (ERC) and insulin-sensitive GLUT4 storage vesicles (GSVs). These compartments are distinct from one another. This is evident from studies that have abolished the entire endosomal pool (and thus removed most of the cellular transferrin receptor (TfR)), but found that between 40% and 60% of GLUT4 remains (Livingstone et al. 1996; Martin et al. 1996). The two intracellular pools of GLUT4 can be separated from each other based on density. The less dense pool is the ERC and contains markers of endosomes such as the TfR. The second, denser pool comprises of small vesicles 50 - 70 nm in size, which do not contain markers of the endosomal recycling systems and are selectively mobilised to the cell surface by insulin. These are termed GLUT4 storage vesicles (GSVs) as they represent a store of GLUT4 that can be mobilised rapidly in response to insulin stimulation (Hashiramoto & James 2000; Martin et al. 2000).

As well as being found in vesicles throughout the cytosol, GLUT4 is also found in the perinuclear region. Here GLUT4 colocalises with sub-domains of the TGN that are enriched in syntaxin 6 and 16 but not TGN38 (Shewan et al. 2003). The GLUT4 within this perinuclear compartment does not translocate to the cell surface in response to insulin (Fujita et al. 2010). This pool of GLUT4 therefore likely represents a GLUT4 trafficking and sorting site, where GLUT4 is passed from the ERC and packaged up into insulin sensitive GSVs.

Examining the cycling of GLUT4 between these intracellular compartments is challenging as the compartments are morphologically similar and GLUT4 cycles between each of them. However, one method to distinguish between them is based on their biochemical composition. GLUT4 containing vesicles within the ERC contain TfR and cellugyrin. On the other hand GSVs do not contain significant amounts of TfR and are devoid of cellugyrin but contain IRAP, which traffics in an identical manner to GLUT4 (Kupriyanova & Kandror 2000; Kupriyanova et al. 2002). The difference in localisation of TfR has been used to dissect the trafficking itinerary of GLUT4.

1.2.2 GLUT4 trafficking

As mentioned, GLUT4 is present in a number of intracellular compartments including the endosomal system and in specialised insulin-sensitive GSVs. Although these pools are distinct from one another, they are inter-linked. GLUT4 pools do not exist in isolation, and GLUT4 is engaged in continual cycling between these intracellular compartments and the plasma membrane.

From the plasma membrane GLUT4 is internalised via both clathrin and cholesterol dependent endocytosis to the endosomal recycling compartment (Ros-Baro et al. 2001; Shigematsu et al. 2003; Blot & McGraw 2006; Leto & Saltiel 2012), where it colocalises with TfR. GLUT4 recycles from the ERC into GSVs, via recycling endosomal compartments and the TGN (Slot et al. 1991; Guilherme et al. 2004; Zeigerer et al. 2002).

To establish if the ERC and the GSV pools of GLUT4 are linked Zeigerer et al. (2002) determined the amount of GLUT4 in each pool when traffic through the endosomal system was blocked. They measured the amount of GLUT4 in each pool using the endosomal ablation technique as developed previously (Livingstone et al. 1996; Martin et al. 1996). In this techniques the amount of GLUT4 in the ERC is determined by measuring GLUT4 loss when cells were incubated with HRP-Tf/DAB. To measure the amount of GLUT4 in ERC and GSVs Zeigerer et al. (2002) used the same technique but delivered HRP to both the ERC and GSVs by expressing a chimeric protein containing TfR and the cytoplasmic domain of IRAP. Under these conditions the amount of GLUT4 in GSVs is equal to the amount abolished using IRAP-TfR chimera minus the amount

abolished using TfR. In line with previous studies, around half the GLUT4 was found to be localised in the ERC and half in GSVs (Livingstone et al. 1996; Martin et al. 1996; Zeigerer et al. 2002). When the same experiments were performed alongside perturbation of endosomal trafficking, most of the GLUT4 was removed when either the wild type TfR or the chimeric IRAP-TfR protein was used. This suggests that when endosomal trafficking is prevented, GLUT4 is inaccessible to the TfR negative, IRAP positive, GSV compartment and remains in the TfR positive ERC. Therefore, GSVs must be formed, at least in part, from the endosomal (ERC) pool of GLUT4.

While it is clear that the ERC and GSV pools are linked, GSVs can also be formed directly from newly synthesised GLUT4 (Watson et al. 2004). Watson et al. (2004) examined the trafficking of newly synthesised GLUT4. They transfected 3T3 L1 adipocytes with cDNA encoding a version of GLUT4 tagged in the first extracellular loop with HA, and at the C terminus with EGFP (Watson et al. 2004). Although it took between 9 and 12 hours for newly synthesised HA-GLUT4-EGFP to become insulin sensitive (a proxy for trafficking into GSVs), GSV formation was unaffected by preventing endocytosis. Moreover HA-GLUT4-GFP did not traffic to the plasma membrane before being incorporated into GSVs (Watson et al. 2004).

These studies provided evidence that although newly synthesised GLUT4 can enter GSVs directly, recycling GLUT4 traffics through the ERC *en-route* to GSVs. GLUT4 also traffics through the Golgi apparatus. This is clear from morphological studies that have localised GLUT4 to subdomains of the Golgi apparatus (Slot et al. 1991; Shewan et al. 2003). The importance of the Golgi is highlighted by the finding that the disruption of trafficking of GLUT4 through the Golgi prevents the formation of GSVs (Williams et al. 2006). Many proteins localised within the Golgi stack have been identified as being required for the formation of GSVs. This includes the TGN proteins syntaxin 6 and 16 as well golgin 160, a protein localised to the Golgi cisternae. Depletion of these proteins inhibits the formation of insulin-sensitive GLUT4 compartments (Perera et al. 2003; Proctor et al. 2006; Williams et al. 2006).

The data discussed in sections 1.2.1 and 1.2.2 has led to the generation of a generally accepted model of GLUT4 cycling, which is depicted in Figure 1.2. In

this model GLUT4 is internalised from the cell surface into the endosomal recycling compartment.

Passage of GLUT4 out of the early endosome into the recycling endosome segregates GLUT4 away from the rapidly recycling loop that acts between the early endosome and the plasma membrane. Around half of the GLUT4 stays in the ERC and the remaining GLUT4 is shuttled, via the *trans* Golgi network, into specialised insulin-sensitive GSVs. GSVs are only recruited to the plasma membrane following insulin-stimulation. The segregation of GLUT4 into GSVs not only effectively sequesters GLUT4 away from the cell surface under basal conditions, but it also provides a rapidly available pool of GLUT4 that is mobilised upon insulin stimulation. The mechanism governing the retention of GSVs under basal conditions has been a hotly debated topic and is discussed in detail in section 1.2.6. However, on balance the available data suggests that in the absence of insulin GLUT4 cycles slowly back into the ERC, where it undergoes another round of cycling.

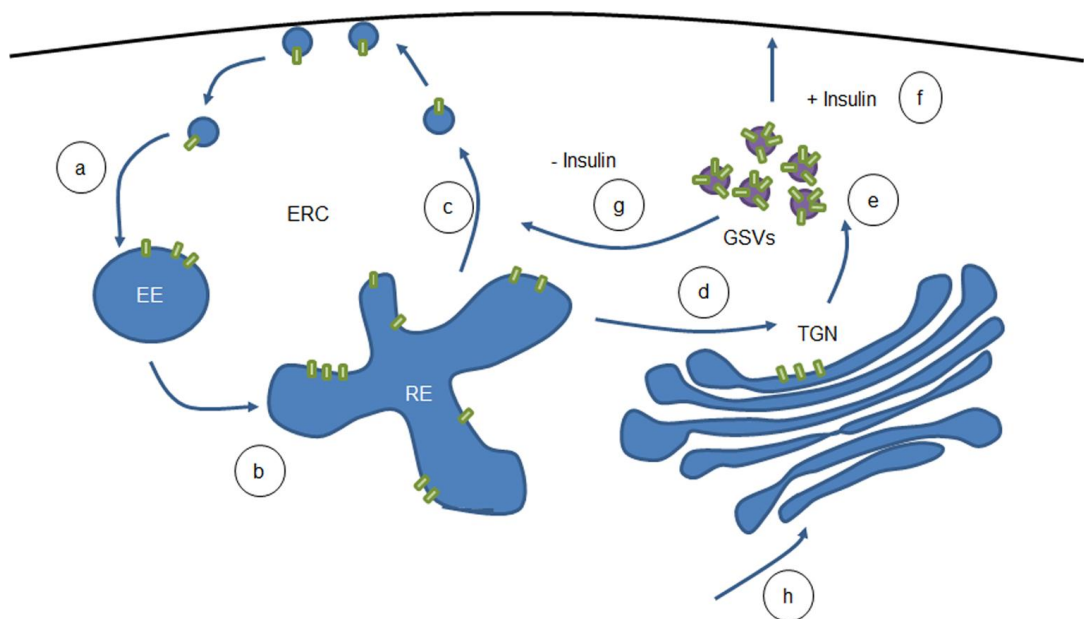


Figure 1-3: GLUT4 continuously cycles through two inter-linked pools.

GLUT4 is internalised from the plasma membrane to early endosomes (a) and is passed onto recycling endosomes (b). From the recycling endosomes it is either trafficked back to the plasma membrane. This cycle forms the endosomal recycling compartment (ERC). Alternatively, GLUT4 is passed to the TGN (d) where it is sorted into GSVs (e). GSVs provide a readily available store of GLUT4 that is recruited to the plasma membrane in the presence of insulin (f). In the absence of insulin, GLUT4 cycles back into the ERC (g) and re-enters the cycle. Newly synthesised GLUT4 can directly enter GSVs (h).

1.2.3 Targeting motifs within GLUT4

The formation of GSVs requires GLUT4 to be targeted to the correct intracellular compartments and away from the endosomal recycling system. The intracellular targeting of GLUT4 is dependent on motifs within the GLUT4 molecule. As discussed, GLUT4 traffics through a number of compartments *en route* to GSVs (Figure 1-3). Each trafficking step is dependent on different motifs on GLUT4. Four key motifs have been identified so far, three of these are present on the C terminal end, and one in the N terminal end.

Substitution of the final 30 amino acids of either GLUT1 or TfR with those of GLUT4 is sufficient to increase their retention to levels similar to that of GLUT4. This phenotype is abolished if the double leucine motif at position 489/490 is mutated. (Corvera et al. 1994; Verhey & Birnbaum 1994; Blot & McGraw 2006; Blot & McGraw 2008). Therefore the LL motif is important for GLUT4 trafficking. Mutation of the LL motif does not affect the internalisation of GLUT4 but does slow the return of GLUT4 retention to basal levels following insulin removal (Blot & McGraw 2006). This suggests one of two scenarios. The first is that the double leucine motif is not involved in endocytosis *per se* but in the intracellular trafficking of GLUT4. The second is that endocytosis under basal conditions and following insulin withdrawal is through different routes, and that the route following insulin withdrawal is dependent on the LL motif but the basal route is not. GLUT4 is internalised by both cholesterol dependent and independent mechanisms. Under basal conditions the majority of internalisation is through cholesterol dependent mechanisms. Insulin-stimulation inhibits the cholesterol dependent mechanism. Following insulin removal GLUT4 internalisation is cholesterol dependent, and requires the LL motif as well as a motif in the N termini (FQQI - discussed below) (Blot & McGraw 2006). Mutation of the LL motif increases the size of the pool of rapidly recycling GLUT4, suggesting GLUT4 is not effectively sequestered into GSVs. These findings are consistent with the LL motif acting in the trafficking of GLUT4 from the ERC into GSVs. In line with this, it has been suggested that the LL motif acts to modulate the trafficking of GLUT4 from the early to the recycling endosome (Blot & McGraw 2008; Figure 1-4).

There are other motifs down-stream of the LL motif that are also important for GLUT4 trafficking. This includes motifs within the T⁴⁹⁸ELEYLGP⁵⁰⁵ domain that makes up the final 12 amino acids of GLUT4 (Shewan et al. 2000). Mutations within this domain lead to the localisation of GLUT4 in the ERC (Shewan et al. 2000). This implies that motifs within the TELEYLGP domain are required for the effective passage of GLUT4 out of the ERC and into GSVs. In line with this it has subsequently been shown that the mutation of E⁴⁹⁹ and E⁵⁰¹ to alanine reduces the amount of GLUT4 in GSV compartments. A reduction in the amount of GLUT4 in GSVs could either be through a reduction in the formation of GSVs or through increased recycling of GLUT4 out of GSVs. In order to differentiate between these two possibilities, the effect of the EE mutations was compared to that of knock down of AS160. AS160 acts to retain GLUT4 within GSVs and the EE mutations were not additive to AS160 depletion. This suggests that the E⁴⁹⁹ E⁵⁰¹ domain and AS160 act at the same step in the cycling of GLUT4, and thus E⁴⁹⁹ E⁵⁰¹ likely functions in the retention of GSVs (Blot & McGraw 2008). Another motif within the C terminal region of GLUT4 has been identified as affecting GSV formation. The mutation of L⁵⁰⁰, L⁵⁰³, P⁵⁰⁵ to alanine causes GLUT4 to be segregated away from GSVs into a compartment free of endogenous GLUT4 that possibly represents a pre-lysosomal compartment (Song et al. 2008). This suggests that these residues act to stabilise GLUT4 and prevent its degradation.

The N terminus also appears to be important for the trafficking of GLUT4 into GSVs. Chimeric proteins expressing the first 8 amino acids of GLUT4 are targeted to perinuclear compartments and localise with endogenous GLUT4 (Piper et al. 1993). Within these 8 amino acids, the fifth phenylalanine (F⁵) seems particularly important. Mutations of F⁵ have different effects depending on the amino acid that F⁵ is substituted with. Mutation of F⁵ to serine prevents entry of GLUT4 into the perinuclear compartment and forces GLUT4 into the degradative pathway (Palacios et al. 2001). This suggests F⁵ is important in the formation of GSVs. Therefore, the mutation of F⁵ might be expected to decrease the sequestration of GLUT4 under basal conditions. In line with this prediction, the mutation of F⁵ to alanine decreases GLUT4 sequestration, and increases GLUT4 in the ERC (Blot & McGraw 2006; Blot & McGraw 2008). However, contrary to this prediction, the mutation of F⁵ to tyrosine increases retention (Blot & McGraw 2008).

Decreases in sequestration could be through the decreased synthesis of GSVs or the increased recycling of GLUT4 out of GSVs. Increases in retention could be through the increased synthesis of GSVs or the trapping of GLUT4 somewhere in its cycle from ERC to GSVs. The increased retention seen with the F⁵ to tyrosine mutation was not due to increased GSV formation as although it increased the amount of GLUT4 in the GSV fraction, as measured by the endosomal ablation technique, the insulin stimulated translocation of GLUT4 was blunted. This suggests that GLUT4 is not truly in GSVs. Therefore it is likely the increased sequestration was due to trapping GLUT4 in the GSV donor compartment. In this way GLUT4 is sequestered away from the ERC compartment but does not reach a compartment that is sensitive to insulin. The decreased retention seen with the F⁵ to alanine mutation was additive to the effects of depletion of AS160, suggesting that the decreased retention was due to decreased synthesis of GSVs. Together these data suggest that the FQQI motif is important for the targeting of GLUT4 into the GSV donor compartment and trafficking through this compartment. Mutations of F⁵ either prevent GLUT4 entering the donor compartment and thus decrease retention, or prevent GLUT4 from exiting the compartment and thus increase retention (Blot & McGraw 2008).

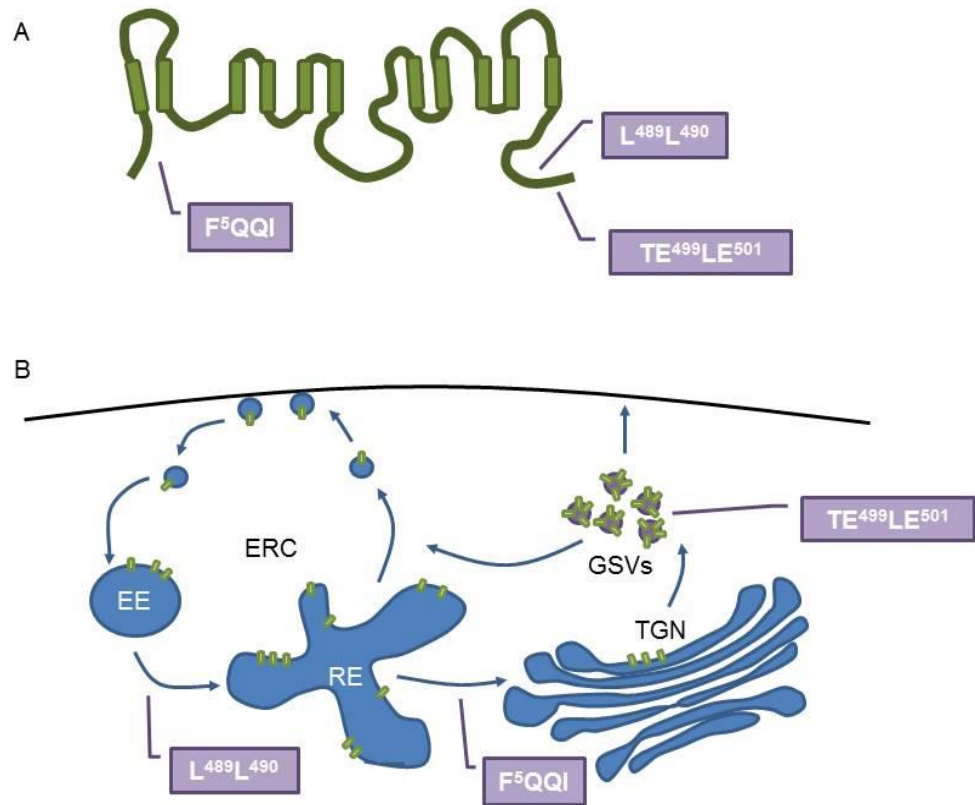


Figure 1-4: Targeting motifs in GLUT4 trafficking.

Motifs of GLUT4 that have been implicated in its intracellular trafficking (A) and the trafficking steps they are proposed to act in (B). The LL motif at the c terminus seems to be involved in the trafficking of GLUT4 out of the rapidly recycling endosomal pool, the N terminal FQQI motif in the trafficking of GLUT4 through the GSV donor compartment, and the TELE motif in the retention of GSVs.

1.2.4 Formation of GSVs

Proteomic analysis of insulin-sensitive GLUT4 membranes has identified many proteins that localize with GLUT4 (Larance et al. 2005; Jedrychowski et al. 2010). Those that translocate with GLUT4 to the plasma membrane in response to insulin are deemed to be present on GSVs and thus are likely to be important in either the formation of GSVs or the insulin response. There are many different groups of proteins that have been identified on GSVs. This includes secretory proteins, adaptor and coat proteins, membrane trafficking proteins and cargo proteins. The GSV cargo proteins that have received particular attention and are deemed to be of high importance in the formation of GSVs are GLUT4, IRAP, sortilin and LRP-1. Each of these cargo proteins plays different but essential roles. GLUT4 is the key component of GSVs, providing the glucose transport machinery and allowing the GSV to fulfil its ultimate role in glucose transport. Sortilin is involved in the formation of GSVs, whereas IRAP and LRP-1 are involved in the insulin-simulated translocation of GSVs (see citations below).

The driving force in GSV formation seems not to be GLUT4, but sortilin. Sortilin is both necessary and sufficient for the formation of GSVs. Sortilin expression increases in line with the acquisition of insulin-responsiveness and the generation of the GSV pool of GLUT4 during adipocyte differentiation (Hatakeyama & Kanzaki 2011). In pre-adipocytes ectopically expressing GLUT4, the GLUT4 is rapidly degraded. However, the expression of sortilin alongside GLUT4 stabilizes GLUT4 and allows it to be trafficked into GSVs and gain insulin responsiveness (Shi & Kandror 2005; Hatakeyama & Kanzaki 2011). GLUT4 and sortilin interact at the GSV donor compartment. Sortilin is targeted to the GSV donor compartment through its luminal domain. Accordingly the luminal domain is required for the formation of GSVs. In the absence of GLUT4, GSV like compartments can be formed in pre-adipocytes through the exogenous expression of sortilin alone. These compartments are morphologically GSVs. However, they lack GLUT4 and IRAP. This shows that GLUT4 is not required for GSV formation. However, despite IRAP being endogenously expressed in pre-adipocytes to a similar level as adipocytes, the GSV compartments do not contain IRAP. IRAP is only incorporated into GSVs when GLUT4 and sortilin is expressed (Shi et al. 2008). Therefore sortilin is required for GLUT4 entry into GSVs, and GLUT4 is required for IRAP entry into GSVs. Sortilin can interact with GLUT4 through the Vps10p domain of sortilin and the first extracellular loop of GLUT4 (Shi et al. 2008). GLUT4 in turn interacts with IRAP (Shi et al. 2008). The finding that interactions between sortilin and GLUT4, and GLUT4 and IRAP are required for GSV formation has led to the proposal of the self-assembly hypothesis (Shi et al. 2008). The self-assembly hypothesis proposes that GLUT4, IRAP and sortilin are targeted to the same membranes of the perinuclear compartment, they interact with one another and enter GSVs together. The entry of this cargo protein complex into GSVs is facilitated by interactions between sortilin and a group of adaptor proteins, termed GGAs (Nielsen et al. 2001; Li & Kandror 2005; Shi & Kandror 2005; Shi et al. 2008).

A recent study identified LRP-1 as another key component of GSVs. The importance of LRP-1 in GSV formation and/or stability is evident from studies depleting adipocytes of LRP-1. This leads to a reduction in the levels of GLUT4, IRAP and sortilin and concomitantly reduces insulin-stimulated glucose uptake (Jedrychowski et al. 2010). LRP-1 interacts with GLUT4, IRAP and sortilin,

although how LRP-1 fits into the 'self-assembly' hypothesis is not yet clear as the mode of the interactions between LRP-1 and the other GSV cargo are as yet unknown.

As mentioned, the packaging of the assembled GSV cargo complex into GSVs requires adaptor proteins. One family of adaptor proteins that are required for this process are Golgi-localised, γ -ear-containing, Arf-binding protein adaptors (GGAs). GGAs are required for the entry of both newly synthesised and recycling GLUT4 into GSVs (Watson et al. 2004; Li & Kandror 2005). GGAs are adaptor proteins that recruit clathrin to the TGN (Puertollano et al. 2001). Expression of dominant negative versions of GGAs that can bind their substrate, but not the clathrin coat, in 3T3 L1 adipocytes results in the trapping of GLUT4 in GSV donor membranes (Li & Kandror 2005). GLUT4 does not directly interact with GGAs. Initially the primary mode of interaction between GGAs and GSVs was proposed to be through sortilin. However, more recently it has been noted that although GGAs contain an ubiquitin binding domain and GLUT4 is ubiquitinated. The ubiquitination of GLUT4 is required for entry into GSVs (Lamb et al. 2010). This therefore may be another way by which GLUT4 can interact with GGAs.

At present it seems that the role of GGAs is to recruit clathrin to the site of GSV formation. However, GGAs may not be the only proteins to do this. GLUT4 interacts with the GTPase activating protein ACAP1, which in turn interacts with clathrin (Leto & Saltiel 2012). Depletion of either ACAP1 or clathrin heavy chain does not affect the targeting of GLUT4 to the perinuclear GSV donor compartment, but does reduce insulin-stimulated GLUT4 translocation, which is suggestive of a reduction in the formation of GSVs (J. Li et al. 2007).

From the data described above the following model of GSV formation can be proposed. GSV cargo proteins are individually targeted to the *trans* Golgi network, where they interact with one another through their luminal domains. GGAs interact with the GSV cargo through sortilin and also possibly through ubiquitinated GLUT4. Clathrin is recruited by GGAs and potentially GLUT4 (via ACAP-1) and facilitates vesicle budding. The newly formed vesicles bud off and form a population of small GLUT4 storage vesicles (GSVs), this process is represented in Figure 1-5.

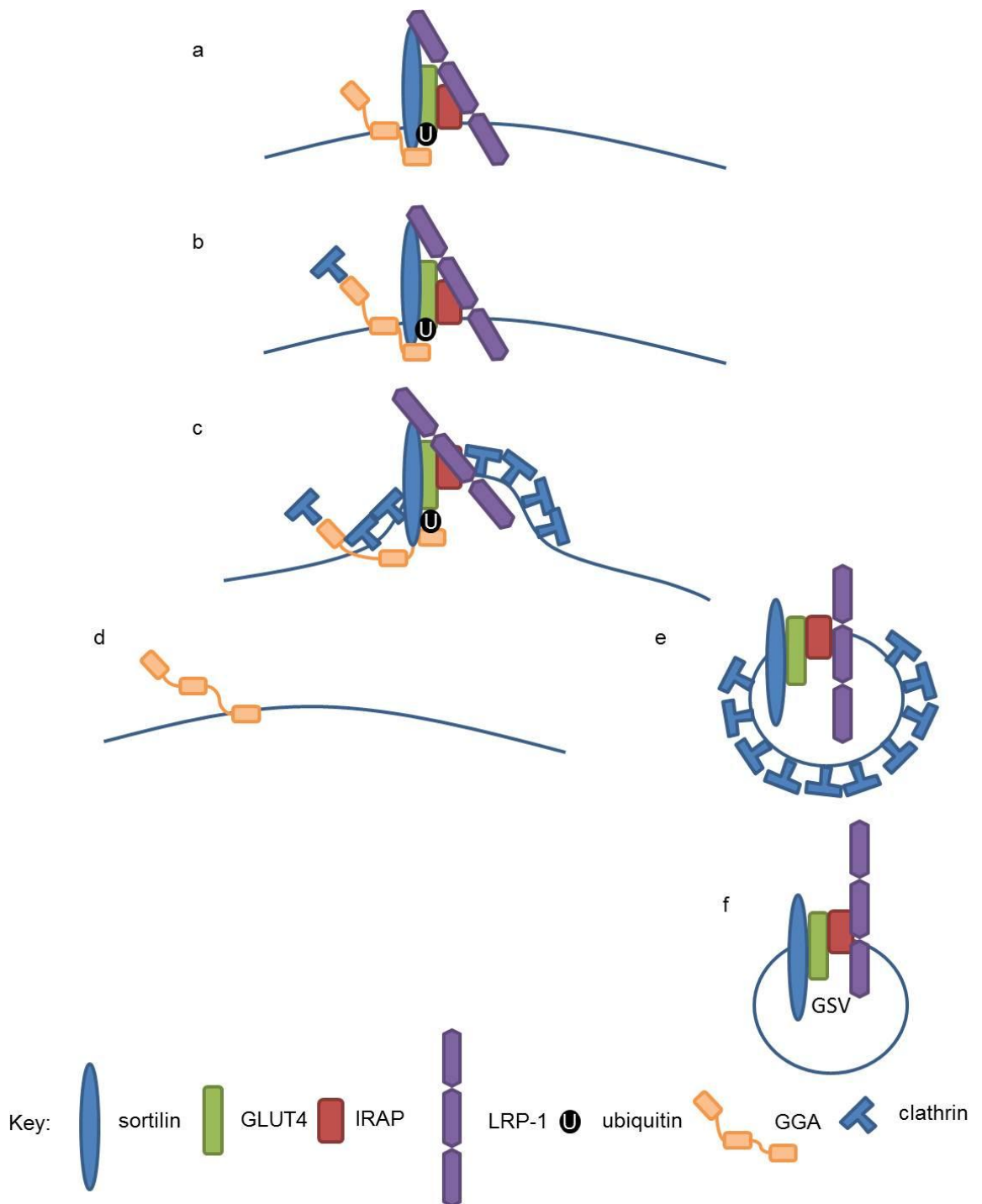


Figure 1-5: GSV formation.

A: the components of GSVs are targeted to the *trans* Golgi Network where they interact with one another via their luminal domains, GLUT4 is ubiquitinated, GGA proteins interact with the cargo protein complex via sortilin and possibly also through the ubiquitin bound to GLUT4. B: GGA recruits clathrin. C: clathrin continues to bind the membrane until the membrane buds off, leaving GGAs on the membrane (D). Since GSVs are not clathrin coated, the vesicles must be uncoated, leaving a newly formed GSV. This GSV then enters the recycling pathway described in Figure 1-3.

1.2.5 Insulin sensitivity of GSVs

For these newly formed GSVs to be functional they must be sensitive to insulin, however it is unclear what gives GSVs their characteristic insulin responsiveness. It does not seem to be GLUT4, as IRAP translocation following insulin stimulation was unaffected by GLUT4 depletion (Yeh et al. 1995). In contrast, the ability of GSVs to respond to insulin appears to be endowed by the presence of IRAP and/or LRP-1. IRAP and LRP-1 are major components of GSVs, however they appear to be dispensable for the formation of GSVs. They may however, be required for giving GSVs their characteristic insulin-responsiveness. Depletion of IRAP has no effect on the basal distribution of GLUT4 but renders GSVs insensitive to insulin-stimulation (Yeh et al. 1995). LRP-1 interacts with the Akt effector AS160 (Jedrychowski et al. 2010). AS160 is found on GSVs and when phosphorylated it stimulates the mobilisation of GSVs to the cell surface (section 1; Figure 1-2), meaning LRP-1 may provide a site of interaction between the insulin-signaling pathway and GSVs.

1.2.6 Retention of GSVs

As described in Section 1.2.1 it is well established that GLUT4 is found within two intracellular pools; the ERC and GSVs, and that in the absence of insulin GSVs are sequestered away from the cell surface. Early research examining GLUT4 recycling using membrane impenetrable photolabelling agents to label endogenous GLUT4, and then following the molecule's internalisation, showed that GLUT4 constitutively recycles to and from the plasma membrane under basal conditions (Yang & Holman 1993). Despite this trafficking itinerary, the majority of GLUT4 is retained within intracellular deposits. This raises the question of how GLUT4 is retained and at the same time cycles to and from the plasma membrane. This phenomenon can be explained by there being an intracellular pool of GLUT4 that is not mobilised to the cell surface under basal conditions. However, the mechanism of this sequestration is debated. One school of thought suggests that GSVs are retained at an intracellular storage site and in the absence of insulin they do not see the cell surface. This is referred to as the "static retention" model. The alternative proposal states that GLUT4 continually cycles to the cell surface under basal and insulin stimulated conditions and that insulin increases the rate of recycling of GLUT4 - the so-

called “dynamic retention” model. The two retention models dictate different and testable hypothesis regarding GLUT4 appearance and traffic through the plasma membrane. The static model dictates that only the ERC pool of GLUT4 will traffic through the plasma membrane under basal conditions, whereas the dynamic model dictates that the entire GLUT4 pool will encounter the plasma membrane under both basal and insulin stimulated conditions. The basis for the static retention model came from Govers et al. (2004) demonstrating that only a small proportion of the total cellular GLUT4 trafficked to the cell surface under basal conditions. Support for the static retention model comes from the identification of a putative intracellular anchoring protein, TUG, and the study of single molecule velocities under basal and insulin stimulated conditions (Bogan et al. 2003; Govers et al. 2004). Furthermore, in insulin-sensitive GSV containing adipocytes, but not in fibroblasts, GLUT4 displays a remarkably static behaviour (Fujita et al. 2010; Hatakeyama & Kanzaki 2011); Fujita et al. (2010) found that in adipocytes, there were three classes of GLUT4 molecules. GLUT4 is either moving rapidly, slowly or is completely static. Insulin reduces the proportion of GLUT4 in the static pool from 60% to 20%.

At the core of the static retention system is the tethering protein TUG (Tether, containing a UBX domain, for GLUT4). TUG binds GLUT4 in basal but not insulin stimulated cells (Bogan et al. 2003). TUG depletion or overexpression of a dominant negative version of TUG decreases the retention of GLUT4 under basal conditions and abolishes the insulin-stimulated increase in GLUT4 translocation (Bogan et al. 2003; Yu et al. 2007). It has recently been shown that TUG depletion redistributes GLUT4 and VAMP2, but not TfR, to the plasma membrane, and that mobilisation that results from TUG depletion is of small GLUT4 containing vesicles that are the same size as GSVs. This suggests that TUG acts specifically on GSVs not endosomes (Xu et al. 2011). These findings strongly suggest a role for TUG in the recycling and retention of GLUT4.

Despite these findings that support the static retention model there are a number of lines of evidence that contradict this model. First of all, bearing in mind that GSVs are formed from GLUT4 within the ERC, and there is always some ‘flux’ of GLUT4 through this pool, if GLUT4 were retained in a static manner the ERC pool would eventually become depleted of GLUT4. This is not the case, ergo GLUT4 must recycle out of GSVs back into the ERC in the absence

of insulin. There is evidence supporting this dynamic model of GLUT4 retention where the entire pool of GLUT4 traffics through the cell surface (and thus through the ERC) under basal conditions. This trafficking is slow as it takes up to 600 minutes for the entire pool of GLUT4 to traffic through the cell surface (Martin et al. 2006). This finding that the recycling is slow allows the findings of the studies supporting the static retention model to be examined more closely. Grovers et al. (2004) found that only a small portion of the total pool of GLUT4 trafficked to the cell surface, however in this study trafficking was only examined for 180 minutes. Furthermore in aforementioned studies that have examined the kinetic properties of GLUT4, velocities were only measured for 10 seconds, meaning very slowly moving GLUT4 may have been observed as static (Fujita et al. 2010).

Taking these observations into consideration allows the proposal of a model of GLUT4 trafficking that encompasses both the dynamic and static properties of GLUT4 that have been observed. This model is displayed in Figure 1-3. In this model GSVs are formed from the TGN. Once formed they may be retained in a static manner for a period of time possibly through interactions with the intracellular anchor TUG, before in the absence of insulin, slowly recycling back into the ERC. In the presence of insulin GSVs are rapidly mobilised to the cell surface, from the cell surface. Once the insulin-stimulus is removed, GLUT4 is internalised and enters the cycling pathway again (Figure 1-3).

At this point it is prudent to note that the debate regarding the retention mechanism of GLUT4 (“static” or “dynamic”) is largely irrelevant in a physiological setting. Under physiological conditions there will always be some level of insulin stimulation, thus GLUT4 will be continually recycling.

1.2.7 Insulin response of GLUT4

The primary effect of insulin in adipose tissue is to increase the rate of glucose uptake. This occurs through a dose dependent increase in the amount of GLUT4 at the cell surface. This arises through a large increase in GLUT4 exocytosis and a slight reduction in endocytosis (Zeigerer et al. 2004). Following insulin stimulation there is a rapid increase in GLUT4 at the cell surface within ~5 minutes, followed by a slower prolonged increase which reaches maximum at

between 15 and 20 minutes (Coster et al. 2004). Ablation of the endosomal system reduces but does not prevent the translocation of GLUT4 to the cell surface in response to insulin. Since there is still a robust insulin response, the endosomal pool is not required for GLUT4 to translocate to the plasma membrane. Therefore, GSVs must be able directly fuse with the plasma membrane without first trafficking into the endosomal system (Livingstone et al. 1996; Millar et al. 2000). However, other data demonstrates that although the endosomal pool is not required for insulin-stimulated GLUT4 translocation, it does play a role in the insulin response. Insulin-stimulation results in the exocytosis of GSVs and increases the recycling of GLUT4 through the endosomal compartment (Ramm et al. 2000). The increase in the recycling of the endosomal compartment is much smaller (2-fold) (Tanner & Lienhard 1987) compared to the mobilisation of the specialised GSV compartment (10-fold).

Not only do the two pools of GLUT4 contribute to the overall insulin response to differing degrees, the temporal pattern of their contribution differs throughout the insulin response. Recent studies using TIRF microscopy, alongside pH-sensitive probes that fluoresce as vesicles fuse with the plasma membrane, have shown that the initial increase in GLUT4 in the cell surface is from GSVs. However, GLUT4 that is delivered at later stages of the insulin response is not from GSVs, but from the ERC. While the insulin-stimulus is present, GSVs are not regenerated. Once the GSV pool is depleted GLUT4 is trafficked to the cell surface in larger vesicles, which likely originate in the ERC (Stenkula et al. 2010; Xu et al. 2011). Xu et al. (2011) identified that the initial increase in cell surface GLUT4 comes from the fusion of small GLUT4 vesicles (average of 56nm) which probably represent pre-formed GSVs. However, GLUT4 inserted into the plasma membrane at later time points (>15 minutes) comes from larger carriers of GLUT4 (~150nm) (Xu et al. 2011). In support of this hypothesis utilizing similar techniques Stenkula et al. (2010) found that the fusion of IRAP (a marker of GLUT4 in GSVs rather than GLUT4 in the ERC) containing vesicles with the plasma membrane increased to its peak at between 3 and 4 minutes then decayed to a level slightly elevated above basal during the remainder of the insulin-stimulation (Stenkula et al. 2010). Therefore, insulin stimulation results in the rapid exocytosis of GSVs and a longer term increase in the exocytosis of GLUT4 vesicles in the ERC.

As well as mobilizing GLUT4 from intracellular deposits to the cell surface, insulin acts at other steps of the GLUT4 trafficking cycle. These include altering the rate of docking and fusion of GLUT4 containing vesicles, and stimulating the dispersal of GLUT4 in the plasma membrane.

Single molecule tracking studies have shown that insulin increases the time GLUT4 remains in the region surrounding the cell surface, the frequency and tightness of docking, the frequency of fusion events and the speed of fusion pore opening (Lizunov et al. 2005; Bai et al. 2007; Fujita et al. 2010; Xu et al. 2011). These all act to increase the probability and rate of GLUT4 entry into the plasma membrane. Another effect of insulin that has only recently been discovered is that it also stimulates the dispersal of GLUT4 within the cell surface. This reduces the amount of GLUT4 that is found in clusters, and may function to reduce the probability of GLUT4 endocytosis (Stenkula et al. 2010; Lizunov et al. 2013). Finally, there is also evidence that insulin-stimulation increases the activity of GLUT4 inserted in the plasma membrane (Funaki et al. 2006). The effects of insulin-stimulation work in collaboration to increase glucose uptake into insulin-sensitive tissues and reduce blood glucose levels.

The key processes that govern the insulin-induced increase in glucose uptake, including the recycling of GLUT4, the formation of insulin-sensitive GSVs, and insulin-stimulated increases in GLUT4 in the plasma membrane are all examples of targeted membrane trafficking. All membrane trafficking events require SNARE proteins. In the following sections research dissecting the involvement of SNAREs in the trafficking of GLUT4 is examined.

1.3 SNAREs and SM Proteins

1.3.1 SNARE proteins

Membrane trafficking requires vesicles from a donor compartment to bud, be targeted, dock and fuse with the correct target membrane. The fusion of membranes is catalysed by the action of SNARE proteins (soluble N-ethylmaleimide-sensitive fusion protein attachment receptors).

1.3.1.1 Discovery of SNARE proteins

The identification of the machinery required for membrane fusion in mammalian cells began with the discovery that membrane fusion, blocked by incubation of membranes with N-ethylmaleimide (NEM) could be recovered by addition of a 'NEM sensitive factor' (NSF) which was present in extracts of brain cytosol. This factor was later identified and purified (Block et al. 1988). This in turn led to the discovery of soluble NSF attachment proteins (SNAPs), which were also purified (Clary et al. 1990). Using purified SNAP and myc tagged NSF, proteins able to bind to and form complexes with NSF/SNAP were isolated from crude bovine brain membrane extracts. Remarkably, the amino acid sequences of these proteins were found to match those of proteins involved in synaptic vesicle fusion. These were SNAP25 (synaptosome-associated protein of 25kDa), syntaxin 1 and VAMP/synaptobrevin and were termed soluble NSF attachment receptors (SNAREs) (Söllner, Bennett, et al. 1993). SNARE proteins have been shown to provide the minimal machinery for membrane fusion (Weber et al. 1998; Hu et al. 2003). Since the discovery of the first SNARE proteins many more isoforms of SNAP, syntaxin and VAMP/synaptobrevin have been identified. The human genome codes 35 SNARE proteins (Bock et al. 2001). This includes seven isoforms of the VAMP family, VAMP1 and 2 (also termed synaptobrevin 1 and 2), VAMP3 (cellubrevin), VAMP4, VAMP5 (myobrevin), VAMP7 (Tetanus insensitive (TI)-VAMP) and VAMP8 (endobrevin). Each VAMP shows differences in tissue distribution as well as the fusion events they are involved in.

1.3.1.2 SNARE protein structure

SNARE proteins reside on opposing membranes. They catalyze fusion by forming a tight SNARE complex which brings the two membranes into close proximity, overcoming the repulsive forces pushing them apart. Central to SNARE protein function is the conserved SNARE domain, a 60 - 70 amino acid sequence made up of heptad repeats. In isolated SNARE proteins the SNARE domain is rather unstructured. However, when a SNARE domain comes into contact with other SNARE domains they form a highly stable, tight alpha-helical coiled-coil bundle, termed the SNARE complex. In this complex, side chains of the individual amino acids making up the SNARE domains interact and these interactions form 'layers'. Each layer is hydrophobic, except the central '0' layer which is made up of three

glutamine residues and one arginine residue (Hong 2005; Jahn & Scheller 2006; Figure 1-5).

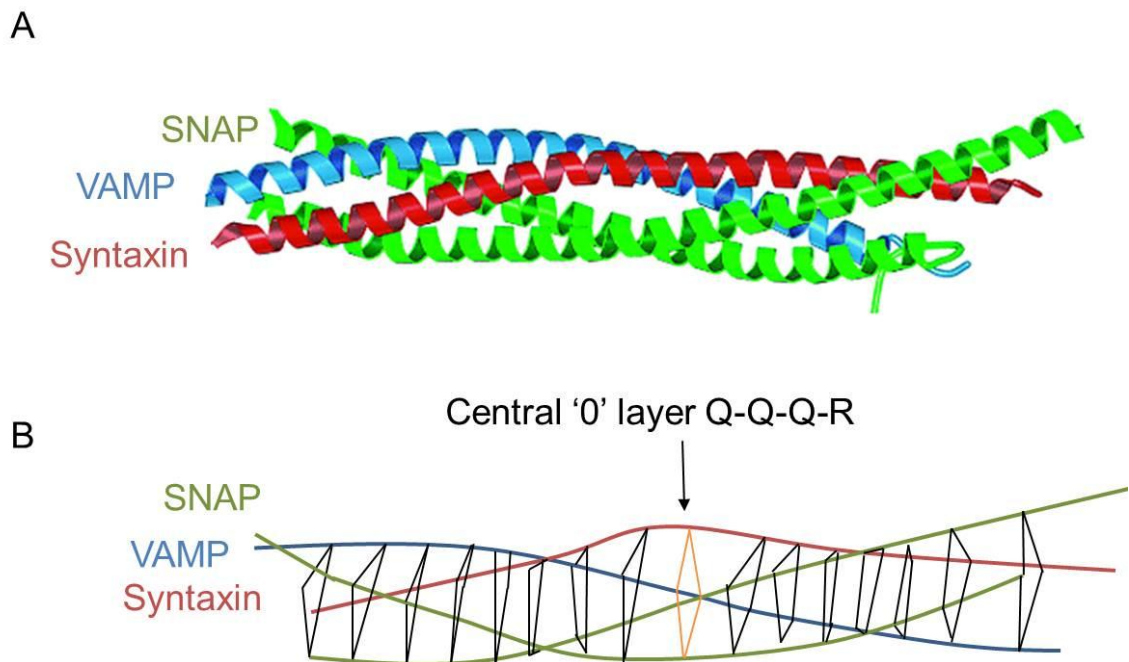


Figure 1-6 SNARE complex structure.

A: The crystal structure of an assembled SNARE complex made up of the SNARE domains of syntaxin 1a (red), SNAP25 (green) and VAMP (blue). **B** Skeleton diagram showing interactions between the side-chains of each of the SNARE complexes, central '0' layer is represented in orange, others in black. Adapted from Sutton et al. (1998).

SNARE proteins can be characterised according to their central '0' layer amino acid (by composition) or by the membrane they localize to (localisation). Initial characterisation was based on localisation; those that were present on target membranes were termed target or tSNAREs and those present on vesicle membranes were termed vesicle or vSNAREs. Although characterisation based on localisation is straightforward, it can be misleading. An example of this is when fusion occurs between membranes that are not easily classifiable into vesicle and target membranes, such as in the fusion of endosomes. Therefore SNARE proteins have also been classified based on their structure. If the central '0' amino acid is glutamine they are termed Q-SNAREs, and if it is arginine they are termed R-SNAREs (Fasshauer et al. 1999). The Q-SNAREs can be further divided up into Q_a, Q_b and Q_c SNAREs. The division of Q SNAREs into these categories is based on the similarities each SNARE has with members of the neuronal SNARE complex. In this complex, syntaxin 1 is the Q_a and the two SNARE motifs of SNAP25 provide the Q_b and c SNARE domains. The alignment of amino acid sequences of other SNAREs with the sequences of syntaxin 1, the two SNARE

domains of SNAP23 or the R-SNARE in this complex, VAMP, has allowed all SNAREs to be classified as either Qa Qb Qc or R (Bock et al. 2001). For SNARE complexes to be functional in mediating membrane fusion, the SNARE complex must contain one of each of these classes of SNARE protein (Qa,b,c and R).

While the SNARE domain is highly conserved, many SNARE proteins contain variable domains at their N termini (Figure 1-6 A). These N terminal extensions range in structure and function. Members of the syntaxin family contain a Habc domain prior to the SNARE domain. The Habc domain can fold back on itself and interact intramolecularly with the SNARE domain forcing the syntaxin into a closed conformation (Fernandez et al. 1998; Misura et al. 2000; Furgason et al. 2009; Figure 1-5 B). In this conformation, a cleft formed between the Hc and b domains interacts with the first 15 amino acids of the SNARE domain (Figure 1-5 B; Misura et al. 2000). As well as the Habc domain, some syntaxins also contain a short N-terminal regulatory domain that can facilitate binding with SNARE regulating proteins, such as Sec-1/Munc 18 (SM) proteins (Section 1.5). Some R SNAREs also have N terminal extensions and the function of this domain varies between each protein. The N terminal domain of VAMP4 contains a *trans* Golgi network targeting motif (Zeng et al. 2003). Similar to the Habc domain of syntaxins, the N terminal login domain of VAMP7 interacts with the SNARE domain and this has been identified to be inhibitory to its association with SNAP25 (Martinez-Arca et al. 2000; Schäfer et al. 2012). SNARE proteins are typically anchored to the membrane through their transmembrane domain. However, SNARE proteins of the SNAP family are notable exceptions. These Qbc SNAREs are anchored to the membrane through palmitoylation (Vogel & Roche 1999; Hong & Lev 2014; Figure 1-6). The structures of SNARE proteins that have been implicated in the trafficking of GLUT4 are represented in Figure 1-6.

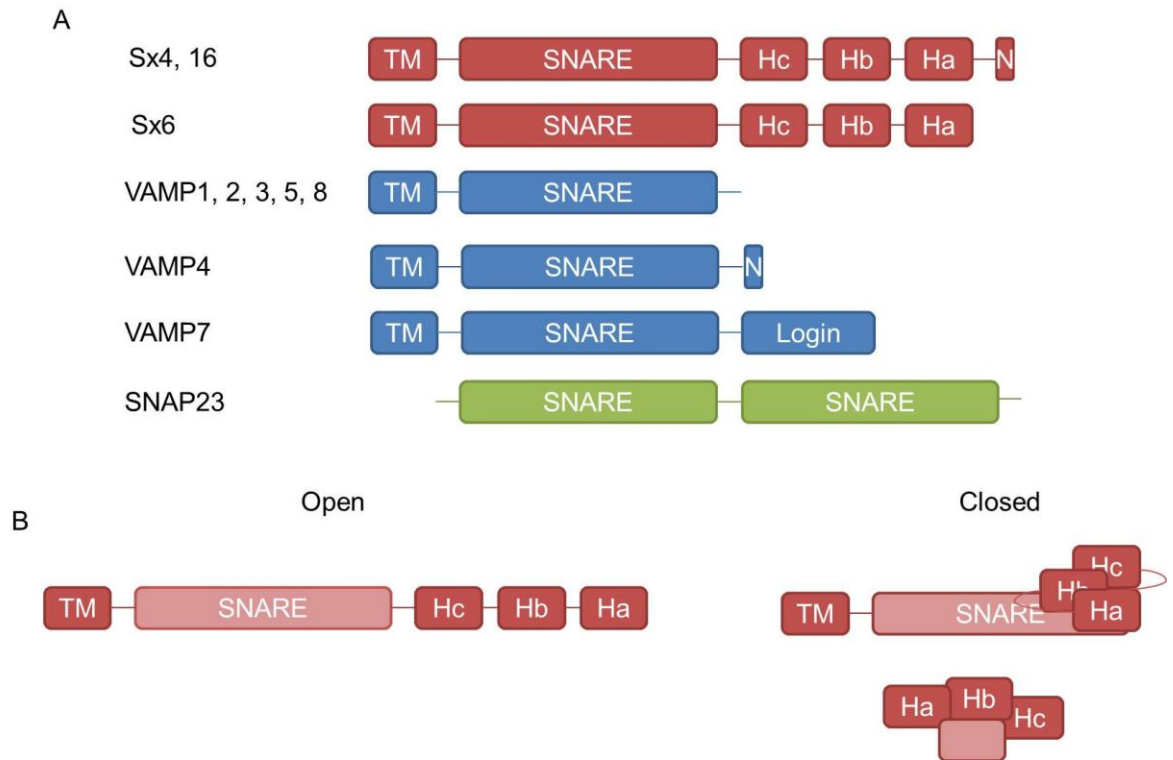


Figure 1-7: Structure of SNAREs discussed in this thesis.

All SNARE proteins contain a conserved SNARE domain, many SNARE proteins also contain transmembrane domains and N terminal extension domains (**A**). The syntaxins contain a Habc domain, and VAMP7 contains a login domain. These domains can fold back and interact with the SNARE domain, giving the SNARE protein a closed conformation (**B**). As well as the Habc domain syntaxin 6 contains a N terminal domain that interacts with its SM protein. VAMP 4 contains an N terminal domain that is important for its TGN localisation. With the exception of the SNAP family, most SNARE proteins are anchored in membranes by their transmembrane (TM) domain. **B** Syntaxin in its open and closed conformation. When in the closed conformation, a cleft between the Ha and Hb domains interacts with the SNARE domain, the top right shows a side view of the syntaxin in its closed conformation, and the bottom right shows the syntaxin in a closed conformation from above.

1.3.1.3 SNARE Complex formation

A stable SNARE complex is formed when four SNARE domains come together. For the complex to be functional in membrane fusion the complex must contain three Q-SNAREs (Qab and c) and one R-SNARE. SNARE complexes that bridge the gap between two membranes are termed *trans* SNARE complexes. SNARE complexes found on the same membrane are termed *cis* SNARE complexes. The formation of *trans* SNARE complexes is sufficient to drive membrane fusion *in vitro*. Therefore SNARE complexes are deemed to be the minimal machinery to drive fusion (Weber et al. 1998).

SNARE complex formation begins at the N terminal end. The side chains of each amino acid interact, and these interactions proceed in a step wise fashion to the C terminal membrane anchored region. This ‘zippering’ action pulls the two membranes into close proximity overcoming the repulsive forces that act

between the membranes. More recently it has been shown that SNARE complex assembly occurs in two discrete stages. First the N terminal portion zippers, then once this has been achieved, the remaining regions of the SNARE domain form a complex. The second stage of SNARE complex formation has been shown to produce enough energy to fuse liposomes *in vitro* (Li et al. 2014). There is also evidence that the domain between the SNARE and transmembrane domain, termed the juxta-membrane domain, assists in membrane fusion. The juxta-membrane domains of VAMP and syntaxin contain many basic residues, and these are attracted to the negative charges of the phospholipids that make up the membrane. Once the SNARE domains have zippered, the basic residues of these domains interact with the negatively charged membranes. This may provide extra force to overcome the barrier to fusion (Williams et al. 2009).

1.3.1.4 Specificity of Fusion

The original SNARE hypothesis stated that SNARE proteins provide both the driving force and the specificity for fusion events (Söllner, Whiteheart, et al. 1993; Rothman 1994). It dictated that each tSNARE has a cognate vSNARE partner and that SNARE complexes only form between cognate SNARE partners. However, this view is now somewhat outdated, as it has become apparent that SNARE proteins are unlikely to dictate fusion specificity alone. One problem with the idea that SNARE proteins provide specificity for fusion is that they are often present on multiple membranes, including membranes they are not involved in the fusion of. This situation arises because, following a fusion event, SNARE proteins must be recycled back to their donor compartment, and is particularly apparent in the endosomal system. Endosomes have been shown to contain SNAREs that participate in both early and late endosomal fusion events and exocytotic fusion events (Brandhorst et al. 2006). Another problem is that many SNARE proteins are involved in more than one fusion event. Furthermore, some fusion events can occur with multiple vSNAREs, but the same tSNARE (Polgár et al. 2002). In line with such problems, SNARE complex formation has been shown to be promiscuous *in vitro*. Providing there is a member of each SNARE subfamily present, many combinations of purified SNAREs can form highly stable SDS resistant complexes (Fasshauer et al. 1999; Yang et al. 1999; Scales et al. 2000). Although these complexes form promiscuously, the formation of fusogenic SNARE complexes, and SNARE complexes formed *in vivo*, seem to be more specific

(Fasshauer et al. 1999; Scales et al. 2000). Therefore although SNARE proteins may provide some level of specificity, other factors must be involved in the targeting and specificity of fusion events.

The ability of SNAREs to act in fusion events can be measured in the cellular environment by observing the inhibiting effect different soluble SNAREs have on fusion events. Using this method the specificity of SNARE complexes involved in the fusion of neuroendocrine carrying vesicles with the cell surface and endosomal fusion has been assessed in PC12 cells. Under these conditions (*in vivo*), SNARE protein interactions appear specific. While there is some degree of cross talk between syntaxins 1 and 4 and VAMPs 2 and 4, but not other syntaxins/VAMPs, in exocytotic fusion events, the inhibition of fusion of endosomes is highly specific to the cognate SNAREs (Fasshauer et al. 1999; Scales et al. 2000).

The data discussed above highlights that SNARE proteins alone cannot drive the specificity of membrane fusion. Consequently roles for tethering factors and SNARE binding proteins have been proposed.

1.4 Tethers

SNARE complexes can clearly mediate fusion events. However, as discussed in section 1.3.1.4, SNAREs may not be sufficient to determine the specificity of fusion events. Furthermore, SNARE complexes only begin to form when membranes are between 4nm and 8nm apart (F. Li et al. 2007). Therefore there needs to be a mechanism by which membranes can be targeted to the correct site, and membranes can be brought into close enough proximity so that SNARE complexes can form. Both these mechanisms can be achieved by the action of tethers.

Tethers can be divided in to two sub classes; long coiled-coil complexes or large multi-subunit tethering complexes (MTCs). Long coiled-coil tethers can interact with membranes that are over 200nm apart, whereas MTCs act over much shorter distances (~30nm) (Hong & Lev 2014). Of the numerous mammalian tethers only a few have been implicated in GLUT4 trafficking. There is direct evidence for the involvement of the exocyst and more indirect evidence for the

conserved oligomeric Golgi complex. The exocyst has been implicated in the tethering of GLUT4 containing vesicles with the plasma membrane (Ewart et al. 2005; Inoue et al. 2003). The overexpression of a mutant subdomain of the exocyst complex prevents insulin-stimulated increases in glucose uptake and insertion of GLUT4 into the plasma membrane, but does not prevent the movement of GLUT4 from the interior of the cell to the cell periphery (Inoue et al. 2003). There is also indirect evidence that the conserved oligomeric Golgi complex (COG) may be involved in the intracellular trafficking of GLUT4. The COG complex assists in the assembly of the SNARE complex made up of syntaxin 6 and 16 (Laufman et al. 2011) which has in turn been implicated in the cycling of GLUT4 into insulin-sensitive vesicles (Perera et al. 2003; Shewan et al. 2003; Proctor et al. 2006). Therefore the COG complex may also be involved in the trafficking of GLUT4.

1.5 SM Proteins

Proteins of the Sec-1/Munc-18 family (SM) proteins are essential components of the fusion machinery. Alongside tethers they may act to provide specificity to membrane fusion. SM proteins have been shown to be both positive and negative regulators of fusion (Toonen & Verhage 2003).

SM proteins bind to their cognate syntaxins through three binding modes. The first, mode 1 binding, is inhibitory to SNARE complex formation. In this binding mode the syntaxin is held in a closed conformation with the Habc domain binding the SNARE motif. The second, mode 2, is the most conserved mode of binding. In this mode the extreme N terminus of the syntaxin binds a hydrophobic pocket of the SM protein. The final mode of binding is between an assembled SNARE complex and the SM protein (Toonen & Verhage 2003; Carr & Rizo 2010; Figure 1-7). Two SM proteins have been implicated in the trafficking of insulin-sensitive GLUT4, Munc18c and mVps45. These act in GLUT4 vesicle fusion with the plasma membrane and formation of GSVs respectively (see citations below).

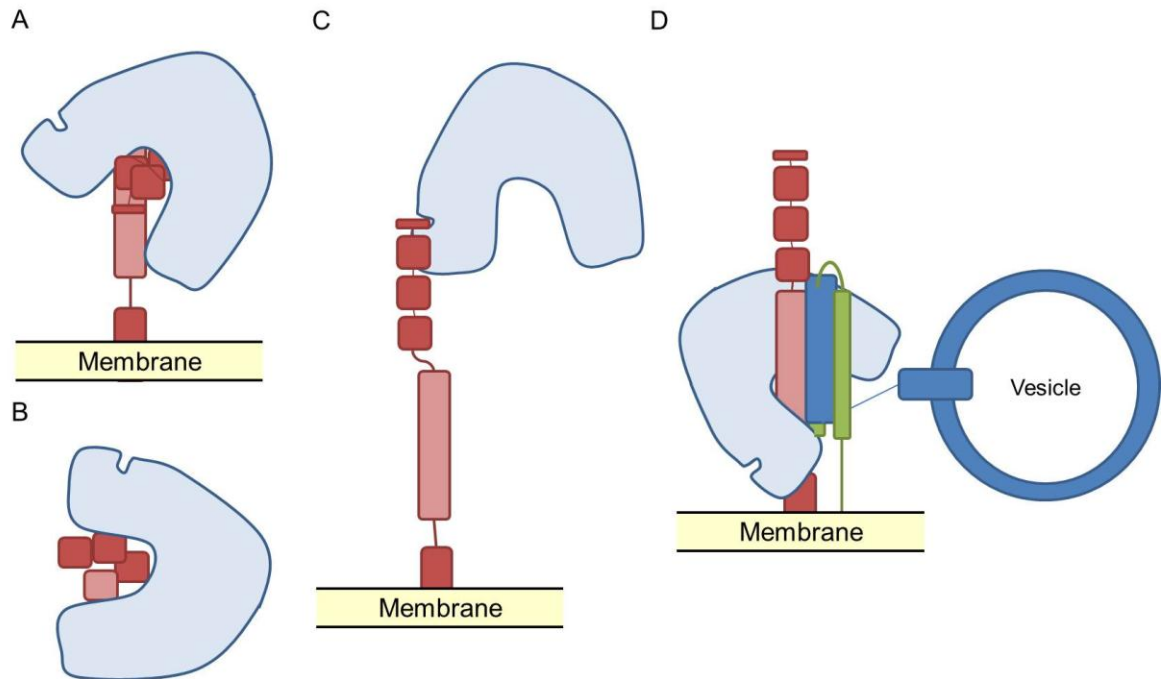


Figure 1-8: Different binding modes of SM proteins interacting with syntaxins.

The SM protein interacts with the syntaxin in a closed conformation, side view (A), top view (B). The SM protein interacts with the N terminal domain of the syntaxin (C). The SM protein interacts with an assembled SNARE complex; this can occur with SNARE complexes either in *cis* or *trans* configuration (D).

1.5.1 Munc18c

Munc18c is required for insulin-stimulated GLUT4 translocation to the PM and glucose uptake (Thurmond et al. 2000). It can bind its cognate syntaxin, syntaxin 4, via the N terminal domain of syntaxin 4 and the hydrophobic pocket of Munc18c (Latham et al. 2006) or through binding of the syntaxin in a closed conformation (Brandie et al. 2008). Munc18c can also bind syntaxin 4 through the final binding mode, mode 3, with the SNARE complex syntaxin4/SNAP23/VAMP2 (Latham et al. 2006).

Munc18c has been found to be both facilitative and inhibitory to SNARE complex formation (Latham et al. 2006; Brandie et al. 2008). Therefore Munc18c could provide a mechanism by which insulin can regulate SNARE complex formation. In this model, Munc18c is inhibitory to fusion when it binds the closed form of syntaxin (mode 1), and facilitative when it binds the N-terminal region (mode 2). One model proposes that insulin stimulates Munc18c phosphorylation, preventing its mode 1 binding to syntaxin 4 (Aran et al. 2011; Jewell et al. 2011). This allows the syntaxin to switch from the closed to the open conformation allowing SNARE complexes to form.

1.5.2 mVps45

Vps45 has been extensively studied in yeast, where it is required for the delivery of proteins to the pre-vacuolar compartment (Cowles et al. 1994; Bryant et al. 1998). Mammalian Vps45 (mVps45) binds to the *trans* Golgi network tSNAREs, syntaxin 6 and 16 (Bock et al. 1997; Tellam et al. 1997; Dulubova et al. 2002) and is essential for the correct targeting of GLUT4 to the insulin sensitive pool (Roccisana et al. 2013).

mVps45 can interact with syntaxin 16 via the N terminal domain (Dulubova et al. 2002), and through an N terminal independent mechanism, although this mode of binding is lower affinity (Burkhardt et al. 2008). The binding of Vps45p to the N terminal region of Tlg2 (yeast syntaxin 16) is required for Tlg2 to bind its cognate SNAREs (Bryant & James 2001). These data suggest that Vps45p, like Munc18c, may be able to regulate SNARE complex formation. Further to potential roles in the regulation of SNARE complex formation, Vps45 also acts as a chaperone for its cognate syntaxin. Studies in both yeast and mammalian cells have shown that depletion of Vps45 leads to a reduction in the levels of Tlg2p/syntaxin 16 (Bryant & James 2001; Roccisana et al. 2013).

1.6 SNAREs in GLUT4 trafficking

GLUT4 is engaged in continual trafficking between multiple membrane compartments. Each trafficking step requires SNARE proteins. In terms of insulin-stimulated GLUT4 translocation, research has focused on two key stages: the fusion of insulin-sensitive GLUT4 storage vesicles (GSVs) with the plasma membrane, and the sorting of GLUT4 into GSVs. Much research has focused on uncovering the roles of SNAREs in these trafficking steps.

1.6.1 SNAREs in GSV fusion with plasma membrane

The tSNAREs required for the fusion of GLUT4 containing vesicles with the plasma membrane have been identified as syntaxin 4 and SNAP23. The introduction of antibodies against SNAP23 or the microinjections of the cytoplasmic domain of syntaxin 4 reduces insulin-stimulated GLUT4 translocation (Cheatham et al. 1996; Rea et al. 1998; Foster et al. 1999). Similarly, knock down of syntaxin 4 or SNAP23 in 3T3 L1 adipocytes impairs both the docking and

subsequent fusion of GLUT4 containing vesicles with the plasma membrane in response to insulin (Kawaguchi et al. 2010).

It is well established that SNAP23 and syntaxin 4 are involved in the fusion of GSVs with the plasma membrane in response to insulin. However, it is less clear which vSNAREs are involved in this process. VAMP2 has been shown to interact with the syntaxin4/SNAP23 tSNARE complex (Rea et al. 1998), and in the presence of SNAP23 with syntaxin 4 (Cheatham et al. 1996; Kawanishi et al. 2000). The interactions seen between VAMP2 and syntaxin4/SNAP23 point to VAMP2 being the vSNARE involved in GLUT4 vesicle fusion with the plasma membrane in response to insulin. In line with this, the disruption of VAMP2, through the injection of VAMP2 peptides (Martin et al. 1998) or the cytoplasmic domain of VAMP2 (Millar et al. 1999), or through RNAi interference (Williams & Pessin 2008; Kawaguchi et al. 2010), reduces insulin-stimulated GLUT4 translocation in 3T3 L1 adipocytes. Such studies support a role for VAMP2 in insulin-stimulated GLUT4 translocation.

However, as well as containing VAMP2, GLUT4 membranes contain VAMP3 and VAMP8 (Volchuk et al. 1995; Larance et al. 2005; Zhao et al. 2009), both of which may also be involved in GSV fusion with the plasma membrane. In keeping with this, Olson et al. (1997) found that the cytoplasmic domains of either VAMP2 or 3 were capable of inhibiting GSV fusion with the plasma membrane (Olson et al. 1997). Further, one study showed that toxin-specific cleavage of VAMP2 and 3 does not impair insulin stimulated GLUT4 translocation, suggesting that another VAMP may be involved in the insulin response (Hajduch et al. 1997). Others dispute this finding (Randhawa et al. 2000).

Recently, VAMP8 has been shown to be able to compensate for the loss of VAMP2 and 3 in the fusion of GLUT4 containing vesicles with the plasma membrane (Zhao et al. 2009). Zhao et al. (2009) used a combination of knock out mice models alongside Tetanus-toxin cleavage of VAMP2 and 3 to study the translocation of GLUT4 in response to insulin. They studied GLUT4 translocation and glucose uptake in adipose cells derived from mouse embryonic fibroblasts (MEFs), taken from a VAMP2 knockout mouse. In these adipose cells insulin-stimulated glucose uptake or GLUT4 vesicle fusion with the plasma membrane was unchanged compared to adipocytes derived from MEFs from wild type

animals. Taking this a step further they found that the cleavage of both VAMP2 and 3 with Tetanus toxin was also without effect. Basal and insulin-stimulated GLUT4 translocation was only impaired when VAMP2, 3 and 8 were absent. In these experiments the reintroduction of either VAMP2, 3 or 8 was sufficient to recover insulin-stimulated GLUT4 translocation. This study highlights that there may be mechanisms of redundancy between SNARE proteins (Zhao et al. 2009). However, neither the origin of the GLUT4 fusing with the plasma membrane nor the mechanism of redundancy between the vSNAREs was assessed. The GLUT4 could have originated from different pools under each condition, and either trafficked through the same pathway using the same tSNARE complex, or through different pathways.

1.6.2 SNAREs in sorting

As mentioned in section 1.2.2 GSVs can be formed from recycling or newly synthesised GLUT4, with both pathways converging at the *trans* Golgi network (TGN). GLUT4 has been shown to traffic through a domain of the TGN that is enriched in two TGN tSNAREs, syntaxin 6 and 16 (Shewan et al. 2003). A tSNARE complex made up of syntaxin 6/16 and Vti1a has been implicated in the formation of insulin sensitive GLUT4 compartments. The formation of GSVs effectively sequesters GLUT4 away from the cell surface under basal conditions. Therefore, preventing the formation of GSVs increases the pool of recycling GLUT4 under non-insulin stimulated conditions. In accordance with this model, syntaxin 6 and 16 are required for the reversal of glucose uptake upon insulin removal (Perera et al. 2003; Proctor et al. 2006). Similarly, the sorting of GLUT4 into GSVs is perturbed when the action of syntaxin 6 is inhibited by the injection of dominant-negative interfering fragments of this protein (Perera et al. 2003), or the disruption of Vti1a (Bose et al. 2005).

Precisely where in the trafficking cycle of GLUT4 the tSNAREs syntaxin 6 and 16 act is unclear. However, they are present in sub-domains of the TGN and on GSVs and they translocate to the plasma membrane along-side GLUT4 in response to insulin (Perera et al. 2003; Shewan et al. 2003; Proctor et al. 2006). Therefore it seems likely they are involved in the later stages of GSV formation, the trafficking of GLUT4 through the TGN to the insulin sensitive compartment (Figure 1-3 step d/e).

The vSNARE VAMP4 is a binding partner of the tSNARE complex made up of syntaxin 6 and 16. Therefore, it has been proposed to play a role in the recycling of GLUT4. Williams and Pessin (2008) used RNAi to selectively remove each of the VAMP isoforms in 3T3 L1 adipocytes expressing a myc-GLUT4-GFP transporter to examine GLUT4 translocation. They found that VAMP2 knock down impaired the insulin-stimulated translocation of myc-GLUT4-GFP, in line with its proposed involvement in the fusion of GSVs with the plasma membrane (section 1.6.1). Surprisingly they found that basal trafficking of myc-GLUT4-GFP to the plasma membrane was unaffected by depletion of any of the VAMPs. However, when VAMP4 was depleted prior to myc-GLUT4-GFP expression, there was an increase in the basal level of myc-GLUT4 in the plasma membrane, suggesting reduced formation of GSVs. This highlights a role for VAMP4 in the entry of newly synthesised, but not recycling, GLUT4 into GSVs. Williams and Pessin (2008) also asserted that since insulin-stimulated GLUT4 trafficking was only attenuated with VAMP2 depletion, VAMP2 may be involved in the formation of GSVs.

The research described in sections 1.6.1 and 1.6.2 illustrate that although roles for VAMP2, 3, 4 and 8 are likely, there is still a great deal of uncertainty in the vSNAREs involved in the intracellular trafficking of GLUT4 under both basal and insulin-stimulated conditions. This study aims to dissect the roles of each of the vSNAREs in the intracellular trafficking of GLUT4.

1.7 SNAREs in diabetes

As mentioned in section 1.2, insulin resistance and Type 2 diabetes are growing problems that face the developed and developing world. One major characteristic of these conditions is an inability of insulin to mobilise GLUT4 from intracellular deposits to the cell surface (Garvey et al. 1988). This may reflect defective GLUT4 sorting into GSVs (Maier & Gould 2000) or defective translocation to the plasma membrane. Both of these trafficking events involve SNARE proteins. As such the status of some of the SNARE proteins that have been implicated in GLUT4 trafficking has been assessed in insulin resistant tissues and/or models of insulin resistance.

When insulin resistance is induced in rats by hyperinsulinemia, there was an increase in the protein levels of VAMPs 2 and 3 and syntaxin 4 in adipose tissue.

This increase was reversed by treatment with the anti-diabetic drug rosiglitazone (Maier et al. 2000). Likewise, in mice with insulin resistance induced by a high fat diet or through overexpression of lipoprotein lipase, elevated adipocyte Munc18c protein levels were observed (Schlaepfer et al. 2003). Similarly, in skeletal muscle from human insulin-resistant subjects, the levels of SNAP23 are increased (Boström et al. 2010). However, no causality between these events has been established. The upregulation of these SNAREs and related proteins may be a compensatory mechanism, or may lead to and/or contribute to the development of insulin resistance.

There is more direct evidence implicating changes in SNARE protein levels in insulin resistance from studies using cell lines. It is well established that treatment of 3T3 L1 adipocytes with fatty acids increases lipid droplet size and induces insulin resistance. An increase in lipid droplet size occurs through lipid droplet fusion; a process that involves SNAP23, syntaxin 5 and VAMP4. Concurrent to this increase in lipid droplet fusion, there is a ‘high-jacking’ of SNAP23 away from the plasma membrane to the site of lipid droplet fusion. In this study, microinjection with SNAP23 restored insulin-sensitivity (Boström et al. 2007). This is consistent with the notion that this specific SNARE protein is crucial for the development of insulin sensitivity/resistance. A state of elevated fatty acid availability and lipid droplet fusion is similar to that seen in obesity. Thus, it is tempting to speculate that this ‘high-jacking’ hypothesis could occur in obesity and contribute to insulin resistance. Although this phenomenon has not been studied in human tissues, it highlights the importance of understanding the membrane trafficking events that underpin the insulin response in both health and disease states, and suggests that defects in the SNARE machinery should be considered as potential defects in Type 2 diabetes.

1.8 Aims of this study

The main aims of this study are to further dissect the roles of the post-Golgi vSNAREs expressed in 3T3 L1 adipocytes (VAMP2, 3, 4, 5, 7 and 8) in the intracellular trafficking of the insulin regulated glucose transporter GLUT4.

1.8.1 Aims of Chapter 3

The trafficking of GLUT4 from intracellular deposits to the cell surface in response to insulin-stimulation is dependent on the tSNARE complex made up of syntaxin 4 and SNAP23. Although the vSNARE VAMP2 has been implicated in this SNARE complex, recent data has suggested roles for other VAMPs. Therefore, Chapter 3 aims to systematically examine the interactions between VAMPs and the tSNARE syntaxin 4.

1.8.2 Aims of Chapter 4

There are discrepancies in the literature regarding compensation and plasticity between VAMP isoforms in GLUT4 trafficking. In order to shed light on the mechanisms of plasticity it is necessary to determine the absolute levels of each VAMP protein in 3T3 L1 adipocytes, and to examine their subcellular distribution in relation to insulin-sensitive GLUT4. Chapter 4 aims to compare the protein levels of each VAMP in 3T3 L1 fibroblasts and adipocytes, and to determine the absolute level of each VAMP in 3T3 L1 adipocytes. Furthermore, the subcellular distribution and localisation of each VAMP with insulin-sensitive GLUT4 is examined.

1.8.3 Aims of Chapter 5

The tSNARE syntaxin 16 and the SM protein mVps45 have both been implicated in the trafficking of GLUT4 from the ERC into GSVs. However, it is unclear which vSNARE acts in this trafficking pathway. Therefore, in Chapter 5 the interactions of each VAMP protein with syntaxin 16 and mVps45 is examined.

1.8.4 Aims of Chapter 6

Previous research has highlighted potential roles for both VAMP2 and 4 in the formation of GSVs, and of VAMP8 in the endocytosis of GLUT4. The overall aim of Chapter 6 is to deplete cells of these VAMP proteins and examine the global distribution of GLUT4. To meet this aim the chapter is split into two sections, the first section aims to replicate the previous data regarding the roles of VAMP2, 4 and 8 in a different cell type, using a different GLUT4 construct (HeLa cells expressing HA-GLUT4-GFP). The second section aims to develop an inducible vector system that will allow the depletion of proteins in mammalian cells to be controlled.

Chapter 2 - Materials and Methods

2.1 Materials

2.1.1 General reagents and enzymes

BD Biosciences, Oxford UK

Syringes

24 Gauge needles

26 $\frac{5}{8}$ Gauge needles

BioRad Laboratories Ltd, Hemel Hemstead, Hampshire, UK

Precision Plus Protein™ All Blue Standards (#161-0373)

Clontech, France

TakaRa rapid Ligation kit

Fisher Scientific UK Ltd., Loughborough, Leicestershire, UK

2-[4-(2-hydroxyethyl)-1-piperazine] ethanesuphonic acid (HEPES)

Ethanol

3mm filter paper

Glycine

L-Glucose

ImmunoMount

Pierce™ Micro BCA™ Protein Assay Kit

Tris(hydroxymethyl)aminoethane Base (Tris Base)

Formedium Ltd., Hunstanton, Norfolk, UK

Amino acid drop-out media -URA

Bacterial agar

Peptone

Tryptone

Yeast extract powder

Yeast nitrogen base without amino acids

GE Healthcare BioSciences Ltd, Chalfont, Buckinghamshire, UK

Dharmafect-4 transfection reagent

Glutathione-S-Sepharose 4B

IgG Sepharose 6 Fast Flow

ON-TARGETplus SMARTpool siRNA

Protein A Sepharose Fast-Flow

Melford Laboratories Ltd., Chelsworth, Ipswich, UK

Dithiothreitol (DTT)

Isopropyl- β -D-thiogalactopyranoside (IPTG)

New England Bioscience (UK) Ltd., Hitchin, Hertfordshire, UK

All endonucleases used in this study

1 kb DNA ladder

100 bp DNA ladder

6x DNA loading buffer

Life Technologies, Paisley, UK

Dulbecco's Modified Eagle Medium (DMEM),
Foetal Bovine Serum (FBS)
Gateway® LR Clonase® II enzyme mix
Lipofectamine® 2000 transfection reagent
Newborn Calf Serum (NCS)
One Shot Chemically Competent BL21 (DE3) E. coli
One Shot Chemically Competent TOP10 E. coli
One Shot® ccdB Survival™ 2 T1R Chemically Competent Cells
One Shot® Stbl3™ Chemically Competent E. coli
Opti-MEM®
Penicillin-Streptomycin (10,000 U/mL)
Subcloning Efficiency™ DH5α™ Competent Cells
smartPOOL siRNA
SYBR® Safe DNA Gel Stain
Trypsin-EDTA (0.05%), phenol red

Pall Life Sciences, Portsmouth, UK

Nitrocellulose transfer membrane, 0.2 µM pore size

Promega, Southampton, UK

Wizard® Plus SV Minipreps DNA Purification System

Qiagen Ltd., Crawley, West Sussex, UK

QIAfilter™ Plasmid Maxi Kit
QIAquick Gel Extraction Kit

Roche Diagnostic Ltd., Burgess Hill, UK

Agarose MP
Complete™ Protease Inhibitor Cocktail Tablets
Complete™ EDTA-free Protease Inhibitor Cocktail Tablets

Severn Biotech Ltd., Kidderminster, Worcestershire, UK

30 % Acrylamide [Acrylamide: Bis-acrylamide ratio 37.5:1]

Sigma-Aldrich Ltd., Gillingham, Dorset, UK

Ammouinum acetate
Ammonium persulphate (APS)
Ampicillin
β-mercaptoethanol
Bovine serum albumin (BSA)
Brilliant Blue-R
Bromophenol blue
Dimethyl sulphoxide (DMSO)
Dexamethasone
Ethylenediaminetetracetic acid (EDTA)
Gelatin from cold water fish skin
Goat serum
L-Glutathione reduced
Glycerol
G418 disulfate salt

3-isobutylmethylxanthine (IBMX)
 Isopropanol
 Kanamycin
 Methanol
 N,N,N',N'-Tetramethylethylenediamine (TEMED)
 Paraformaldehyde
 Ponceau S
 Porcine insulin
 Potassium hydroxide (KOH)
 Reduced glutathione
 Sodium fluoride (NaF)
 Sodium hydrogen carbonate (NaHCO₃)
 Sodium dihydrogen phosphate (NaH₂PO₄)
 Sodium orthovanadate (Na₄VO₃)
 Sodium dodecyl sulphate (SDS)
 Thrombin (Bovine)
 Triton-X100
 Troglitazone
 Tween -20

Spectrum Europe BV., Breda, The Netherlands

Float-a-lyzer, 5 ml 5 kDa MWCO
 Float-a-lyzer, 5 ml 20 kDa MWCO

VWR International Ltd., Lutterworth, Leicestershire, UK

Glacial Acetic Acid
 Glass cover slips (3mm diameter)
 Disodium hydrogen orthophosphate (Na₂HPO₄)
 Potassium Acetate
 Potassium Chloride (KCl)
 Potassium dihydrogen orthophosphate (KH₂PO₄)
 Sodium Chloride (NaCl)
 Sodium Hydroxide (NaOH)

2.1.2 Solutions

2x Laemmli Sample Buffer (LSB)	100mM Tris, HCl pH 6.8, 4% (w/v) SDS, 20% (v/v) glycerol, 0.2% (w/v) bromophenol blue, 10% (v/v) β-mercaptoethanol
2YT	1.6% (w/v) tryptone, 1.0% (w/v) yeast extract, 0.5% (w/v) NaCl (20% Agar)
Coomassie	0.05% (w/v) Coomassie brilliant blue R-250 , 50% (v/v)methanol, 10% (v/v) acetic acid
Coomassie Destain	15% (v/v) methanol, 15% (v/v) acetic acid
ECL solution 1	100mM Tris-HCl, pH 8.5, 2.25mM luminol in 2% (v/v) DMSO, 0.4 mM p-coumaric acid in 1% (v/v) DMSO

ECL solution 2	100mM Tris-HCl, pH 8.5, 0.018% (v/v) H ₂ O ₂
HEPES/EDTA/Sucrose (HES) buffer	250 mM Sucrose, 20 mM HEPES pH 7.4, 1 mM EDTA
immunoprecipitation (IP) buffer	50 mM HEPES pH 7.5, 5 mM EDTA, 10 mM sodium pyrophosphate, 10 mM NaF, 150 mM NaCl, 2 mM β-Glycerophosphate, 1 mM DTT
PBS	140mM NaCl 3mM KCl, 1.5mM KH ₂ HPO ₄ , 8mM Na ₂ HPO ₄
PBST	140mM NaCl 3mM KCl, 1.5mM KH ₂ HPO ₄ , 8mM Na ₂ HPO ₄ , 0.1% (v/v) Tween-20
Ponceau S	0.2% (w/v) Ponceau S, 1% (v/v) acetic acid
RIPA Buffer	50mM Tris, HCl pH8, 150mM NaCl, 2mM MgCl ₂ , 1% Triton, 0.5% sodium deoxycholate (w/v), 0.1% (w/v) SDS, 1mM DTT, 50 units/ml Benzonase
SDS-PAGE running buffer	25mM Tris, 190mM glycine, 0.1% (w/v) SDS
SDS-PAGE transfer buffer	25 mM Tris-HCl, 192 mM glycine, 20% (v/v) methanol
SDS-PAGE transfer buffer (alcohol free)	12.5mM Tris HCl pH 7.4, 200mM glycine
SDS-PAGE transfer buffer (semi-dry)	50 mM Tris base, 40 mM glycine, 0.1% (w/v) SDS, 10% (v/v) methanol
selective defined (SD) medium	0.67% (w/v) yeast nitrogen base without amino acids, 2% (w/v) glucose
SOC	2% tryptone, 0.5% yeast extract, 10 mM NaCl, 2.5 mM KCl, 10 mM MgCl ₂ , 10 mM MgSO ₄ , and 20 mM glucose
TAE buffer	40mM Tris, 1mM EDTA
TBST	20 mM Tris-HCl, pH 7.5, 137 mM NaCl, 0.1% (v/v) Tween-20
TE buffer	1 M Tris pH 8.0, 100 mM EDTA
TST	50mM Tris Hcl pH7.6, 150mM NaCl, 0.05% (v/v) Tween-20
Yeast lysate binding buffer	40mM HEPES pH7.4 KOH, 150mM KCl, 1mM DTT, 1 mM EDTA 0.5% Triton X 100

2.1.3 Plasmids

Table 2-1: Plasmids used in this study.

Plasmid	Description	Source	Reference
pGEX-GST	<i>E. coli</i> expression plasmid encoding GST	Dr. Richard Scheller (Stanford, CA).	(Brandie et al. 2008)
pGEX-GST-VAMP1	<i>E. coli</i> expression plasmid encoding GST tagged truncated VAMP1 residues 1-97	Dr. Richard Scheller (Stanford, CA).	(Martin et al. 1998)
pGEX-GST-VAMP2	<i>E. coli</i> expression plasmid encoding GST tagged truncated VAMP2, residues 1-94	Dr. Richard Scheller (Stanford, CA).	
pGEX-GST-VAMP3	<i>E. coli</i> expression plasmid encoding GST tagged truncated of VAMP3 residues 1-81	Dr. Richard Scheller (Stanford, CA).	(Martin et al. 1998)
pGEX-GST-VAMP4	<i>E. coli</i> expression plasmid encoding GST tagged truncated human VAMP4 pGEX residues 1-119.	Dr. Andrew Peden (University of Sheffield)	(Brandie et al. 2008)
pGEX-GST-VAMP5	<i>E. coli</i> expression plasmid encoding GST tagged truncated mouse VAMP5, residues 2-69.	Dr. Andrew Peden (University of Sheffield)	
pGEX-GST-VAMP7	<i>E. coli</i> expression plasmid encoding GST tagged truncated rat VAMP7, residues 2-188	Dr. Andrew Peden (University of Sheffield)	(Newell-Litwa et al. 2009)
pGEX-GST-VAMP8	<i>E. coli</i> expression plasmid encoding GST tagged truncated human VAMP8, residues 1-75	Dr. Andrew Peden (University of Sheffield)	(Brandie et al. 2008)
pALA001 (Sx16-PrA)	<i>E. coli</i> expression plasmid encoding C-terminally PrA-tagged Syntaxin 16A, residues 1-269	Alicja Drozdowska	(Struthers et al. 2009)
pCOG022	<i>E. coli</i> expression vector encoding two IgG-binding domains of <i>S. aureus</i> PrA		(Carpp et al. 2006)

2.1.4 Yeast Strains

Table 2-2: Yeast strains used in this study

Yeast Strains	Genotype
9DaΔ45 (LCY008)	<i>MATα</i> , <i>ura3-52 leu2-3 112 his4-519, ade6, gal2, pep4-3, vps45Δ::Kanr</i>
	(Piper et al. 1994; Roccisana 2010)

2.1.5 Bacterial Strains

Table 2-3: Bacterial strains used in this study

Strain	Genotype	Source
BL-21 (DE3)	$F^- omp T hsdSB(rB^- mB^-) gal dcm$ (DE3)	Invitrogen, Life Technologies
DH5 alpha	$F \Phi 80 lacZ \Delta M15 \Delta(lacZYA-argF)U169 recA1 endA1 hsdR17(r_k^-, m_k^+) phoA supE44 thi-1 gyrA96 relA1 \lambda$	Invitrogen, Life Technologies
Top 10	$F-mcrA _ (mrr-hsdRMS-mcrBC) \phi 80 lacZ_M15_ lacX74 nupG recA1 araD139 _ (ara-leu)7697 galE15 galK16 rpsL(StrR) endA1 \lambda$	Invitrogen, Life Technologies
ccdB Survival™ 2T1R	$FmcrA \Delta(mrr-hsdRMS-mcrBC) \Phi 80 lacZ \Delta M15 \Delta lacX74 recA1 ara\Delta 139 \Delta(ara-leu)7697 galU galK rpsL(Str^R) endA1 nupG fhuA::IS2$	Invitrogen, Life Technologies
Stbl3	$FmcrB mrr hsdS20(r_B, m_B) recA13 supE44 ara-14 galK2 lacY1 proA2 rpsL20(Str^R) xyl-5 \lambda leumtl-1$	Invitrogen, Life Technologies

2.1.6 Mammalian Cell Lines

Table 2-4: Mammalian cell lines used in this study

Cell Line	Source
3T3 L1	American Tissue Culture Collection (ATCC)
HeLa	American Tissue Culture Collection (ATCC)

2.1.7 Antibodies

Table 2-5: Antibodies used in this study

Antigen	Working dilution	Description	Supplier
GLUT4	IB: 1:1000; 1% milk PBST	rabbit polyclonal, affinity purified antibody against C terminal 14 amino acids of GLUT4	Synaptic Systems (235 003)
Synaptobrevin 1 (VAMP1)	IB: 1:10 000; 1% milk PBST	rabbit polyclonal, antiserum	Synaptic Systems (104 002)
Synaptobrevin 2 (VAMP2)	IB: 1:250/4µl/ml; 1% milk PBST	rabbit polyclonal, antiserum	Synaptic Systems (104 202)
cellubrevin (VAMP3)	IB: 1:1000/1µl/ml; 1% milk PBST	rabbit polyclonal affinity purified	Synaptic Systems (104 103)
VAMP4	IB: 1:8000/0.125µl/ml; 1% milk PBST	rabbit polyclonal, antiserum	Synaptic Systems (136 002)
myobrevin (VAMP5)	IB: 1:1000/1µl/ml; 1% milk PBST	rabbit polyclonal affinity purified	Synaptic Systems (176 003)
VAMP7	IB: 1:5000/0.2µl/ml; 1% milk PBST	rabbit polyclonal affinity purified	Synaptic Systems (232 003)
endobrevin (VAMP8)	IB: 1:5000/0.2µl/ml; 1% milk PBST	rabbit polyclonal antiserum	Synaptic Systems (104 302)
GAPDH	IB: 1:80,000	mouse monoclonal, (clone 6C5) against GAPDH, affinity purified	Ambion (AM4 300)
IRAP	IB: 1:1000/1µl/ml; 1% milk TBST	mouse polyclonal, affinity purified	Cell Signalling (3808)

IRAP	IB: 1:1000/1 μ l/ml; 1% milk PBST	rabbit polyclonal, antiserum	Kind gift from Prof. Paul F Pilch (Boston University)
Syntaxin 4	IB: 1:2500; 1% milk PBST	rabbit polyclonal, antiserum raised against the cystolic domain of rat syntaxin 4.	Synaptic Systems (110 042)
Syntaxin 16	IB: 1:1000; 1% milk PBST	rabbit polyclonal, antiserum	Synaptic Systems (110 162)
Human transferrin receptor	IB: 1:1000/1 μ l/ml; 1% milk in PBST	mouse monoclonal, affinity purified	Life Technologies (13-6800)
HA 11	IF: 1:500/2 μ l/ml in PBS/Glycine/BSA IB: 1:100 1% milk	mouse monoclonal (clone 16B12), affinity purified	Covance Research Products (MMS 101P)
Calnexin	IB: 1:2000/0.5/ml; 1% milk in PBST	rabbit polyclonal, antiserum	Sigma (C4731)
VPS45	IB: 1:1000/1 μ l/ml; 1% milk in PBST	rabbit polyclonal, antiserum	Synaptic Systems (137 002)
Donkey anti rabbit HRP linked	1:3000, 1% milk PBST	HRP conjugated secondary antibodies against rabbit IgG from donkey	GE Healthcare (RPN1004)
Sheep anti mouse HRP linked	1:2000, 1% milk PBST	HRP conjugated secondary antibodies against mouse IgG from sheep	GE Healthcare (NA931)
Donkey anti rabbit 800	1:10 000 in LI-COR blocking buffer 1:1 PBST	infrared dye-labeled secondary antibodies against rabbit IgG from donkey	LICOR Biosciences (926-32213)
Donkey anti mouse 680	1:10 000 in LI-COR blocking buffer 1:1 PBST	infrared dye-labeled secondary antibodies against mouse IgG from donkey	LICOR Biosciences (26-68072)
Goat anti mouse AlexaFluor 647	IF: 1:200	AlexaFluor 647 conjugated anti mouse IgG from goat	Life Technologies (A-11001)

2.2 Molecular Biology Methods

2.2.1 Plasmid DNA purification

Cultures were inoculated from single colonies and grown overnight with shaking in 10 ml 2YT (1.6% (w/v) tryptone, 1.0% (w/v) yeast extract, 0.5% (w/v) NaCl) containing appropriate antibiotic (usually 100µg/ml ampicillin or 50µg/ml G418). Plasmid DNA was isolated using the Promega Wizard® Plus SV Mini Prep system according to the manufacturer's instructions. Plasmid DNA was digested with restriction endonucleases where required and analysed using agarose gel electrophoresis.

2.2.2 Agarose gel electrophoresis

Agarose gels were made up of between 1% and 1.5% agarose (w/v) in TAE buffer (40mM Tris, 1mM EDTA) stained with 0.5µg/ml ethidium bromide. Gels were run in TAE buffer at a constant voltage of 70V. Samples were mixed with New England BioLabs 6x DNA loading buffer. 10µl of each sample was run alongside 5µl of New England BioLabs Quick-Load 1Kb DNA Ladder. DNA fragments were extracted from agarose gels using the QIAquick gel extraction kit (Qiagen) according to the manufacturer's instructions.

2.2.3 Digestion using restriction endonucleases

DNA was incubated with the appropriate restriction endonucleases according to manufacturers' recommendations for between 1 and 4 hours in a final volume of 20µl - 30µl. 1 unit of enzyme was used per µg of DNA, and unless otherwise stated 1µg DNA was digested. When plasmids required digesting at two sites two restriction enzymes were used. Under these conditions the buffer used was compatible with least stable restriction enzyme.

2.2.4 Transformation of plasmid into bacterial cells

Commercially available competent bacterial cells were thawed on ice. Once thawed, 50µl of competent bacterial cells was added to 2µl of mini-prep DNA and incubated on ice for 1 hour. Cells were heat shocked for 45 seconds at 42°C.

300µl SOC media was added and cells were incubated for 1 hour at 37°C. 100µl of this culture was then plated onto pre-warmed 2YT bacto-agar plates containing the appropriate antibiotic and incubated for 16 hours at 37°C.

2.3 Protein Methods

2.3.1 Purification of recombinant fusion proteins from *E.coli*

Fusion proteins were expressed in *E. coli* BL-21 (DE-3) cells. 10 ml of 2YT containing the appropriate antibiotic (100µg/ml ampicillin or 50 µg/ml G418) was inoculated using a single colony of the appropriate transformant and incubated at 37°C for 16 hours with shaking (230 rpm). The 10ml culture was used to inoculate a 1L culture which was grown until $OD_{600} = 0.6$. Protein expression was induced with 0.5mM IPTG for 16 hours at 22°C with shaking. Cells were harvested by centrifugation and resuspended in 200mls PBS containing protease inhibitors (1 tablet EDTA-Free Protease Cocktail Inhibitor/50 ml volume of PBS: 140 mM NaCl, 3 mM KCl, 1.5 mM KH_2PO_4 , 8 mM Na_2HPO_4).

Homogenisation was achieved by passing the suspension through a Microfluidizer M-110P cell disrupter set to 20,000 psi and treating cells with lysozyme (1 mg/ml) on ice for 30 minutes. A cleared lysate was produced by centrifugation at 22,500 x g at 4°C for 30 minutes.

2.3.2 GST tagged proteins

For purification of GST tagged proteins, the cleared lysate was incubated with glutathione-Sepharose beads (GE Healthcare Bio-Sciences Ltd) with rotation at 4°C overnight (approximately 1ml glutathione-Sepharose bead slurry (50% (v/v) bead bed volume) was used per 1L original culture). Prior to use, glutathione-Sepharose beads were equilibrated by 6 washes with PBS. Immobilised proteins and beads were washed three times with ice cold PBS to remove non-specifically bound proteins. Samples of the unbound material and washes were collected and analysed by SDS-PAGE. Bound protein was then eluted with 1mM reduced glutathione solution in 50mM Tris base, pH8. Beads were incubated with elution buffer for 30 min and eluted protein was collected. This process was repeated 3 times, a sample of each elute was collected and analysed by SDS-PAGE. Elutes were then pooled and dialysed overnight in Float-a-Lyzer columns with 20kDa pores against 4L PBS.

2.3.3 Protein A tagged proteins

For purification of Protein A tagged proteins, the cleared lysate was incubated with IgG Sepharose™ 6 Fast Flow (GE Healthcare Bio-Sciences Ltd) with rotation at 4°C overnight (approximately 1ml IgG bead slurry (50% (v/v) bead bed volume) per 1L original culture). Prior to use IgG beads were equilibrated by 4 washes with TST (50 mM Tris-HCl, pH 7.6, 150 mM NaCl, 0.05% (v/v) Tween-20), followed by 4 washes alternating between TST and 0.5M acetic acid pH5. Immobilised proteins and beads were washed 5 times with TST and once with 5mM ammonium acetate pH5. Protein was then eluted using 0.5 M acetic acid, pH 3.4. This process was repeated 3 times, a sample of each elute was collected and analysed by SDS-PAGE. Elutes were then pooled and protein was then dialysed overnight in Float-a-Lyzer columns with 5kDa pores against 4L of PBS.

2.3.4 SDS-Polyacrylamide gel electrophoresis

SDS-Polyacrylamide gel electrophoresis (SDS-PAGE) was used to resolve proteins. A 30% (w/v) acrylamide/bisacrylamide mix was used to make stacking and resolving gels. The stacking gel was made up of 5% acrylamide, 0.37M Tris HCl pH 6.8, 0.1% (w/v) SDS. The resolving gel was made up of between 7.5% and 15% acrylamide and 0.37M Tris HCl pH 8.8, 0.1% (w/v) SDS both stacking and resolving gels were polymerised with 8mM ammonium persulfate (APS) and 200nM tetramethylethylenediamine (TEMED). The gels were cast using BioRad mini-Protean III apparatus. Samples were thawed on ice and combined with 2 x Laemmli sample buffer (LSB; 100mM Tris, HCl pH 6.8, 4% (w/v) SDS, 20% (v/v) glycerol, 0.2% (w/v) bromophenol blue, 10% (v/v) β-mercaptoethanol), then heated at 95°C for 5 minutes, or 65°C for 10 minutes when using samples to blot for GLUT4. Samples were then cooled, subject to brief centrifugation to pellet condensation and loaded into gel wells. Samples were run alongside BioRad Precision Plus Protein Standards All Blue Markers. Gels were run in SDS-PAGE running buffer (25mM Tris, 190mM glycine, 0.1% (w/v) SDS) at 70V through both the stacking and resolving gels.

2.3.5 Coomassie staining

Proteins separated by SDS PAGE were visualised through Coomassie staining. Resolved gels were stained with Coomassie Brilliant Blue R-250 (0.25% (w/v), 45

% (v/v) methanol, 10% acetic acid (v/v)) for 1 hour and de-stained in Coomassie destain (15% methanol, 15% acetic acid) solution overnight, or until fully de-stained.

2.3.6 Immunoblotting

For antibody staining, proteins were transferred to nitrocellulose membrane (BioTrace™, pore size 0.2µm). Protein samples were resolved by SDS-PAGE as described above. For semi-dry transfers, gels, membranes and filter papers were soaked in semi-dry transfer buffer (50 mM Tris base, 40 mM glycine, 0.1% (w/v) SDS, 10% (v/v) methanol). The membrane and gel were sandwiched between 6 sheets of 3mm filter paper on BioRad Trans-Blot® SD semi-dry electrophoretic transfer cell and air bubbles were gently removed. Transfer was completed by applying a constant current of 180mA for between 40 and 80 minutes depending on the number, thickness and percentage of gels being transferred.

For wet transfers the membrane gel and filter papers were soaked in SDS-PAGE transfer buffer (25 mM Tris-HCl, 192 mM glycine, 20% (v/v) methanol). Membrane and gel were sandwiched between 6 sheets of filter paper and 2 transfer sponges, soaked in transfer buffer then housed in BioRad mini Protean III trans-blot system transfer cassettes. The cassette was immersed in transfer buffer and transfer was achieved by applying a constant current of 200mA for 2 hours.

Wet transfer in alcohol free transfer buffer was performed as described above using an alcohol free transfer buffer (12.5mM Tris HCl pH 7.4, 200mM glycine).

Following transfer, nitrocellulose membranes were stained with Ponceau S solution (0.1% (w/v) Ponceau S, 5% (v/v) acetic acid) to assess transfer efficiency. Membranes were blocked for 45 minutes in either 1% or 5% (w/v) milk made up in either PBST (85 mM NaCl, 1.7 mM KCl, 5 mM Na₂HPO₄, 0.9 mM KH₂PO₄, 0.1% (v/v) Tween-20) or TBST (20 mM Tris-HCl, pH 7.5, 137 mM NaCl, 0.1% (v/v) Tween-20) depending on the antibody (see Table 2-5). Primary antibodies were diluted to desired concentrations in 1% or 5% milk PBST/TBST as required (see Table 2-5) and applied to membranes for 16 hours at 4°C with rotation. Membranes were then washed three times for 10 minutes in either

PBST or TBST. The secondary antibody was applied for one hour at room temperature with rotation. Membranes were washed a further three times, twice in PBST/TBST and once in PBS/TBS and blots were visualised using enhanced chemiluminescence (ECL) or infra-red imaging (LICOR). For ECL, the secondary antibodies were horseradish peroxidase (HRP) linked, (GE Healthcare Bio-Sciences Ltd) and for infrared imaging secondary antibodies were labelled with infrared dye (LI-COR Biosciences Ltd). To minimise bleaching of the image signal when using the LICOR system secondary antibodies and subsequent wash steps were all completed under dark conditions.

For ECL detection, ECL was applied to the membranes for 10 seconds, the excess removed, and membranes were exposed to X-ray film in a light proof cassette, and developed in a Kodak x-omat 2000. For infrared imaging membranes were imaged using the Odyssey Infrared Imaging System (LI-COR Biosciences).

2.3.7 Estimation of protein concentrations

2.3.7.1 Tagged proteins

Purified protein samples were thawed on ice. Once thawed samples were diluted in dH₂O as necessary to bring them to a concentration between 0.1- 2mg/ml. Samples were then diluted 1:2 in 2 x Laemmli Sample Buffer (LSB) and run on 15% SDS-PAGE gels alongside BSA standards (0.1 µg, 0.2 µg, 0.4 µg, 1µg, 2µg). Gels were stained with Coomassie for 1 hour and destain (15% (v/v) methanol, 15% (v/v) acetic acid) was applied for 16 hours with agitation at room temperature. Protein concentrations were estimated with the aid of densitometry using Image J software.

2.3.7.2 Micro BCA

Total protein content of 3T3 membrane fractions and lysates was determined in a 96 well plate using Pierce Micro BCA solutions. Increasing concentrations of BSA (0 to 12µg) were added into the first two rows of a 96 well plate and 1µl of sample was added into the remaining wells, dH₂O was added to all rows to adjust the volume to 100µl. Finally 100µl microBCA solution was added (50% (v/v) of Solution A (Proprietary alkaline tartrate-carbonate solution), 48% (v/v) of Solution B (Proprietary bicinchonic acid solution) and 2% (v/v) of Solution C

(Proprietary copper sulphate solution)) to each well. Samples were incubated at 37°C for 30 minutes and absorbance at 570nm was measured using Flmorostar Optima plate reader (BMG LabTech, Aylesbury, UK).

2.3.7.3 GST and Protein A pull-down assays with yeast lysate

400ml cultures of yeast lacking endogenous Vps45p, but expressing mVps45 were grown to $OD_{600} = 0.6$. Cells were harvested by centrifugation and washed in $1/50^{\text{th}}$ the volume of binding buffer (40mM HEPES pH7.4 KOH, 150mM KCl, 1mM DTT, 1 mM EDTA 0.5% Triton X 100). Cells were then resuspended in $1/100^{\text{th}}$ their original volume of binding buffer. Cells were homogenised by vortexing with glass beads (Sigma, 425-600 μ). Cells were vortexed for 30 seconds and rested on ice for 60 seconds, this was repeated 4 times. A sample of lysate was retained for analysis. 5 μ g recombinant protein was immobilised to 20 μ l of appropriate beads (50% bead slurry in PBS). Prior to this beads were equilibrated as described in Sections 2.3.1-2.3.3. Recombinant protein was immobilised to beads for 2 hours at room temperature, unbound protein was removed, and beads were washed three times in PBS. 200 μ l yeast lysate was added and the solution was made up to 1ml with binding buffer. The lysate was incubated with the immobilised protein for 16 hours at 4°C with rotation. Unbound proteins were washed from the beads by four washes with PBS (for glutathione Sepharose beads) or TST (for IgG Sepharose 6 Fast Flow beads) and bound protein was eluted with 2xLSB. Samples were subjected to SDS-PAGE and immunoblot analysis.

2.3.7.4 GST pull-down assays with recombinant protein

0.1 μ g - 0.5 μ g recombinant GST-VAMP protein or GST alone was immobilised to 20 μ l equilibrated glutathione-Sepharose beads (50% bead slurry) in a total volume of 100 μ l for 2 hours at 4°C. Beads were washed 3 times in PBS to remove any unbound protein. A sample of GST-VAMPs bound to beads was retained for analysis. Bound proteins were then incubated with a 10 fold excess of recombinant, thrombin cleaved syntaxin 16 or syntaxin 4 in binding buffer. Binding buffer was made up of PBS, 5mM β -mercaptoethanol, and supplemented with 100 μ g/ml BSA. GST-VAMPs and syntaxin were incubated for 0, 10, 30, 60, 120 minutes or overnight in a total volume of 100 μ l, at 4°C. Following incubation

unbound protein was retained and bound protein washed 3 times. A variety of washing steps were employed to abolish non-specific binding, these included PBS alone, PBST, PBS supplemented with 100µg/ml BSA, PBS + 5% gelatin, and PBS + 5% glycerol. Bound proteins were eluted by addition of 20 µl 2xLSB. Samples were subjected to SDS-PAGE and immunoblotting for protein detection.

2.3.7.5 SNARE complex assembly assay (CAA)

Equimolar (approximately 4µM) amounts of GST tagged VAMP protein (or GST alone), His tagged SNAP23 and thrombin cleaved syntaxin 4 or 16 were combined in a volume of 500µl PBS supplemented with 100µg/ml BSA and incubated for 2 hours at 4°C with rotation. Reactions were stopped by the addition of the appropriate volume of 5xLSB and immediately heated to 95°C for 5 minutes. For measurement of SNARE complex assembly at 0 minutes the tSNARE complex was combined with the appropriate volume of 5xLSB and heated to 95°C prior to the addition of the vSNARE, the entire mixture was then heated to 95°C for 5 minutes. Samples were subjected to SDS-PAGE and immunoblot analysis on the same day as the experiment.

2.4 Cell Culture Methods

2.4.1 Yeast cell culture

Yeast were grown in selective defined (SD) medium (0.67% (w/v) yeast nitrogen base without amino acids, 2% (w/v) glucose) supplemented with the appropriate amino acids (Sherman 1991).

2.4.2 Mammalian cell culture

2.4.2.1 Growth of 3T3 L1 adipocytes

3T3 L1 murine adipocytes were purchased from ATCC (USA), cells expressing HA-GLUT4-GFP were previously made within the lab. Cells were cultured in DMEM (Dulbecco's Modified Eagle's Medium), 10% (v/v) Newborn Calf Serum (NCS), 1% (v/v) Penicillin (10,000 U)/Streptomycin (10,000 U) (P/S). Cells were incubated at 37°C in a humid atmosphere of 10% CO₂. Media was changed every other day until cells were ready for splitting or differentiation.

2.4.2.2 Passage of 3T3 L1 adipocytes

Cells were split at 70% Confluence, and were not used past passage 12. Media was aspirated and cells washed in 5ml pre-warmed, sterile PBS, 5ml 0.05% trypsin (Invitrogen) was added. Cells were incubated at 37°C for 5 minutes or until the cells had detached from the bottom of the flask. The desired volume of growth medium was added and the cell suspension was mixed. 10ml of the cell suspension was added to each 10cm plate, 15ml to each 75cm² flask, 1ml to each well of a 12 well plate, 500 µl to each well of a 24 well plate. Media was changed every other day until differentiation was initiated.

For seeding onto glass coverslips, coverslips were sterilised by dipping 3 times in ethanol, placed onto the side of a well and left to air dry in a cell culture hood for 1 hour, then exposed to UV light for 2 hours. Before seeding cells onto coverslips, the coverslips were washed twice in growth media to remove any residual ethanol. Between 0.5ml and 2ml of cell suspension was added to each well. Cells were cultured as described.

2.4.2.3 Differentiation of 3T3 L1 adipocytes

Differentiation was initiated 2 days post confluence, differentiation media was made up of DMEM supplemented with 10% (v/v) FCS (Fetal Calf Serum), 1% (v/v) Penicillin/Streptomycin (P/S), 0.5 mM 3-isobutyl-1-methylxanthine (IBMX), 1 µM insulin, 0.25 µM dexamethasone, and 1nM troglitazone. 3 days after differentiation media was changed for DMEM supplemented with 10% (v/v) FCS, 1% (v/v) P/S, 1 µg/ml insulin and 1nM troglitazone which was left on cells for a further 3 days. On day 6 post differentiation media was replaced with DMEM supplemented with 10% (v/v) FCS, 1% (v/v) P/S, this process was repeated every other day until day 8-12 post differentiation.

2.4.2.4 Freezing of 3T3 L1 adipocytes

Cells were frozen down at 70% confluence in freeze down media (Foetal Calf Serum US supplemented with 10% (v/v) DMSO) and stored in liquid nitrogen until use. Cells were trypsinised as for passaging, 12ml growth media was added and cells were pelleted by centrifugation at 500 x g for 5 minutes. The resulting pellet was re-suspended in freeze down media (1ml per flask). Cells were

transferred to 1.8ml cyro-vials on ice, and stored in Nalgene “Mr Frosty” containing isopropanol for 16 hours at -80°C . They were then transferred to liquid nitrogen for long term storage.

2.4.2.5 Resurrection of cells

Cells were removed from liquid nitrogen and thawed in a water bath at 37°C . Cells were added to 15ml pre-warmed growth media in a 75cm^2 flask, 24 hours later growth media was replaced to remove DMSO.

2.4.2.6 Growth of HeLa cells

Human cervical carcinoma HeLa cells were purchased from ATCC (USA), HeLa cells expressing HA-GLUT4-GFP have been previously generated within the lab. Cells were cultured in DMEM (Dulbecco’s Modified Eagle’s Medium), 10% (v/v) Foetal Calf Serum (FCS), 1% Glutamine (v/v) 1% (v/v) Penicillin (10,000 U)/Streptomycin (10,000 U) (P/S). Cells were incubated at 37°C in a humid atmosphere of 5% CO_2 . Media was changed every other day until cells were ready for splitting or use.

2.4.2.7 Passage of HeLa cells

Cells were split when at 70% Confluence. Media was aspirated and cells washed in 5ml pre-warmed, sterile PBS, then 5ml 0.05% (w/v) trypsin (Invitrogen) was added. Cells were incubated at 37°C for 5 minutes or until the cells had detached from the bottom of the flask. The desired volume of growth medium was added and the cell suspension was mixed. 10ml of the cell suspension was added to each 10cm plate, 15ml to each 75cm^2 flask, 2ml to each well of a 6 well plate, 1ml to each well of a 12 well plate, 500 μl to each well of a 24 well plate. Media was changed every other day until cells were ready for use. HeLa cells were passaged onto glass coverslips as described for 3T3 L1 adipocytes as described in section 2.4.2.1.

2.4.2.8 Transfection of HeLa cells with plasmid DNA

HeLa cells were cultured on glass coverslips as described (section 2.4.2.2). Cells were transfected with plasmid DNA using Lipofectamine™ 2000 according to manufacturer’s instructions. Briefly, for one well of a 24 well plate, 0.8 μg DNA

was combined with 50µl of Opti-MEM® reduced serum medium. 2 µl Lipofectamine™ 2000 was diluted in 50µl Opti-MEM® and mixed. These solutions were incubated separately for 5 minutes at room temperature. The diluted DNA and Lipofectamine™ 2000 were then combined and incubated for 20 minutes at room temperature. The desired volume of antibiotic free HeLa growth media was added to give the desired concentration of DNA (0. 8µg per well) and 125µl was added to each well of a 24 well plate. Cells were processed 24-72 hours later.

2.5 Production of HeLa cell lysates

HeLa cells were washed 3 times in ice cold PBS and scraped in 100µl RIPA buffer (50mM Tris, HCl pH8, 150mM NaCl, 2mM MgCl₂, 1% Triton, 0.5% sodium deoxycholate (w/v), 0.1% (w/v) SDS, 1mM DTT, 50 units/ml Benzonase) containing EDTA free protease inhibitor cocktail (Roche). Samples were homogenised by passage through a 26 ½ gauge needle 10 times. Samples were rested on ice for 20 minutes and then this process was repeated. Homogenates were centrifuged at 12470 x g for 20 minutes at 4°C to pellet any insoluble material. Lysates were stored at -20°C until use.

2.6 Protein depletion in cell culture

2.6.1 siRNA treatment of HeLa cells

HeLa cells expressing HA-GLUT4-GFP have been previously made in the lab using a HA-GLUT4-GFP construct provided by Cynthia Mastick (University of Nevada). Cells were grown in 6 well plates with two wells containing 13mm sterile glass coverslips as described above. HeLa cells were transfected with SMARTpool siRNA against VAMP2, 3, or 8 (GE Healthcare Ltd) at 70% confluence. All treatments were carried out under conditions to minimize potential contact with nucleases and in a fume hood. siRNA was diluted to 200nM with Opti-MEM® in a volume of 100µl, 2µl DharmaFECT 4 was diluted in 100µl Opti-MEM® and left to equilibrate at room temperature for 5 minutes. The two diluted mixtures were then combined and incubated for 20 minutes at room temperature to allow the formation of siRNA-transfection reagent complexes. The solution was made up to the desired volume in antibiotic free HeLa growth media and 0.5ml was added

to each well of a 6 well plate. 48 hours later 0.5ml fresh HeLa growth media was added to the cells. Cells were used 68 hours post transfection with siRNA.

2.6.2 Generation of inducible shRNA vector for use in 3T3 L1 adipocytes

2.6.2.1 shRNA Production

shRNA hairpins were designed using RNAi Codex (<http://cancan.cshl.edu/cgi-bin/Codex/Codex.cgi>), the first 18 nucleotides were deleted from the 5' end and the first 16 nucleotides were deleted from the 3' end of the 22mer. The sequence AGCG was added to the 5' end of the sense strand and ACGG was added to the 5' end of the antisense strand. Oligonucleotides were purchased from Sigma-Aldrich. Oligonucleotides were diluted to 50 μ M in TE buffer (1 M Tris pH 8.0, 100 mM EDTA) and stored at -20°C until use. To anneal oligonucleotides, 10 μ l of the sense and antisense strands were mixed with 0.2 μ l 5M NaCl in thinwall PCR tubes. The mixture was heated to 95°C for 5 minutes, transferred to a water bath at 70°C for 10 minutes, the water bath was turned off and oligonucleotides were left to anneal in the water bath overnight.

2.6.2.2 Shuttling oligonucleotides into pEN vector

The pEN_TmiRc2 and pEN_TGmiRc2 vectors were provided by Dr Robert Semple (University of Cambridge). The pEN vector was digested with BfUA1 (New England Biolabs) to remove the toxic ccdB gene. The linearised pEN vector was gel purified using the QIAquick gel extraction kit (Qiagen) according to the manufacturer's instructions. Ligation of the annealed oligonucleotides with the pEN vector was completed using TakaRa rapid Ligation kit. The resulting pEN vector was transformed into commercially available DH5alpha / HB101 cells (Life Technologies). Diagnostic digests of the resultant colonies with BsRG1 (New England Biolabs) were carried out to ensure the shRNA oligonucleotide had been inserted into the pEN vector.

2.6.2.3 Shuttling pEN vector into pSLIK Vector

The pEN vectors were shuttled into pSLIK-Neo destination vectors using Gateway Clonase II (Life Technologies) according to manufacturer's instructions, 100ng of pEN was combined with 150ng of pSLIK destination vector in a volume of 8 μ l, 2 μ l

clonase was added and reaction was incubated at 25°C for 1 hour. 2µg of proteinase K was added and mixture was incubated at 37°C for 10 minutes. 2µl of the mixture was used to transform Sltb3™ cells.

2.7 Subcellular Fractionation Methods

2.7.1 Preparation of total membrane fractions

Adipocytes were used between 8 and 12 days post differentiation, growth media was aspirated off and cells were washed three times in 5mls ice cold HEPES/EDTA/Sucrose (HES) Buffer (250 mM Sucrose, 20 mM HEPES pH 7.4, 1 mM EDTA, supplemented with EDTA-Free Protease Cocktail Inhibitor tablets, 1 tablet per 50ml HES). Cells were then scraped in ice-cold HES and homogenised by passing through a 24 gauge needle 10 times and subsequently twice through a 26 ½ gauge needle. Homogenates were stored at -20°C until use.

Homogenates were centrifuged at 500 x g for 10 minutes at 4°C to pellet nuclei and insoluble material. Supernatants were transferred into fresh TLA110 ultracentrifuge tubes (Beckman Coulter) and centrifuged at 95, 000 x g for 1 hour to pellet all membranes. The pellet, which is the membrane fraction, was resuspended in 100 µl HES buffer per 10cm plate (approximately 10⁶ cells). Samples were stored at -20°C until use. Protein content of membrane fractions was determined by micro BCA as described in section 2.3.7.2.

2.7.2 Preparation of subcellular fractions

Subcellular fractions of 3T3 L1 adipocytes were obtained as described (Piper et al. 1991). 3T3 L1 adipocytes were used between day 8 and 10 post differentiation. Twelve 10cm plates were used for each subcellular fractionation, cells were serum starved for 2 hours and half the plates were treated with 1µM insulin for the last 30 minutes. Cells were washed, scraped and homogenised as described in section 2.7.1. Homogenates were centrifuged at 10,000 x g for 20 minutes at 4°C to pellet the nuclei, mitochondria and the plasma membrane (PM). The pellet was resuspended in 1ml HES buffer, layered on to a high sucrose HES cushion (1.12M sucrose in HES buffer) and centrifuged at 41,000 x g in swing out rota (TLS55, Beckman Coulter) for 60 minutes at 4°C. The layer containing the plasma membrane fraction was collected, resuspended

in 5ml HES and centrifuged at 140,000 x g in for 60 minutes to pellet the PM fraction which was resuspended in 150 μ l of 1 x LSB. The supernatant from the original spin was centrifuged at 12,500 x g for 20 minutes at 4°C to pellet the high density membrane fraction (HDM), which was resuspended in 150 μ l of 1 x LSB. The supernatant of the 12,500 x g spin was centrifuged at 140,000 x g for 60 minutes to pellet the light density membrane fraction (LDM), which was resuspended in 150 μ l 1 x LSB. The soluble protein was recovered from the supernatant by TCA precipitation and was resuspended in 150 μ l 1 x LSB. Fractions were stored at - 20°C until use. A schematic representation of the subcellular fractionation procedure is displayed in Figure 2-1.

2.7.3 Preparation of iodixanol gradients

In order to further separate out the LDM fraction Iodixanol gradient experiments were carried out (Hashiramoto & James 2000; Perera et al. 2003). LDM fractions were produced as described in section 2.7.2, diluted in HES buffer, mixed with 60% (v/v) Iodixanol to a final concentration of 14% (v/v) and heat-sealed into Beckmann Quick Seal polyallomer tubes. Tubes were inverted three times to mix, and secured into a pre-chilled Beckmann TLN 100 Rotor and centrifuged at 295,000 x g for 1 hr at 4°C. Fractions were collected by first piercing the top then piercing the bottom of the tubes to dislodge the air lock in the sealed tubes. 300 μ l fractions were dripped out of the bottom of the tubes, collected and mixed with 4 x LSB. Samples were analysed by immunoblotting.

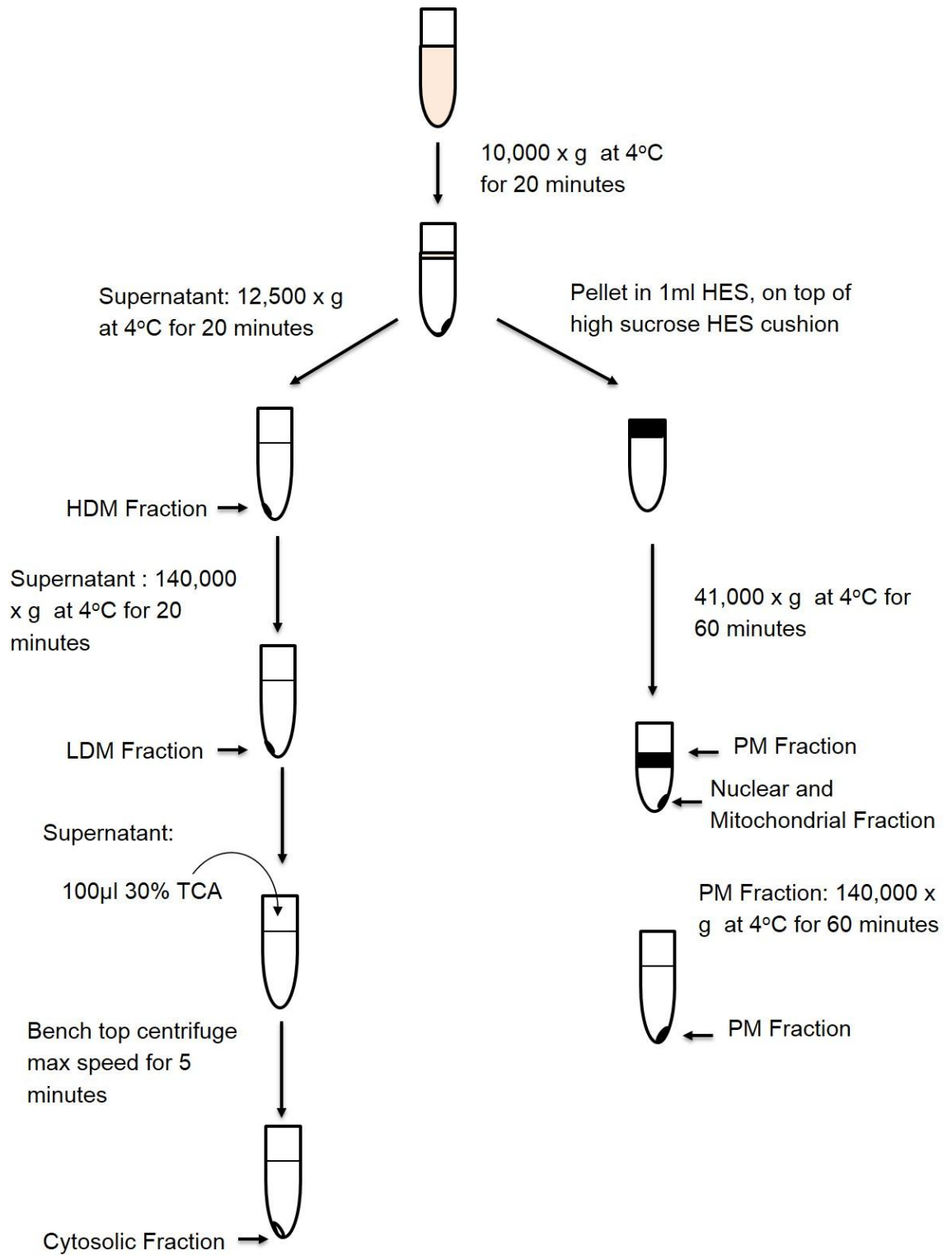


Figure 2-1: Flow chart displaying the subcellular fractionation procedure of 3T3 L1 adipocytes.

2.8 Immunoprecipitation from 3T3 L1 adipocytes

3T3 L1 adipocytes were grown and differentiated as described, they were used between day 8 and 12 post differentiation. On day of use cells were serum starved for 2 hours, and treated with 1mM NEM or 1mM NEM + 1 μ M insulin for the last 30 minutes. Cells were washed 3 times in ice cold PBS and scraped in immunoprecipitation (IP) buffer (50 mM HEPES pH 7.5, 5 mM EDTA, 10 mM sodium pyrophosphate, 10 mM NaF, 150 mM NaCl, 2 mM β -Glycerophosphate, 1 mM DTT and EDTA-protease inhibitor cocktail tablet) supplemented with 1% (v/v) Triton X-100. Lysates were homogenised by passage through a 26 $\frac{5}{8}$ gauge needle 12 times and then incubated on ice for 30 minutes.

Homogenates were centrifuged at 12,470 x g for 20 min at 4°C to pellet insoluble material; supernatants were decanted into fresh tubes and used for immunoprecipitation. Lysates were pre cleared by incubation with 40 μ l protein A beads (50% slurry) for 1 hour at 4°C. Protein A beads were equilibrated by 4 washes with IP buffer prior to use.

1.5mg of lysate was combined with 5 μ l (approximately 50 μ g) antibody (syntaxin 16 antibody, syntaxin 4 antibody or random rabbit IgG) in a volume of 500 μ l for 2 hours on ice. Samples were briefly vortexed every 30 minutes to ensure the antibody and lysates were adequately mixed. 20 μ l of Protein A beads (50% slurry) were then added to the lysate and antibody and incubated for 2 hours at 4°C. Samples were then centrifuged at 12,470 x g for 1 minute at 4°C, the supernatant (unbound material) were transferred to fresh tubes and retained for analysis. The pellet washed 3 times in 1ml IP buffer supplemented with 1% (v/v) Triton X-100, then once in IP buffer containing 0.1% (v/v) Triton. The final pellet was resuspended in 20 μ l 2XLSB, boiled at 95°C for 5 min and then stored at -20°C. Samples were subjected to SDS-PAGE and immunoblotting for protein detection.

2.9 Indirect immunofluorescence

3T3 L1 adipocytes or HeLa cells were seeded onto sterilised 13mm glass coverslips in 24-well plates as described. 3T3 L1 Cells were used between day 8

and 12 post differentiation, HeLa cells were used once confluent. Cells were washed in DMEM and serum starved for 2 hours before being treated with or without 1 μ M insulin for 20 minutes. Cells were washed 3 times in 1ml ice cold PBS and fixed in 200 μ l 3% (w/v) paraformaldehyde (PFA) for 20 minutes. Cells were washed three times in PBS supplemented with 20mM glycine to quench the PFA and blocked for 20minutes in PBS supplemented with glycine, 1mg/ml BSA and 5% (v/v) goat serum (Sigma) (PBS/glycine/BSA + goat serum). Primary antibody was then applied for 45 minutes, antibodies were diluted to the appropriate concentrations in PBS/glycine/BSA (Table 2-5). Cells were washed four times in PBS/glycine/BSA and Alexa-Fluor conjugated secondary antibody was applied for 30 minutes. Cells were washed a further four times with the final wash in PBS. For nuclear staining the third wash contained DAPI stain (4',6-diamidino-2-phenylindole, v/v 1:10 000). Coverslips were mounted onto glass slides face down using ImmunoMount and left overnight in the dark to dry. Coverslips were imaged using the 63 x oil-immersion objective lens fitted to a Zeiss LSM Pascal Exciter confocal microscope, images were captured and processed using Zeiss LSM software

Chapter 3 - Interactions between the tSNARE complex syntaxin 4/SNAP23 and VAMP proteins.

3.1 Introduction

3.1.1 SNARE complex involvement in GLUT4 fusion with the plasma membrane

The insertion of GLUT4 into the plasma membrane requires vesicles carrying GLUT4 to fuse with the plasma membrane. This is an example of a membrane fusion event and as such is reliant on SNARE complexes. The tSNAREs required for this process have been identified as syntaxin 4 and SNAP23. It has been shown that preventing syntaxin 4 or SNAP23 function or depleting syntaxin 4 or SNAP23 inhibits insulin-stimulated GLUT4 insertion to the plasma membrane (Olson et al. 1997; Rea et al. 1998; Foster et al. 1999; Kawaguchi et al. 2010).

However, the vSNARE requirements for GLUT4 vesicle fusion with the plasma membrane are less clear. Many studies have identified VAMP2 as playing an important role in the fusion of insulin-sensitive GSVs with the plasma membrane. This research has primarily utilised loss of function models. VAMP2 function has been impaired through the introduction of toxins to cleave VAMPs 2 and 3, competitive inhibition (injection of VAMP2 peptides and cytoplasmic domain of VAMP2) or through RNAi interference (Cheatham et al. 1996; Martin et al. 1998; Williams & Pessin 2008; Kawaguchi et al. 2010). All of these studies support a role for VAMP2 in insulin-stimulated GLUT4 translocation. However, some studies have noted that removal of VAMP2 and 3 does not completely inhibit the fusion of GLUT4 containing vesicles with the plasma membrane (Hajduch et al. 1997; Zhao et al. 2009). Hajduch et al. (1997) found that cleavage of VAMPs 2 and 3 with Tetanus neurotoxin (TeNT) did not impair insulin-stimulated glucose uptake or mobilisation of GLUT4 from intracellular deposits to the plasma membrane (Hajduch et al. 1997). Zhao et al. (2009) found that insulin-stimulated GLUT4 translocation and glucose uptake were only impaired when VAMPs 2, 3 and 8 were simultaneously depleted. In this study glucose uptake was not impaired in adipocytes derived from embryonic fibroblasts from VAMP2 knockout mice, or in 3T3 L1 adipocytes treated with TeNT, which cleaves both VAMP2 and VAMP3. GLUT4 translocation was only impaired when TeNT treatment was applied to adipocytes lacking VAMP8. These data suggest that there is some degree of plasticity or redundancy in the vSNARE requirements for GSV fusion with the plasma membrane. Discrepancy in these results could be due to a

number of factors. This includes incomplete and differing effects of siRNA, and the length of time cells were treated with TeNT. Variations in methodology and treatment, as well as differences in the cell type studied may lead to differences in the conclusions drawn on compensatory mechanisms and pathways.

Other factors, as well as insulin, stimulate the translocation of GLUT4 to the cell surface. Two of these stimuli are osmotic shock and GTP γ S (Chen et al. 1997; Millar et al. 1999; Williams & Pessin 2008). While these stimuli result in insulin like recruitment of GLUT4 to the plasma membrane, they seem to recruit GLUT4 from a different pool (or different pools) than insulin. GLUT4 translocation in response to both osmotic shock and GTP γ S is independent of VAMP2. GLUT4 translocation in response to osmotic shock is dependent on VAMP7 and translocation in response to GTP γ S is dependent on VAMP3 (Millar et al. 1999; Williams & Pessin 2008). Both VAMP3 and VAMP7 have been implicated in the recycling of cargo through the endosomal system (Galli et al. 1994; Galli et al. 1998). In order to examine the role of the endosomal system in GLUT4 translocation in response to different stimuli Millar et al. (1999) abolished the endosomal pool by incubating cells with HRP conjugated transferrin. They then ablated any pools that contained HRP by treating cells with diaminobenzidine (DAB) and hydrogen peroxide. They found that ablation of the endosomal system inhibited insulin-stimulated GLUT4 translocation by 30%. In contrast, endosomal ablation reduced GTP γ S-stimulated GLUT4 translocation by 80% (Millar et al. 1999). The contribution the endosomal pool plays to osmotic shock induced GLUT4 translocation has not been directly tested. However, osmotic shock induced translocation of GLUT4 is depend on VAMP7, an endosomal vSNARE (Galli et al. 1998; Williams & Pessin 2008). Thus, GTP γ S and osmotic shock seem to simulate GLUT4 translocation from the endosomal pool of GLUT4 not from the insulin-sensitive pool.

However, although the recruitment of GLUT4 in response to osmotic shock, GTP γ S and insulin require different vSNAREs, they may all use the same tSNARE. It has been demonstrated that both insulin-stimulated and osmotic shock stimulated insertion of GLUT4 into the plasma membrane is inhibited by the expression of the cytoplasmic portion of syntaxin 4 (Chen et al. 1997).

This research reveals that there are a number of pools from which GLUT4 can be mobilised to the plasma membrane in response to different stimuli. This highlights a possible mechanism behind the plasticity between VAMP2, 3 and 8 in GLUT4 insertion into the plasma membrane. It could be that VAMP2, 3 and 8 are present on different pools of GLUT4 and that the degree of mobilisation from each pool is altered by depletion of certain VAMP isoforms. Alternatively, these vSNAREs could all be present on insulin-sensitive GLUT4, and in the absence of certain VAMPs others compensate in fusion activity. The localisation of each VAMP with insulin-sensitive GLUT4 is examined in Chapter 4. However, irrespective of whether VAMP 2, 3 and 8 are present on different pools of GLUT4 or the same pool of GLUT4, for them to act in the fusion of GLUT4 containing vesicles with the plasma membrane they must be able to form fusiogenic SNARE complexes with tSNAREs. The three vSNAREs may act in the fusion of GLUT4 containing vesicles with the plasma membrane through the same pathway, with the tSNARE SNAP23/syntaxin 4. Alternatively, each VAMP could traffic GLUT4 to the plasma membrane through interactions with different tSNARE complexes. If VAMP2, 3 and 8 traffic GLUT4 to the plasma membrane through the same pathway, then they should all form complexes with syntaxin 4 and SNAP23.

3.1.2 Interactions between syntaxin 4/SNAP23 and VAMPs

Syntaxin 4 has been shown to interact with VAMP2 *in vivo* (Cheatham et al. 1996; Kawanishi et al. 2000). However, this interaction only occurs in the presence of SNAP23 (Kawanishi et al. 2000). Kawanishi et al. (2000) studied protein-protein interactions by co-immunoprecipitation following expression of recombinant syntaxin 4, myc-VAMP2 and HA-SNAP23. Interactions between syntaxin 4 and VAMP2 were only seen in the presence of HA-SNAP23. Conversely, *in vitro* experiments show that recombinant VAMP2 can directly interact with recombinant syntaxin 4 but not recombinant SNAP23 (Kioumourtzoglou et al. 2014). This suggests that *in vivo*, there is inhibition of binary interactions between syntaxin 4 and VAMP2. It also highlights the importance of studying interactions between proteins both *in vitro* and *in vivo*. Interactions between VAMP proteins and the tSNAREs syntaxin 4 or SNAP23 have not been systematically examined either *in vivo* or *in vitro*. However, since the existence of any SNARE protein interactions is governed by the specificity of SNARE complex formation, research examining SNARE complex specificity can provide

insights into possible v and tSNARE interactions. Specificity in SNARE complex formation is discussed below.

The human genome codes for more than 35 different SNARE proteins. These are present in different cellular compartments and participate in different membrane fusion events. For cells to function, the integrity of membrane trafficking events must be maintained. Therefore SNARE protein interactions must be specific. The original SNARE hypothesis proposed that SNARE proteins provided both the energy and the specificity for membrane fusion (McNew et al. 2000). Opposing this theory is the finding that SNARE complexes formed with purified SNARE proteins *in vitro* are promiscuous and rather non-specific (Fasshauer et al. 1999; Yang et al. 1999; Scales et al. 2000). SDS resistant SNARE complexes can form between the tSNARE complex made up of syntaxin 1/SNAP25 and VAMPs 2, 4, 7 or 8. They can also form between tSNARE complexes made up of either syntaxin 2, 3 or 4, and SNAP25 and the vSNARE VAMP2 (Fasshauer et al. 1999; Scales et al. 2000).

Despite the promiscuity of SNARE complex formation *in vitro*, Scales et al. (2000) found that SNARE proteins participate selectively in fusion events *in vivo*. They demonstrated that the cytoplasmic domains of syntaxin 4 and 1, and VAMPs 2 and 4, but not those of other SNAREs, inhibited the fusion of norepinephrine-containing vesicles with the plasma membrane in PC12 cells. This inhibition was greater for the cognate SNAREs (syntaxin 1 and VAMP2) than for the non-cognate SNAREs (syntaxin 4 and VAMP4) (Scales et al. 2000). Similarly, Brandhorst et al. (2006) examined the effect of soluble SNAREs on homotypic endosome fusion. They found that only early endosomal SNAREs, not the neuronal or late endosomal SNAREs inhibited fusion. This is despite both sets of SNARE proteins being present on early endosomes (Brandhorst et al. 2006). However, in the same study, in a cell free system with proteoliposomes reconstituted with recombinant SNARE proteins there was much more promiscuity in fusion. Liposomes containing early endosomal SNAREs fused with those containing VAMP2, 4 or 8 (Brandhorst et al. 2006). Furthermore, fusion of liposomes containing early endosomal SNAREs and VAMP4 could be inhibited by the addition of soluble portions of either VAMP2, 4 or 8. Finally Hu et al. (2007) showed that cells containing VAMP3 on the external face of the plasma membrane, could fuse with cells containing tSNARE complexes made up of

syntaxin 1/SNAP25, syntaxin 1/SNAP23 or syntaxin 4/SNAP25, but not with cells containing syntaxin 4/SNAP23 on the outside of the plasma membrane (Hu et al. 2007).

These studies demonstrate that SNARE complex formation is promiscuous *in vitro*. Yet, the formation of SNARE complexes that function in membrane fusion events is more specific. This highlights the necessity of examining SNARE complex formation both *in vitro* and *in vivo*. This research also makes it evident that multiple pairing combinations between v and tSNAREs are not only possible, but these SNARE complex may be fusiogenic, and therefore able to mediate fusion events.

The promiscuity of SNARE complex formation is of importance in light of the research discussed in section 3.1.1 regarding plasticity between multiple VAMP isoforms in GLUT4 translocation. It has been demonstrated that VAMPs 2, 3 and 8 can function in the fusion of GLUT4 containing vesicles with the plasma membrane (Zhao et al. 2009). It is unclear whether these VAMPs utilize the same or different tSNARE complexes to fuse GLUT4 containing vesicles with the plasma membrane. The tSNARE complex that is responsible for the fusion of insulin-sensitive GLUT4 with the plasma membrane is made up of syntaxin 4 and SNAP23 (Foster et al. 1999; Chamberlain & Gould 2002; Kawaguchi et al. 2010). Which vSNAREs can form complexes with this tSNARE both *in vitro* and *in vivo* has not been systematically examined and uncovering this information is an important step in understanding the mechanisms by which VAMPs 2, 3 and 8 can compensate for one another in mediating membrane fusion events.

3.2 Aims of Chapter

This chapter aims to systematically examine the interactions that can and do occur between the tSNARE complex involved in the fusion of insulin sensitive GLUT4 vesicles with the plasma membrane and the VAMP proteins expressed in adipocytes. Here, interactions that can occur between each of the VAMP proteins and the tSNARE complex syntaxin 4/SNAP23 have been systematically examined *in vitro* through the formation of SDS-resistant SNARE complexes. Interactions that do occur and *in vivo* have been examined by co-immunoprecipitation experiments.

3.3 Results

3.3.1 Purification of recombinantly expressed tagged proteins

N terminally GST tagged VAMP proteins and C terminally protein A tagged syntaxin 4 were purified and tags were cleaved as described (sections 2.3.2 and 2.3.3). Purified recombinant protein was subjected to SDS-PAGE to confirm that the protein had been correctly synthesised and to determine concentration of the purified protein stocks (Figure 3-1, Figure 3-2). Figure 3-1 shows many of the purified VAMPs exhibited multiple bands; if these were found to be immunoreactive they were included in the concentration analysis (section 2.3.7). Figure 3-2 shows the purification and thrombin cleavage of syntaxin 4. Purified C terminally His tagged SNAP23 was provided by Dr. D.Kioumourtzoglou.

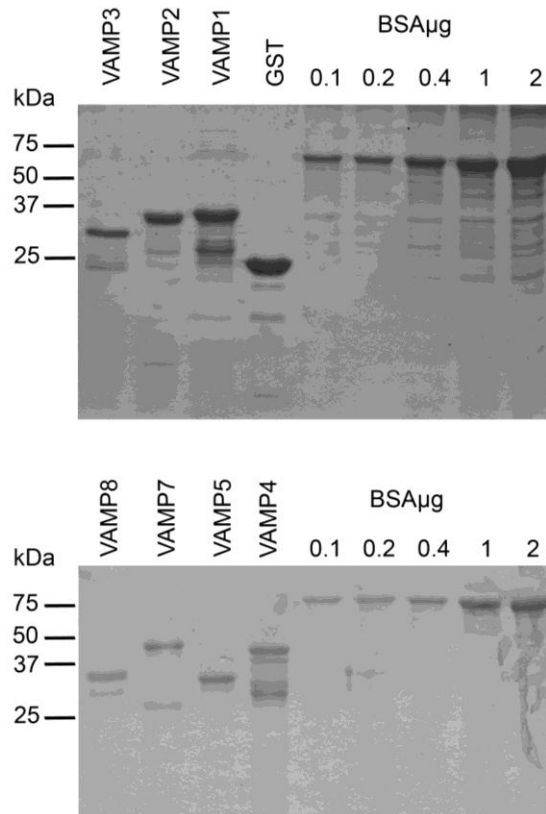


Figure 3-1: Purification of VAMP proteins.

GST tagged VAMPs were expressed in BL21 DE3 cells and purified as described (section 2.3.1 – 2.3.3). 10 μ l samples of each purified VAMP were analysed alongside known amounts of BSA on SDS-PAGE and stained with Coomassie Brilliant Blue. Shown are data from a typical experiment. molecular weights in kDa are shown.

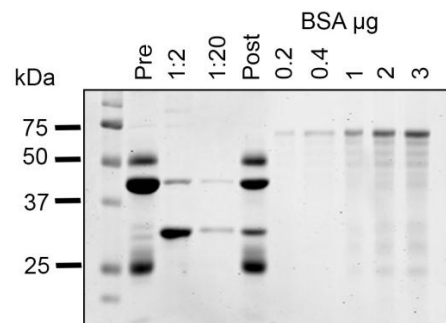


Figure 3-2: Purification and thrombin cleavage of protein A tagged syntaxin 4.

Protein A tagged syntaxin 4 was expressed in BL21 DE3 cells and the protein was purified as described (section 2.3.1 – 2.3.3). The protein A tag was thrombin cleaved as described (section 2.3.3). Shown is a representative experiment. Protein A tagged syntaxin 4 bound to IgG beads (Pre), thrombin cleaved syntaxin 4 (diluted 1:2 and 1:20) and any protein that remained bound to IgG beads post thrombin cleavage (Post) was analysed by SDS-PAGE and stained with Coomassie Brilliant Blue alongside known amounts of BSA. Shown are data from a typical experiment, molecular marker sizes are shown in kDa. Cleaved syntaxin 4 is ~30kDa, protein A tagged syntaxin 4 is ~40kDa.

3.3.2 SNARE Complex Assembly Assay (CAA)

Previous research has demonstrated that purified SNARE proteins can form stable SDS-resistant complexes alone *in vitro* (Fasshauer et al. 1999; Scales et al. 2000). Providing that a Qa,b,c and R SNARE are present, a stable SDS resistant SNARE complex can be formed without the addition of any external factors; this is the SNARE complex assembly assay. The SNARE complex assembly assay allows the requirements for each of the individual SNARE proteins in the formation of SNARE complexes to be examined. GST-VAMP proteins were incubated with His-SNAP23 and thrombin cleaved syntaxin 4 for two hours. The presence of a SNARE complex was determined through SDS-PAGE and immunoblotting. Figure 3-3 demonstrates that each of the VAMP proteins, but not GST, were capable of forming SDS-resistant SNARE complexes with syntaxin 4 and SNAP23. This complex is seen between 100kDa and 150kDa, and again at >250kDa, and contains syntaxin 4 (Figure 3-3B), SNAP23 (Figure 3-3C) and the indicated VAMP protein (Figure 3-3D). It is likely that the larger complex is a dimer of the smaller complex as both the smaller and larger complexes contain syntaxin 4, and SNAP23. Although the presence of the relevant VAMP in this larger complex is not detectable by immunoblotting (Figure 3-3C) its presence can be inferred by the molecular weight differences in the complexes. As previously demonstrated the formation of these complexes was not possible when any one of the SNARE domains (Qa, Qbc or R SNARE) were omitted from the assay (data not shown; Antonin et al. 2000).

The results presented in Figure 3-3 provide clear evidence that each of the VAMP proteins is capable of forming complexes with the tSNARE made up of syntaxin 4 and SNAP23. However, it provides no information on whether these complexes exist in the cell and therefore whether they are functional. To determine this, the co-immunoprecipitation of VAMP isoforms with syntaxin 4 was examined.

3.3.3 Interactions between syntaxin 4 and VAMP proteins in 3T3 L1 adipocytes

In order to determine if the VAMP proteins are present in complexes with syntaxin 4 the cellular environment immunoprecipitation and co-immunoprecipitation experiments were performed as described (section 2.8). As shown in Figure 3-4 the syntaxin 4 antibody but not the random rabbit IgG antiserum successfully immunoprecipitated syntaxin 4 from both basal and insulin-stimulated 3T3 L1 adipocyte lysates. As expected SNAP23 co-immunoprecipitates with syntaxin 4, and there is no observable increase in this interaction in lysates from insulin-stimulated cells compared to basal lysates. No interactions between syntaxin 4 and VAMPs 3, 4, 7 or 8 were detectable under basal or insulin-stimulated conditions. The syntaxin 4 antibody did not appear to co-immunoprecipitate VAMP2 from basal lysates. However co-immunoprecipitation was observed following insulin-stimulation (Figure 3-4). There was also substantial co-immunoprecipitation of VAMP5 with the anti-syntaxin 4 antibody from both basal and insulin-stimulated lysates (Figure 3-4). These data indicate that *in vivo*, syntaxin 4 interacts with both SNAP23 and VAMP5 and that following insulin-stimulation, syntaxin 4 also interacts with VAMP2. No interactions between syntaxin 4 and the other VAMPs were observed under either basal or insulin-stimulated conditions.

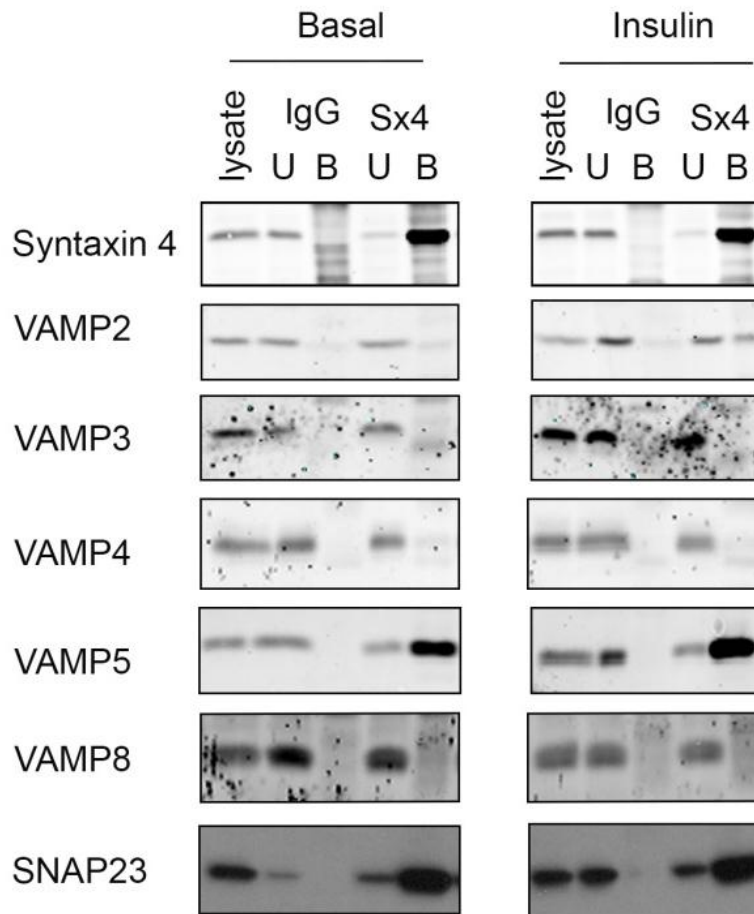


Figure 3-4: Immunoprecipitation of syntaxin 4 and co-immunoprecipitation of VAMP proteins in 3T3 L1 adipocytes.

Syntaxin 4 was immunoprecipitated from serum starved 3T3 L1 adipocytes treated with (insulin) or without (basal) 1 μ M insulin for 20 minutes as described (section 2.8). Proteins were immunoprecipitated from 1.5mg 3T3 L1 lysate (lysate) with 5 μ l anti-syntaxin 4 (Sx4) or random rabbit IgG (IgG). Immunoprecipitated proteins and associated material was isolated by centrifugation and unbound material retained (U), bound material (B) was washed and eluted in 2xLSB. Samples were subjected to SDS-PAGE and immunoblotting with anti-syntaxin 4 and anti-VAMP antibodies. Samples from basal and insulin-stimulated cells were subjected to immunoblotting on the same membrane and the irrelevant lanes excised, the original image is shown in the appendix (Appendix; Figure 8-1). Shown are data from a typical experiment.

3.4 Discussion

The results described in sections 3.3.1 - 3.3.3 demonstrate that *in vitro* all the VAMP proteins are capable of interacting with the tSNARE complex made up of syntaxin 4 and SNAP23. However *in vivo* only VAMP2 and 5 are found to interact with syntaxin 4. These novel findings shed light on the mechanisms of plasticity that have been observed between VAMPs 2, 3 and 8 in insulin-stimulated GLUT4 translocation to the plasma membrane (Zhao et al. 2009).

3.4.1 Methodological considerations

These studies have examined interactions between VAMP proteins and the syntaxin 4/SNAP23 tSNARE complex in two ways. Firstly, through the SNARE complex assembly assay and secondly, through co-immunoprecipitation of these proteins with syntaxin 4. Both methods, although providing valuable information regarding protein-protein interactions, have their limitations. The SNARE complex assembly assay allows the formation of SNARE complexes to be studied in the most minimalistic way. Thus, it allows the requirement for each SNARE in the overall complex to be examined. However, this method does not allow the stoichiometry of the complexes formed to be examined. For example, although each complex clearly contains at least one of each of the SNARE proteins (Figure 3-3), it may contain more than one of some proteins; the complex may be made up of, for example, one VAMP, one SNAP23 and three syntaxins, or three VAMPs, two SNAP23s and one syntaxin. Furthermore, the SNARE complex assembly assay provides no measure of the ability of the formed SNARE complexes to act in membrane fusion. At the other end of the spectrum the co-immunoprecipitation of syntaxin 4 binding partners allows measurement of the interactions that take place in the cellular environment. However, it is entirely possible that interactions that are not detectable in the cellular environment are able to participate in membrane fusion. This caveat is important in the context of examining plasticity when certain SNARE proteins are depleted or disrupted. Moreover, in co-immunoprecipitation experiments cells are lysed prior to detection of interactions, therefore the possibility that changes in interactions occur post-cell lysis cannot be excluded. Further, this technique relies on antibody detection of co-immunoprecipitated material. This means that

interactions might be missed and also means that no quantitative data obtained. Finally, interactions observed could be pairwise between the two proteins, or could require other proteins as well for example VAMP5 could interact with syntaxin 4, or be present in a complex with syntaxin 4 and SNAP23.

3.4.2 Discussion of findings

This is the first study to systematically examine the binding between the SNAREs syntaxin 4, SNAP23 and VAMP proteins *in vitro*, and to survey the interactions between the VAMP proteins and syntaxin 4 *in vivo*. The main findings are that all the VAMPs expressed in 3T3 L1 adipocytes are capable of forming SDS-resistant SNARE complexes with the tSNARE complex syntaxin 4/SNAP23 *in vitro* (Figure 3-3). However, this does not appear to translate to interactions with syntaxin 4 in the cellular environment, as only VAMPs 2 and 5 interact with syntaxin 4 *in vivo* (Figure 3-4).

In agreement with the SNARE complex assembly findings, previous studies investigating the specificity in SNARE complex formation found high levels of binding promiscuity between recombinant SNARE proteins (Fasshauer et al. 1999; Scales et al. 2000). Yang et al. (1999) examined the interactions between three different tSNARE complexes and the VAMP proteins VAMP2, 4, 7 and 8. The tSNARE complexes examined in this study were syntaxin 1/SNAP25, syntaxin 4/SNAP23 and syntaxin 13/SNAP29. They found that all 4 VAMP isoforms could form SDS-resistant SNARE complexes with syntaxin1/SNAP25 and syntaxin 13/SNAP29. However, only VAMP4 and 8 formed SDS resistant complexes with syntaxin 4/SNAP23. Conversely, Fassauer et al. (1999) found that the tSNARE complex SNAP25/syntaxin 4 could form SDS-resistant complexes with VAMP2 but not VAMP8. Here, it has been shown that all 6 VAMP isoforms can form SDS resistant SNARE complexes with syntaxin 4/SNAP23 (Figure 3-3). This adds to the existing literature regarding the promiscuity of SNARE complex formation. All the available data regarding the formation of SDS resistant SNARE complexes with different tSNAREs and VAMP protein is compiled in Table 3-1. Importantly, only a single set of experimental conditions have been examined here. Each VAMP may form complexes with the tSNARE at different rates, and there may be different affinities between the tSNARE complex and each VAMP. This may

provide a level of specificity or preference in interactions between t and vSNAREs. Further work will need to be carried out to explore this.

Table 3-1: SNARE proteins that can form SDS-resistant SNARE complexes *in vitro*.

vSNARE	tSNARE	Reference
VAMP2	Syntaxin 1/SNAP25 Syntaxin 13/SNAP29 Syntaxin 4/SNAP23	Yang et al. (1999) Fassauer et al. (1999); Figure 3-3
VAMP3	Syntaxin 4/SNAP23	Figure 3-3
VAMP4	Syntaxin 1/SNAP25 Syntaxin 13/SNAP29 Syntaxin 4/SNAP23	Yang et al. (1999); Figure 3-3
VAMP5	Syntaxin 4/SNAP23	Figure 3-3
VAMP7	Syntaxin 1/SNAP25 Syntaxin 13/SNAP29 Syntaxin 4/SNAP23	Yang et al. (1999) Figure 3-3
VAMP8	Syntaxin 1/SNAP25 Syntaxin 13/SNAP29 Syntaxin 4/SNAP23	Yang et al. (1999); Figure 3-3

The research described above and in Table 3-1 demonstrates that there is a large degree of promiscuity in the formation of SNARE complexes *in vitro*. However, although the *in vitro* SNARE complex assembly assay constitutes the minimal machinery for SNARE complex formation and gives information on the ability of v and tSNAREs to interact, it only measures complex formation and gives no information on the functional relevance of these complexes. SNARE complexes formed using this method (Fassauer et al. 1999; Yang et al. 1999; Scales et al. 2000; Figure 3-3,) may not function in membrane fusion events. Therefore it is important to establish the interactions that take place in the cellular environment.

Many lines of evidence support the notion that although SNARE complex formation is promiscuous *in vitro*, not all SNARE complexes that are formed are functional. Brandhorst et al. (2006) found that whilst endosomes contain multiple sets of SNAREs, including the early and late endosomal SNAREs and exocytotic SNAREs, only soluble early endosomal SNAREs inhibit endosome fusion (Brandhorst et al. 2006). Similarly, Scales et al. (2000) examined SNARE complex specificity *in vivo* by examining the inhibition of fusion of noradrenaline containing vesicles with the plasma membrane of PC12 cells using soluble SNARE proteins. This fusion event requires the tSNARE syntaxin 1/SNAP25. They found

that even though VAMPs 2, 4, 7 and 8 form SDS-resistant SNARE complexes with syntaxin 1/SNAP25 (Yang et al. 1999), only VAMP2, and to a lesser extent VAMP4, inhibited the exocytosis of noradrenaline from PC12 cells (Scales et al. 2000). This is suggestive of some cross talk between VAMP2 and 4 with but not the other VAMPs.

Studies using yeast SNAREs reconstituted into liposomes have further demonstrated that although SNAREs may be able to form multiple complexes, that these may not all be fusogenic. When pairs of yeast SNAREs are co-expressed in bacterial cells they form complexes promiscuously (Tsui & Banfield 2000). However, fusion of liposomes containing different combinations of many of the same tSNAREs and vSNAREs is much more specific (Parlati et al. 2002; Paumet et al. 2004).

In summary, although a high level of promiscuity between SNARE partners is seen *in vitro*, much more specificity is seen in the cellular environment. This study has demonstrated that this situation is evident for SNARE complexes containing syntaxin 4. The findings of co-immunoprecipitation experiments conducted here illustrate that although interactions between the VAMP proteins and syntaxin 4/SNAP23 *in vitro* are promiscuous, interactions between syntaxin 4 and VAMP proteins in the cellular environment are highly selective. *In vivo*, the only detectable interactions between syntaxin 4 and VAMP proteins were with VAMP2 and VAMP5. The interaction between syntaxin 4 and VAMP2 has been observed previously (Cheatham et al. 1996). However, unlike Cheatham et al. (1996), here this interaction was not detectable in basal lysates; it only became apparent in insulin-stimulated lysates (Figure 3-4). This discrepancy is likely to be a function of the anti-VAMP2 antibody used in this study. A limitation with using co-immunoprecipitation to characterise interactions is that it is entirely reliant on antibodies to detect the co-immunoprecipitated proteins. The anti-VAMP2 antibody used here, although specific for VAMP2, produces a weak signal, therefore interactions in basal lysates may have been present but not detectable.

Quite recently Zhao et al. (2009) found that VAMPs 2, 3 and 8, but not VAMPs 4, 5 or 7, can act in the fusion of insulin-sensitive GLUT4 containing vesicles with the plasma membrane. The possible mechanisms underlying this plasticity are

discussed in more detail in Chapter 4. However, Figure 3-4 shows that *in vivo* VAMPs 3 and 8 do not interact with syntaxin 4, but VAMP2 does. It is possible that the lack of observable interactions between VAMP3 and syntaxin 4, is due to an inability of the antibodies used to detect the interaction as apposed to the interaction not being present. However, when the co-immunoprecipitation data is viewed in the context of previous research that has shown that membranes containing VAMP3 are not capable of fusing with those containing the tSNARE sytaxin4/SNAP23 *in vitro*. It seems that, in fact VAMP3 does not interact with syntaxin 4. The ability of VAMP8 to form fusiogenic SNARE complexes with syntaxin 4/SNAP23 has not yet been addressed. However, the VAMP8 antibody used in this study produces a strong signal and at the concentration used detects very low quantities of recombinant VAMP8 (0.1ng; data not shown). Therefore it seems that the lack of observable interaction between VAMP8 and syntaxin 4 is due to there not being an interaction, not due to detection issues. In summary, the co-immunoprecipitation data provided here, alongside previous findings, demonstrate that under conditions where VAMP2 is present, VAMPs 3 and 8 do not interact with syntaxin 4. These VAMP isoforms therefore either do not play a role in the fusion of insulin-sensitive GLUT4 vesicles with the plasma membrane, or if they do play a role, they do so with a tSNARE complex that does not contain syntaxin 4. On balance, the former situation seems more likely as, to date, there is no evidence that any tSNAREs other than syntaxin 4 and SNAP23 are involved in the fusion of GLUT4 vesicles with the plasma membrane in response to insulin (Foster et al. 1999; Kawaguchi et al. 2010).

Interestingly VAMP5, as well as VAMP2, was found to co-immunoprecipitate with syntaxin 4. Little is known regarding the role of VAMP5 in adipose cells. In muscle cells it is found predominantly in the sarcolemma (Zeng et al. 1998) and in cardiomyocytes it is required for the trafficking of insulin sensitive-GLUT4 to the plasma membrane in response to insulin (Schwenk et al. 2010). It is noteworthy that although VAMP5 interacts with syntaxin 4 in adipocytes (Figure 3-4), it cannot compensate for the loss of VAMP2 (Zhao et al. 2009) in the same cell type. Potential reasons for this are discussed in Chapter 4.

As anticipated syntaxin 4 interacts with SNAP23 in lysates from both basal and insulin-stimulated cells (Figure 3-4). Insulin-stimulation has no discernible effect on this interaction. This is in agreement with previous data collected using a

different approach. Using an assay that measures the proximity of proteins *in situ* (Proximity Ligation Assay; PLA) it has been shown that insulin increases associations between SNAP23 and VAMP2, but not SNAP23 and syntaxin 4, or VAMP2 and syntaxin 4 (Kioumourtzoglou et al. 2014). These findings led to the proposal of a model whereby under basal conditions there are two pools of syntaxin 4. One of these pools of syntaxin 4 associates with SNAP23 and the other associates with VAMP2. Insulin-stimulation is proposed to induce a switch in these associations so that a SNARE complex is formed between syntaxin 4/SNAP23 and VAMP2. It is important to note however that the PLA assay measures proximity not interaction. Figure 3-4 shows that under insulin-stimulated but not basal conditions VAMP2 co-immunoprecipitates, and therefore interacts, with syntaxin 4. This suggests that either interactions between VAMP2 and syntaxin 4 increases upon insulin-stimulation, or that the strength of this interaction increases with insulin-stimulation, so that the interaction is not disrupted during cell lysis. Taking this data alongside the PLA data allows the generation of a model by which, under basal conditions, syntaxin 4 and VAMP2 are either in close proximity but not in complex with one another, or in a weak complex that is disrupted by the cell lysis procedures. Insulin-stimulation then either stimulates VAMP2 and syntaxin 4 to form a complex or results in an increase the strength of the interaction between these proteins so that it is now not disrupted by cell lysis and becomes detectable by co-immunoprecipitation.

The data presented here and by others provides clear evidence of promiscuity in SNARE complex formation *in vitro* (Figure 3-3; Fasshauer et al. 1999; Yang et al. 1999; Scales et al. 2000). Yet, interactions seen in the cellular environment are much more tightly regulated (Figure 3-4). The assembly of non-fusogenic SNARE complexes *in vivo* must be avoided as these will result in dead-end fusion reactions. Since the specificity of SNARE complex formation is not encoded in the SNARE proteins themselves some extra layer of specificity must exist *in vivo*. This may be achieved by the spatial segregation of cognate and non-cognate SNARE proteins or through the actions of tethers.

The spatial segregation of SNARE proteins to separate membrane compartments is discussed in Chapter 4. SNARE proteins may also be segregated from one another on membranes; on isolated plasma membrane lawns tSNAREs are found

in discrete clusters, which provide platforms for membrane fusion events (Lang et al. 2001; Predescu et al. 2005). This clustering is cholesterol and SNARE motif dependent (Chamberlain & Gould 2002; Low et al. 2006; Sieber et al. 2006). Segregation is not only evident on the plasma membrane, it is also evident on vesicle membranes. In artificially enlarged fusing endosomes, which contain both VAMP2 (non-cognate) and VAMP4 (cognate), VAMP2 (the non-cognate SNARE) is excluded from the contact site (Bethani et al. 2007) . This spatial segregation might contribute to the specificity of membrane fusion alongside the action of tethers.

3.5 Conclusion

In summary the data presented here builds on previous research and demonstrates that *in vitro* SNARE complex assembly is promiscuous. However this promiscuity is not maintained in the cellular environment. The finding that *in vivo* neither VAMP3 nor 8 interact with one of the tSNAREs required for the fusion of GLUT4 containing vesicles with the plasma membrane in response to insulin suggests that the plasticity seen between VAMP2, 3 and 8 in insulin-stimulated GLUT4 containing vesicle fusion with the plasma membrane (Zhao et al. 2009) is not evident when VAMP2 is present. This data does not address the mechanisms by which VAMPs 3 and 8 can act in GSV fusion with the plasma membrane when VAMP2 is depleted; this is examined in Chapter 4.

Chapter 4 - Endogenous Levels and Subcellular Distribution of VAMPs and in 3T3 L1 Adipocytes.

4.1 Introduction

As described in Chapter 3, there has been considerable debate as to what provides the specificity of SNARE complex formation and membrane fusion. There is a large body of evidence suggesting that SNARE complex formation *in vivo* is highly selective. However, it has recently become evident that there is some level of cross talk and plasticity in SNARE complex formation and the membrane fusion events different SNARE proteins function in. With regard to insulin-stimulated GLUT4 translocation Zhao et al. (2009) recently found that VAMPs 2, 3 and 8 could act in the insulin-stimulated fusion of GLUT4 vesicles with the plasma membrane (Zhao et al. 2009). In Chapter 3 it was demonstrated that *in vitro* the interactions between VAMPs and the tSNAREs syntaxin 4 and SNAP23 are not selective. However, *in vivo* only VAMPs 2 and 5 interact with syntaxin 4 (Chapter 3, section 3.3.3). This indicates that under physiological conditions VAMP2 is the predominant VAMP involved in the fusion of GSVs with the plasma membrane. It also raises the question as to why no plasticity is seen between VAMP2 and VAMP5, since VAMP5 can clearly interact with syntaxin 4, and therefore should be able to function in the fusion events involving this tSNARE. This chapter aims to gain further insight into the function of and plasticity between VAMPs in 3T3 L1 adipocytes by quantifying their levels, examining their changes in expression upon differentiation from fibroblasts to adipocytes, and determining their subcellular localisation under basal and insulin-stimulated conditions.

4.1.1 Current Understanding of Roles and Localisation of VAMPs

Different sets of SNARE proteins function in different membrane fusion events and therefore show different tissue distribution patterns. VAMPs 3, 4, 7 and 8 are all broadly expressed. VAMP5 is preferentially expressed in skeletal and cardiac muscle. VAMP2 is expressed at highest levels in tissues which display high levels of secretory activity such as neurones and neuroendocrine cells (McMahon et al. 1993; Rossetto et al. 1996; Advani et al. 1998; Zeng et al. 1998).

As well as showing different tissue distributions, SNARE proteins also show different subcellular distributions depending on the membrane trafficking events they are involved in. VAMP2 is found on vesicles that are mobilised in response

to external stimuli; it is found on insulin responsive GLUT4 containing vesicles in muscle and adipose tissues and on synaptic vesicles in neuronal tissues. In line with this distribution pattern VAMP2 is involved in the regulated exocytosis of both GSVs and synaptic vesicles (Verderio et al. 1999; Williams & Pessin 2008). VAMP3 is ubiquitously expressed and has been identified on GLUT4 containing vesicles within the endosomal recycling pathway (McMahon et al. 1993; Volchuk et al. 1995; Martin et al. 1996; Randhawa et al. 2000). VAMP4 is localised to both the *trans*-Golgi network and endosomes (Steggmaier et al. 1999; Mallard et al. 2002) and has been found to participate in retrograde but not antigrade trafficking (Shitara et al. 2013). VAMP5 is predominantly expressed in skeletal and cardiac muscle where it associates with the sarcolemma and vesicles in perinuclear compartments (Zeng et al. 1998; Takahashi et al. 2013), including GLUT4 containing vesicles (Larance et al. 2005; Rose et al. 2009). VAMP7 is primarily localised within the lysosomal pathway. In adipose and muscle tissues it is also found on GLUT4 containing vesicles, where it facilitates their fusion with the plasma membrane in response to osmotic shock (Randhawa et al. 2004; Williams & Pessin 2008). VAMP8 is localised within the endosomal pathway and found at the plasma membrane and TGN (Advani et al. 1998; Wong et al. 1998). In line with this distribution pattern it has been implicated in the fusion of early and late endosomes and in the endocytosis of GLUT4 (Antonin et al. 2000; Williams & Pessin 2008).

4.1.2 Identification of VAMPs on GLUT4 containing vesicles

Although each VAMP protein shows a distinct subcellular distribution pattern and its primary localisation is to membrane compartments in which it acts in the fusion of, many membranes contain multiple VAMPs. These VAMPs could be involved in membrane fusion events or they could be present in a passenger capacity. Indeed, although in insulin-sensitive tissues VAMP2 predominantly localised to insulin-sensitive GLUT4 membranes, it is not the only VAMP protein to have been identified here. Many studies have observed that GLUT4 containing vesicles contain VAMPs 3, 5, 7 and 8 as well as VAMP2. These observations have been made primarily through the immunoprecipitation of GLUT4 containing membranes from L6 muscle cells and adipose cells with anti-GLUT4 antibodies and assessing the presence of VAMP proteins with antibodies or through mass spectrometry (Volchuk et al. 1994; Martin et al. 1996; Ross et al. 1996; Larance

et al. 2005). This method of isolation does not differentiate the species of the GLUT4 membranes. The GLUT4 membranes isolate could be from the endosomal recycling pool, from the insulin-sensitive pool or from vesicles transporting GLUT4 to one of these compartments or the lysosome. Further, this methodology does not give any information on the amount of each VAMP on these GLUT4 containing vesicles; there could be one or one hundred molecules of the identified VAMP on the GLUT4 containing membrane. These issues mean that currently there is confusion as to which VAMP isoforms are where, and with which pool of GLUT4. One method to separate the GLUT4 vesicles in the endosomal pool from those in the insulin sensitive pool is to isolate the intracellular pools of GLUT4 and then separate these out using iodixanol gradients (Hashiramoto & James 2000; Perera et al. 2003). In this method the iodixanol is combined with the sample that is to be separated, the mixture is centrifuged, and the iodixanol forms a gradient through which organelles are separated out based on density. Using this method syntaxins 16 and 6 and VAMPs 2 and 3 have been identified to localise with GSVs (Hashiramoto & James 2000; Perera et al. 2003). Here, the localisation of all the VAMP proteins has been addressed using this method.

4.1.3 Levels of VAMPs in 3T3 L1 adipocytes

As discussed in section 4.1.1, the tissue distribution of SNARE proteins can give some indication as to their functions. Consequently, any VAMP proteins expressed at high levels in insulin-sensitive tissues, compared to insulin-insensitive tissues may be important in the acquisition and/or maintenance of insulin sensitivity and play a role in GLUT4 trafficking. For this reason many groups have studied the change in expression of proteins in response to differentiation of 3T3 L1 fibroblasts to adipocytes. This differentiation process leads to the acquisition of insulin-sensitivity (Ross et al. 1996; El-Jack et al. 1999; Roccisana et al. 2013). Therefore it is necessary to examine the differences in the levels of each of the VAMP proteins in adipocytes as well as their expression levels in fibroblasts compared to adipocytes.

Although to date there has been no systematic analysis of the expression level of all of the post-Golgi vSNAREs in adipocytes, the levels of the some of the t and vSNAREs implicated in the insulin-stimulated trafficking of GLUT4 to the plasma

membrane have been studied. Hickson and colleagues (2000) examined the levels of the vSNAREs VAMP2 and 3 and the tSNAREs syntaxin 4 and SNAP23 as well as the SM protein Munc18c in 3T3 L1 adipocytes. It was found that each cell contained 374,000 copies of syntaxin 4, 452,000 copies of Munc18c, 1,150,000 copies of SNAP23, 495,000 copies of VAMP2 and 4,300,000 copies of VAMP3 (Hickson et al. 2000). Here, for the first time in any cell type, the expression levels of all 6 members of the VAMP subfamily expressed in adipose tissue, and their response to adipocyte differentiation has been examined.

4.1.4 Mobilisation of VAMPs in response to insulin

It is well documented that insulin mobilises GLUT4 from intracellular deposits to the cell surface. Concurrent with this mobilisation there is also a translocation of proteins that localise with insulin-sensitive GLUT4 containing vesicles such as IRAP, syntaxin 6 and syntaxin 16 (Ross et al. 1996; Perera et al. 2003; Shewan et al. 2003). In adipose tissue VAMPs 2, 3, 7 and 8 are found on GLUT4 containing vesicles and in muscle cells VAMP5 also localises to GLUT4 containing vesicles (Larance et al. 2005; Rose et al. 2009). In adipose cells both VAMP2 and VAMP3 translocate to the plasma membrane in response to insulin (Volchuk et al. 1995; Martin et al. 1996; Xu et al. 2011). In muscle cells GLUT4, VAMP5 and VAMP7 translocate to the cell surface in response to contraction and in both muscle and adipose tissue, VAMP7 translocates along with GLUT4 to the cell surface in response to osmotic shock (Williams & Pessin 2008; Rose et al. 2009). However, despite these VAMPs being present on GLUT4 containing vesicles the translocation of VAMP5, 7 or 8 to the cell surface in response to insulin in adipose cells has not been examined. Translocation of proteins to the plasma membrane alongside insulin-sensitive GLUT4 suggests that they are present on insulin-sensitive GLUT4 containing vesicles (GSVs). However, it should be noted that their presence on GSVs does not necessarily translate to functionality in terms of involvement in the insulin response.

4.1.5 Roles of VAMPs in insulin response

Many studies have identified that VAMP2 is required for GSV fusion with the plasma membrane, this has been achieved by removing VAMP2 from cells and examining their response to insulin-stimulation (Cheatham et al. 1996; Martin et

al. 1998; Williams & Pessin 2008; Kawaguchi et al. 2010). A variety of methods have been employed to deplete cells of VAMP2 or impair VAMP2 action. This includes using cells derived from knockout mice, treating cells with RNAi or tetanus neurotoxins (TeNT), or by the injection of peptides to block the action of endogenous VAMPs. These studies have provided valuable insight into the role of VAMPs in GLUT4 trafficking, however they have their limitations. The first and largest is that measurements are taken in an artificial system; removal or inhibition of proteins may stimulate others to compensate, particularly when the protein of interest is chronically removed (as seen in knock out models). RNAi may also result in off target or non-specific effects, and may not result in full removal of the protein. Similar problems arise with the use of TeNT, as this removes both VAMP2 and VAMP3 thus preventing these proteins from being distinguished. Putting these issues aside, there are also issues with the methods used to measure the insulin response. The insulin response is measured by the appearance of GLUT4 at the plasma membrane. However, as discussed in section 1.2.1 GLUT4 is found within multiple intracellular pools. None of the studies mentioned above have differentiated between GLUT4 in the endosomal recycling system and that in the specialised insulin-sensitive store. Here, in an attempt to circumvent these issues, the subcellular distribution of VAMP proteins and their localisation with GSVs in 3T3 L1 adipocytes has been determined.

4.2 Aims

This chapter has three main aims. Firstly, to determine whether the levels of the VAMP proteins change upon differentiation of 3T3 L1 fibroblasts into adipocytes. Secondly, to determine the absolute levels of the VAMP proteins expressed in 3T3 L1 adipocytes. Finally, to determine the subcellular distribution of each of the VAMP isoforms both in the absence and presence of insulin, and to determine the extent to which each VAMP protein localises with insulin-sensitive GLUT4, as defined using iodixanol gradient separation of this compartment.

4.3 Results

4.3.1 Testing of VAMP antibodies

Before any work using commercially purchased VAMP antibodies could be carried out it was necessary to characterise each antibody. Commercially available

antibodies against VAMPs 1, 2, 3, 4, 5, 7 and 8 were purchased from synaptic systems (Table 2-5). Antibody specificity was tested with GST tagged recombinant VAMP proteins and antibodies were optimised for use in 3T3 L1 adipocytes using membrane fractions from this cell type.

Figure 4-1 shows that each of the VAMP antibodies was specific for the named VAMP. Slight cross reactivity of the anti-VAMP3 antibody was seen with recombinant VAMP4. However, this cross reactivity was seen with a large amount (10ng) of recombinant protein which is unlikely to be come across in the cellular environment. Furthermore, the two proteins can be differentiated from one another by their differing molecular weights (approximately 11kDa for VAMP3 and 16kDa for VAMP4). At higher amounts of recombinant purified VAMP protein than those used in Figure 4-1 not all antibodies were entirely selective. However, this was only found using large (>10ng) amount of recombinant protein; this level of protein is not likely to be found in samples from 3T3 L1 adipocytes.

To determine the optimum antibody concentration for detecting endogenous VAMP proteins in 3T3 L1 adipocytes 20µg of membrane fraction was subjected to immunoblotting with VAMP antibodies at different concentrations. An example of the steps taken to optimise antibody use is displayed in Figure 4-2. Initial experiments were carried out using a standard alcohol rich transfer buffer (20% (v/v) methanol). Under these conditions detection of endogenous protein was only possible at high concentrations of antibody, and in some cases was not possible at all. Since SNARE proteins are hydrophobic it was theorised that they might be attracted to, and become trapped in the alcohol in the transfer buffer and therefore not transfer to the nitrocellulose membrane. So, in an attempt to improve the transfer efficiency, an alcohol free transfer buffer was used (12.5mM Tris HCl pH 7.4, 200mM glycine). This allowed much better detection of endogenous VAMP proteins (Figure 4-2 A vs. B). Following optimisation of the transfer efficiency, the blocking solution and antibody dilutions were also optimised. Membranes were blocked, and antibodies made up, in 1% or 5% milk (Figure 4-2 C vs.D). It was clear that detection was best when transfer was completed in alcohol-free transfer buffer and blocking was in 1% milk. The dilutions of the antibodies used are described in (Table 2-5), and these conditions gave consistent results and were used throughout this thesis.

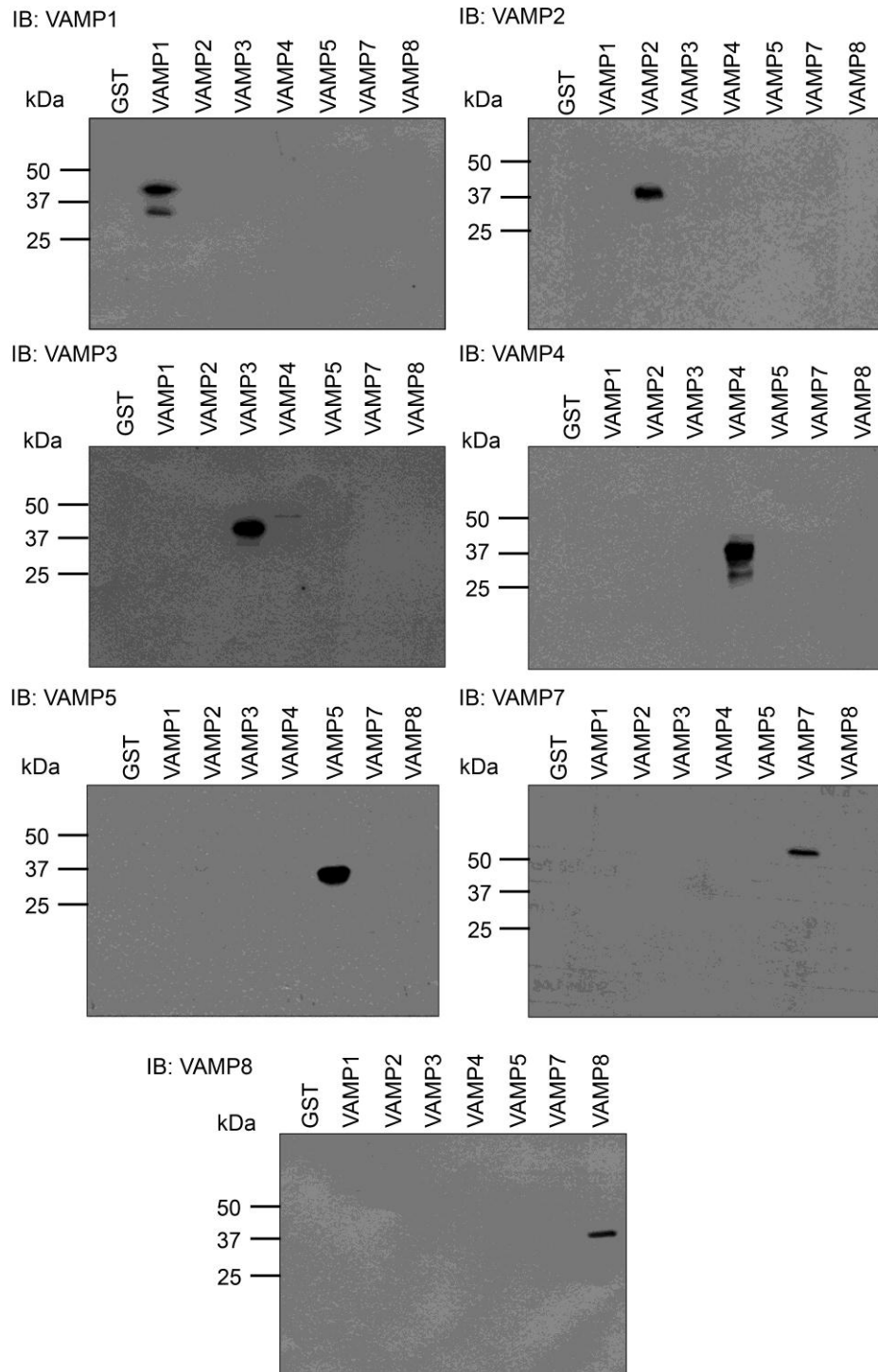


Figure 4-1: VAMP antibodies are specific.

10 ng (or 1ng for testing of anti-VAMP8) GST and recombinant VAMPs were subjected to SDS-PAGE followed by immunoblotting with anti-VAMP antibodies. Anti-VAMP1, anti-VAMP4, anti-VAMP5 and anti-VAMP7 were used at 1:1000, anti-VAMP2 and anti-VAMP3 at 1:10 000 and anti-VAMP8 was used at 1:50 000. Shown are data from a typical experiment, molecular marker sizes are shown in kDa.

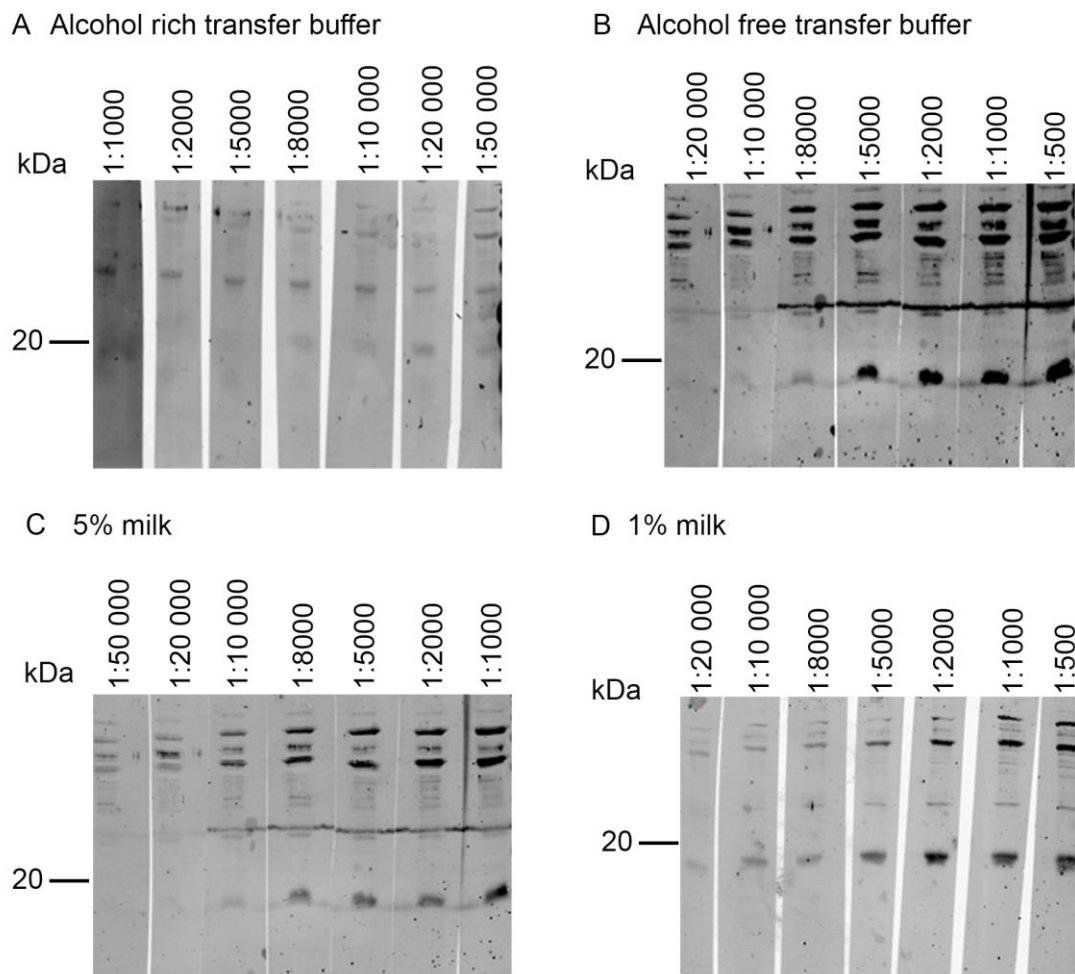


Figure 4-2: Example of the steps taken to optimise antibodies for use in 3T3 L1 adipocytes. 20 μ g of 3T3 L1 adipocyte membrane fraction was subjected to SDS-PAGE followed by immunoblotting, membranes were sliced and probed with the indicated concentration of anti-VAMP4 antibody in either 5% (**A, B, D**) or 1% milk (**C**), transfer was conducted in either alcohol rich transfer buffer (**A**) or alcohol free transfer buffer (**B, C, D**). Predicted molecular weight of VAMP4 is 16kDa. Shown are data from a typical experiment, molecular marker sizes are shown in kDa.

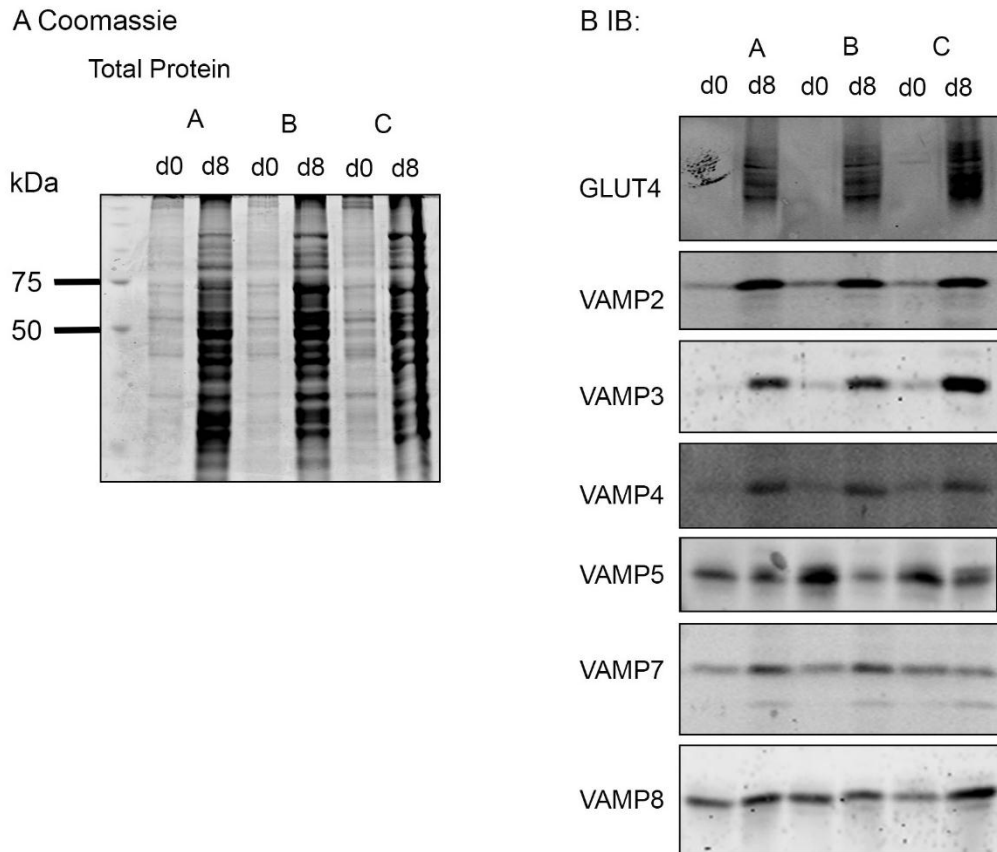
4.3.2 Determination of changes in expression levels upon adipocyte differentiation.

The 3T3 L1 cell line is a preadipocyte cell line derived from mouse embryos. 3T3 L1 cells can be propagated in culture and upon the addition of media containing 3-isobutyl-1-methylxanthine (IBMX), dexamethasone, insulin, troglitazone and foetal bovine serum they begin to accumulate triglycerides and turn into adipocytes.

Differentiation of 3T3 L1 fibroblasts into adipocytes is associated with an increase in GLUT4 protein content, which is concurrent with the acquisition of insulin-sensitivity. This coincides with the formation of the specialised insulin-

sensitive pool of GLUT4 vesicles (GSVs) (El-Jack et al. 1999). Differentiation is also associated with increases in the levels of the proteins required to synthesise GSVs and recycle GLUT4. This includes sortilin, IRAP and the tSNARE syntaxin 16 (Shi & Kandror 2005; Ross et al. 1996; Roccisana et al. 2013). To determine the effect of differentiation on the levels of VAMP proteins, equal numbers of fibroblast and adipocyte cells were subjected to immunoblotting with VAMP antibodies. To ensure that equal numbers of fibroblast and adipocyte cells were examined, fibroblasts were seeded onto coverslips and either fixed on day 0 or differentiated into adipocytes and fixed on day 8. Cell nuclei were stained with DAPI and the number of cells within a field of view was counted (data not shown). This demonstrated that the number of fibroblasts and adipocytes in a field of view (and 10cm dish) are equal, and therefore membrane fractions of fibroblasts and adipocytes from the same number of 10cm plates, produced in the same manner, could be directly compared.

Figures 4-3 A and B show equal volumes of 3T3 L1 membrane fractions from the same number of fibroblast and adipocyte cells (1/10th of a 10cm plate, 1×10^6 cells). It is evident from Figure 4-3 A that differentiation results in a large increase in the total cellular protein content. There are increases in the levels of GLUT4, VAMP 2, 3 and 4, but the levels of VAMP 5, 7 and 8 remain unchanged (Figure 4-3).



C

Fold Change in VAMP Protein Levels following Differentiation.

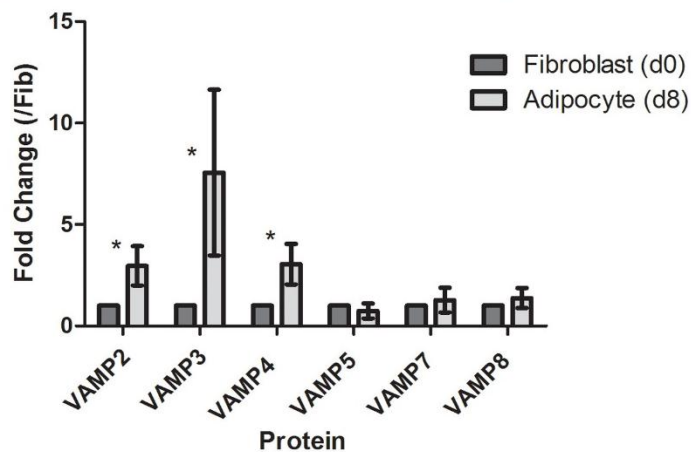


Figure 4-3: Changes in VAMP protein levels upon adipocyte differentiation.

Equal numbers of fibroblast and adipocyte cells were homogenised and subjected to centrifugation at 95 000 x g for 1 hour to pellet to the total membranes as described (section 2.7.1). Samples were then subjected to SDS-PAGE followed by staining with Coomassie Brilliant Blue to assess total protein content (**A**) or immunoblotting with anti-GLUT4 and anti-VAMP antibodies to determine change in protein content of specific proteins (**B**). 3 experiments are displayed on each gel (A, B and C), d0 = fibroblasts, d8 = fully differentiated adipocytes. Compared to an equal number of fibroblast cells the levels of VAMP 2 3 and 4 are elevated in fully differentiated adipocytes (**C**). Values represent the means of 3 separate experiments, values were compared with a Student's t-test, * = $p < 0.05$ (C).

4.3.3 Determination of expression levels in 3T3 L1 adipocytes

As well as examining the changes in VAMP protein levels upon adipocyte differentiation, the expression levels of each of the VAMP isoforms in 3T3 L1 adipocytes has also been determined for the first time. In these experiments, increasing amounts of recombinant purified VAMP protein was subjected to immunoblotting alongside samples of 3T3 L1 adipocyte membrane fractions. Figure 4-4 shows analysis of 1µg of each recombinant VAMP protein. These stocks were further diluted and used to determine the amount of VAMP protein in 3T3 L1 membrane fractions. This demonstrates that the amount of recombinant protein used to quantify the absolute levels of each VAMP in adipocytes were equal, and therefore that the values produced from the quantification are accurate and comparable to one another. A representative immunoblot of the quantification process is shown in Figure 4-5. The intensity values obtained for the VAMP content in 3T3 L1 membrane fractions were compared to the intensity values obtained for the increasing amounts of recombinant protein. This was used to determine the amount of VAMP in the membrane fractions, which was then converted to copy number per 10cm dish (1×10^7 cells; (Biber & Lienhard 1986)), and then to copy number per cell (Table 4-1, Figure 4-6).

The levels of each of the VAMP isoforms differed greatly. VAMP 8 was the most abundant VAMP isoform with 3.5×10^6 copies per cell, this was followed by VAMP3 with 4.8×10^6 copies per cell. VAMP2 and 4 were expressed at moderate levels with 8.6×10^5 and 4.8×10^5 copies per cell respectively and VAMP5 and 7 were expressed at similar, very low levels, with 5.8 and 5.3×10^4 copies per cell (Table 4-1, Figure 4-6, $p < 0.05$).

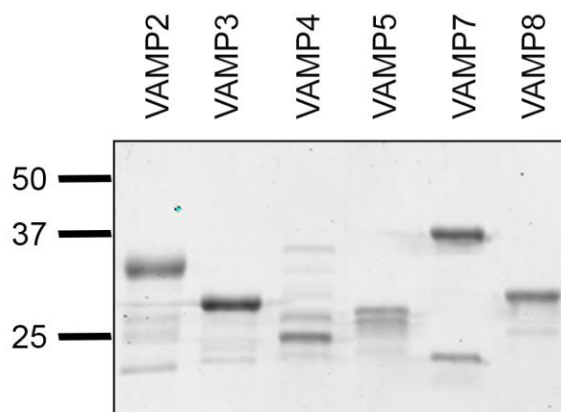


Figure 4-4: SDS-PAGE analysis of recombinant proteins.

1 μ g of purified recombinant protein was subjected to SDS-PAGE and stained with Coomassie Brilliant Blue. The top bands for VAMP2, 3 and 7 were found to be immunoreactive so were used in analysis, whereas all bands present for VAMP4 and 5 were immunoreactive and used in analysis. Shown are data from a typical experiment, molecular marker sizes are shown in kDa.

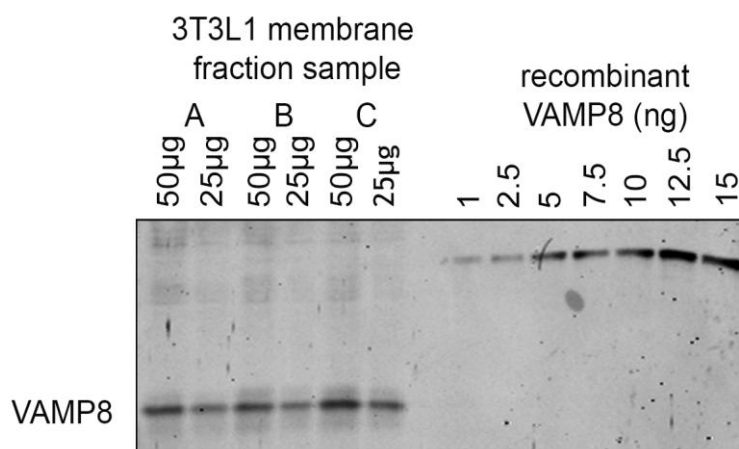


Figure 4-5: Representative immunoblot showing the method used to quantify the levels of VAMP protein in 3T3 L1 adipocytes.

Fully differentiated 3T3 L1 adipocytes were homogenised and centrifuged at 95 000 xg for 1 hour to pellet the total membrane fraction as described (section 2.7.1). This was subjected to SDS-PAGE and immunoblotting with anti-VAMP proteins alongside increasing amounts of bacterially expressed recombinant VAMP protein. Each immunoblot contains membrane fractions from three separate batches of cells (A, B and C). Data shown are from a typical experiment determining the levels of VAMP8 as an example.

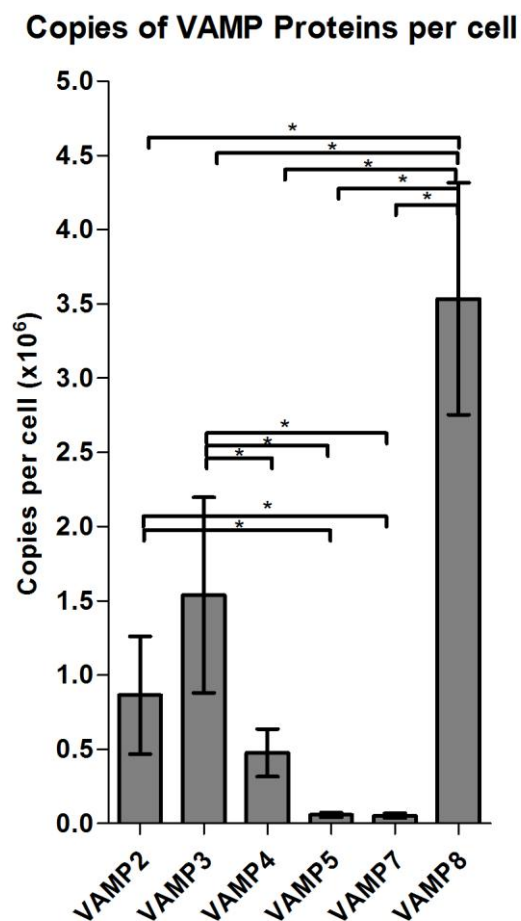


Figure 4-6: Copy number of each VAMP protein in 3T3 L1 adipocytes.

Copy number of each of the VAMP proteins was determined from values obtained for ng VAMP per μg membrane fraction (Figure 4-5). Values are the means \pm SD of 3 separate experiments and were compared using a one way ANOVA * = $p < 0.05$.

Table 4-1: Copies of each VAMP protein in 3T3 L1 adipocytes,

Copy number of each of the VAMP protein from was determined from immunoblot experiments seen above (Figure 5-4). One 10cm dish contains 1×10^7 cells, made up of 2.5mg membrane protein (Biber & Lienhard 1986; Hickson et al. 2000). Values obtained for g VAMP/ 1×10^7 cells was divided by the molecular weight of the protein to give moles/ 1×10^7 cells. The mole value was multiplied by Avagadro's number to determine copy number per 1×10^7 cells, and thus the copy number per cell.

Protein	Copies per μg Membrane	Copies per Cell
VAMP2	3.5×10^9	8.6×10^5
VAMP3	6.1×10^9	1.5×10^6
VAMP4	1.9×10^9	4.8×10^5
VAMP5	2.3×10^8	5.8×10^4
VAMP7	2.1×10^8	5.3×10^4
VAMP8	1.4×10^{10}	3.5×10^6

4.3.4 Subcellular distribution of VAMP proteins in 3T3 L1 adipocytes

Having identified which VAMPs are up-regulated upon adipocyte differentiation and determined the abundance of each VAMP protein, the next step was to examine whether any of the VAMPs co-localised with insulin-sensitive GLUT4 in 3T3 L1 adipocytes. Under non-insulin-stimulated conditions the majority of the insulin-sensitive GLUT4 is found within intracellular organelles (Slot et al. 1991). These intracellular organelles can be separated by subcellular fractionation. In this process 3T3 L1 adipocytes were either left untreated or subjected to insulin-stimulation for 20 minutes; they were then subjected to a well-established subcellular fractionation protocol (Simpson et al. 1983; Piper et al. 1991; section 2.7.2). The subcellular localisation of each VAMP isoform was determined through immunoblotting, and representative blots of these experiments are shown in Figure 4-7.

As anticipated, under basal conditions GLUT4 was sequestered away from the plasma membrane (PM) fraction in the low density membrane fraction (LDM; Figure 4-7, Figure 4-8 A). Insulin-stimulation redistributed GLUT4 out of the LDM and led to a 1.7-fold increase in the amount of GLUT4 within the PM ($p < 0.01$, Figure 4-9), resulting in the majority of the cellular GLUT4 being found within the PM fraction in insulin-stimulated cells ($p < 0.05$, Figure 4-8 B).

Before examining the subcellular distribution of VAMPs, it was necessary to determine the purity of each of the fractions. To this end each fraction was subjected to immunoblotting with antibodies against proteins expected to be within each fraction. For the plasma membrane (PM) fraction the tSNARE protein syntaxin 4 (Sx4) was used, for the low density membrane fraction (LDM) fraction the cation-dependent mannose-6-phosphate receptor (CDMPR), for the high density membrane fraction (HDM) the endoplasmic reticulum (ER) resident protein calnexin was used, and for the soluble fraction glyceraldehyde 3-phosphate dehydrogenase (GAPDH) was used. The transferrin receptor (TfR) was used as a marker of GLUT4 vesicles within the constitutive recycling system and IRAP was used as a marker for GSVs. Figure 4-10 shows the distribution of these proteins under basal and insulin stimulated conditions. Most of the marker proteins were found in their expected locations. However, there was

contamination of the LDM with the soluble fraction (GAPDH was found in the LDM). Calnexin, which was used as a marker for the HDM, was found across all fractions, suggesting that there was contamination of all fractions with the ER.

Under basal conditions VAMP2 and 3 were found to be predominantly localised with insulin-sensitive GLUT4 in the LDM fraction (62% and 61% $p < 0.05$, Figure 4-8A). Similar to GLUT4, insulin led to a significant 2.2-fold increase in VAMP2 in the PM fraction and a concurrent reduction in the LDM fraction ($P < 0.01$, Figure 4-9). Insulin stimulation also redistributed VAMP3 out of the LDM (40% reduction $p < 0.05$, Figure 4-9) and increased the level seen in the PM fraction, although this increase was not significant ($p = 0.13$). The mobilisation of VAMPs 2 and 3 in response to insulin led to both VAMPs 2 and 3 being predominantly localised in the PM fraction in insulin-stimulated cells (54% and 46% respectively, $p < 0.05$, Figure 4-8 B).

In contrast to VAMPs 2 and 3, VAMP4 was similarly distributed across all 3 fractions and there was no significant redistribution of VAMP4 in response to insulin (Figure 4-8). VAMP5 was found to be evenly split between the PM and LDM fractions under basal conditions (Figure 4-8 A). Insulin-stimulation led to a significant 0.7-fold reduction in the level of VAMP5 in the LDM ($p < 0.01$, Figure 4-9). This resulted in 56% of VAMP5 being within the PM fraction following insulin-stimulation, significantly more than in any other fraction ($p < 0.05$, Figure 4-8 B).

In basal adipocytes VAMP7 was found predominantly within the LDM (43%, $p < 0.05$, Figure 4-8 A). Insulin did not result in any significant mobilisation of VAMP7 (Figure 4-9). VAMP8 was split evenly between the membrane fractions under both basal and insulin-stimulated conditions, and although insulin-stimulation mobilised VAMP8 out of the LDM, this had no significant impact on its subcellular distribution pattern (Figure 4-8, Figure 4-9).

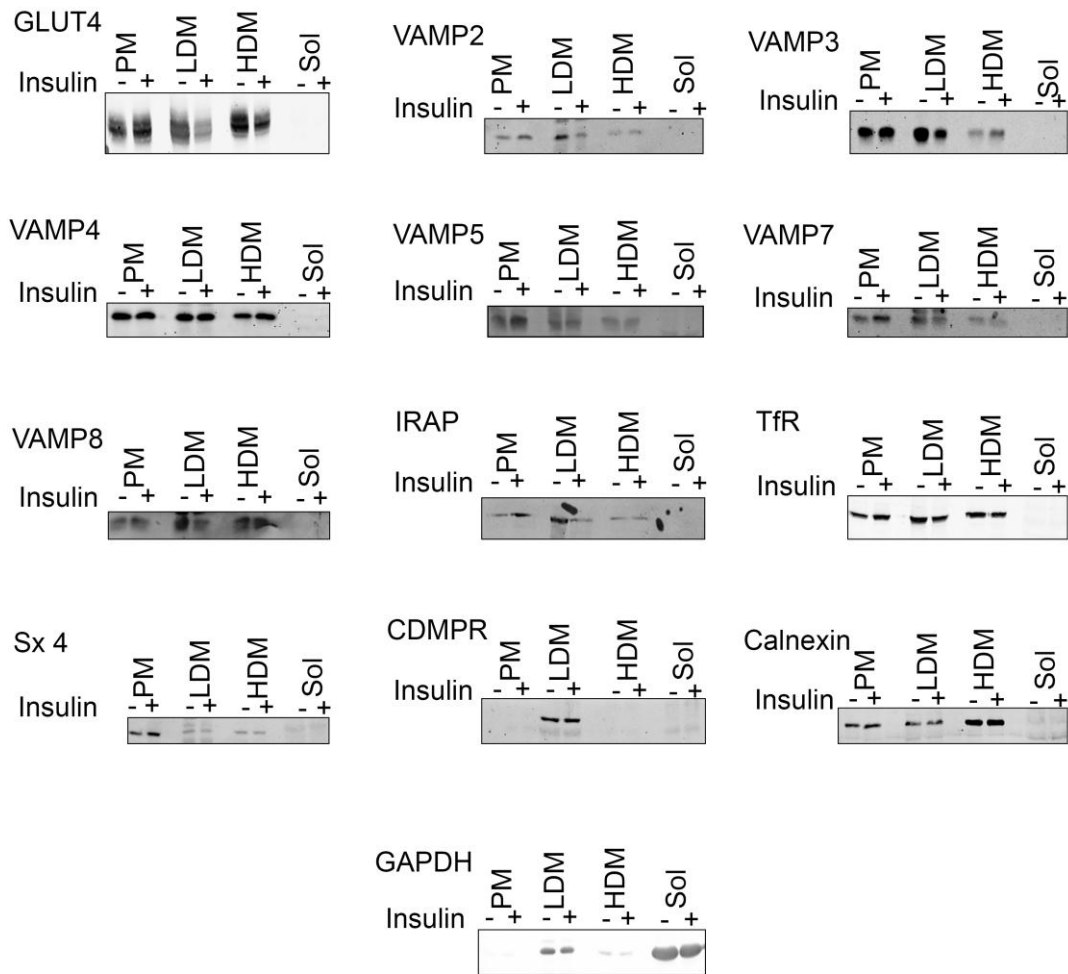


Figure 4-7: Representative immunoblots showing the subcellular distribution of each VAMP protein in 3T3 L1 adipocytes.

Fully differentiated 3T3 L1 adipocytes were serum-starved and then treated with (+) or without (-) 1 μ M insulin for 20 minutes. Subcellular fractionation was performed as described in Materials and Methods (section 2.7.2). The resultant fractions were the plasma membrane (PM), low density membranes (LDM), high density membranes (HDM) and soluble fraction (Sol). Fractions were resuspended in equal volumes of 1xLSB and subjected to SDS-PAGE and immunoblotting with the indicated antibodies. Shown are representative immunoblots of more than 3 separate experiments. IRAP=insulin responsive aminopeptidase, TfR = transferrin receptor, Sx4 = syntaxin 4, CDMPR = cation-dependent mannose 6-phosphate receptor, GAPDH = glyceraldehyde 3-phosphate dehydrogenase.

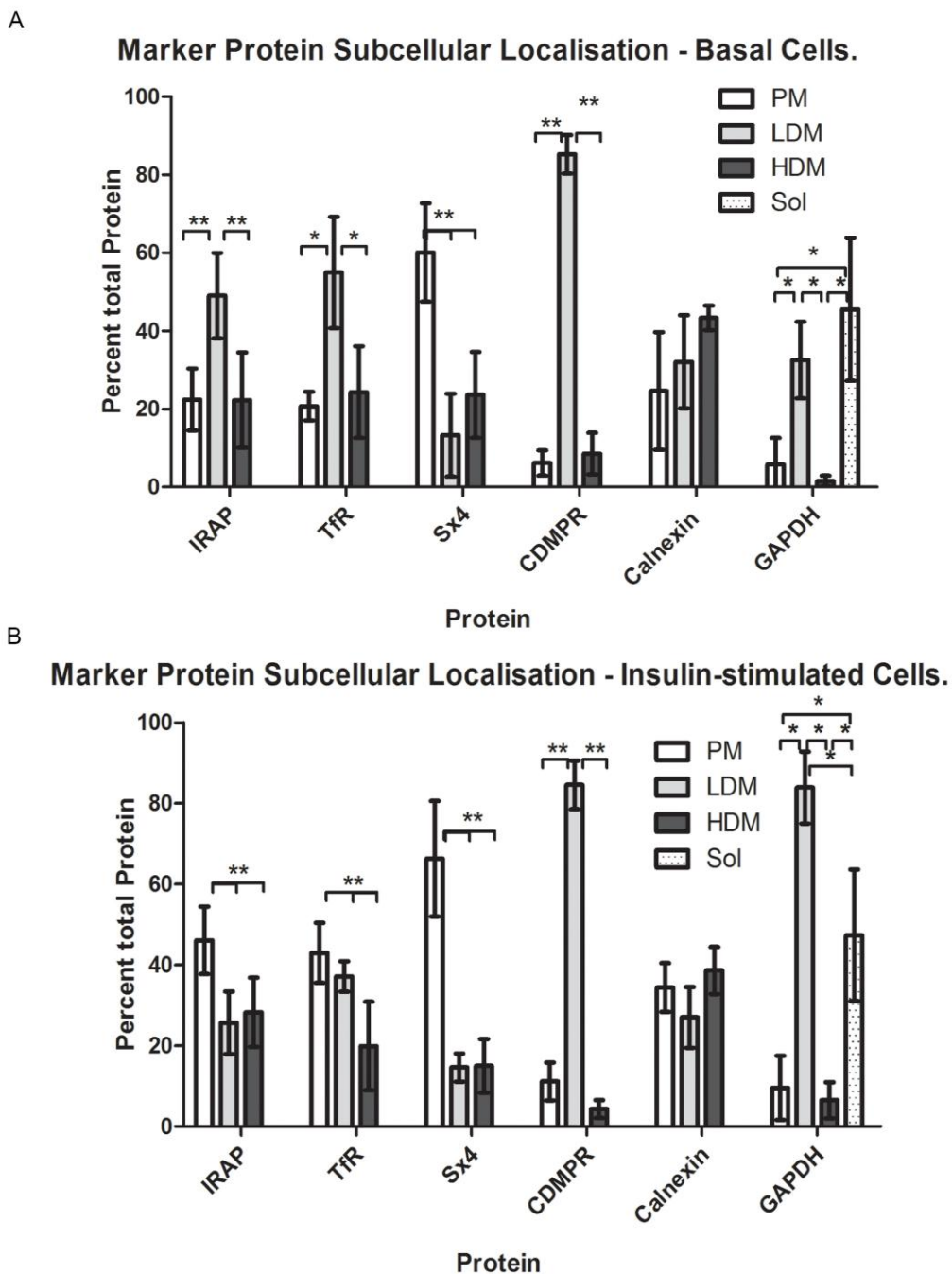


Figure 4-8: Localisation of marker proteins in basal (A) and insulin-stimulated 3T3 L1 adipocytes (B).

Percentage of the indicated protein in the PM, LDM, HDM and soluble fractions in basal (A) and insulin-stimulated (1 μ M insulin for 20 minutes) 3T3 L1 adipocytes (B) was determined. Values are the means \pm SD of 3 separate experiments, fractions were compared using a one way ANOVA, * = $p < 0.05$, ** = $p < 0.01$. IRAP=insulin responsive aminopeptidase, TfR = transferrin receptor, Sx4 = syntaxin 4, CDMPR = cation-dependent mannose 6-phosphate receptor, GAPDH = glyceraldehyde 3-phosphate dehydrogenase.

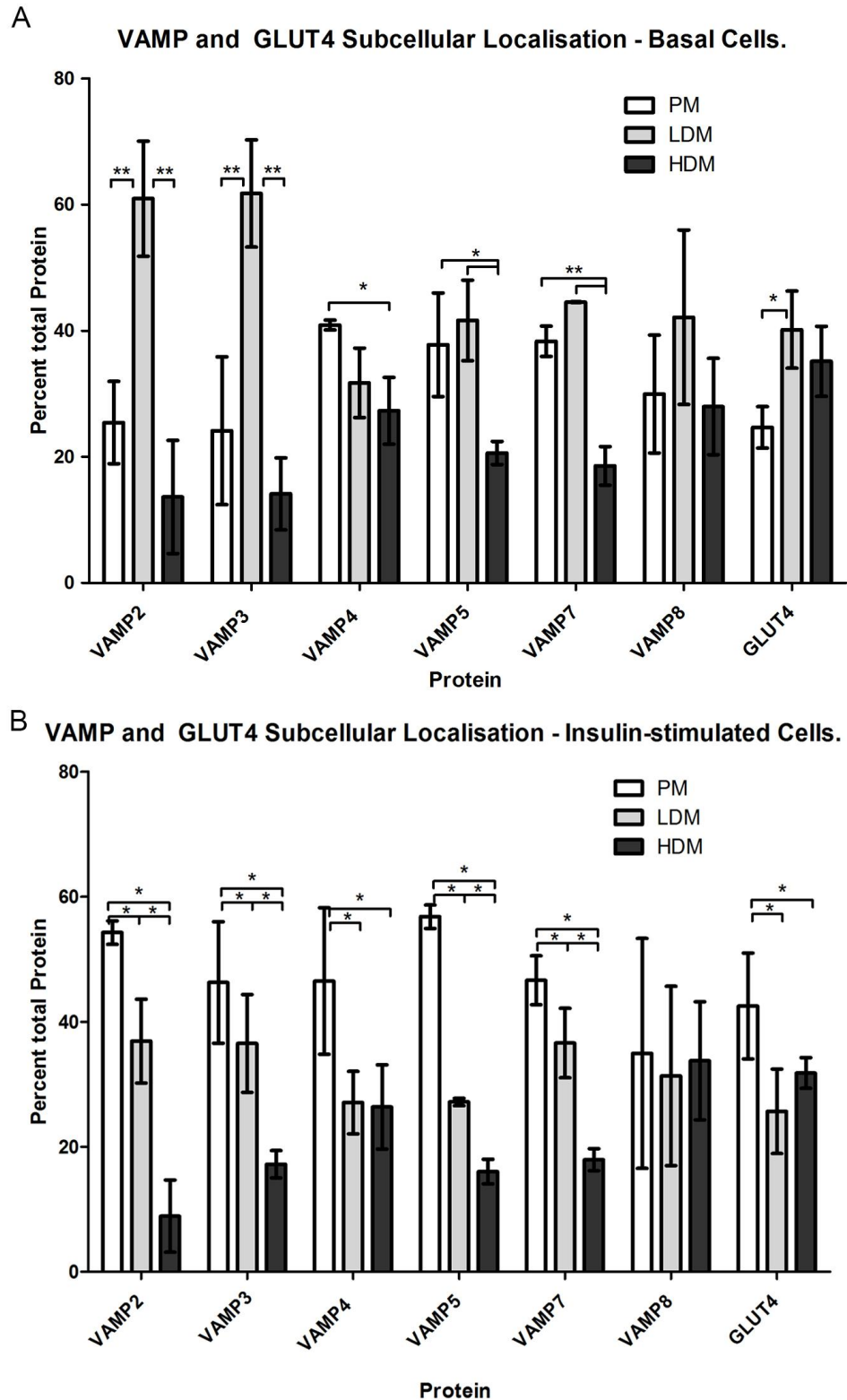


Figure 4-9: localisation of the vSNAREs and GLUT4 in basal (A) and insulin-stimulated (B) 3T3 L1 adipocytes.

Percentage of the indicated protein in the PM, LDM, HDM and soluble fractions in basal (A) and insulin-stimulated ($1\mu\text{M}$ insulin for 20 minutes) 3T3 L1 adipocytes (B) was determined. Values are the means \pm SD of 3 separate experiments, fractions were compared using a one way ANOVA, * = $p < 0.05$, ** = $p < 0.01$.

GLUT4 and VAMP Subcellular Localisation - Fold Change following Insulin-stimulation.

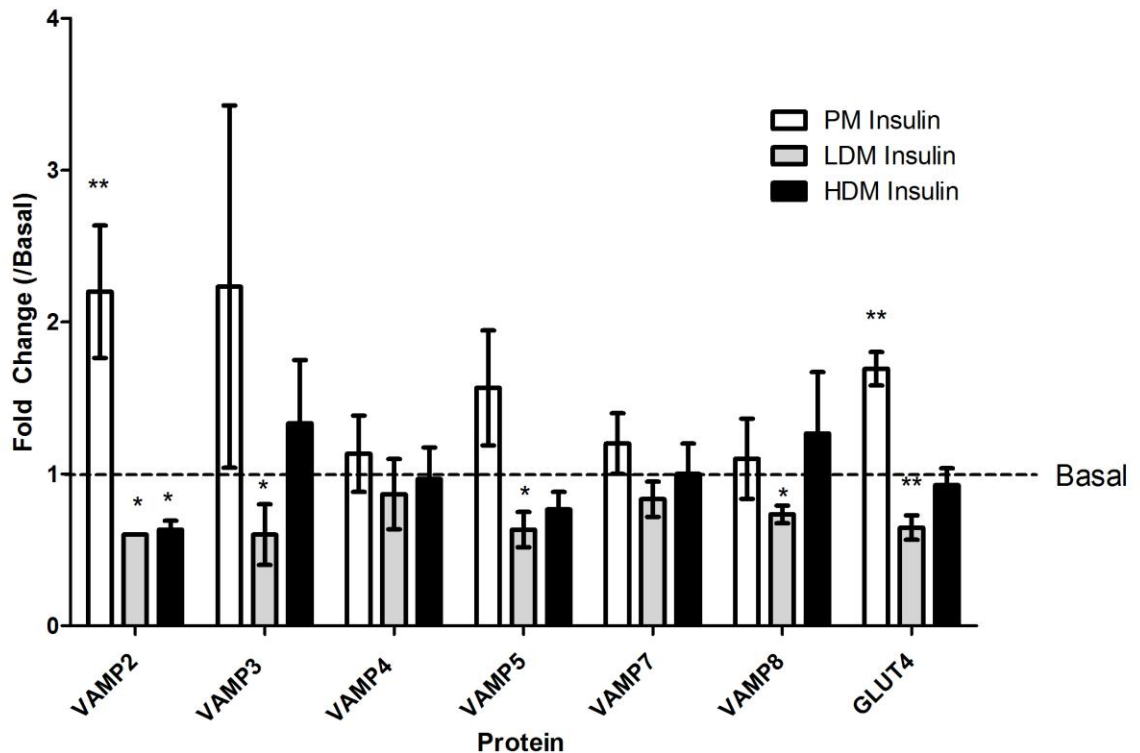


Figure 4-10: Effect of insulin stimulation on the distribution of GLUT4 and VAMP proteins in 3T3 L1 adipocytes.

Percentage protein in each fraction under insulin-stimulated (1 μ M insulin for 20 minutes) conditions was compared to the percentage in each fraction under basal conditions to give the fold change in protein content of each fraction in response to insulin-stimulation. Values represent means \pm SD of 3 separate experiments, fold change compared to basal values were compared using the Students t-test, * = $p < 0.05$, ** = $p < 0.01$.

4.3.5 Iodixanol gradient analysis of LDM fractions.

The subcellular distribution data (section 3.3.5) highlights that each VAMP protein is present in the fraction that contains insulin-sensitive GLUT4 (the LDM). However, the LDM contains GLUT4 in both the endosomal recycling pool (the ERC) and in the insulin sensitive pool (GSVs). These two pools can be separated out using iodixanol gradient centrifugation. This process has been described by Hashiramoto and James (2000). Briefly, the LDM fraction is isolated and resuspended in HES buffer, mixed with iodixanol, and subjected to centrifugation. Iodixanol acts as a self-forming gradient, separating out organelles based on density. Here, twelve 300 μ l fractions were collected from the bottom of the tube and subjected to immunoblotting with GLUT4 (Figure 4-11) and VAMP proteins (Figure 4-13). In order to confirm that the first denser peak (fractions 1 - 5) corresponds to GSVs and the second lighter peak (fractions 9 - 12) corresponds to the endosomal pool the distribution of GLUT4, the

transferrin receptor and IRAP was examined in fractions produced from basal and insulin-stimulated 3T3 L1 adipocytes. As anticipated, IRAP was predominantly localised to the first peak and the transferrin receptor in the second peak (Figure 4-12). GLUT4 was found within both the GSV and ERC peaks with more localised within the GSV peak (50% vs. 40%, $p < 0.01$) and insulin-stimulation led to a selective reduction in GLUT4 content in this peak (Figure 4-11, $p < 0.01$).

The distribution of the VAMP proteins was determined in the same manner as GLUT4, IRAP and the transferrin receptor. Representative immunoblots are shown in Figure 4-13. All proteins were localised within both the GSV and ERC pools, however their pattern of distribution between the two pools differed. VAMPs 2, 5 and 8 were evenly distributed between the GSV and ERC pools. VAMPs 3, 4 and 7 were found predominantly with the endosomal pool of GLUT4 (Figure 4-13 $p < 0.05$). This was most striking for VAMP3, which showed more than 75% was localised to the endosomal pool.

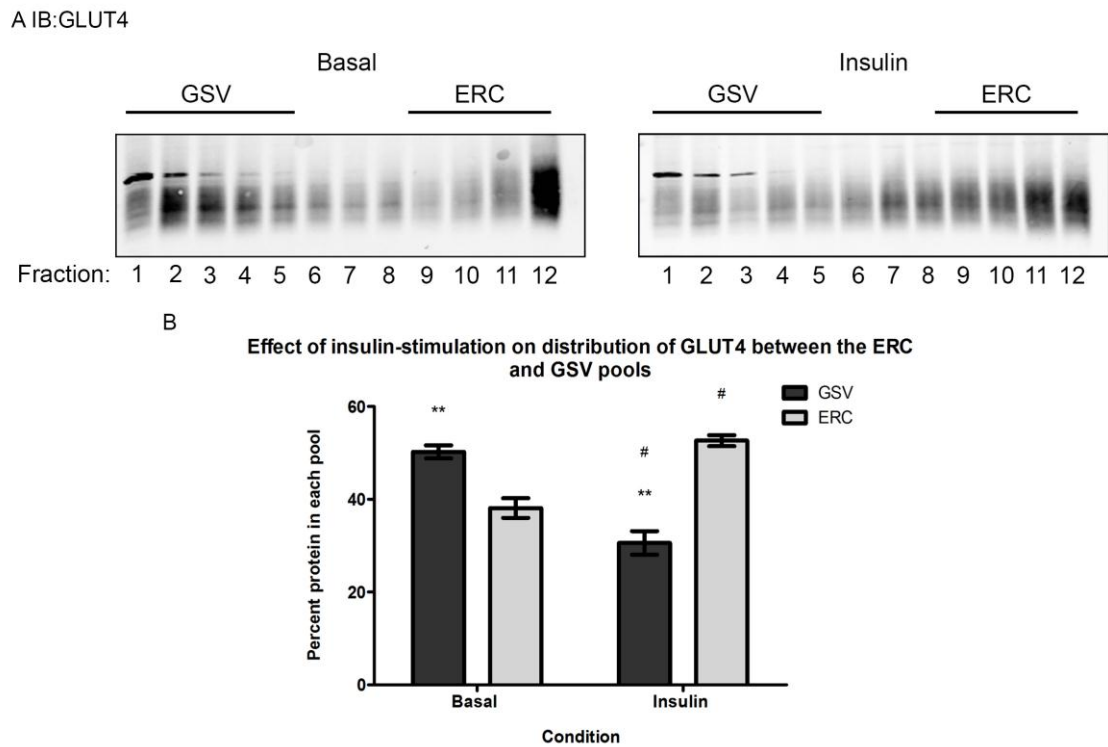


Figure 4-11: Localisation of GLUT4 in GSVs and the endosomal recycling compartment (ERC) fractions of 3T3 L1 adipocytes.

Low density membrane fractions (LDM) from serum-starved (basal) or insulin-stimulated ($1\mu\text{M}$ insulin for 20 minutes) 3T3-L1 adipocytes were resuspended in HES buffer and centrifuged at $295\,000\text{ xg}$ for 1 hour on a self-forming iodixanol gradient as described (section 2.7.3). Twelve equal volume fractions were collected and subjected to SDS-PAGE followed by immunoblotting with anti-GLUT4. Fractions were loaded in order of decreasing density, fractions 1 - 5 represent GSVs and 9 - 12 endosomal recycling compartment (ERC). Shown are immunoblots from a typical experiment (A). the mean values \pm SD for percentage of GLUT4 found in the GSV and ERC pools from 5 separate experiments were calculated by comparing the intensity signal in this fraction (1-5 or 9-12) to the intensity signal across all fractions (B) values were compared using the Student's t-test ** = $p < 0.01$ vs ERC, # = $p < 0.01$ vs basal.

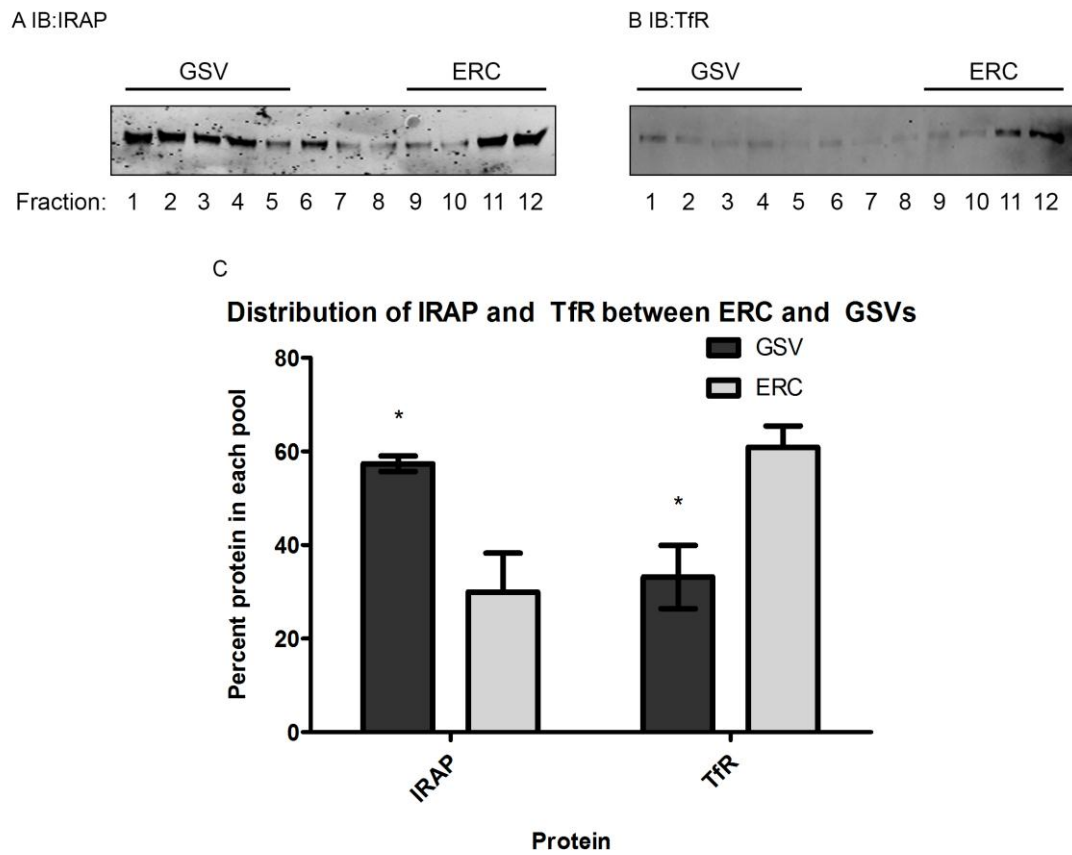


Figure 4-12: Localisation of IRAP and TfR in GSVs and ERC fractions of 3T3 L1 adipocytes. Iodixanol gradients prepared as in Figure 4-11 and used to determine the distribution of IRAP and TfR. Fractions were loaded in order of decreasing density, fractions 1 - 5 represent GSVs and 9 - 12 ERC. Shown are immunoblots from a typical experiment (**A**: IRAP, **B**:TfR) and the mean values \pm SD for percentage of total protein across all fractions found in the GSV and ERC pools from 3 separate experiments (**C**) values were compared using the Student's t-test * = $p < 0.05$ ERC.

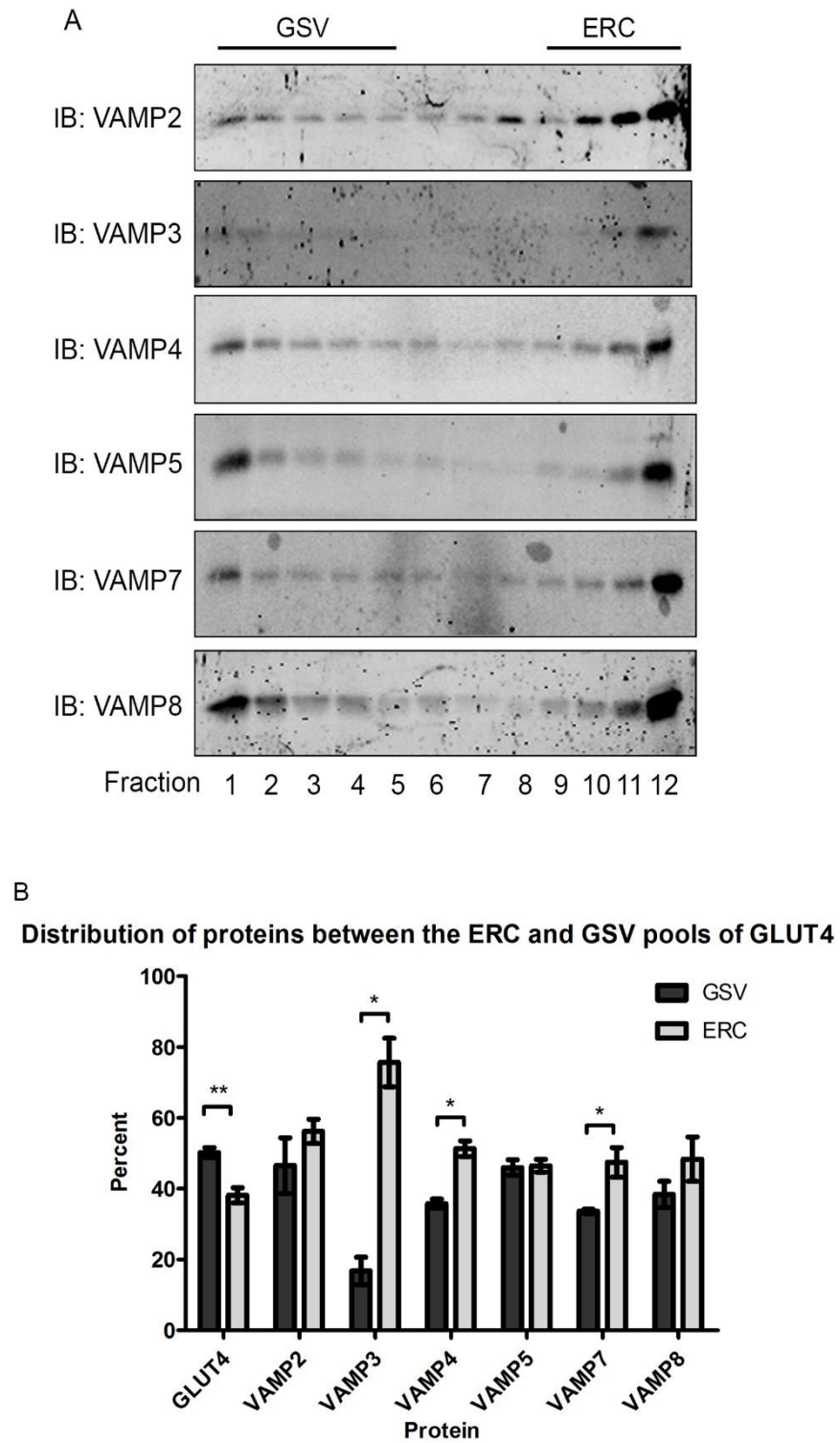


Figure 4-13: Localisation of VAMP proteins in GSVs and ERC fractions of 3T3 L1 adipocytes. Iodixanol gradients prepared as in Figure 4-11 and used to determine the distribution of VAMP proteins. Fractions were loaded in order of decreasing density, fractions 1 - 5 represent GSVs and 9 - 12 ERC. Shown are immunoblots from a typical experiment (**A**) and the mean values \pm SD for percentage of total protein across all fractions found in the GSV and ERC pools from 3 separate experiments (**B**) values were compared using the student's t test * = $p < 0.05$, ** = $p < 0.01$.

4.4 Discussion

The data presented here shows that the expression level of VAMPs 2, 3 and 4 is increased in response to differentiation. It has been demonstrated that, in 3T3 L1 adipocytes, VAMP8 is the most abundant isoform, followed by VAMPs 3, 2, and 4. In contrast, VAMPs 5 and 7 are expressed at very low levels in this cell type. Through the subcellular fractionation of 3T3 L1 adipocytes, it has been shown that although all VAMPs expressed in adipocytes localise with insulin-sensitive GLUT4, they do so to varying degrees, and each of VAMP shows different translocation responses to insulin-stimulation.

4.4.1 Methodological Considerations

It is important to note a few caveats with the methodology used to produce this data. The estimation of copy number of each of the VAMP proteins is reliant on a number of assumptions. First, that the VAMP antibodies are specific to the named VAMP. This was tested by assessing the binding of each antibody to recombinant VAMP proteins (Figure 4-1). Each VAMP antibody was found to selectively react with the named VAMP. Second, it assumes that the VAMP antibodies bind the GST-tagged VAMPs to the same degree as to endogenous VAMP. This is likely to be the case as the only differences between the recombinant VAMPs and endogenous VAMP were that the recombinant VAMPs lack their transmembrane domains and are tagged at their N terminus with GST. It is also important to note that the quantification analysis only took into account signals from antibodies reacting with proteins found at the predicted molecular weight for each VAMP. Therefore, it is possible that some VAMP was present in an SDS resistant SNARE complex and thus excluded from analysis.

There are also some caveats with the subcellular fractionation protocol. The first being the cross contamination of fractions, particularly the contamination of fractions with components of the ER (Figure 4-8; Simpson et al 1983). Simpson et al. (1983) used a similar subcellular fractionation protocol in rat adipocytes and examined the activity of organelle-specific enzymes to determine their localisation within each fraction. Based on the relative densities of the PM, Golgi, endoplasmic reticulum (ER) and mitochondria these should have been localised to the PM, LDM, HDM and mitochondrial fraction respectively. However, Simpson et al. (1983) found there was significant cross contamination

of these organelles within each fraction (Simpson et al. 1983). Here, calnexin, an ER resident enzyme, was distributed across the PM, LDM and HDM, and GAPDH, a soluble enzyme, was found in both the soluble fraction and the LDM (Figure 4-10). This means the determination of GLUT4 in the HDM and soluble fraction may be an underestimate. However, it may explain the high levels of GLUT4 seen in the PM under basal conditions here (Figure 4-7; Figure 4-8).

Although under basal conditions GLUT4 was predominantly localised to the LDM fraction, it was also present in the HDM and the PM, which is in contrast to previous studies that have used similar protocols (Simpson et al. 1983; Piper et al. 1991), and those examining GLUT4 distribution using microscopy (Slot et al. 1991). Localisation to within the PM fraction does not mean that the GLUT4 is inserted into the plasma membrane and the high localisation of GLUT4 within the PM could be due to vesicles docked on material that is pelleted alongside the PM. Some of the material recovered in the PM fractions is likely to be from the ER as there was significant contamination of this fraction with calnexin (Figure 4-8). The amount of non-PM material isolated with the PM fraction will be dependent on the homogenisation method used. Here, homogenisation was achieved by passing cell lysates through a 24 gauge needle 10 times, then a 26 gauge needle twice, which may not have been sufficient to detach all material surrounding the plasma membrane from the PM. Despite the high level of GLUT4 in the PM under basal conditions, there was a robust insulin-stimulated mobilisation out of the LDM and into the PM (Figure 4-10)Figure 4-10.

4.4.2 VAMPs involved in fusion of GLUT4 containing vesicles with the PM.

There has been much debate as to the vSNARE requirements for fusion of GLUT4 containing vesicles with the plasma membrane in response to insulin in adipose tissue. Most data supports the role of VAMP2, however some suggest roles for VAMP3 and 8 as well. This comes from the identification of VAMPs 2, 3 and 8 on GLUT4 containing membranes (Martin et al. 1996; Larance et al. 2005; Zhao et al. 2009) and from studies that have found insulin-stimulated GLUT4 translocation is not impaired following VAMP protein removal (Hajduch et al. 1997; Zhao et al. 2009). However, immunoisolation of GLUT4 membranes does not separate the source of GLUT4 membrane, and the use of toxins and knock

out mice models to deplete cells of VAMPs disrupts the natural physiological environment, meaning there may be compensation by other VAMPs or upregulation of other GLUT4 trafficking pathways. The data presented in this chapter on the absolute levels of each of the VAMP proteins, their response to adipocyte differentiation and their subcellular distribution and localisation alongside insulin-sensitive GLUT4 under physiological conditions, supports the view that the fusion of GSVs with the plasma membrane predominantly involves VAMP2.

VAMPs 2 and 3 but not VAMP8 are upregulated upon adipocyte differentiation (Figure 4-3). It is well documented that key regulators of the insulin-response in adipocytes such as GLUT4, IRAP, sortilin and syntaxin 16 are upregulated with adipocyte differentiation (El-Jack et al. 1999; Ross et al. 1996; Shi & Kandror 2005; Roccisana et al. 2013). That VAMP8 levels remain unchanged upon differentiation, despite large increases in cellular total protein content, suggests that the requirement for VAMP8 is not upregulated in adipocytes compared to fibroblasts. Therefore VAMP8 is unlikely to be involved in the fusion of GLUT4 containing vesicles with the plasma membrane.

Here, large increases in the levels of VAMPs 2, 3 and 4 were seen following differentiation. In contrast to this Williams and Pessin (2008) found only small changes in the levels of VAMP protein with adipocyte differentiation. This difference could be due to the methodology used. Although Williams and Pessin (2008) did not state if equal numbers of cells or equal total protein levels were compared, if the levels of VAMP protein are compared per mg of protein changes may be missed due to the large increase in total protein content in adipocytes compared to fibroblasts.

VAMP2, 3 and 8 are all found on GLUT4 containing membranes (Martin et al. 1996; Larance et al. 2005; Zhao et al. 2009). By separating out GLUT4 containing compartments it can be seen that VAMP2 localises to the same compartment as insulin-sensitive GLUT4 (the LDM; Figure 4-7 Figure 4-9A), translocates to the PM alongside GLUT4 in response to insulin (Figure 4-10) and when the pools of GLUT4 within the LDM are separated VAMP2 localises to the insulin-sensitive pool (Figure 4-13). VAMP3 also localises to the LDM and translocates to the PM with insulin (Figure 4-9A, Figure 4-10) However, unlike VAMP2, the VAMP 3 in the LDM

is predominantly (>75%) localised with GLUT4 in the endosomal system (Figure 4-13).

The finding that VAMP2 and 3 are present with separate pools of GLUT4 is in agreement with ablation and immunoelectron studies (Martin et al. 1996). These studies have shown that VAMP2 and 3 are on different populations of GLUT4 containing vesicles, and that VAMP3 but not VAMP2 is localised with the transferrin receptor. The data presented here supports a role for VAMP2 in the fusion of GLUT4 containing vesicles with the plasma membrane from the insulin-sensitive store (GSVs) and VAMP3 in the fusion of GLUT4 containing vesicles from the endosomal recycling pool (ERC).

4.4.3 Plasticity in vSNARE requirements for GLUT4 fusion with the plasma membrane – Possible Mechanisms

Although VAMP2 seems to be the vSNARE involved in the fusion of GSVs with the plasma membrane in response to insulin-stimulation, there is clear evidence of plasticity between VAMP2, 3 and 8 but not 4, 5 or 7 in the fusion of GLUT4 containing vesicles with the plasma membrane (Zhao et al. 2009). The results presented here help to uncover the possible mechanisms of this plasticity.

It is important to note that the studies by Zhao et al. (2009) were conducted in an artificial environment, as VAMP proteins were removed either by using mouse embryonic fibroblasts from knock out animals (VAMP2 or 8 knockout) or by treatment with TeNT to cleave VAMP2 and 3 for 2 days. These conditions may allow compensatory mechanisms to be upregulated. Furthermore, VAMP2 knockout has been proposed to prevent the entry of GLUT4 into GSVs and VAMP8 has been identified as being involved in GLUT4 endocytosis (Williams & Pessin 2008; see Chapter 6). Therefore under the conditions employed by Zhao *et al.* (2009) to examine plasticity, GLUT4 may not have been correctly sorted and the results obtained may not be representative of the processes that occur *in vivo*. Putting these considerations to one side, the quantification and subcellular fractionation data presented here can help to dissect why some VAMP isoforms but not others are able to compensate in GLUT4 trafficking to the PM in response to insulin.

As described, VAMP2 is present on GSVs, whereas VAMP3 is present on GLUT4 containing vesicles within the endosomal recycling system (Martin et al. 1996; Figure 4-13). Therefore in the absence of VAMP2, the GLUT4 translocation seen by Zhao et al. (2009) may have been from the endosomal recycling compartment. Figure 4-6 shows VAMPs 2, 3 and 8 are expressed at the highest levels in 3T3 L1 adipocytes (with 8.6×10^5 , 1.5×10^6 and 3.5×10^6 copies per cell respectively; Figure 4-3), and the values reported for VAMP2 and 3 are in agreement with those previously reported using a similar approach (Hickson et al. 2000). The finding that the VAMPs expressed at the highest levels in 3T3 L1 adipocytes are those that show plasticity (VAMPs 2, 3 and 8,) is intriguing as it highlights the possibility that the reason that VAMPs 3 and 8, but not any other VAMPs can compensate for the loss of VAMP2 is due to their high levels of expression (Zhao et al 2009).

Both VAMP5 and 7 have been identified on immunoprecipitated GLUT4 vesicles in muscle (Rose et al. 2009). In cardiomyocytes VAMP5 has been shown to have a role in the trafficking of GLUT4 to the plasma membrane in response to insulin (Schwenk et al. 2010). The subcellular fractionation data presented here suggests that VAMP5 is also present on GSVs in adipose cells. VAMP5 is localised with insulin-sensitive GLUT4 and it translocates out of this compartment in response to insulin (Figure 4-8, Figure 4-9, Figure 4-13). VAMP5 also interacts with the tSNARE involved in insulin-stimulated GLUT4 translocation, syntaxin 4, *in vivo* (Chapter 3; Figure 3-4). Taken together these observations make it tempting to speculate that VAMP5 is involved in the fusion of GSVs with the plasma membrane in both muscle and adipose cells, but that in 3T3 L1 adipocytes, the contribution it plays is small due to its low expression level. In contrast to this, VAMP7 did not mobilise in response to insulin so is unlikely to be present on insulin-sensitive GLUT4 vesicles in any significant amount, although it is involved in the fusion of GLUT4 containing vesicles with the PM in response to osmotic shock (Randhawa et al. 2004; Williams & Pessin 2008), and therefore must be present on some population of GLUT4 containing vesicles. These observations predict that both VAMP5 and 7 should be able to compensate in the fusion of GLUT4 containing vesicles with the plasma membrane when VAMP2, is removed. However, neither VAMPs 4, 5 nor 7 can (Zhao et al. 2009).

This may be a function of these proteins' expression levels and subcellular distributions. The levels of VAMP5 and 7 are very low compared to levels of the other VAMP proteins (Figure 4-6). The subcellular fractionation data indicates that although VAMPs 4 and 7 are found within the same compartments as insulin-sensitive GLUT4, they are not present on insulin-sensitive GLUT4 containing vesicles. The subcellular fractionation protocol does not selectively isolate GLUT4 containing vesicles. However the presence of proteins on insulin-sensitive GLUT4 vesicles can be inferred by their translocation, alongside GLUT4, in response to insulin. Neither VAMP4 nor VAMP 7 translocated with GLUT4 to the plasma membrane in response to insulin-stimulation. They are therefore probably not present on insulin-sensitive GLUT4 containing vesicles.

Zhao et al. (2009) found that VAMP8 was able to compensate for the loss of VAMP2 and 3. Yet, VAMP8 did not translocate to the plasma membrane in response to insulin (Figure 4-10), and the levels of VAMP8 did not increase with differentiation (Figure 4-3)). These data suggest that, similar to VAMPs 4 and 7, VAMP8 is not present on insulin-sensitive GLUT4 containing vesicles and is not normally involved in the fusion of GLUT4 vesicles with the plasma membrane. However, VAMP8 is expressed at very high levels (Figure 4-6), so although it is not selectively sorted onto GLUT4 containing vesicles, some VAMP8 may be mis-sorted onto GLUT4 vesicles. This value is probably low in terms of percentage of the total VAMP8 within adipose cells, but may be a sufficient amount to act in the fusion of GLUT4 vesicles with the plasma membrane.

4.4.4 How many VAMPs per insulin sensitive GLUT4 vesicle?

The information presented here regarding the copy number and subcellular distribution of each of the VAMP proteins and GLUT4 allows the number of each of the VAMP proteins found with a single insulin sensitive GLUT4 molecule to be estimated.

There are 2.8×10^5 copies of GLUT4 in a 3T3 L1 adipocyte cell (Calderhead et al. 1990). 40% of the total GLUT4 is in the LDM (Figure 4-9A), this corresponds to 112,000 copies of GLUT4 in the LDM, 50% of the GLUT4 within the LDM is in GSVs. Assuming all GLUT4 present in the GSV fraction is actually on GSVs, this gives 56,000 GLUT4 molecules on GSVs. Using the same calculations (8.5×10^5

copies VAMP2, 60% in the LDM, 46% in GSVs) there are 241,453 copies of VAMP2 on insulin-sensitive GLUT4 vesicles, this is four per GLUT4, using the same calculations there are two VAMP3 molecules per GLUT4 (1.5×10^6 copies VAMP3, 60% in the LDM, 14.4% on GSVs).

There are 3.5×10^6 copies of VAMP8, of which 40% are in in the LDM and 38% of VAMP8 in the LDM colocalises with insulin-sensitive GSVs. Insulin-stimulation had no effect on the distribution of VAMP8, so it is likely VAMP8 is not selectively sorted onto GSVs, its presence alongside insulin-sensitive GLUT4 is likely due to its localisation with other organelles of similar densities. However, the sorting of SNARE proteins on to the correct membranes is unlikely to be completely accurate meaning some mis-sorting of proteins is inevitable. If 20% of the total VAMP8 within the compartments containing insulin-sensitive GLUT4 is mis-sorted and localised to GSVs, this corresponds to 108,646 copies of VAMP8, which is roughly 2 per GLUT4.

Estimates of the number of SNARE proteins required for membrane fusion vary from between 1 and 15 complexes. These estimations come from studies that have examined *in vitro* fusion of liposomes with varying numbers of SNARE proteins. Van den Bogaart et al. (2010) found that liposomes containing a single SNARE are capable of fusion, and isolated synaptic vesicles require only one tSNARE for fusion (van den Bogaart et al. 2010). Shi et al. (2013) found that nanodiscs were capable of fusing with only one SNARE complex being present (Shi et al. 2013). However they found that for the fusion pore to be open for long enough for content mixing, 3 SNARE complexes were required. Conversely, Karatekin et al. (2010) found that between 5 and 10 SNARE complexes are required for fusion (Karatekin et al. 2010).

The major difference in these studies can be explained by the protein density of the liposome membranes. Karatekin et al. (2000) used polyethylene glycol (PEG) to increase the protein density of the liposome. At high protein densities lateral diffusion of the SNAREs is limited, whereas at lower densities there is free lateral diffusion (van den Bogaart et al. 2010). Free lateral diffusion of the SNARE means that the VAMP can engage with the tSNARE more readily, as the VAMP can diffuse through the membrane to the site of the tSNAREs, therefore fusion is independent of the orientation of the vesicle. However, when lateral

diffusion is limited, the probability of the VAMP engaging with the tSNARE is reduced and thus the estimation of the number of VAMPs being required for fusion may be higher. The protein composition of GSV is largely unknown, and the requirement for lateral diffusion of vSNAREs is also unknown. Although this has not been examined, it is possible that one role of docking factors might be to help to orientate the GSV so the vSNARE is in the correct position to form complexes with tSNAREs, thus allowing fusion to occur with lower vSNARE densities.

Other studies examining the number of SNARE complexes required for membrane fusion have done so *in vivo* by blocking SNARE complex formation. These studies have used titration assays to block fusion with mutant SNAP25 (Mohrmann et al. 2010), selective proteolysis of SNAP25 (Keller et al. 2004; Montecucco et al. 2005) and VAMP2 peptides (Hua & Scheller 2001), and found between 1 and 15 SNARE complexes are required for fusion.

It has also been noted that the vesicle size and membrane curvature may be important when determining the number of SNARE proteins required to facilitate membrane fusion events. The critical vSNARE density below which liposome fusion cannot occur is 1.5 to 3 times larger for large (80nm diameter) liposomes than small liposomes (25nm diameter) (Hernandez et al. 2014). The total number of vSNARE proteins required on a small liposome for fusion to occur was approximately three. In contrast, between 23 to 30 vSNAREs were required to fuse large liposomes. It must be noted that this is the total number of vSNAREs on the entire liposome not the local concentration of vSNAREs at the contact site. Nevertheless, GSVs are small (~50nm in diameter), this is somewhere between the two sizes of vesicle assessed by Hernandez et al. (2014) so this would correspond to somewhere around a total of 15 vSNAREs spread around the surface area of the vesicle. A vesicle of 50nm diameter has a surface area of $7.8\mu\text{m}^2$. Assuming an equal distribution of vSNAREs throughout the vesicle, 15 vSNAREs in a vesicle of 50nm in diameter would give approximately one vSNARE every 500nm^2 on the surface of the vesicle.

Although the studies discussed above have been informative, they have all provided estimates on SNARE requirements for fusion based on indirect measurements or measurements *in vitro*. A more direct measure has been

provided by Sinha et al. (2011), pHluorin tagged VAMP2 was used to quantitatively examine the number of VAMP proteins required for synaptic vesicle fusion when wild type VAMP2 was removed and replaced by pHluorin VAMP2. The results of these studies suggested that two VAMP2 molecules were sufficient for membrane fusion to occur (Sinha et al. 2011).

On balance there seems to be a general consensus in the literature that around 3 SNARE complexes are sufficient for fusion. These estimations are not dissimilar to the estimations of the numbers of VAMP2 found per GLUT4 molecule made above. Calculations based on the copy number and distribution of VAMP2 give values of four VAMP2 molecules per GLUT4. If there were one GLUT4 per GSV, this would give four VAMP2 molecules per GSV, which may be sufficient to facilitate membrane fusion. However, there is some evidence that GSVs contain more than one molecule of GLUT4 (Kupriyanova et al. 2002). If this were the case then the number of VAMP proteins on a GSV would increase accordingly, two molecules of GLUT4 would give 8 of VAMP2 and so on. This brings the predicted number of VAMP2 molecules per GSV well into the range of estimations of SNARE complex requirements for fusion.

However these estimations of both SNARE complex requirements for fusion and VAMP per GSV, are vastly different to the number of VAMP2 found on synaptic vesicles (Takamori et al. 2006). Takamori et al. (2006) found that synaptic vesicles contain, on average, 70 copies of VAMP2. This difference may reflect differences in the time scale required for these two fusion events. Synaptic vesicles must fuse within milliseconds. A high density of VAMP2 may assist in this rapid fusion by ensuring that whatever orientation the vesicle is in when it docks with the synaptic membrane, there is always a vSNARE available to engage with the tSNARE so fusion can occur rapidly. Conversely, compared to synaptic vesicle fusion, in GSV fusion with the plasma membrane occurs on within a relatively slow time scale. This means there is more time available for either the VAMP to diffuse to the docking site and the site of the tSNAREs, or for the vesicle to re-orientate so the VAMP can engage with the tSNARE complex.

It must be noted that the calculations of the number of VAMPs per GLUT4 molecule are based on a few large assumptions. Firstly the calculations assume that all the GLUT4, VAMP2 and VAMP3 (and 20% of the VAMP8) present in the

GSV peak is actually on GSVs and not on other compartments of similar density (for example, other vesicles within the LDM such as trafficking vesicles). Secondly, that the VAMPs found in the GSV peak distribute among GLUT4 containing vesicles evenly.

4.5 Conclusions

In summary the data presented in this chapter supports previous suggestions that VAMP2 is the predominant VAMP on GSVs. The data also indicates that under conditions of VAMP2 loss, compensation seen by VAMP3 may be due to translocation from the ERC pool of GLUT4. It has also been demonstrated that although VAMP8 is not selectively sorted onto GLUT4 containing membranes it may be present on GSVs in sufficient numbers to allow for the translocation of GLUT4 to the plasma membrane. Thus data presented here explains possible mechanisms for plasticity amongst the vSNAREs VAMP2, 3 and 8 in GLUT4 translocation to the plasma membrane.

Chapter 5 - Interactions between VAMPs and syntaxin 16 and mVps45.

5.1 Introduction

5.1.1 tSNAREs involved in recycling of GLUT4

As described, GLUT4 traffics from the plasma membrane to early endosomes. From here approximately half of the total cellular GLUT4 is then trafficked into specialised insulin sensitive GSVs (Livingstone, James, Rice, Hanpeter, & Gould, 1996; Martin et al., 1996; Figure 4-11). GLUT4 traffics into GSVs via a subdomain of the TGN that is enriched in both syntaxin 6 and 16, but lacks TGN38 (Martin et al. 1994; Shewan et al. 2003). Syntaxin 6 and 16 are both present on isolated GLUT4 containing membranes and translocate to the plasma membrane in response to insulin (Perera et al. 2003; Shewan et al. 2003). This suggests that both syntaxin 6 and 16 are components of GSVs. Indeed, iodixanol gradient analysis separating out the specialised insulin-sensitive GSV pool from GLUT4 containing membranes in the endosomal recycling pool, has shown that syntaxin 6 and 16 both co-sediment with GSVs (Perera et al. 2003). The localisation of these tSNAREs with GSVs indicates that syntaxin 6 and 16 may be essential components of the GLUT4 recycling machinery involved in the formation of GSVs.

Roles for syntaxin 6 and 16 in the recycling of GLUT4 have been uncovered through experiments that have expressed the cytosolic portions of these proteins and examined GLUT4 trafficking. Cytosolic portions of SNARE proteins act as competitive inhibitors of their endogenous counterparts by forming dead-end complexes with their SNARE partners. Expression of the cytosolic domain of syntaxin 6 increases basal glucose uptake (Perera et al. 2003). Similarly, expression of the syntaxin 16 cytosolic domain reduces insulin simulated glucose transport (Proctor et al. 2006). Furthermore, expression of the cytosolic domains of either syntaxin 6 or 16 significantly reduces the internalisation of GLUT4 following insulin withdrawal (Perera et al. 2003; Proctor et al. 2006). Taken together these data suggest that a SNARE complex that includes both syntaxin 6 and 16 may function in the formation of insulin sensitive GSVs.

However, as yet the vSNARE involved in this SNARE complex has remained undefined. Syntaxin 6 has been shown to have multiple SNARE partners. It has been implicated in multiple SNARE complexes and membrane trafficking events,

ranging from secretory granule maturation to exocytosis (Wendler & Tooze 2001). This raises the possibility that the effects of disruption of syntaxin 6 activity on GLUT4 trafficking may not be via its involvement with syntaxin 16, but through involvement with other SNARE complexes. With this in mind, although there is no direct evidence that syntaxin 6 acts with syntaxin 16 to mediate the trafficking of GLUT4 into GSVs, the available data suggests that this is likely. It has been shown in HeLa cells that a tSNARE complex made up of syntaxin 6/16 and Vti1a is required for the retrograde trafficking of the Shiga toxin from the early/recycling endosome to the TGN (Mallard et al. 2002). This trafficking pathway is the proposed route that GLUT4 takes en route to GSVs (Chapter 1, Figure 1-3). Mallard et al. (2002) found that inhibition of the activity of syntaxin 6, 16 or Vti1a prevented the passage of the Shiga toxin from the early/recycling endosome to the TGN. To determine if syntaxin 6 and 16 were acting in the same step as part of a complex, they determined whether the effects of the syntaxin 6 and 16 inhibition were additive and whether syntaxin 6 and 16 co-immunoprecipitated with one another. Through these methods, they determined that syntaxin 6 and 16, and Vti1a, act as a tSNARE complex to traffic the Shiga toxin from the early/recycling endosome to the TGN. It seems likely this tSNARE complex also acts in retrograde GLUT4 trafficking in 3T3 L1 adipocytes. The phenotypes seen with depletion or inhibition of either syntaxin 6 or 16 on GLUT4 localisation in this cell type are consistent with impaired retrograde trafficking of GLUT4 from the endosomal pool into GSVs (Perera et al. 2003; Proctor et al. 2006). Therefore, although it is possible that syntaxin 6 is involved in the trafficking of GLUT4 in a manner independent of syntaxin 16, the available data suggests that syntaxin 6 and 16 act together to form a tSNARE complex that is required for the trafficking of GLUT4 from the endosomal compartment into GSVs.

Although, as discussed in Chapter 3, SNARE protein binding seems to be highly promiscuous *in vitro*, *in vivo* measurements of SNARE protein binding partners provides a valuable starting point in determining the SNARE proteins involved in fusion events. Syntaxin 6 and 16 have been identified as important in the trafficking of GLUT4 into GSVs (Perera et al. 2003; Shewan et al. 2003; Proctor et al. 2006), and it is likely they do so by acting in the same complex. The vSNARE involved in this membrane fusion event has not yet been defined.

Syntaxin 6 has multiple vSNARE partners including VAMPs 2, 3, 4, 7 and 8 (Wendler & Tooze 2001). Furthermore, the tSNARE complex made up of syntaxin 6 and 16 interacts with both VAMPs 3 and 4 in HeLa cells (Mallard et al. 2002). As well as performing co-immunoprecipitation experiments to determine the tSNARE complex involved in retrograde trafficking, Mallard et al. (2002) performed co-immunoprecipitation experiments to determine the vSNARE involved in this pathway. They found that syntaxins 6 and 16, as well as Vti1a could co-immunoprecipitate VAMP3 and VAMP4, however VAMP4 did not co-immunoprecipitate VAMP3. This suggests that both VAMP3 and 4 independently form complexes with the tSNARE made up of syntaxin 6/16/Vti1a (Mallard et al. 2002). Therefore, either VAMP3 or VAMP4 could be the vSNARE with the tSNARE required for the trafficking of GLUT4 from endosomes to the TGN and into GSVs.

As yet there is no evidence implicating VAMP3 in the formation of GSVs. However, it is involved in endosomal recycling. VAMP3 is found on GLUT4 vesicles within the endosomal recycling system (Martin et al. 1996), and the transferrin receptor localises to VAMP3 positive endosomal vesicles (Daro et al. 1996). Since GLUT4 traffics through the endosomal pool *en route* to GSVs, it is plausible that VAMP3 is involved in the membrane fusion event that facilitates this transport step. Furthermore, in HeLa cells VAMP3 acts with syntaxin 6 to traffic internalised membrane receptors from the endosomal pool to the TGN (Riggs et al. 2012).

In contrast to this, there is evidence that VAMP4 plays a role in GSV formation (Williams & Pessin 2008). Similar to the effect of inhibition of endogenous syntaxin 6, VAMP4 depletion leads to increased basal recycling of GLUT4, which is suggestive of impaired trafficking of GLUT4 into GSVs. However, VAMP4 depletion does not impair the insulin-stimulated translocation of GLUT4 to the plasma membrane (Williams & Pessin 2008). This GLUT4 translocation in response to insulin could be due to increased recycling of the enlarged endosomal compartment. An alternative explanation is that under conditions of VAMP4 depletion, some GLUT4 may still be accessible to GSVs. This research highlights that the vSNARE involved in the formation of GSVs, alongside the tSNAREs syntaxin 6 and 16, remains unclear. Likely candidates include VAMPs 3 and 4 as these have been identified to form complexes with syntaxins 6 and 16,

and have been implicated in trafficking from the endosomal system to the TGN (Mallard et al. 2002; Riggs et al. 2012).

5.1.2 SM proteins in intracellular sorting of GLUT4

Although SNARE proteins are the minimal membrane fusion machinery, there are many regulatory proteins that also act in the fusion process. One class of such proteins is the Sec-1/Munc-18 like (SM) protein family (see section 1-5). SM proteins regulate membrane fusion events through interactions with their cognate SNARE proteins. The cognate SM protein of syntaxin 16 is mVps45. The importance of the SNARE complex made up of syntaxin 16 and the SM protein mVps45 in the recycling of GLUT4 is highlighted by the finding that depleting 3T3 L1 adipocytes of mVps45 impairs the sorting of GLUT4 into GSVs (Roccisana et al. 2013).

Vps45 regulates the levels of its cognate SNARE partners in mammals and in yeast. In yeast lacking Vps45p, there is a reduction in the levels of the yeast syntaxin (Tlg2) and the yeast vSNARE (Snc2) (Shanks et al. 2012). In 3T3 L1 adipocytes, mVps45 depletion reduces levels of syntaxin 16 (Roccisana et al. 2013). However, the effect of mVps45 depletion on the levels of vSNAREs in 3T3 L1 adipocytes is unknown.

5.2 Aims

Both the tSNARE syntaxin 16 and its regulatory SM protein mVps45 have been implicated in the intracellular sorting of GLUT4 into GSVs. To uncover the vSNAREs involved in this process, firstly, the effect of mVps45 depletion on VAMP protein levels will be determined, and secondly, the interactions between both mVps45 and syntaxin 16 with VAMP proteins will be characterised. Interactions will be characterised through *in vitro* pull down experiments and co-immunoprecipitation experiments.

5.3 Results

5.3.1 Effect of mVps45 depletion on VAMP protein levels

Whole cell lysates from 3T3 L1 adipocytes treated with scrambled shRNA, or shRNA targeted against mVps45 were provided by Dr. Roccisana (Roccisana et al. 2013). These were subjected to immunoblotting with antibodies against VAMP proteins (Figure 5-1 A). Values obtained for the intensity of each band were adjusted for protein loading by comparison with GAPDH, and normalised against values obtained from cells treated with scrambled shRNA (Figure 5-1 B). As previously reported mVps45 knock down significantly reduced the levels of GLUT4 (Roccisana et al. 2013). mVps45 knock down also significantly reduced the levels of both VAMP2 and 4, but had no specific effect on any of the other VAMPs (Figure 5-1).

Reducing the cellular content of Vps45 either in mammalian or yeast cells results in reductions in the levels of its cognate syntaxin, syntaxin 16/Tlg2 (Bryant & James 2001; Roccisana et al. 2013). In yeast, a reduction in Vps45p leads to increased proteosomal degradation of Tlg2 (Bryant & James 2001). In yeast, Vps45p depletion also reduces the level of Snc2, the cognate vSNARE of the syntaxin Tlg2 (Shanks et al. 2012). Therefore, it is possible that, like in yeast, the reductions in VAMP2 and 4 could occur as a consequence of reduced mVps45 levels. However, VAMP2 is also found on GSVs, and mVps45 knock down reduces the sorting of GLUT4 into GSVs (Roccisana et al. 2013). Therefore, the reduction in VAMP2 could also be indirect, through a reduction in the number of GSVs. To examine the mechanisms behind the reductions in VAMP proteins seen with mVps45 depletion, the ability of mVps45 to bind directly to VAMP proteins has been assessed (Figure 5-2). It was hypothesised that, if the reduction in the vSNARE protein levels was due to destabilisation of the SNARE complex or mVps45 depletion *per se*, the vSNARE would interact with mVps45. Conversely, if the reduction were indirect, due to a reduction in the number of GSVs, then the vSNARE would not interact with mVps45.

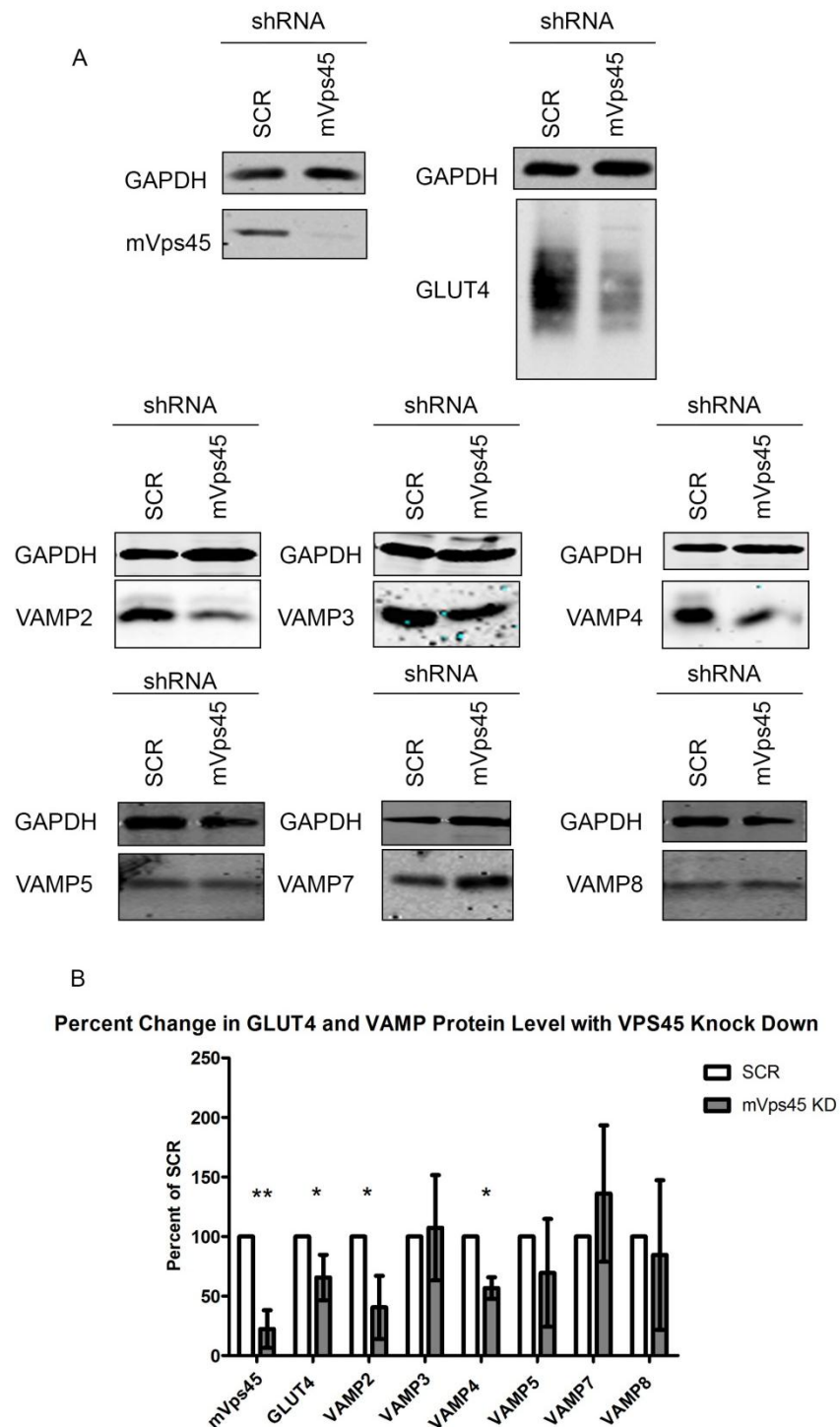


Figure 5-1: mVps45 Knock-down reduces the levels of VAMPs 2 and 4 in 3T3 L1 adipocytes. Knock-down of mVps45 was achieved through infection with lentivirus containing shRNA constructs against mVps45 or scrambled control sequence. mVps45, GLUT4 and VAMP protein levels were determined by SDS-PAGE followed by immunoblotting with the indicated antibody. Shown are immunoblots from a typical experiment following treatment with control shRNA (SCR) or shRNA targeting mVps45 (mVps45) (**A**). Immunoblot signals were normalised to GAPDH signals obtained from the same gel, and values from mVps45 treated 3T3 L1 adipocytes were compared to SCR (**B**). Values are mean \pm SD of three separate experiments. Values were compared using a Students t-test * = $p < 0.05$, ** = $p < 0.01$ vs scrambled control.

5.3.2 Interactions between mVps45 and VAMP proteins

Since mVps45 knock down reduces the cellular levels of VAMPs 2 and 4 (Figure 5-1), the hypothesis that mVps45 interacts directly with VAMPs 2 and/or 4 was tested. This was achieved by performing pull down experiments with GST-VAMPs bound to a solid phase incubated with yeast lysates lacking Vps45p, but expressing epitope tagged mVps45. Despite the mVps45 being functional and able to bind syntaxin 16 (Roccisana 2010 p132; Figure 5-2), no detectable interaction between mVps45 and any of the VAMP proteins was observed (Figure 5-2).

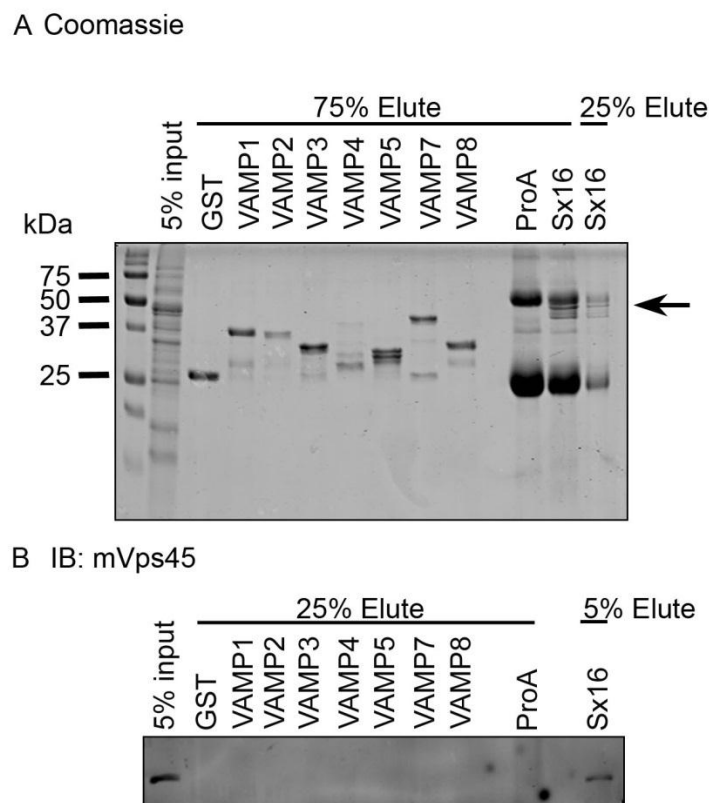


Figure 5-2: mVps45 does not directly interact with any of the VAMP proteins but does interact with syntaxin 16.

5 μ g recombinant tagged protein was bound to the appropriate beads (Glutathione-Sepharose or IgG beads). Beads and associated proteins were incubated with equal volumes of yeast lysate expressing HA-tagged mVps45 over-night as described (section 2.3.7.3). Beads and associated material were recovered by centrifugation, washed in yeast cell lysis buffer and bound protein was eluted in 2xLSB. 75% of the elute was subjected to SDS-PAGE and stained with Coomassie Brilliant Blue to examine the amounts of each protein bound to beads, arrow identifies syntaxin 16 (A). 25% of the elute was subjected to SDS-PAGE followed by immunoblotting with anti-HA tag to determine the presence of mVps45 (B), due to the high levels of interaction seen between mVps45 and syntaxin 16, 5% of this elute was examined. Shown are data from a typical experiment that was repeated 3 times using 3 separate batches of yeast lysate. Molecular marker sizes are shown in kDa.

The finding that none of the VAMPs directly interact with mVps45 does not rule out the possibility that the reduction in levels of VAMPs 2 or 4 is due to a destabilisation of a SNARE complex formed with syntaxin 16. These VAMPs may directly interact with syntaxin 16. In this situation, VAMP2 or 4 protein levels would be reduced when mVps45 levels are depleted as a consequence of increased syntaxin 16 degradation. Therefore, interactions between VAMP proteins and syntaxin 16 were examined.

5.3.3 Interactions between syntaxin 16 and VAMP proteins

Initially, interactions between syntaxin 16 and VAMP proteins were examined *in vitro*. Experiments to pull out GST tagged VAMP proteins from bacterial lysates using recombinantly expressed syntaxin 16 immobilised to a solid phase identified the ability of syntaxin 16 to interact with VAMPs 1, 2, 4, 7 and 8, but not VAMPs 3 or 5 (Figure 5-3; Data produced by Minttu Virolainen under my supervision).

This approach has a number of limitations. The expression levels of the VAMP proteins in the bacterial lysates differed, and there was no antibody available that could clearly detect the GST tag in the lysates (or the material bound to syntaxin 16). This meant that it was not possible to quantify the levels of interaction between syntaxin 16 and these VAMP proteins.

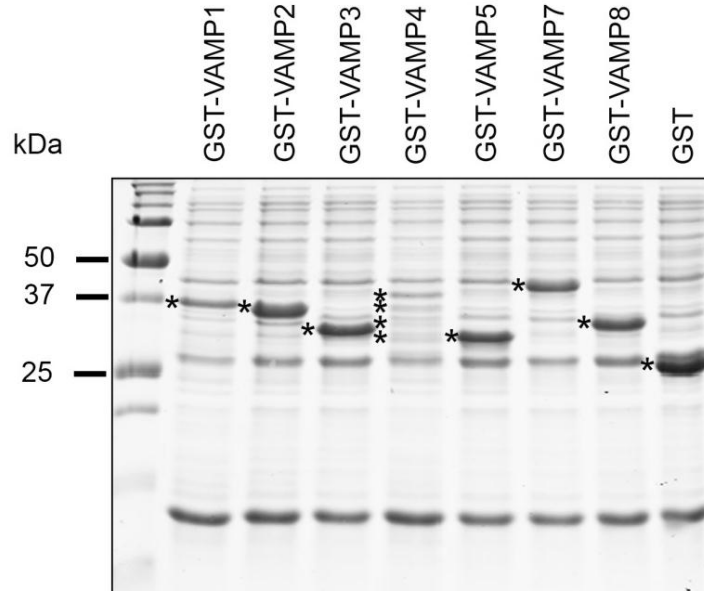
Therefore, the reciprocal approach was used. GST-VAMPs were immobilised to a solid phase and incubated with purified recombinantly expressed syntaxin 16. The results of a representative experiment are shown in Figure 5-4.

Unfortunately, using this approach it was not possible to abolish non-specific binding between syntaxin 16 and GST, despite trying multiple adaptations of the protocol.

Initial experiments were carried out using syntaxin 16 tagged with protein A at its C terminus. Under these conditions the protein A tag interacted strongly with GST. Therefore, in subsequent experiments, the protein A tag was removed by thrombin cleavage (Figure 5-5). However, this did not reduce the binding of syntaxin 16 to GST. To address this, a number of different wash buffers and binding conditions were used. These included varying the incubation time,

varying the molar ratios of the binding partners, varying the salt and detergent concentrations, and including various blocking reagents in the binding and wash buffers. None of these alterations to the protocol had any significant impact on the interactions observed between GST and syntaxin 16. Therefore, this method of determining interactions could not be used.

A: Input lysates



B: Pull Down with syntaxin 16-ProA

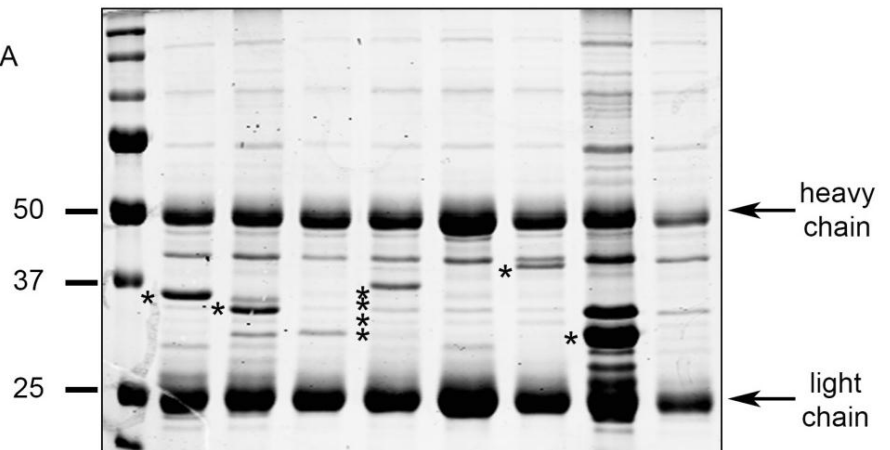


Figure 5-3: Protein A tagged syntaxin 16 can pull GST-VAMPs out of bacterial lysate

Syntaxin-16 was bound to IgG beads and incubated with 1ml of bacterial lysate expressing the indicated GST tagged VAMP protein for 2 hours at 4°C with rotation. Beads and associated material were recovered by centrifugation, washed in PBS and eluted in 2xLSB. The elute was subjected to SDS-PAGE and stained with Coomassie Brilliant Blue, and both heavy and light chains are marked. This data was produced by Minttu Virolainen whilst completing a placement project under my supervision.

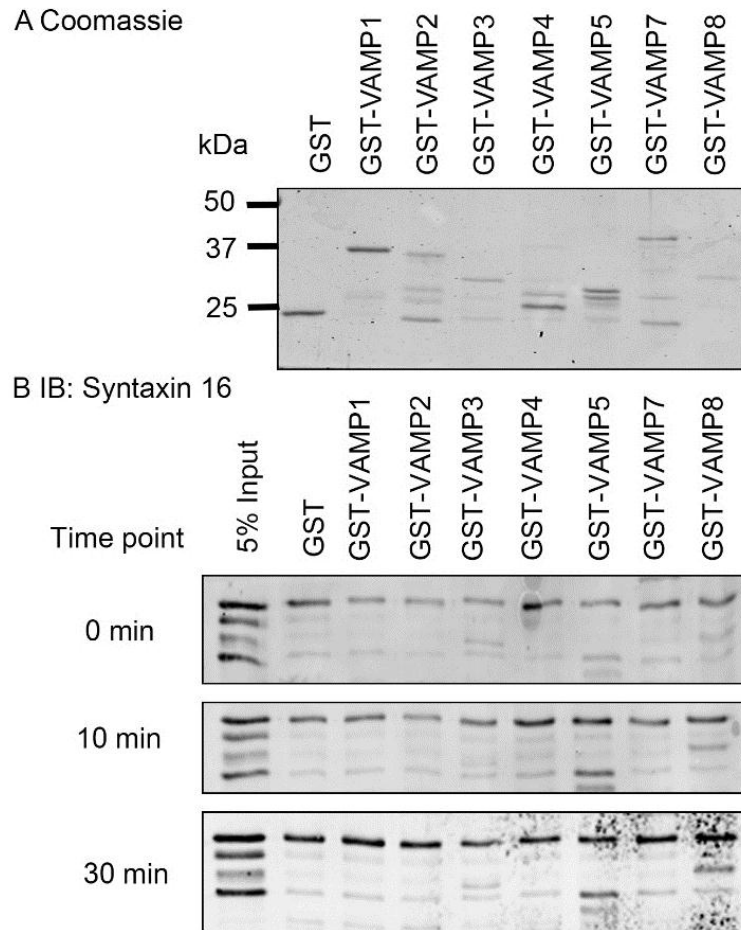


Figure 5-4: Interactions between GST-VAMPs and cleaved syntaxin 16

0.15 μ M GST alone or GST-VAMP proteins were immobilised on Glutathione-Sepharose beads. Beads and associated proteins were incubated with 10x molar excess of recombinant, thrombin cleaved, syntaxin 16 for the indicated time points (0, 10, 30 minutes). Beads and associated material were recovered by centrifugation, washed in PBST and bound protein was eluted in 2xLSB as described (section 2.3.7.4). Samples were subjected to SDS-PAGE followed by staining with Coomassie Brilliant Blue (A) or immunoblotting with anti-syntaxin16 (B). Shown are data from a typical experiment. Experiments were repeated using a variety of wash buffer and incubation times in attempts to remove the non-specific interactions seen between GST and syntaxin 16 (lane 2), without success.

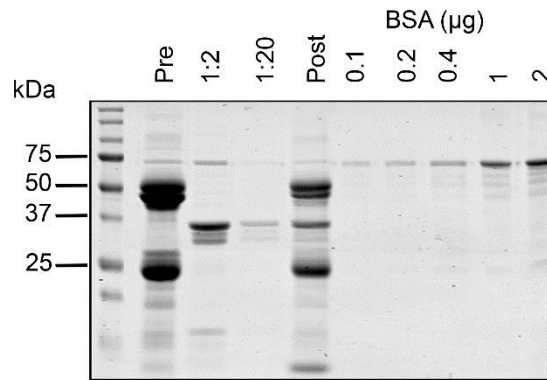


Figure 5-5: Purification and thrombin cleavage of protein A tagged syntaxin 16.

Protein A-tagged syntaxin 16 was expressed in BL21 DE3 cells, purified and the protein A tag thrombin cleaved as described (section 2.3.3). Shown is a representative experiment of analysis of purified, thrombin cleaved syntaxin 16. Protein A tagged syntaxin 4 bound to IgG beads (Pre), thrombin cleaved syntaxin 16 (diluted 1:2 and 1:20) and any protein that remained bound to IgG beads post thrombin cleavage (Post) was analysed by SDS-PAGE and stained with Coomassie Brilliant Blue alongside known amounts of BSA. Shown are data from a typical experiment, molecular marker sizes are shown in kDa.

As discussed in section 1.3.1, SNARE complexes are made up of four SNARE domains. A SNARE complex contains a Qa, Qb, Qc, and an R SNARE. It was therefore hypothesised that the binding between the tSNARE syntaxin 16 and the GST-VAMPs may be more specific when a SNARE domain of each type was incubated. Therefore, syntaxin 16 was combined with, SNAP23 and GST-VAMP, or GST alone. In this situation syntaxin 16 is the Qa SNARE, the VAMP is the R SNARE and SNAP23 provides the Qb and Qc SNARE domains. Under these conditions, selective SDS-resistant complex formation was seen. SDS-resistant SNARE complexes formed with all the VAMPs, but not GST (Figure 5-6). This provides further evidence of the promiscuity of SNARE interactions *in vitro* (Figure 5-6;3-3; discussed in more detail in Chapter 3, section 3.6.2) but does not give any indication as to the origin of the reduction in VAMP2 and 4 levels in cells depleted of mVps45. Therefore, the interactions between syntaxin 16 and VAMP proteins in the cellular environment were analysed through co-immunoprecipitation experiments. Representative immunoblots of syntaxin 16 co-immunoprecipitation experiments are displayed in Figure 5-7. These experiments show VAMP4, but not any of the other VAMPs, co-immunoprecipitate with syntaxin 16.

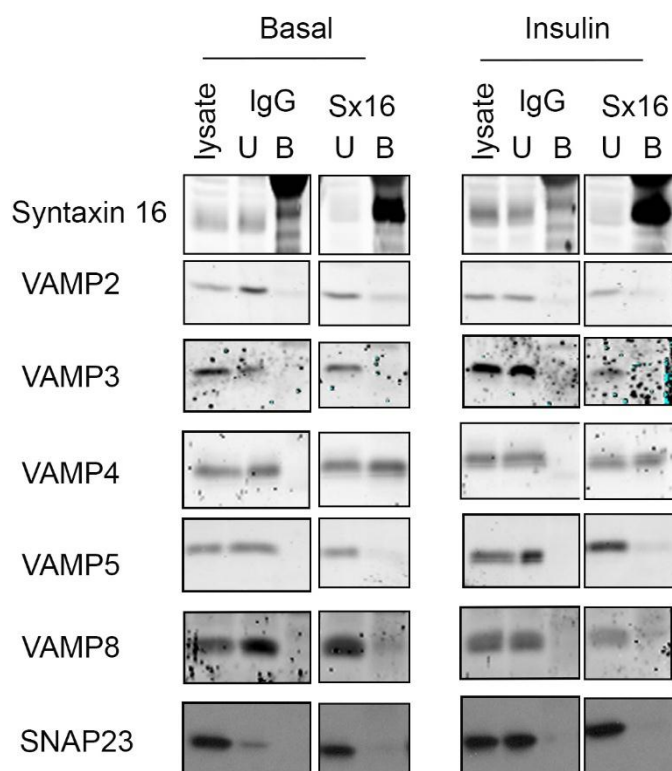


Figure 5-7: Immunoprecipitation of syntaxin 16 and co-immunoprecipitation of VAMP proteins from basal and insulin-stimulated 3T3 L1 adipocytes.

Syntaxin 16 was immunoprecipitated from serum starved 3T3 L1 adipocytes treated with 1mM NEM and with (insulin) or without (basal) 1 μ M insulin, as described (section 2.8). Proteins were immunoprecipitated from 1.5mg 3T3 L1 lysate (lysate) with 5 μ l anti syntaxin 16 (Sx16) or random rabbit IgG (IgG). Immunoprecipitated proteins and associated material was isolated by centrifugation and unbound material retained (U). Bound material (B) was washed and eluted in 2xLSB. Samples were subjected to SDS-PAGE and immunoblotting with anti-syntaxin 16 and anti-VAMP antibodies. Each immunoblot shown is the output from the IP of 1.5mg 3T3 L1 lysate. Samples from basal and insulin-stimulated cells were subjected to immunoblotting on the same membrane and the irrelevant lanes excised. The original image is shown in the appendix (Appendix; Figure 8-1). Shown are data from a typical experiment, repeated >3 times.

5.4 Discussion

The tSNARE syntaxin 16 is involved in the sorting of GLUT4 into GSVs, and is regulated by the SM protein mVps45. Depletion of mVps45 levels in 3T3 L1 adipocytes also depletes syntaxin 16 and perturbs the entry of GLUT4 into GSVs (Roccisana et al. 2013). Here it has been demonstrated that mVps45 knock down selectively depletes cells of VAMPs 2 and 4, but not of the other VAMPs.

Both VAMP3 and 4 are known to interact with syntaxin 16 (Mallard et al. 2002) and thus could be involved, with syntaxin 16, in the recycling of GLUT4. However, no role for VAMP3 has yet been proposed in this process and VAMP3 levels are unaffected by mVps45 knockdown (Figure 5-1). Together, these findings imply that VAMP3 is not involved in the recycling of GLUT4 through the TGN and into GSVs. This idea is strengthened by the findings of co-immunoprecipitation experiments showing that, unlike in HeLa cells, in 3T3 L1 adipocytes VAMP3 does not interact with syntaxin 16. In contrast to VAMP3, roles for both VAMP2 and 4 in the formation of GSVs have been proposed (Williams & Pessin 2008).

Williams and Pessin (2008) used RNA interference technologies to deplete adipocytes of VAMPs 2 or 4, and proposed that VAMP4 is required for the entry of newly synthesised GLUT4 into GSVs. They examined the requirements for VAMP4 in the formation of insulin-sensitive GLUT4 vesicles from newly synthesised GLUT4 by exposing cells to VAMP4 siRNA prior to the expression of myc-GLUT4-GFP. Under these conditions, but not when myc-GLUT4-GFP was expressed prior to VAMP4 depletion, there was significantly more GLUT4 present in the plasma membrane of basal cells. This is suggestive of a situation where GLUT4 cannot enter GSVs and is therefore trafficked back into the ERC. However, under these conditions, although there was a reduction in the fold increase in GLUT4 in the plasma membrane with insulin-stimulation, the absolute level of GLUT4 translocation was unchanged compared to control cells. This led Williams and Pessin (2008) to propose that under conditions of VAMP4 depletion, some GLUT4 is still able to gain access to the GSV compartment. Williams and Pessin (2008) also observed that insulin stimulated GLUT4 translocation was only impaired when VAMP2 was depleted. These data were interpreted to mean that both VAMP2 and 4 are required for sorting of GLUT4 into GSVs, but they act on

different sources of GLUT4. They proposed that VAMP2 is required for the cycling of GLUT4 into GSVs, and that VAMP4 is required for the entry of newly synthesised GLUT4 into GSVs (Williams & Pessin 2008). However, this explanation does not take into account a number of factors. Firstly, the well documented role that VAMP2 plays in the fusion of GSVs with the plasma membrane in response to insulin (Cheatham et al. 1996; Martin et al. 1998; Kawaguchi et al. 2010). Since VAMP2 is involved in the fusion of GLUT4 with the plasma membrane, VAMP2 depletion would be expected to impair the insulin response even if GSVs were fully formed. Secondly, if VAMP2 were required for GSV formation, depletion of this isoform would be expected to have some effect on the basal distribution of GLUT4. However, this was not observed. Finally, it is entirely feasible the insulin-response seen following VAMP4 depletion may have been a result of insulin-stimulation of the enlarged endosomal pool of GLUT4, and not due to GSVs still being formed following VAMP4 depletion. Therefore, to examine the role VAMP2 and 4 play in the formation of GSVs, their interactions with the tSNARE syntaxin 16 and its SM protein mVps45 were examined. These proteins have been implicated in the trafficking of GLUT4 from the endosomal system into GSVs (Perera et al. 2003; Shewan et al. 2003; Roccisana et al. 2013).

The reduction in both VAMP2 and 4 levels with mVps45 depletion (Figure 5-1) supports a role for these proteins in the formation of GSVs. However, the reductions in VAMP2 and 4 could either be direct or indirect. Direct effects would occur through the destabilisation of the syntaxin 16 containing SNARE complex, and indirect effects through a reduction in the number of GSVs. Therefore, the interactions between VAMP proteins and both syntaxin 16 and mVps45 were examined.

Pull down experiments showed that none of the VAMP proteins directly interact with mVps45 in yeast lysates. This is despite mVps45 being fully functional and able to bind syntaxin 16 (Roccisana 2010 p132; Figure 5-2). This is in discord with findings in yeast, where Vps45p directly binds to the vSNARE Snc2 (Carpp et al. 2006) and findings with another SM protein, Munc18c, which directly binds VAMP2 *in vitro* (Brandie et al. 2008). It is of course possible, that there were interactions between mVps45 and VAMP proteins that were not detectable. However, this is unlikely as the interaction observed with syntaxin 16 and mVps45 was substantial. In Figure 5-2, four times more VAMP bound material

was examined than syntaxin 16 bound material. Despite this, no interaction was detected between mVps45 and the VAMPs. There is also the possibility that the recombinantly expressed VAMP proteins were not-functional. Again this is unlikely as they were capable of forming SDS resistant complexes with both syntaxin 4 and 16 (Figure 5-6; Figure 3-3).

In bacterial lysates, syntaxin 16 interacts with VAMPs 1, 2, 4, 7 and 8 (Figure 5-3). Stable SDS resistant SNARE complexes form between all VAMP proteins and syntaxin 16 when all four classes of SNARE protein are present (Qa, Qb, Qc and R SNAREs) (Figure 5-6). This observation is not surprising, as it has been well established that SNARE complex formation is highly promiscuous (discussed in more detail in Chapter 3, section 3.6.2). However, in the cellular environment syntaxin 16 only interacts with VAMP4. There is no detectable interaction between syntaxin 16 and VAMP2. It cannot be ruled out that interactions between VAMP2 and syntaxin 16 are present, but not detectable. This seems unlikely as in the same experiments interactions between VAMP2 and syntaxin 4 were detectable (Appendix, Figure 8-1). For a discussion of the limitations of the co-immunoprecipitation approach see Chapter 3, section 3.6.1.

Therefore, this research demonstrates for the first time, that *in vivo*, VAMP4 but not VAMP2 interacts with syntaxin 16. This data, alongside previous reports highlighting that VAMP2, but not VAMP4 is present on GSVs (Larance et al. 2005) suggests that the reduction in VAMP2 seen with mVps45 depletion is an indirect result, and due to a reduction in the number of GSVs. Furthermore, the finding that VAMP2 cannot be found to interact with syntaxin 16 implies either it is not involved in the formation of GSVs, or that if it is involved this is via a tSNARE complex that does not contain syntaxin 16.

5.5 Conclusion

Syntaxin 6, 16 and mVps45 are all involved in the formation of GSVs (Perera et al. 2003; Shewan et al. 2003; Proctor et al. 2006; Roccisana et al. 2013). The experiments in this Chapter aimed to dissect the vSNARE requirements for GLUT4 sorting into GSVs by examining interactions between VAMP proteins, mVps45 and syntaxin 16. Previous research has suggested roles for VAMPs 2, 3 and 4 in this trafficking step. mVps45 depletion reduces both VAMP2 and VAMP4

levels, however VAMP4 but not VAMPs 2 or 3 interact with syntaxin 16. This supports previous findings that have implicated VAMP4 in the intracellular trafficking of GLUT4 from endosomes to the TGN and in the formation of GSVs (Mallard et al. 2002; Williams & Pessin 2008).

Chapter 6 - Knock down of VAMP proteins in mammalian cells.

6.1 Introduction

Although many studies have identified VAMP2 as being required for the delivery of GLUT4 to the cell surface in response to insulin, the role of each VAMP protein in the intracellular trafficking of GLUT4 is less clear. To date, only one study has systematically examined the role of each VAMP protein in GLUT4 sorting in adipocytes (Williams & Pessin 2008). This study depleted 3T3 L1 adipocytes of each VAMP isoform using siRNA and examined GLUT4 trafficking by following the translocation of the GLUT4 reporter protein, myc-GLUT4-GFP. Their findings suggested a role for VAMP4 in the trafficking of newly synthesised GLUT4 into the insulin sensitive pool. Depletion of VAMP4 in cells already expressing myc-GLUT4-GFP had no significant effect on GLUT4 trafficking. However, depletion of VAMP4 prior to the expression of myc-GLUT4-GFP significantly increased the presence of GLUT4 in the plasma membrane of untreated cells. This is indicative of a situation where GLUT4 cannot be sorted into the insulin-sensitive compartment (GSVs) and is trafficked into the endosomal recycling pool. Despite the decreased sorting of GLUT4 in GSVs, insulin still increased GLUT4 at the cell surface. Although the absolute value of GLUT4 at the cell surface was similar to control cells, the fold-change in cell surface GLUT4 was reduced. Williams and Pessin (2008) interpreted this to mean that in the absence of VAMP4, a proportion of GLUT4 is still sorted into GSVs. There is however another explanation. This is that VAMP4 knockdown prevents entry of GLUT4 into GSVs, and the increase in GLUT4 at the cell surface seen with insulin-stimulation is due to increased traffic through the endosomal pool.

In line with the role of VAMP2 in insulin-stimulated GLUT4 translocation (see Chapter 3; Chapter 4), Williams and Pessin (2008) found that insulin-stimulated increases in myc-GLUT4-GFP appearance in the plasma membrane was only impaired when VAMP2 was depleted. They suggested that the attenuated insulin response may be because VAMP2 is required for the recycling of GLUT4 into GSVs. However, this was not directly tested.

Williams and Pessin (2008) also examined the role each VAMP plays in GLUT4 endocytosis. To do this, VAMP proteins were selectively depleted and the internalisation of myc-GLUT4-GFP following insulin removal was measured. Myc-GLUT4-GFP internalisation was measured through the internalisation of anti-myc

antibodies. VAMP8 depletion reduced the internalisation of myc-GLUT4-GFP following insulin-stimulation. Therefore, VAMP8 was suggested to be involved in the endocytosis of GLUT4 from the plasma membrane. That the effect of VAMP8 knock down was not apparent prior to insulin stimulation is possibly because under basal conditions, there is low traffic through the system. Since this VAMP isoform is expressed at high levels (Chapter 4, Figure 4-6), the depletion of VAMP8 was unlikely to be complete. So when traffic through the system is low, the remaining VAMP8 may be able to fulfil the requirements for endocytosis. It is only when endocytosis rates are elevated and there is pressure on the system its role becomes apparent.

In summary, data collected using RNAi in 3T3 L1 adipocytes reveals that VAMP4 and VAMP2 may be involved in the trafficking of GLUT4 into GSVs. However, there are a few questions that remain to be answered and this data must be independently replicated. Therefore, a similar approach to explore the roles of these VAMP proteins further has been taken here. Although the approach is broadly similar, alterations have been made. The first is in the GLUT4 transporter used and the second in the cell type studied.

The study discussed above utilised a myc-GLUT4-GFP reporter, here a HA-GLUT4-GFP construct has been used. This HA-GLUT4-GFP construct contains a HA tag in the first exofacial loop and a GFP tag at the C terminus. This allows the trafficking of GLUT4 to the cell surface to be examined in a quantitative manner. The HA-GLUT4-GFP reporter has been thoroughly characterised and shown to traffic in an identical manner to endogenous GLUT4 (Lampson et al. 2000; Martin et al. 2006). Although it is likely that the myc-GLUT4-GFP transporter used in previous studies also traffics in a similar manner as endogenous GLUT4, this has not been extensively examined. The other alteration here is in the cell type used, as previous studies have used 3T3 L1 adipocytes. 3T3 L1 adipocytes are insulin-sensitive and express endogenous GLUT4. This makes them a good model to study insulin-responsiveness. However, it may also cause problems, particularly when GLUT4 reporter proteins (such as HA-GLUT4-GFP) are introduced on top of endogenous GLUT4, as this may lead to over-expression artefacts and subsequent perturbation in trafficking pathways. This overexpression may cause the system to over-load and force the cell to employ 'extra' pathways to sort GLUT4. Therefore, HeLa cells have been used

here. The benefits and caveats of using these are discussed in detail in section 6.1.3. Briefly, HeLa cells have been shown to be insulin-sensitive and seem to contain the machinery required to form GSVs.

6.1.1 Use of RNAi

Previous studies have utilised RNA interference to deplete cells of proteins and examine GLUT4 trafficking (Williams & Pessin 2008). RNA interference (RNAi) is a widely used method to silence gene expression. Short interfering RNA (siRNA) sequences can be transfected into cells, where they result in specific protein knock down (Elbashir et al. 2001). siRNAs are between 21 and 23 nucleotides long, double stranded RNA duplexes. siRNAs are transfected into cells either chemically or through electroporation. Once in the cytoplasm they are incorporated into the RNA inducing silencing complex (RISC) where they unwind. The antisense strand then guides the RISC complex to the target mRNA which is cleaved. In mammalian cells, siRNAs are not replicated meaning their functionality is limited by their transient nature. For more prolonged RNAi, DNA-vector mediated RNAi systems can be used. In these systems, DNA is transcribed into siRNA by RNA polymerase III. The siRNA double strand is usually expressed as a sense and antisense strand from two promoters. These strands come together to form a siRNA molecule. Alternatively, a single promoter can be used to express a single stranded RNA that folds into a hairpin structure (shRNA). shRNA molecules are then processed by members of the Dicer family of RNase III enzymes to produce miRNAs (microRNAs). These short RNA sequences bind to complementary sites on mRNA, repressing mRNA translation and protein synthesis (Dykxhoorn & Lieberman 2005).

6.1.2 Studying GLUT4 trafficking using RNAi

Traditionally, studies examining the role of proteins in GLUT4 trafficking and insulin-stimulation have done so in adipose and muscle cell lines. These cell lines are advantageous because they express GLUT4 and are insulin-sensitive. However, there are some limitations with these cell lines, particularly when studying the effect of depletion of proteins through RNAi interference. When studying any biological pathway through RNAi interference, it is important that the transfection of cells is both consistent across the population and

reproducible. This is often a problem when using 3T3 L1 adipocytes as they are typically difficult to transfect. Indeed, initial studies in this cell line using previously published siRNA sequences (Williams & Pessin 2008) produced inconsistent knockdown (data not shown). Therefore, the use of other cell lines had to be considered.

6.1.3 HeLa cells

Any cell lines used in this study needed to be readily transfectable and responsive to insulin. A number of cell lines have been used to study insulin mediated GLUT4 trafficking, including CHO cells (Wei et al. 1998) and HeLa cells (Hernandez et al. 2001). Here, HeLa cells were used. One consideration when using HeLa cells to study the trafficking of GLUT4 is that these cells do not express GLUT4. This provides a benefit in that there will be no competition for trafficking machinery, however, it also presents the possibility that they are not insulin-sensitive or that they do not traffic GLUT4 in the same manner as adipocytes. However, when GLUT4 is ectopically expressed in cell lines that do not express GLUT4, it is present in endosomal vesicles and a subpopulation of small vesicles, similar to those seen in adipocytes (Herman et al. 1994). Furthermore, HeLa cells respond to insulin (Figure 6-1; Haga et al. 2011). This suggests that HeLa cells contain the basic machinery to form insulin sensitive GLUT4 compartments and respond to insulin, and are therefore a suitable cell line in which to study the trafficking of GLUT4.

6.1.4 Inducible vector system

HeLa cells were chosen to study intracellular trafficking and sorting of GLUT4 to circumvent some of the issues that occur when studying this process in adipocytes or muscle cells. A particular problem with using 3T3 L1 adipocytes is inconsistent transfection and RNAi uptake, and thus inconsistent protein knock down. One method to overcome this is to transfect cells with RNAi as fibroblasts (Roccisana et al. 2013). In this process shRNA constructs are designed and packaged into viral particles, which are then used to infect fibroblast cells. This results in a population of fibroblast cells that are depleted of the protein of interest. The fibroblasts are then differentiated into adipocytes, and can be assayed. While this does circumvent some of the problems that commonly occur

when trying to transfect differentiated adipocytes, it has a number of limitations. One limitation is that since knockdown occurs prior to differentiation, there is the possibility that the knock down of proteins may impair or alter the differentiation of cells into adipocytes. A system that allows the regulated expression of shRNA constructs has been designed. This should overcome any problems associated with protein depletion prior to differentiation. In this system, a microRNA fragment is placed downstream of a tetracycline promoter within a lentiviral vector platform. This platform, termed pSLIK (single lentivector for inducible knockdown), has been described previously (Shin et al. 2006). Here, the first steps have been taken to develop the pSLIK platform to express shRNA constructs targeting VAMP2 and 4 in 3T3 L1 adipocytes.

6.2 Aims

The overall aim of this final chapter was to further examine the roles of VAMP2, 4 and 8 in the trafficking of GLUT4, by studying the effects of the knock down of these proteins on GLUT4 distribution under basal and insulin-stimulated conditions in HeLa cells. A second aim was to develop the pSLIK inducible vector system for use in 3T3 L1 adipocytes.

6.3 Results

6.3.1 VAMP protein knock down in HeLa cells

Previous studies have implicated VAMP2, 4 and 8 in the trafficking of GLUT4 in 3T3 L1 adipocytes (Williams & Pessin 2008). In order to further define the roles of these VAMP isoforms in GLUT4 trafficking, HeLa cells expressing GLUT4 tagged in the first extracellular loop with HA, and at the C terminus with GFP (HA-GLUT4-GFP), have been selectively depleted of VAMP proteins. Following protein depletion, the distribution of GLUT4 was examined by indirect immunofluorescence and confocal microscopy.

Prior to examining the effects of VAMP protein depletion in HA-GLUT4-GFP expressing HeLa cells, it was necessary to check that these cells did respond to insulin. HeLa cells expressing HA-GLUT4-GFP were grown on glass coverslips and subjected to indirect immunofluorescence staining as described (section 2.9). The HA tag of this construct is positioned on the first extracellular loop of GLUT4. This means that when it is inserted into the plasma membrane, the HA tag is outside the cell. Following serum starvation, cells were either left untreated (basal) or treated with 1 μ M insulin for 20 minutes (insulin). Antibody staining with antibodies against the HA tag was carried out without prior permeabilisation. Under these conditions, only HA outside the cell is accessible to the antibody. Therefore, the HA antibody signal represents HA-GLUT4-GFP inserted into the plasma membrane, and the GFP fluorescence represents total GLUT4. Figure 6-1 shows that HeLa cells expressing HA-GLUT4-GFP were responsive to insulin-stimulation.

Having established that HeLa cells are insulin-responsive, the next step was to determine the effect of depletion of VAMP 2, 4 or 8 on global GLUT4 distribution under basal and insulin-stimulated conditions. HA-GLUT4-GFP expressing HeLa cells were transfected with 200nM siRNA as described (section 2.6.1). Figure 6.2 shows that the siRNA duplexes resulted in depletion of the relevant VAMP. Due to the low level of material obtained in knockdown experiments, immunoblotting with the full set of VAMP proteins for each experiment was not always possible. Therefore, statistical analysis of the knock down cannot be

carried out. However, the phenotype seen in Figure 6.2 was consistently observed.

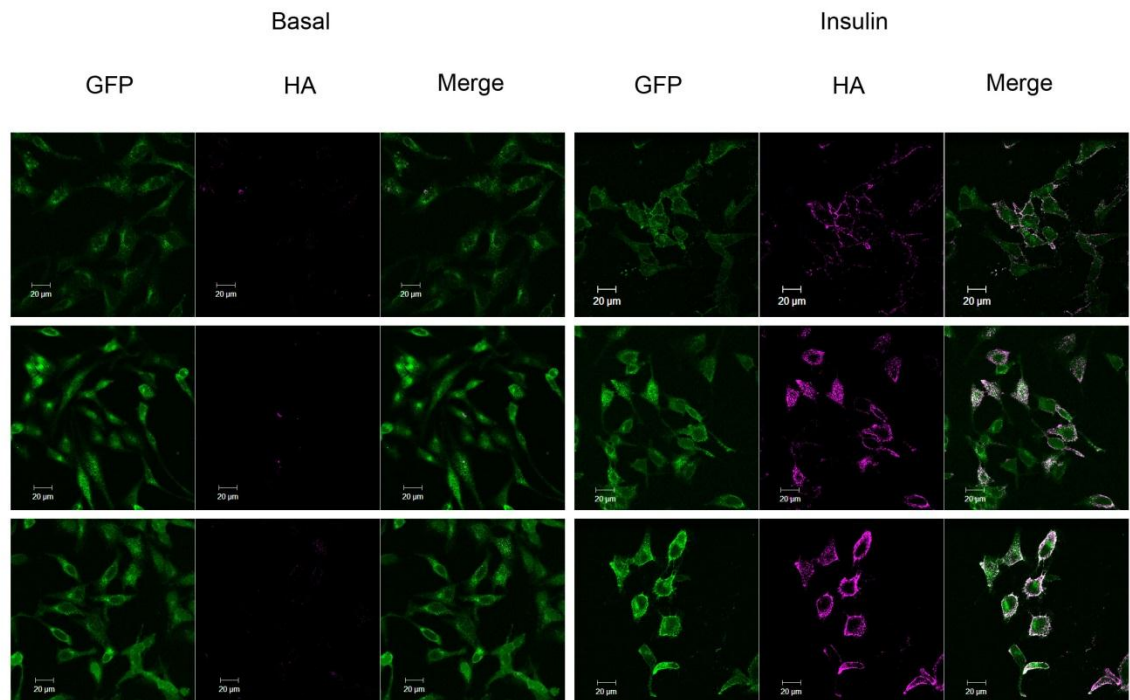


Figure 6-1: Insulin-stimulation causes HA-GLUT4-GFP translocation in HeLa cells.

HeLa cells expressing HA-GLUT4-GFP were grown as described (2.4.2). Cells were serum-starved (basal) before being treated with or without 1 μ M insulin (insulin) for 20 minutes. Cells were fixed and surface HA was stained as described (2.9). Immunofluorescence images were taken using the 63x oil immersion lens and are representative of a typical field of view. 6 images from 2 coverslips were taken for each experiment.

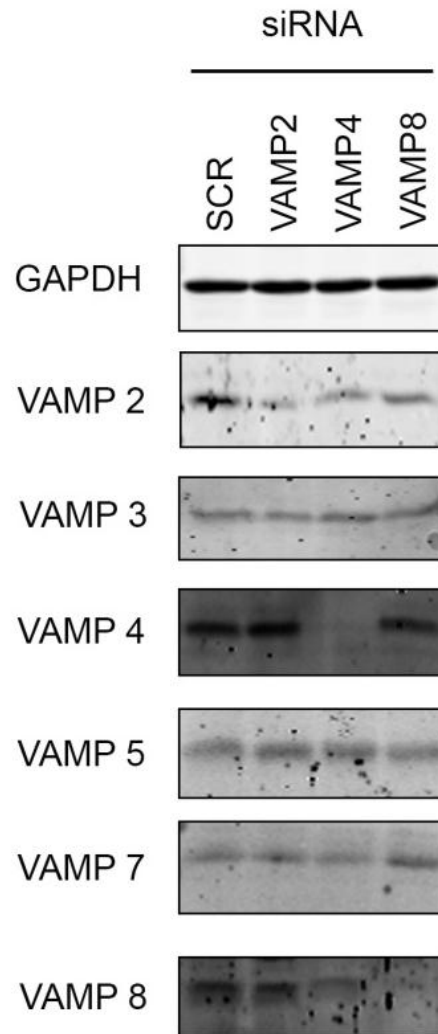


Figure 6-2: Knockdown of, VAMP2, VAMP4 and VAMP8 in HeLa cells

HeLa cells expressing HA-GLUT4-GFP were grown and transfected with 200nM SMARTpool siRNA as described (section 2.6.1). Cells were scraped and homogenised in 100 μ l RIPA buffer, left in ice for 30 minutes and mixed with 6xLSB. Samples were subjected to SDS-PAGE and immunoblotting with indicated antibodies. Images shown are from typical experiments.

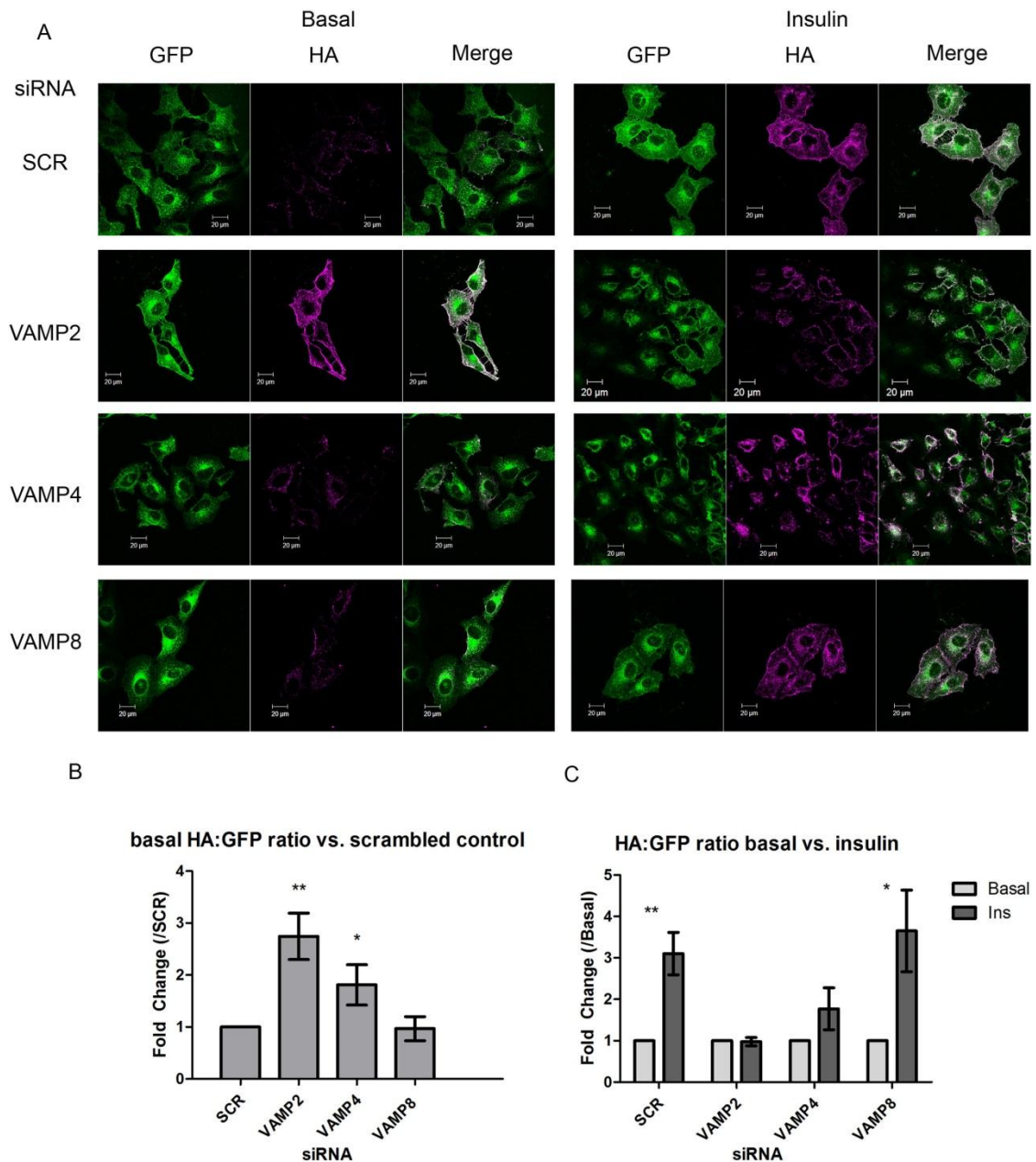


Figure 6-3: Effect of VAMP2, 4 or 8 knockdown on GLUT4 distribution under basal and insulin-stimulated conditions.

HeLa cells expressing HA-GLUT4-GFP were grown and transfected with 200nM scrambled control sequence (SCR) VAMP2, 4 or 8 SMARTpool siRNA as described (section 2.6.1). Cells were serum-starved (basal) before being treated with or without 1 μ M insulin (insulin) for 20 minutes. Cells were fixed and surface HA was stained as described (section 2.9). **A** - Immunofluorescence images were taken using the 63x oil immersion lens and are representative of a typical field of view. 6 images from 2 coverslips were taken for each experiment, this was repeated 4 times. **B** - basal HA:GFP ratio compared to SCR, values represent the means \pm SD of 18 fields of view, taken from 4 independent experiments. Values were compared using the Student's t-test, *= p <0.05, **= p <0.01. **C** - Fold-change in the HA/GFP ratio with insulin-stimulation, values were compared using the Student's t-test *= p <0.05, **= p <0.01.

To assess the trafficking of HA-GLUT4-GFP in HeLa cells depleted of VAMP2, 4 or 8, cells were subjected to indirect immunofluorescence staining with antibodies against the HA tag (as detailed above). As discussed in section 1.2.1 and shown in Figure 6-7 A, GLUT4 is found in two inter-linked cycles. One cycle acts between the plasma membrane and the endosomal recycling compartment (ERC). The other acts between the ERC and insulin-sensitive GLUT4 storage vesicles (GSVs). The cycle that acts between the ERC and GSVs effectively sequesters GLUT4 away from the plasma membrane under basal conditions, whereas the endosomal recycling pool recycles GLUT4 to and from the plasma membrane. Therefore, in the absence of insulin, GLUT4 is only accessible to the plasma membrane when it is in the ERC. Insulin-stimulation results in the mobilisation of GLUT4 from GSVs to the cell surface and to a lesser degree, increases the recycling of GLUT4 out of the ERC. Therefore, the distribution of GLUT4 under basal and insulin-stimulated conditions can be used to dissect the cycling of GLUT4 and the formation of the GSV pool of GLUT4. In the presence of GSVs, under basal conditions, there will be little GLUT4 in the plasma membrane. Insulin-stimulation will increase the presence of GLUT4 in the plasma membrane. In the absence of GSVs, GLUT4 will be directed into the ERC and therefore the basal distribution of GLUT4 in the plasma membrane will be increased and the insulin induced increase in GLUT4 in the plasma membrane will be attenuated.

In line with this, in HeLa cells treated with scrambled control siRNA, under basal conditions, there is little GLUT4 in the plasma membrane. In these cells insulin-stimulation results in a robust increase in surface staining of HA-GLUT4-GFP. This increase was quantified by comparing the HA (surface GLUT4) signal to the GFP (total GLUT4) signal. For scrambled control cells insulin led to a 3-fold increase in GLUT4 in the plasma membrane (Figure 6-3 A Basal vs Insulin; Figure 6-3 C).

Knock down of either VAMP2 or VAMP4 increased the appearance of GLUT4 in the plasma membrane of basal cells by 2.7-fold ($p < 0.01$), and 1.8-fold ($p < 0.05$) respectively. The increases seen with either VAMP2 or 4 knock down were not dissimilar to those seen in control cells treated with insulin. Knock down also abolished any insulin-stimulated increase in GLUT4 in the plasma membrane in

these cells (Figure 6-3). In contrast, VAMP8 depletion had no effect on either the basal appearance of GLUT4 in the plasma membrane, or on the insulin-response.

6.3.2 Generation of inducible vector system to knock down VAMP proteins in 3T3 L1 adipocytes

Studying the effect of VAMP knock down in HeLa cells gives a good indication of the roles these proteins play in GLUT4 trafficking. However, HeLa cells, although clearly insulin sensitive do not endogenously express GLUT4. Therefore, it is also important to study the trafficking of the insulin sensitive glucose transporter in 3T3 L1 adipocytes, which express GLUT4 and are insulin-sensitive.

Initial experiments using siRNA in this cell line showed that 3T3 L1 adipocytes are not readily transfectable (data not shown). Therefore, one of the focuses of this project has been to generate a tetracycline (TET) inducible shRNA containing vector system for use in mammalian cells (Shin et al. 2006). This construct can be transfected into 3T3 L1 cells prior to differentiation, when transfection is much more efficient. Following differentiation, the expression of the shRNA can be induced by the stimulation of the TET promoter with doxycycline. All plasmids used to generate this system were kind gifts from Dr Rob Semple (University of Cambridge) and cloning steps were completed with the guidance of Dr. Nuno Rocha (University of Cambridge).

The method for designing the shRNA oligonucleotides is illustrated in Figure 6-4. shRNA constructs were inserted into two different entry plasmids, pEN_TmiRc2 and pEN_TGmiRc2 (Table 6-1, Figure 6-5 A and B). The second of these contains the GFP gene between the TET promoter and the shRNA fragment. Therefore, expression of the shRNA is linked to GFP expression, and the level of GFP expression is proportional to the shRNA expression. To determine whether the shRNA oligonucleotide had been inserted into the pEN plasmid, plasmid DNA was subjected to digestion with restriction endonucleases. This resulted in changes in the size of the digested fragments (Figure 6-5 A and B). The expected changes in fragment sizes when the empty pEN_TmiRc3 and pEN_TGmiRc3 plasmids or those containing the VAMP2 or 4 oligonucleotides are digested with BsRG1 are shown in Table 6-1. pEN_TmiRc3 and pEN_TGmiRc3 plasmid DNA that was identified as containing the relevant VAMP oligonucleotide was shuttled into the

mammalian expression plasmid pSLIK_Neo. Successful recombination into the pSLIK plasmid was confirmed by a reduction in the size of the largest fragment produced when plasmids were digested with the endonuclease Kpn1 (Figure 6-5 C).

To ensure that activation of the TET promoter would result in gene expression, pSLIK_TG plasmids containing the VAMP2 and 4 oligonucleotides were transfected into HeLa cells. Once transfected, cells were either left unstimulated or stimulated with 1 μ g/ml doxycycline. HeLa cells were chosen for these experiments because of their high transfection efficiency. In the absence of doxycycline stimulation, GFP expression in cells transfected with either pSLIK_TG_VAMP2 or 4 is similar to that of cells transfected with no DNA (Figure 6-6 C and D vs A). With doxycycline stimulation GFP expression is elevated. The GFP transfection rate of cells that contain the pSLIK_TG plasmids is similar to that of those transfected with GFP-cellulogyrin DNA in which GFP is constitutively expressed (Figure 6-6 C and D vs B).

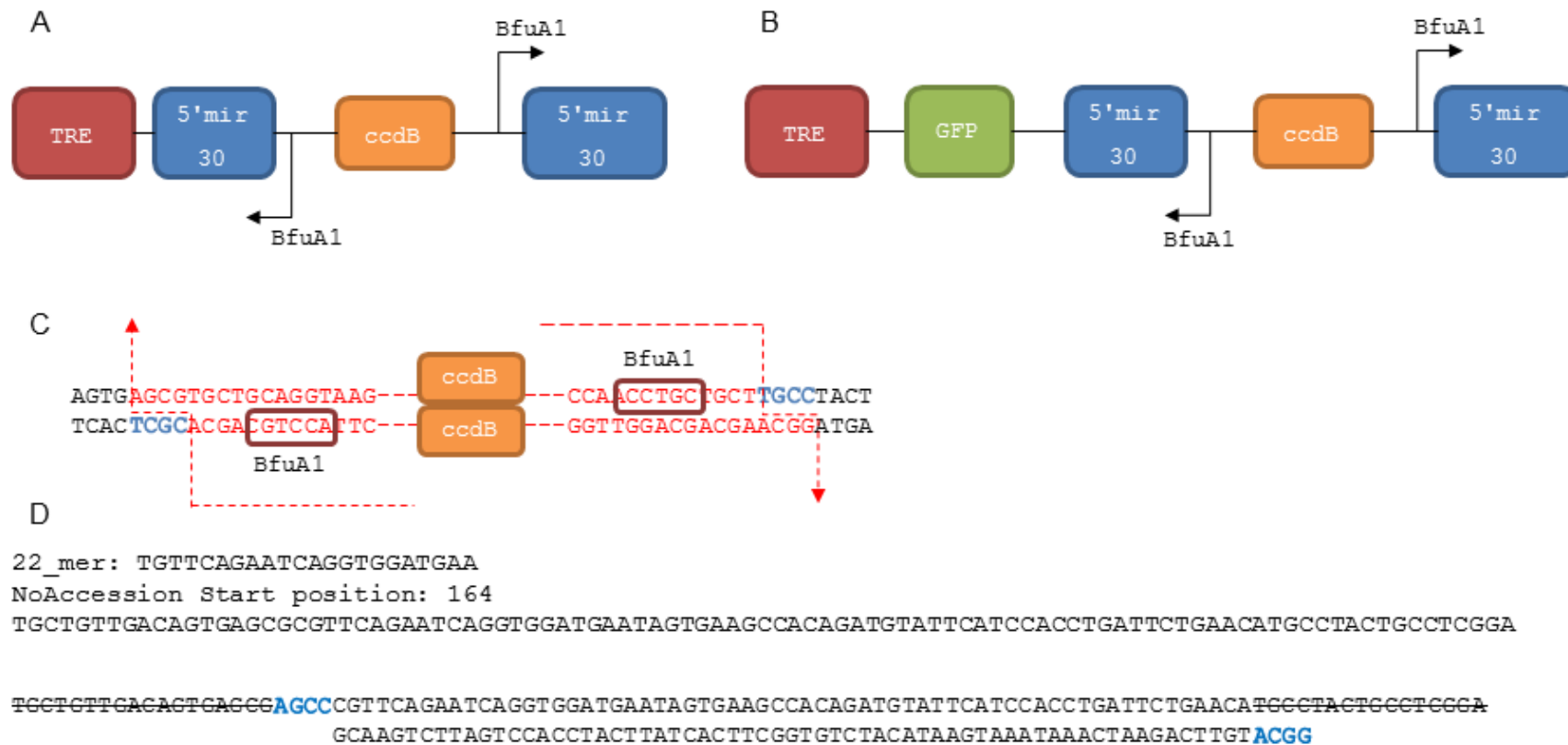


Figure 6-4: Design of shRNA constructs

shRNA constructs were designed as described (section 2.6.2) and (Shin et al. 2006) **A** - Schematic of the pEN_TmiRc3 and **B** - pEN_TGmiRc3 plasmids **C** - Digestion of the plasmid with BfuA1 (BfuA1 recognition site surrounded by red box) removes the toxic ccdB gene and allows for entry of the shRNA construct downstream of the TRE promoter. **D** - Design of the shRNA sequence, sequence was designed using RNAi Codex (<http://cancan.cshl.edu/cgi-bin/Codex/Codex.cgi>). The first 18 nucleotides were deleted from the 5' end and the first 16 nucleotides were deleted from the 3' end (marked with ~~strikethrough~~). AGCG was added to the 5' end of the sense strand and ACGG to the antisense strand, this creates overhangs that are complementary to those created by digestion of the pEN plasmids with BfuA1 (**C**).

Table 6-1: Expected fragment size for each pEN plasmid following digestion with endonucleases.

Plasmid	Fragments produced following digestion with BsRG1 endonuclease
pEN_TmiRc3	1889, 1478, 773, 447
pEN_TmiRc3 + VAMP2	1740, 1478, 730, 215, 149
pEN_TmiRc3 + VAMP4	1740, 1478, 945, 149
pEN_TGmiRc3	1889, 1478,1219, 447, 270
pEN_TGmiRc3+ VAMP2	1889, 1478,1219,227,215
pEN_TGmiRc3+ VAMP4	1889, 1478,1219,442

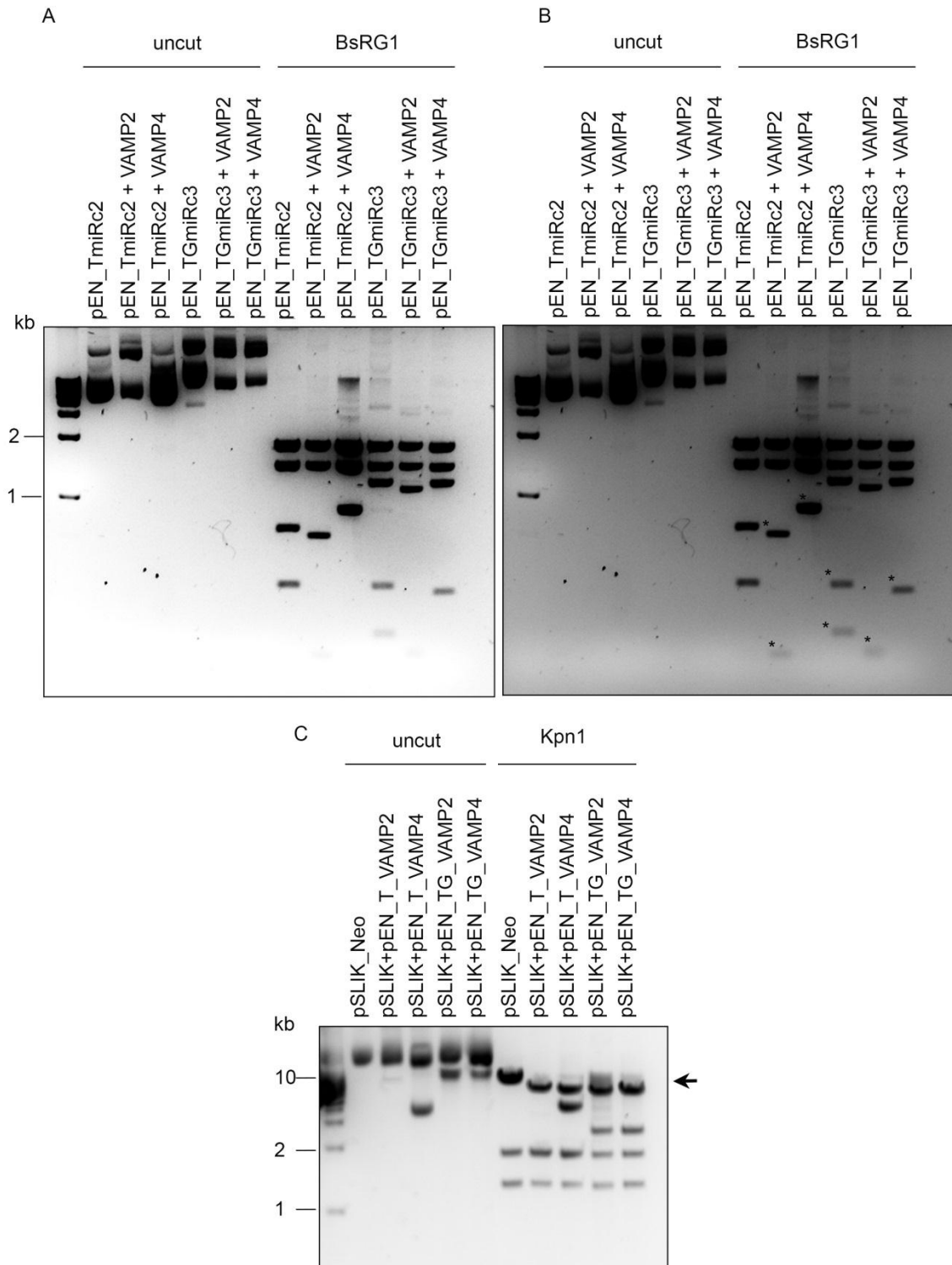


Figure 6-5: Generation of pEN and pSLIK vectors

Purified plasmid DNA samples were separated by electrophoresis in 1.5% agarose gels. Where indicated samples were subjected to restriction digestion with the indicated enzyme at 37°C for 1 hour. **A** and **B** - shRNA constructs against VAMP2 and VAMP4 were ligated into pEN_TmiRc3 or pEN_TGmiRc3, digested with BsRG1 to determine the presence of the shRNA (A and B are the same gel, A is a shorter exposure than B), key fragments are marked with * on B. **C** - pEN_TmiRc3 or pEN_TGmiRc3 containing shRNA constructs were shuttled into pSLIK_Neo, resultant constructs were digested with Kpn1 to determine the presence of the pEN cassette, insertion of the pEN cassette led to a drop in the size of the 10,173 bp band, indicated by arrow (C).

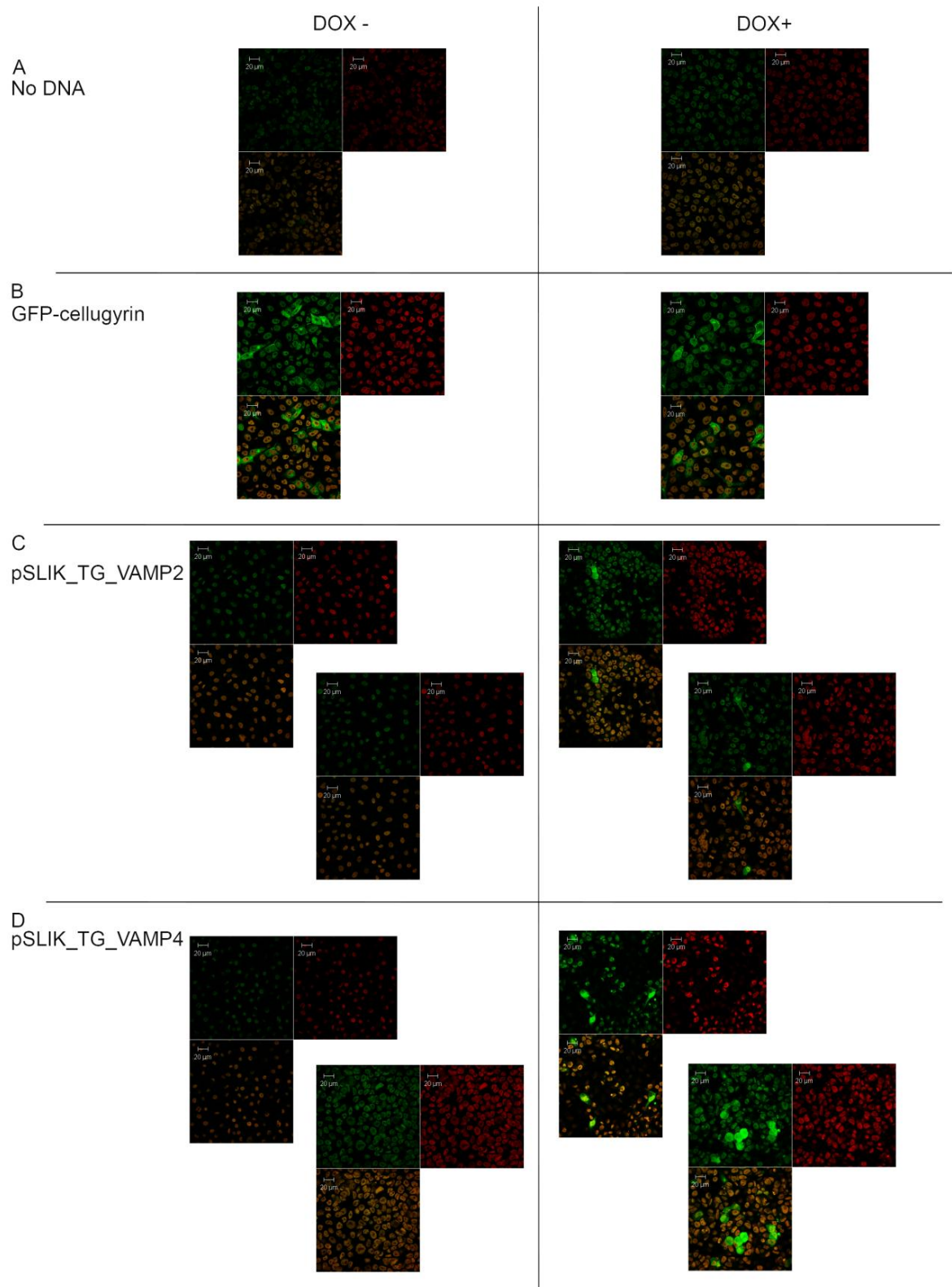


Figure 6-6: Testing of pSLIK_TG_VAMP2 and pSLIK_TG_VAMP4 constructs in HeLa cells. HeLa cells expressing mCherry tubulin (red) were grown on glass coverslips in 12 well plates as described (section 2.4.2) and transfected with 1.25μg DNA per well using Lipofectamine™ 2000. Cells were transfected with **A** - No DNA, **B** - GFP-cellugyrin, **C** - pSLIK_TG_VAMP2 or **D** - pSLIK_TG_VAMP4. 24 hours later DNA expression of pSLIK_TG_VAMP2 and 4 was induced by the addition of 1μg/ml DOX (+ DOX) or left unstimulated (-DOX) for a further 24 hours. GFP-cellugyrin is not under the control of the DOX inducible TET promoter so the GFP is constitutively expressed; both pSLIK_TG_VAMP2 and 4 are under the control of the TET promoter so GFP is only expressed following DOX stimulation. Images were taken using the 63x oil immersion lens and are representative of a typical field of cells n=6.

6.4 Discussion

The first striking finding here was that in HeLa cells expressing HA-GLUT4-GFP both VAMP 2 and 4 knock down increased the basal appearance of GLUT4 in the plasma membrane, and prevented any significant increases in GLUT4 insertion into the plasma membrane following insulin stimulation (Figure 6-3 A, C). This suggests that trafficking steps involving VAMP2 and 4 are required to sequester GLUT4 into the insulin sensitive compartment. Closer examination of the data however allows differences between the effects of VAMP2 and VAMP4 knock down to be seen.

The increase in GLUT4 in the plasma membrane under basal conditions was nearly a third larger following VAMP2 depletion than VAMP4 (Figure 6-3B, 2.7-fold vs 1.8-fold). VAMP2 knock down completely abolished any increase in GLUT4 in the plasma membrane following insulin stimulation. Conversely, following VAMP4 depletion, insulin was still able to increase GLUT4 in the plasma membrane, although the increase was not significant (1.7-fold, compared to 3-fold in control cells, Figure 6-3 C $p=0.18$).

The different phenotypes seen with depletion of VAMP2 vs. depletion of VAMP4 can be explained in two ways. The first is that all GLUT4 passes through a VAMP2-dependent trafficking step, whereas not all GLUT4 passes through a VAMP4-dependent trafficking step. This explanation is in line with the data of Williams and Pessin (2008), who found that VAMP4 was required for the sorting of newly synthesised GLUT4 into GSVs.

The other explanation is that VAMP2 and 4 act at different trafficking steps, and thus depletion of each protein affects GLUT4 localisation in different ways. As shown in Figure 6-7 A, GLUT4 cycles between different compartments *en route* to GSVs. Following internalisation from the plasma membrane, GLUT4 traffics through early endosomes and into recycling endosomes. From here, it either slowly recycles back to the plasma membrane, or is segregated into GSVs via the *trans* Golgi network. In the presence of insulin, GSVs are rapidly recruited to the plasma membrane. In the absence of insulin, GSVs cycle back into the endosomal system and continue through the recycling pathway.

VAMP2 has been implicated in the SNARE complex that is required for trafficking of cargo from early endosomes into recycling endosomes (Prekeris et al. 1998; Aikawa et al. 2006). Although this has not been directly tested, if VAMP2 were required for GLUT4 trafficking from early endosomes to recycling endosomes, VAMP2 depletion would prevent GLUT4 entering the recycling endosomes. Under these conditions GLUT4 would remain in the early endosomes. The consequences of this would be two fold. Firstly, it would prevent GLUT4 being sorted into GSVs. Secondly, it would increase GLUT4 levels in the plasma membrane to near maximal values. This is because cargo from the early endosomes cycles rapidly back to the plasma membrane, whereas cargo that traffics back to the plasma membrane via the recycling endosomes traffics much more slowly. In this model, under conditions of VAMP2 depletion, the formation of GSVs from newly synthesised GLUT4 is not prevented. However, as insulin is not present in HeLa growth media, GLUT4 cycles out of GSVs and back into the endosomal system (Figure 6-7 B), where it becomes trapped in the early endosomes. This model dictates that due to its role in the trafficking of cargo from early to recycling endosomes, VAMP2 depletion increases the presence of GLUT4 in the plasma membrane to near maximal values under basal conditions. Furthermore, since GLUT4 is not sorted into GSVs, insulin does not increase the presence of GLUT4 in the plasma membrane. The predictions of this model are consistent with the data shown in Figure 6-3. Figure 6-3 shows that VAMP2 depletion increases basal GLUT4 appearance at the plasma membrane to levels similar to those seen in control cells following insulin-stimulation, and abolishes any increase in response to insulin.

On the other hand, VAMP4 has been shown to interact with the tSNARE complex syntaxin 16/6/Vti1a in HeLa cells (Mallard et al. 2002) and interacts with syntaxin 16 in 3T3 L1 adipocytes (Chapter 5, Figure 5-7). This tSNARE complex is found within the *trans* Golgi network and is required for the retrograde trafficking of the Shiga toxin (Mallard et al. 2002). tSNARE complexes containing syntaxin 6 and 16 are also required for the trafficking of GLUT4 into GSVs (Perera et al. 2003; Shewan et al. 2003; Proctor et al. 2006). Since VAMP4 interacts with syntaxin 16, it seems likely that VAMP4 is also involved in this trafficking step. In this model, VAMP4 depletion results in disruption of the SNARE complex that is required for trafficking cargo through the TGN (Figure 6-7

C). This in turn prevents GLUT4 entering GSVs. Under these conditions, GLUT4 is shuttled into the endosomal recycling system where it is engaged in a cycle that acts between the plasma membrane, early endosomes and the recycling endosomes. This model predicts that, as seen with VAMP2 depletion, VAMP4 depletion results in all GLUT4 cycling between the endosomal system and the plasma membrane. However, because GLUT4 cycles between three compartments, the rate of cycling is much slower than if it were only cycling between the early endosomes and the plasma membrane. The net result of this would be that the levels of GLUT4 at the plasma membrane under basal conditions increase, but not to the same extent as seen with VAMP2 depletion. Insulin-stimulation would increase the rate of flux through the endosomal compartments and therefore increase GLUT4 in the plasma membrane, but because GLUT4 is not sorted into GSVs the increase would be smaller than that which is seen in control cells. The predictions of this model are entirely consistent with the phenotype that is seen with VAMP4 depletion (Figure 6-3). Figure 6-3 shows that VAMP4 depletion increases the basal appearance of GLUT4 in the plasma membrane, but to a lesser degree than seen with VAMP2 depletion. Insulin-stimulation of HeLa cells expressing GLUT4 but depleted of VAMP4 increased GLUT4 appearance at the plasma membrane by 1-7 fold, although this was not statistically significant ($p=0.18$). The proposed models to explain the roles of VAMP2 and 4 in GLUT4 trafficking and the effects of VAMP2 and 4 depletion compared to control cells are explained in Figure 6-7.

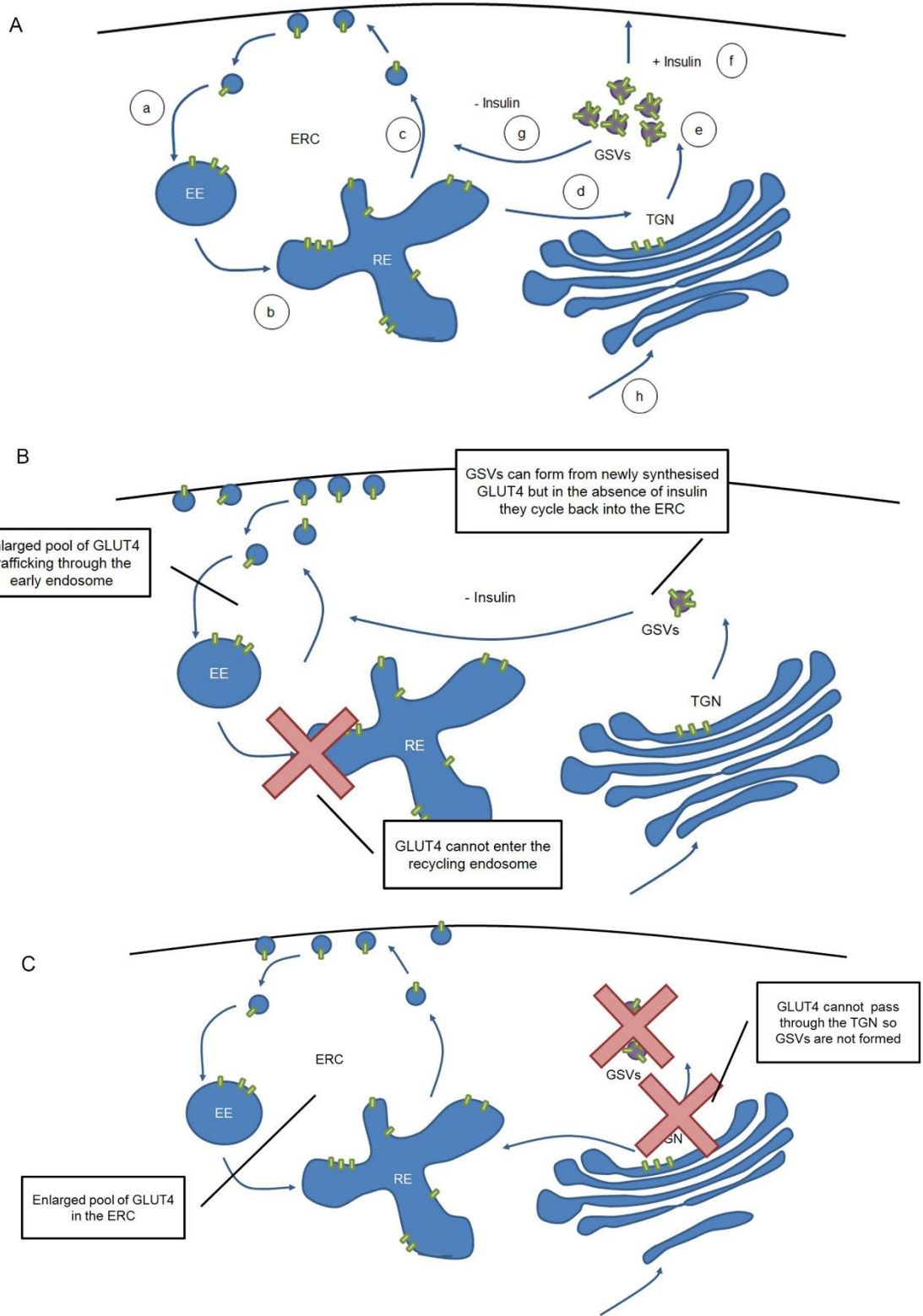


Figure 6-7: GLUT4 recycling.

A: GLUT4 continuously cycles through two inter-linked pools: GLUT4 is internalised from the plasma membrane to early endosomes (a) and is passed onto recycling endosomes (b). From recycling endosomes it is either trafficked back to the plasma membrane. This cycle forms the endosomal recycling compartment (ERC). Alternatively, GLUT4 is passed to the TGN (d) where it is sorted into GSVs (e). GSVs provide a readily available store of GLUT4 that is recruited to the plasma membrane in the presence of insulin (f). In the absence of insulin, GLUT4 cycles back into the ERC (g) and re-enters the cycle. Newly synthesised GLUT4 can directly enter GSVs (h). **B: When VAMP2 is depleted GLUT4 cannot enter the recycling endosome:** GLUT4 is internalised from the plasma membrane to early endosomes (a) however it cannot enter the recycling endosome. It is therefore not trafficked to the TGN or into GSVs. Newly synthesised GLUT4 enters GSVs, but as insulin is absent it cycles back into the endosomal system. Re-entry into GSVs is blocked at the recycling endosome, so GSVs are not formed and there is no insulin response or sequestering of GLUT4 away from the plasma membrane under basal conditions. **C: When VAMP4 is depleted GLUT4 cannot enter GSVs:** GLUT4 is internalised from the plasma membrane, passed to the early endosome and the recycling endosome. However entry into GSVs is blocked. Newly synthesised GLUT4 is also not able to enter GSVs and is targeted to the ERC. GLUT4 remains in the ERC, which increases the basal appearance of GLUT4 at the plasma membrane. Insulin increases the rate of flux through the ERC, and thus can increase GLUT4 appearance at the plasma membrane.

Figure 6-3 displays that irrespective of the model by which this occurs, both VAMP2 and 4 are required for the effective trafficking of GLUT4 into GSVs. The finding that VAMP4 is required for the sorting of GLUT4 into GSVs is in line with data implicating VAMP4 in the sorting of newly synthesised GLUT4 into GSVs (Williams & Pessin 2008). However, in this study Williams and Pessin (2008) only observed an effect of VAMP4 depletion when this was done prior to GLUT4 expression, suggesting that VAMP4 is required for sorting of biosynthetic but not recycling GLUT4 into GSVs. In contrast, the data displayed in Figure 6-3 are from experiments where HA-GLUT-GFP was expressed prior to VAMP2 or 4 depletion. These data demonstrate that VAMP2 and 4 are required for recycling of GLUT4 into GSVs. This difference may be due to differences in cell types studied (3T3 L1 adipocytes vs. HeLa cells).

However, this may also be due to differences in data presentation. Looking closely at the data of Williams and Pessin (2008), under conditions of VAMP2 or 4 depletion there is a non-significant increase in basal GLUT4 at the plasma membrane. This is seen when the absolute values of plasma membrane to total GLUT4 are compared. The representation of data in this manner may be slightly misleading, since what is of interest is how depletion of the protein (VAMP2 or 4) affects the distribution of GLUT4 compared to untreated control cells. The fold-change in GLUT4 presence at the plasma membrane compared to control cells would provide more information, and was therefore used here. Figure 6-3 clearly shows that depletion of VAMP2 or 4 alters the intracellular trafficking of HA-

GLUT4-GFP, this is reflected in a significant difference in the cell surface GLUT4 when normalised to control levels (fold change $p < 0.05$). However, if the data is not normalised to values obtained for control cells then the magnitude of the difference is reduced in statistical terms. Therefore, the differences in the effect of VAMP2 or 4 depletion seen by Williams and Pessin (2008) compared to those seen here may be a function of the method used to display and normalise the data.

Another possible explanation for the differences could be the number of cells included in the analysis. Here, a minimum of 96 cells were used per condition, compared to 45 in studies by Williams and Pessin (2008). However, it seems unlikely that this could account for the differences. Even significant effects were observed in the data here, when a similar number of cells were analysed as those compared by Williams and Pessin (2008).

Although HeLa cells provide a good model for studying GLUT4 trafficking, they do not express GLUT4. This raises the possibility that when GLUT4 is ectopically expressed in these cells, it is trafficked in a different manner than in insulin-sensitive cells. Therefore it is important that these findings are replicated in an insulin-sensitive cell line, such as 3T3 L1 adipocytes. In this regard, a secondary aim of this chapter was to generate a system where shRNA constructs can be transfected into fibroblasts, the cells then differentiated into adipocytes and once cells are differentiated, the shRNA can be expressed.

Using the pSLIK platform (Shin et al. 2006), inducible vectors containing shRNA constructs that target VAMP2 and 4 have been successfully designed, made and tested in HeLa cells (Figure 6-4, Figure 6-6). The next steps in these experiments are to produce viral particles containing these vectors and use these to infect 3T3 L1 fibroblasts. This will allow the ability of the shRNA construct to deplete cells of VAMP2 and 4 to be tested.

6.5 Conclusion

In summary this chapter has highlighted that VAMP2 and 4 play roles in the intracellular trafficking of GLUT4 into GSVs. The first steps have been taken to develop an inducible viral vector system to deplete these proteins in 3T3 L1 adipocytes following differentiation.

Chapter 7 - Discussion

7.1 Summary of findings

The aims of this thesis were to dissect the roles of the post-Golgi vSNAREs of the VAMP subfamily in the intracellular trafficking and sorting of GLUT4. In meeting this aim a number of novel findings have been made.

Firstly, the absolute expression level of each of the VAMP isoforms has been systematically quantified. This represents the first analysis of this kind in any cell type. Strikingly, the levels of each VAMP isoform differed significantly. VAMP8 was expressed at the highest level, followed by VAMP3, VAMP2 and then VAMP4. VAMPs 5 and 7 were expressed at very low levels. This differential expression of each VAMP is likely to be a reflection of the specialisation of adipocytes, which are known to be active in secreting adipocytokines and other polypeptides, and thus may be considered specialised secretory cells. How these VAMP level differences compare across other neuroendocrine or secretory cells will be an interesting subject for future research.

The studies outlined above determined differences in VAMP expression levels on a per cell basis. Further analysis also revealed that these VAMPs showed differences in subcellular distribution and localisation with insulin-sensitive GLUT4 vesicles (GSVs). This generates highly significant variations in 'local' concentrations of VAMPs. Taken together, the localisation and expression level data supports a scenario where VAMP2 is the predominant vSNARE involved in the fusion of GSVs with the cell surface in response to insulin. This is further supported by the finding that, although all VAMPs are able to form stable SDS resistant SNARE complexes with both syntaxin 4/SNAP23 and syntaxin 16/SNAP23, only VAMP2 could be seen to interact with syntaxin 4 in 3T3 L1 adipocytes.

This study also provides evidence suggesting that VAMP4 is involved in the formation of GSVs. It was found that VAMP4, but not any other VAMPs, interact with syntaxin 16 in 3T3 L1 adipocytes. In line with this and the requirement for syntaxin 16 in the formation of GSVs (Proctor et al. 2006), the depletion of VAMP4 seemed to prevent the effective sorting of GLUT4 from the endosomal recycling pool into GSVs.

7.2 Findings in the context of existing literature

An important aspect of this study was to examine the expression levels of each of the VAMP proteins in adipocytes. This, alongside the determination of the subcellular distribution of each VAMP isoform with insulin-sensitive GLUT4, allowed rough calculations of the number of VAMPs localised with each insulin-sensitive GLUT4 molecule to be estimated, at least on a per cell basis assuming equal distribution of the protein(s) in question. It was estimated that for each GLUT4 there were four VAMP2 molecules (section 4.4.4). GSVs have been estimated to contain five molecules of GLUT4 (Kupriyanova et al. 2002), which would give 20 molecules of VAMP2 per GSV, well within the range of estimates of the number of SNARE proteins required for membrane fusion (see section 4-4-4). However, this is around 4 times fewer than the number of VAMP molecules found on synaptic vesicles (Takamori et al. 2006). Takamori et al., (2006) isolated synaptic vesicles through cell fractionation procedures. Similar to here, the number of VAMP molecules per synaptic vesicle was determined using quantitative immunoblotting. They estimated that each synaptic vesicle contains 70 molecules of VAMP2. The difference in SNARE density between synaptic vesicles and GSVs is probably not a function of the methodology used as similar methodology (subcellular fractionation followed by quantitative immunoblotting) was used in both studies. Here, GSVs were not isolated prior to the determination of VAMP concentration, which may account for the 4-fold difference between GSVs and synaptic vesicles. Alternatively, the difference may reflect cell-type differences as synaptic vesicles are involved in neurotransmission and need to fuse with the pre-synaptic membrane within a fraction of a second. Compared to this, the insulin-stimulated fusion of GSVs with the plasma membrane is much slower with a time scale of seconds to minutes. The higher density of SNAREs on synaptic vesicles may help to increase the rate of fusion by increasing the chances of SNARE complex formation or the rate of complex formation.

This study has provided data to support a scenario whereby VAMP2 is the predominant vSNARE involved in GSV fusion with the plasma membrane. Early research examining the vSNARE requirements for insulin-stimulated GLUT4 translocation to the plasma membrane highlighted VAMP2 as being the

predominant vSNARE involved in this process (Cheatham et al. 1996; Martin et al. 1998; Williams & Pessin 2008; Kawaguchi et al. 2010). More recently one key study has found that VAMP3 and 8 may also be able to act in this process (Zhao et al 2009). Therefore this study set out to examine the mechanism behind this 'plasticity'. In particular the ability of VAMP proteins to interact with syntaxin 4 *in vitro* and *in vivo* was examined, and their localisation with insulin-sensitive GLUT4 was determined.

The results presented in Chapter 3 suggest that under physiological conditions, when all VAMPs are present, only VAMP2 interacts with the tSNARE involved in insulin-stimulated GLUT4 insertion into the plasma membrane (syntaxin 4). Furthermore, Chapter 4 highlights that VAMP2 is found to localise with insulin-sensitive GLUT4, and translocates with GLUT4 to the plasma membrane upon insulin-stimulation. Conversely, VAMP3 is found predominantly with GLUT4 in the endosomal recycling compartment (ERC) and VAMP8 does not seem to be selectively localised with insulin-sensitive GLUT4 and does not exhibit insulin-stimulated movement to the plasma membrane. These findings support the original hypothesis that VAMP2 is the vSNARE involved in the insulin-stimulated insertion of GLUT4 into the cell surface. However, it is important to note that these results do not dispute the findings of Zhao and colleagues that show that in the absence of VAMP2, 3 or 8 any of these VAMPs can compensate. Rather, the results presented in Chapter 4 help to clarify the manner in which VAMPs 2, 3 and 8 can act in the fusion of GLUT4 vesicles with the plasma membrane, and shed some light as to why VAMPs 4, 5 and 7 cannot. As discussed, VAMP2 is localised to GSVs. In contrast, although VAMP3 translocates with GLUT4 to the cell surface in response to insulin, it localises with GLUT4 in the ERC. Insulin is known to increase the traffic of endosomal proteins to the cell surface, and the rate of recycling through the ERC (Tanner & Lienhard 1987). Therefore in the absence of VAMP2, VAMP3 may compensate in the fusion of GLUT4 vesicles with the plasma membrane through the mobilisation of GLUT4 from the ERC. VAMP8 has been shown to be expressed at high levels and therefore, although not selectively sorted alongside insulin-sensitive GLUT4, it may be present on GLUT4 containing vesicles, both within the ERC and GSVs. In contrast, VAMP5 and 7 were both expressed at very low levels and although VAMP4 was expressed at levels similar to VAMP2, it did not translocate to the cell surface in response to

insulin, suggesting that it is not present on GSVs. The expression level and subcellular distribution data suggest that VAMP4, 5 and 7 are not found in significant amounts on GSVs. This is supported by data produced by Zhao et al. (2009) who identified VAMP2, 3 and 8 on docking GSVs, and found these VAMPs co-localised with GLUT4 in the low density membrane fraction of adipocytes (the fraction that contains insulin-sensitive GLUT4) (Zhao et al. 2009).

As part of Chapter 4 the protein expression level of each of the VAMPs was examined pre and post differentiation of 3T3 L1 cells into adipocytes. The differentiation of adipocytes leads to an increase in the level of GLUT4, the acquisition of insulin-responsiveness, and the generation of insulin-sensitive GSVs (El-Jack et al. 1999). Differentiation is also associated with an increase in the protein content of a number of proteins implicated in the sorting of GLUT4 into GSVs, such as IRAP and syntaxin 16 (Ross et al. 1996; Roccisana et al. 2013). In line with roles in the trafficking of GLUT4 from the ERC and GSVs to the plasma membrane, the levels of VAMP2 and 3 increase with differentiation. The levels of VAMP8 remain unchanged, further supporting the notion that this protein's involvement in GLUT4 trafficking is more incidental than selective. Similarly, the levels of VAMPs 5 and 7 remain unchanged. Interestingly, the levels of VAMP4 do increase. This is despite VAMP4 not being found on GSVs or being involved in the translocation of GSVs to the cell surface. That the levels of VAMP4 increase with differentiation suggest this protein is important in some aspect of adipocyte-specific function. Indeed VAMP4 has been implicated in GLUT4 trafficking and the formation of insulin sensitive GSVs (Williams & Pessin 2008, Chapter 5 and 6).

Previous research has provided evidence that VAMP4 is required for the entry of newly synthesised, but not recycled, GLUT4 into GSVs (Williams & Pessin 2008). This research also suggested that VAMP2 may also be involved in the formation of GSVs (Williams & Pessin 2008). These conclusions were drawn on the basis of data produced by examining the trafficking of the GLUT4 reporter myc-GLUT4-GFP in 3T3 L1 adipocytes depleted of VAMPs. The conclusion that recycled GLUT4 did not require VAMP4 to enter GSVs was reached based on the finding that when myc-GLUT4-GFP was expressed in the absence of VAMP4, although there was evidence of an enlargement in the ERC compartment, and thus a

reduction in the GSV compartment, there was still a robust insulin-stimulated increase in GLUT4 translocation. Therefore it was postulated that some GLUT4 must still be entering GSVs. However, the insulin-stimulated increase in GLUT4-translocation seen under conditions of VAMP4 depletion may have been a result of insulin increasing the exocytosis of GLUT4 from the ERC compartment. The conclusion that VAMP2 is required for the formation of GSVs came from the finding that insulin-stimulated GLUT4 translocation is only completely inhibited by VAMP2 depletion (Williams & Pessin 2008). However, this could be a result of the well-documented requirement for VAMP2 in the fusion of GSVs with the plasma membrane (Cheatham et al. 1996; Martin et al. 1998; Williams & Pessin 2008; Kawaguchi et al. 2010).

The results of Chapter 5 and 6 support a role for VAMP4 in the formation of GSVs, and suggest that, at least in HeLa cells, VAMP2 may also be involved. The formation of GSVs requires the tSNARE syntaxin 16 (Perera et al. 2003; Proctor et al. 2006). In HeLa cells syntaxin16 interacts with both VAMP3 and VAMP4 (Mallard et al. 2002). Although there is no evidence VAMP3 is involved in the trafficking of GLUT4, it is implicated in trafficking through the ERC (Daro et al. 1996; Martin et al. 1996; Riggs et al. 2012). This raises the possibility that VAMP3 interacts with syntaxin 16 in adipocytes, and may be involved in the trafficking of GLUT4. Chapter 5 shows that, in contrast to in HeLa cells, VAMP4, but not VAMP3 or any other VAMPs, interacts with syntaxin 16 in 3T3 L1 adipocytes. This, alongside previous research showing VAMP3 depletion has no effect on GLUT4 trafficking (Williams & Pessin 2008), seems to rule out VAMP3 in the recycling of GLUT4 into GSVs.

Experiments examining the trafficking of HA-GLUT4-GFP in HeLa cells reveal a requirement for VAMP4 in the trafficking of GLUT4 into GSVs. The phenotype of HA-GLUT4-GFP localisation following VAMP4 depletion, alongside the finding that VAMP4 interacts with the TGN tSNARE syntaxin 16, implies that VAMP4 is required for the passage of GLUT4 through the TGN. These experiments also reveal that VAMP2 is required for the trafficking of GLUT4 from the ERC to GSVs, at least in HeLa cells. In HeLa cells, VAMP2 depletion increases the basal GLUT4 in the plasma membrane to similar levels to insulin-stimulation. In contrast, VAMP4 depletion increases basal GLUT4 in the plasma membrane, but does not

abolish the increase in GLUT4 at the plasma membrane in response to insulin. The different phenotypes seen for GLUT4 distribution between VAMP2 and 4 depletion in HA-GLUT4-GFP expressing HeLa cells can be explained by two different theories. These are described in detail in the discussion section of Chapter 6 (section 6.4). Briefly, the first theory is that all GLUT4 passes through a VAMP2 requiring step, but not all GLUT4 passes through a VAMP4 requiring step. The alternative theory is that the step involving VAMP2 precedes the step involving VAMP4. In this model, VAMP4 acts at the TGN alongside syntaxin 16, whereas VAMP2 acts at the step of sorting GLUT4 out of early endosomes into recycling endosomes. Therefore, in the absence of VAMP2, GLUT4 is trapped in a rapid cycle between the early endosome and the plasma membrane. On the other hand, in the absence of VAMP4, GLUT4 traffics between the plasma membrane, early, and recycling endosomes. Although these theories have not been directly tested here, a number of lines of evidence support the second scenario.

VAMP2 has been implicated in a SNARE complex made up of SNAP25 and syntaxin 13 (Prekeris et al. 1998; Aikawa et al. 2006). In turn, this SNARE complex has been implicated in the trafficking of cargo from the early endosome to the recycling endosome, at least in PC12 cells (Prekeris et al. 1998; Aikawa et al. 2006). Conversely, VAMP4 is localised to the TGN where it interacts with the tSNAREs syntaxin 16 and 6 (Steegmaier et al. 1999; Mallard et al. 2002). Syntaxin 6, 16 and VAMP4 are required for retrograde trafficking of the Shiga toxin and both syntaxin 6 and 16 have been implicated in the trafficking of GLUT4 through the TGN into GSVs (Mallard et al. 2002; Perera et al. 2003; Proctor et al. 2006; Foley & Klip 2014).

These observations, as well as the effects of depletion of VAMPs 2 and 4 in HeLa cells expressing HA-GLUT4-GFP (Chapter 6; Figure 6-3), support a scenario whereby VAMP2 is required for GLUT4 to traffic from the early endosome to the recycling endosome, and VAMP4 is required for GLUT4 to traffic from the recycling endosome to GSVs.

The phenotype seen here with VAMP4 depletion in HeLa cells expressing HA-GLUT4-GFP is largely similar to that seen in previous studies by Williams and

Pessin (2008) using a different cell type and GLUT4 reporter. Williams and Pessin (2008) studied VAMP requirements in 3T3 L1 adipocytes using a myc-GLUT4-GFP reporter for GLUT4 localisation. Although it is likely that the myc-GLUT4-GFP reporter traffics in a similar manner to endogenous GLUT4, this reporter has not been as well characterised as the HA-GLUT4-GFP transporter. Therefore, despite the phenotypes being similar in these studies, it is important that the findings are replicated and further characterised in 3T3 L1 adipocytes using the better characterised HA-GLUT4-GFP reporter. In contrast to the phenotype seen with VAMP4 depletion, the phenotype seen with VAMP2 depletion in HeLa cells is drastically different to that seen in 3T3 L1 adipocytes (Williams & Pessin 2008; Figure 6-3). This may be a reflection of differences in the cell type examined. Therefore future studies will need to examine the effect of VAMP2 depletion on HA-GLUT4-GFP trafficking in 3T3 L1 adipocytes. Experiments will also need to be carried out to determine the role of VAMP3 in the trafficking of GLUT4 in HeLa cells. In HeLa cells, unlike in 3T3 L1 adipocytes where only VAMP4 interacts with syntaxin 16, VAMP3 interacts with syntaxin 16 and is involved in retrograde trafficking in this cell type (Mallard et al. 2002). It is therefore plausible that in HeLa cells VAMP3 plays a role in the retrograde trafficking of GLUT4.

Studies examining the roles of these VAMPs, in both 3T3 L1 adipocytes and HeLa cells using the same well characterised HA-GLUT4-GFP transporter, will not only provide valuable information regarding the trafficking of GLUT4 into GSVs, but will also give insights into any membrane trafficking differences that exist between HeLa cells and 3T3 L1 adipocytes. It is important to characterise GLUT4 trafficking in both these cell lines. An increasing body of work has recently begun to highlight species-specific differences in GLUT4 trafficking and sorting. For example, in humans a specialised Clathrin Heavy Chain, CHC22, is required for normal trafficking of GLUT4. This isoform is notably absent in mice (Vassilopoulos et al. 2009; Esk et al. 2010). Similarly, the SNARE Syntaxin 10 is involved in GLUT4 trafficking in humans, but again is absent from mice (Ganley et al. 2008; Esk et al. 2010). These findings highlight an alternative explanation as to why VAMP2 knockdown provides distinctly different results in HeLa cells and 3T3 L1 adipocytes (Figure 6-3; Williams & Pessin 2008). The differences in results may not be a function of differences in the cell type *per se* but due to

species differences. This demonstrates an important need in the field for standardised human adipocyte cell lines to be used for such mechanistic studies.

7.3 Wider implications

The finding that VAMP4 is implicated in the sorting of GLUT4 into GSVs is particularly interesting with regard to obesity and Type 2 diabetes. Type 2 diabetes is associated with increased adiposity, and increased triglyceride storage. Triglycerides are stored in lipid droplets. Lipid droplets increase in size through fusion with other smaller lipid droplets. Lipid droplet fusion has been shown to require the SNARE proteins SNAP23, syntaxin 5 and VAMP4 (Boström et al. 2007). Increasing the rate of lipid droplet fusion leads to competition for the limited pool of SNAP23. This leads to a 'high-jacking' of SNAP23 away from the plasma membrane to the lipid droplet, where it acts in lipid droplet fusion events, increasing the lipid droplet size (Boström et al. 2007). A similar mechanism may take place for VAMP4. When lipid availability is elevated, as is the case in obesity, VAMP4 may be high-jacked away from the TGN to lipid droplets. Although this has not been examined, the high-jacking of VAMP4 away from the TGN may prevent GLUT4 being recycled into GSVs and therefore may lead to a reduction in insulin-stimulated GLUT4 translocation. This is a possible mechanism by which a high fat diet could contribute to a reduction in insulin-stimulated GLUT4 translocation.

7.4 Conclusions and future directions

Uncovering the mechanisms governing the trafficking of GLUT4 into the insulin-sensitive GSV compartment is a vital part of understanding insulin-stimulated increases in glucose uptake. Here, evidence has been provided supporting the role of VAMP2 in the fusion of GSVs with the plasma membrane in response to insulin. Evidence has also been provided supporting a role for VAMP4 in the trafficking of GLUT4 into the insulin-sensitive compartment.

It has previously been demonstrated that when VAMP2 is absent, VAMP3 and 8 can act in the fusion of GLUT4 with the plasma membrane (Zhao et al. 2009). Here it has been shown that in the presence of VAMP2, these VAMPs do not interact with the tSNARE involved in this process, syntaxin 4. It has also been

demonstrated that these VAMPs are not selectively sorted onto GSVs. Therefore the mechanism by which these VAMPs compensate for VAMP2 loss needs further clarification.

This thesis has also provided data to suggest that, at least in HeLa cells, VAMP2 is involved in the recycling of GLUT4 into GSVs. This may be at the stage of the trafficking of cargo from the early to the recycling endosome. Further clarification regarding the role VAMP2 plays in this trafficking step in 3T3 L1 adipocytes is required.

The role of VAMP4 in the formation of GSVs also requires more investigation. Results presented here suggest that VAMP4 is required for the formation of GSVs. However, it has been proposed that VAMP4 is only required for the entry of newly synthesised GLUT4 into GSVs in 3T3 L1 adipocytes (Williams & Pessin 2008). Whether any GSVs are formed in the absence of VAMP4, or whether the observed insulin response in this study, and in previous studies, is from the enlarged ERC compartment was not directly tested here and requires further clarification.

VAMP4 is involved in both GSV formation and lipid droplet fusion. Both of these cellular processes seem to be dysregulated in obesity-related insulin resistance. Therefore the relationship between these two events should be examined.

Finally, it now seems clear that SNAREs alone do not provide the specificity for fusion (Chapter 3, 5; Fasshauer et al. 1999; Yang et al. 1999; Scales et al. 2000). Identifying the component(s) that provides this specificity will be a key step in understanding the regulation of membrane fusion events.

Chapter 8 - Appendicies

8.1 Immunoprecipitation of syntaxin 4 and syntaxin 16

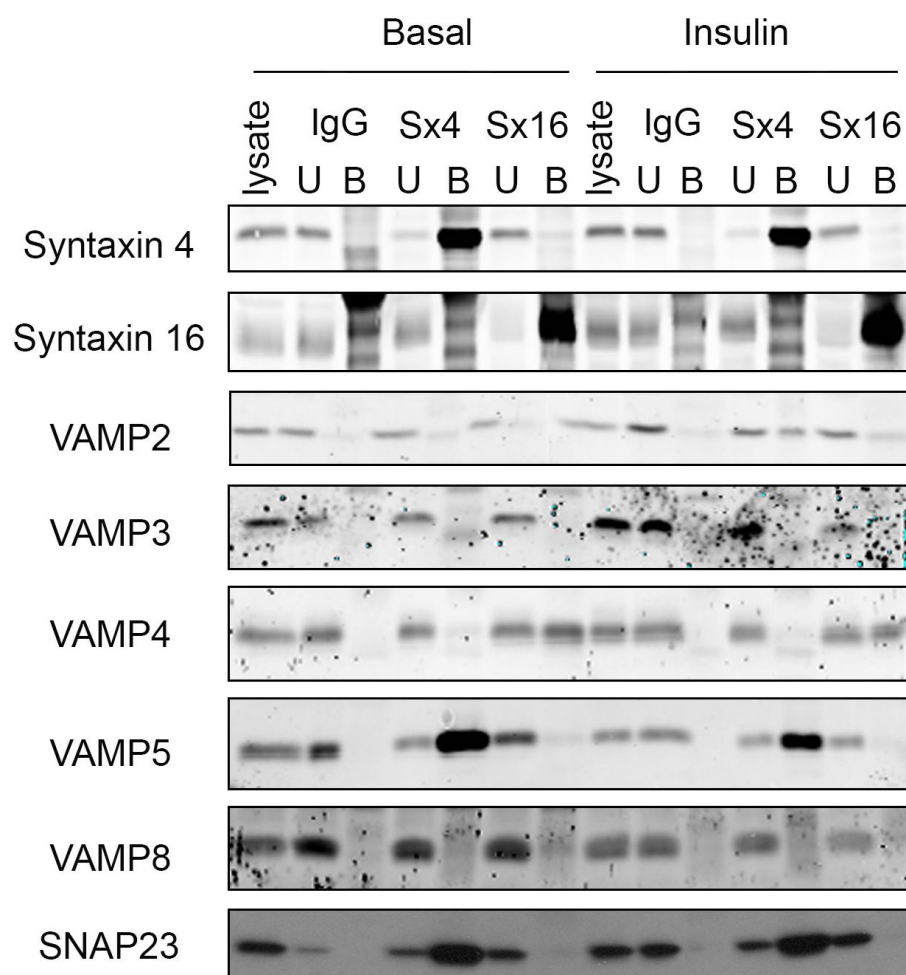


Figure 8-1: Co-Immunoprecipitation of VAMP proteins with syntaxin 4 and syntaxin 16 in 3T3 L1 adipocytes.

Random rabbit IgG, syntaxin 4, and syntaxin 16 were immunoprecipitated from serum starved 3T3 L1 adipocytes treated with (insulin) or without (basal) 1 μ M insulin for 20 minutes as described (section 2.8). Proteins were immunoprecipitated from 1.5mg 3T3 L1 lysate (lysate) with 5 μ l anti-syntaxin 4 (Sx4), syntaxin 16 (Sx16) or random rabbit IgG (IgG). Immunoprecipitated proteins and associated material was isolated by centrifugation and unbound material retained (U). Bound material (B) was washed and eluted in 2xLSB. Samples were subjected to SDS-PAGE and immunoblotting with anti-syntaxin 4, anti-syntaxin 16 and anti-VAMP antibodies (B). Samples from basal and insulin-stimulated cells were subjected to immunoblotting on the same membrane data shown are from a typical experiment, experiments were repeated a minimum of 3 times.

List of References

- Abel, E.D. et al., 2001. Adipose-selective targeting of the GLUT4 gene impairs insulin action in muscle and liver. *Nature*, 409(6821), pp.729-33.
- Advani, R.J. et al., 1998. Seven novel mammalian SNARE proteins localize to distinct membrane compartments. *The Journal of biological chemistry*, 273(17), pp.10317-24.
- Aikawa, Y. et al., 2006. A second SNARE role for exocytic SNAP25 in endosome fusion. *Molecular biology of the cell*, 17(5), pp.2113-24.
- Antonin, W. et al., 2000. The R-SNARE Endobrevin/VAMP-8 Mediates Homotypic Fusion of Early Endosomes and Late Endosomes. *Molecular Biology of the Cell*, 11, pp.3289-3298.
- Aran, V., Bryant, N.J. & Gould, G.W., 2011. Tyrosine phosphorylation of Munc18c on residue 521 abrogates binding to Syntaxin 4. *BMC biochemistry*, 12, p.19.
- Bai, L. et al., 2007. Dissecting multiple steps of GLUT4 trafficking and identifying the sites of insulin action. *Cell metabolism*, 5(1), pp.47-57.
- Bethani, I. et al., 2007. The specificity of SNARE pairing in biological membranes is mediated by both proof-reading and spatial segregation. *The EMBO journal*, 26(17), pp.3981-92.
- Biber, J.W. & Lienhard, G.E., 1986. Isolation of vesicles containing insulin-responsive, intracellular glucose transporters from 3T3-L1 adipocytes. *The Journal of biological chemistry*, 261(34), pp.16180-4.
- Block, M.R. et al., 1988. Purification of an N-ethylmaleimide-sensitive protein catalyzing vesicular transport. *Proceedings of the National Academy of Sciences of the United States of America*, 85(21), pp.7852-6.
- Blot, V. & McGraw, T.E., 2006. GLUT4 is internalized by a cholesterol-dependent nystatin-sensitive mechanism inhibited by insulin. *The EMBO journal*, 25(24), pp.5648-58.
- Blot, V. & McGraw, T.E., 2008. Molecular mechanisms controlling GLUT4 intracellular retention. *Molecular biology of the cell*, 19(8), pp.3477-87.
- Bock, J.B. et al., 2001. A genomic perspective on membrane compartment organization. *Nature*, 409(6822), pp.839-41.
- Bock, J.B. et al., 1997. Syntaxin 6 functions in trans-Golgi network vesicle trafficking. *Molecular biology of the cell*, 8(7), pp.1261-71.
- Van den Bogaart, G. et al., 2010. One SNARE complex is sufficient for membrane fusion. *Nature structural & molecular biology*, 17(3), pp.358-64.

- Bogan, J.S. et al., 2003. Functional cloning of TUG as a regulator of GLUT4 glucose transporter trafficking. *Nature*, 425(6959), pp.727-33.
- Bose, A. et al., 2005. The v-SNARE Vti1a regulates insulin-stimulated glucose transport and Acrp30 secretion in 3T3-L1 adipocytes. *The Journal of biological chemistry*, 280(44), pp.36946-51.
- Boström, P. et al., 2007. SNARE proteins mediate fusion between cytosolic lipid droplets and are implicated in insulin sensitivity. *Nature cell biology*, 9(11), pp.1286-93.
- Boström, P. et al., 2010. The SNARE protein SNAP23 and the SNARE-interacting protein Munc18c in human skeletal muscle are implicated in insulin resistance/type 2 diabetes. *Diabetes*, 59(8), pp.1870-8.
- Brandhorst, D. et al., 2006. Homotypic fusion of early endosomes: SNAREs do not determine fusion specificity. *Proceedings of the National Academy of Sciences of the United States of America*, 103(8), pp.2701-6.
- Brandie, F.M. et al., 2008. Negative regulation of syntaxin4/SNAP-23/VAMP2-mediated membrane fusion by Munc18c in vitro. *PloS one*, 3(12), p.e4074.
- Bryant, N.J. et al., 1998. Retrograde traffic out of the yeast vacuole to the TGN occurs via the prevacuolar/endosomal compartment. *The Journal of cell biology*, 142(3), pp.651-63.
- Bryant, N.J. & James, D.E., 2001. Vps45p stabilizes the syntaxin homologue Tlg2p and positively regulates SNARE complex formation. *The EMBO journal*, 20(13), pp.3380-8.
- Burkhardt, P. et al., 2008. Munc18a controls SNARE assembly through its interaction with the syntaxin N-peptide. *The EMBO journal*, 27(7), pp.923-33.
- Calderhead, D.M. et al., 1990. Insulin regulation of the two glucose transporters in 3T3-L1 adipocytes. *The Journal of biological chemistry*, 265(23), pp.13801-8.
- Carpp, L.N. et al., 2006. The Sec1p/Munc18 protein Vps45p binds its cognate SNARE proteins via two distinct modes. *The Journal of cell biology*, 173(6), pp.927-36.
- Carr, C.M. & Rizo, J., 2010. At the junction of SNARE and SM protein function. *Current opinion in cell biology*, 22(4), pp.488-95.
- Chamberlain, L.H. & Gould, G.W., 2002. The vesicle- and target-SNARE proteins that mediate Glut4 vesicle fusion are localized in detergent-insoluble lipid rafts present on distinct intracellular membranes. *The Journal of biological chemistry*, 277(51), pp.49750-4.

- Cheatham, B. et al., 1996. Insulin-stimulated translocation of GLUT4 glucose transporters requires SNARE-complex proteins. *Proceedings of the National Academy of Sciences of the United States of America*, 93(26), pp.15169-73.
- Chen, D. et al., 1997. Osmotic Shock Stimulates GLUT4 Translocation in 3T3L1 Adipocytes by a Novel Tyrosine Kinase Pathway. *Journal of Biological Chemistry*, 272(43), pp.27401-27410.
- Chen, X.-W. et al., 2007. Activation of RalA is required for insulin-stimulated Glut4 trafficking to the plasma membrane via the exocyst and the motor protein Myo1c. *Developmental cell*, 13(3), pp.391-404.
- Chen, X.-W. & Saltiel, A.R., 2011. Ral's engagement with the exocyst: breaking up is hard to do. *Cell cycle*, 10(14), pp.2299-304.
- Chen, Y. et al., 2012. Rab10 and myosin-Va mediate insulin-stimulated GLUT4 storage vesicle translocation in adipocytes. *The Journal of cell biology*, 198(4), pp.545-60.
- Chen, Y. & Lippincott-Schwartz, J., 2013. Rab10 delivers GLUT4 storage vesicles to the plasma membrane. *Communicative & integrative biology*, 6(3), p.e23779.
- Clary, D.O., Griff, I.C. & Rothman, J.E., 1990. SNAPs, a family of NSF attachment proteins involved in intracellular membrane fusion in animals and yeast. *Cell*, 61(4), pp.709-21.
- Corvera, S. et al., 1994. A double leucine within the GLUT4 glucose transporter COOH-terminal domain functions as an endocytosis signal. *The Journal of cell biology*, 126(4), pp.979-89.
- Coster, A.C.F., Govers, R. & James, D.E., 2004. Insulin stimulates the entry of GLUT4 into the endosomal recycling pathway by a quantal mechanism. *Traffic (Copenhagen, Denmark)*, 5(10), pp.763-71.
- Cowles, C.R., Emr, S.D. & Horazdovsky, B.F., 1994. Mutations in the VPS45 gene, a SEC1 homologue, result in vacuolar protein sorting defects and accumulation of membrane vesicles. *Journal of cell science*, 107 (Pt 1, pp.3449-59.
- Daro, E. et al., 1996. Rab4 and cellubrevin define different early endosome populations on the pathway of transferrin receptor recycling. *Proceedings of the National Academy of Sciences of the United States of America*, 93(18), pp.9559-64.
- Dulubova, I. et al., 2002. How Tlg2p/syntaxin 16 "snares" Vps45. *The EMBO journal*, 21(14), pp.3620-31.
- Dykxhoorn, D.M. & Lieberman, J., 2005. The silent revolution: RNA interference as basic biology, research tool, and therapeutic. *Annual review of medicine*, 56, pp.401-23.

- Elbashir, S.M. et al., 2001. Duplexes of 21-nucleotide RNAs mediate RNA interference in cultured mammalian cells. *Nature*, 411(6836), pp.494-8.
- El-Jack, a K., Kandror, K. V & Pilch, P.F., 1999. The formation of an insulin-responsive vesicular cargo compartment is an early event in 3T3-L1 adipocyte differentiation. *Molecular biology of the cell*, 10(5), pp.1581-94.
- Esk, C. et al., 2010. The clathrin heavy chain isoform CHC22 functions in a novel endosomal sorting step. *The Journal of cell biology*, 188(1), pp.131-44.
- Ewart, M.-A. et al., 2005. Evidence for a role of the exocyst in insulin-stimulated Glut4 trafficking in 3T3-L1 adipocytes. *The Journal of biological chemistry*, 280(5), pp.3812-6.
- Fasshauer, D. et al., 1999. Mixed and non-cognate SNARE complexes. Characterization of assembly and biophysical properties. *The Journal of biological chemistry*, 274(22), pp.15440-6.
- Fernandez, I. et al., 1998. Three-dimensional structure of an evolutionarily conserved N-terminal domain of syntaxin 1A. *Cell*, 94(6), pp.841-9.
- Foley, K.P. & Klip, A., 2014. Dynamic GLUT4 sorting through a syntaxin-6 compartment in muscle cells is derailed by insulin resistance-causing ceramide. *Biology open*, 3(5), pp.314-25.
- Foster, L.J. et al., 1999. SNAP23 promotes insulin-dependent glucose uptake in 3T3-L1 adipocytes: possible interaction with cytoskeleton. *The American journal of physiology*, 276(5 Pt 1), pp.C1108-14.
- Fujita, H. et al., 2010. Identification of three distinct functional sites of insulin-mediated GLUT4 trafficking in adipocytes using quantitative single molecule imaging. *Molecular biology of the cell*, 21(15), pp.2721-31.
- Funaki, M., DiFransico, L. & Janmey, P.A., 2006. PI 4,5-P2 stimulates glucose transport activity of GLUT4 in the plasma membrane of 3T3-L1 adipocytes. *Biochimica et biophysica acta*, 1763(8), pp.889-99.
- Furgason, M.L.M. et al., 2009. The N-terminal peptide of the syntaxin Tlg2p modulates binding of its closed conformation to Vps45p. *Proceedings of the National Academy of Sciences of the United States of America*, 106(34), pp.14303-8.
- Galli, T. et al., 1998. A novel tetanus neurotoxin-insensitive vesicle-associated membrane protein in SNARE complexes of the apical plasma membrane of epithelial cells. *Molecular biology of the cell*, 9(6), pp.1437-48.
- Galli, T. et al., 1994. Tetanus toxin-mediated cleavage of cellubrevin impairs exocytosis of transferrin receptor-containing vesicles in CHO cells. *The Journal of cell biology*, 125(5), pp.1015-24.

- Ganley, I.G., Espinosa, E. & Pfeffer, S.R., 2008. A syntaxin 10-SNARE complex distinguishes two distinct transport routes from endosomes to the trans-Golgi in human cells. *The Journal of cell biology*, 180(1), pp.159-72.
- Garvey, W.T. et al., 1988. Role of glucose transporters in the cellular insulin resistance of type II non-insulin-dependent diabetes mellitus. *The Journal of clinical investigation*, 81(5), pp.1528-36.
- Govers, R., Coster, A.C.F. & James, D.E., 2004. Insulin increases cell surface GLUT4 levels by dose dependently discharging GLUT4 into a cell surface recycling pathway. *Molecular and cellular biology*, 24(14), pp.6456-66.
- Guilherme, A. et al., 2004. Role of EHD1 and EHBP1 in perinuclear sorting and insulin-regulated GLUT4 recycling in 3T3-L1 adipocytes. *The Journal of biological chemistry*, 279(38), pp.40062-75.
- Haga, Y., Ishii, K. & Suzuki, T., 2011. N-glycosylation is critical for the stability and intracellular trafficking of glucose transporter GLUT4. *The Journal of biological chemistry*, 286(36), pp.31320-7.
- Hajdуч, E. et al., 1997. Proteolytic cleavage of cellubrevin and vesicle-associated membrane protein (VAMP) by tetanus toxin does not impair insulin-stimulated glucose transport or GLUT4 translocation in rat adipocytes. *The Biochemical journal*, 321 (Pt 1), pp.233-8.
- Hashiramoto, M. & James, D.E., 2000. Characterization of insulin-responsive GLUT4 storage vesicles isolated from 3T3-L1 adipocytes. *Molecular and cellular biology*, 20(1), pp.416-27.
- Hatakeyama, H. & Kanzaki, M., 2011. Molecular basis of insulin-responsive GLUT4 trafficking systems revealed by single molecule imaging. *Traffic (Copenhagen, Denmark)*, 12(12), pp.1805-20.
- Herman, G.A. et al., 1994. A distinct class of intracellular storage vesicles, identified by expression of the glucose transporter GLUT4. *Proceedings of the National Academy of Sciences of the United States of America*, 91(26), pp.12750-4.
- Hernandez, J.M. et al., 2014. Variable cooperativity in SNARE-mediated membrane fusion. *Proceedings of the National Academy of Sciences of the United States of America*, 111(33), pp.12037-42.
- Hernandez, R., Teruel, T. & Lorenzo, M., 2001. Akt mediates insulin induction of glucose uptake and up-regulation of GLUT4 gene expression in brown adipocytes. *FEBS letters*, 494(3), pp.225-31.
- Hickson, G.R. et al., 2000. Quantification of SNARE protein levels in 3T3-L1 adipocytes: implications for insulin-stimulated glucose transport. *Biochemical and biophysical research communications*, 270(3), pp.841-5.
- Hong, W., 2005. SNAREs and traffic. *Biochimica et biophysica acta*, 1744(2), pp.120-44.

- Hong, W. & Lev, S., 2014. Tethering the assembly of SNARE complexes. *Trends in cell biology*, 24(1), pp.35-43.
- Hu, C. et al., 2003. Fusion of cells by flipped SNAREs. *Science (New York, N.Y.)*, 300(5626), pp.1745-9.
- Hu, C., Hardee, D. & Minnear, F., 2007. Membrane fusion by VAMP3 and plasma membrane t-SNAREs. *Experimental cell research*, 313(15), pp.3198-209.
- Hua, Y. & Scheller, R.H., 2001. Three SNARE complexes cooperate to mediate membrane fusion. *Proceedings of the National Academy of Sciences of the United States of America*, 98(14), pp.8065-70.
- Huang, S. & Czech, M.P., 2007. The GLUT4 glucose transporter. *Cell metabolism*, 5(4), pp.237-52.
- Inoue, M. et al., 2003. The exocyst complex is required for targeting of Glut4 to the plasma membrane by insulin. *Nature*, 422(6932), pp.629-33.
- Jahn, R. & Scheller, R.H., 2006. SNAREs--engines for membrane fusion. *Nature reviews. Molecular cell biology*, 7(9), pp.631-43.
- Jedrychowski, M.P. et al., 2010. Proteomic analysis of GLUT4 storage vesicles reveals LRP1 to be an important vesicle component and target of insulin signaling. *The Journal of biological chemistry*, 285(1), pp.104-14.
- Jewell, J.L. et al., 2011. Munc18c phosphorylation by the insulin receptor links cell signaling directly to SNARE exocytosis. *The Journal of cell biology*, 193(1), pp.185-99.
- Johnson, A.M.F. & Olefsky, J.M., 2013. The origins and drivers of insulin resistance. *Cell*, 152(4), pp.673-84.
- Karatekin, E. et al., 2010. A fast, single-vesicle fusion assay mimics physiological SNARE requirements. *Proceedings of the National Academy of Sciences of the United States of America*, 107(8), pp.3517-21.
- Karylowski, O. et al., 2004. GLUT4 is retained by an intracellular cycle of vesicle formation and fusion with endosomes. *Molecular biology of the cell*, 15(2), pp.870-82.
- Kawaguchi, T. et al., 2010. The t-SNAREs syntaxin4 and SNAP23 but not v-SNARE VAMP2 are indispensable to tether GLUT4 vesicles at the plasma membrane in adipocyte. *Biochemical and biophysical research communications*, 391(3), pp.1336-41.
- Kawanishi, M. et al., 2000. Role of SNAP23 in insulin-induced translocation of GLUT4 in 3T3-L1 adipocytes. Mediation of complex formation between syntaxin4 and VAMP2. *The Journal of biological chemistry*, 275(11), pp.8240-7.

- Keller, J.E., Cai, F. & Neale, E. a, 2004. Uptake of botulinum neurotoxin into cultured neurons. *Biochemistry*, 43(2), pp.526-32.
- Kioumourtzoglou, D., Gould, G.W. & Bryant, N.J., 2014. Insulin stimulates syntaxin4 SNARE complex assembly via a novel regulatory mechanism. *Molecular and cellular biology*, 34(7), pp.1271-9.
- Kraegen, E.W. et al., 1985. Dose-response curves for in vivo insulin sensitivity in individual tissues in rats. *The American journal of physiology*, 248(3 Pt 1), pp.E353-62.
- Kupriyanova, T. a & Kandrор, K. V, 2000. Cellugyrin is a marker for a distinct population of intracellular Glut4-containing vesicles. *The Journal of biological chemistry*, 275(46), pp.36263-8.
- Kupriyanova, T. a, Kandrор, V. & Kandrор, K. V, 2002. Isolation and characterization of the two major intracellular Glut4 storage compartments. *The Journal of biological chemistry*, 277(11), pp.9133-8.
- Lamb, C. a et al., 2010. Insulin-regulated trafficking of GLUT4 requires ubiquitination. *Traffic (Copenhagen, Denmark)*, 11(11), pp.1445-54.
- Lampson, M. a et al., 2000. Demonstration of insulin-responsive trafficking of GLUT4 and vpTR in fibroblasts. *Journal of cell science*, 113 (Pt 2, pp.4065-76.
- Lang, T. et al., 2001. SNAREs are concentrated in cholesterol-dependent clusters that define docking and fusion sites for exocytosis. *The EMBO journal*, 20(9), pp.2202-13.
- Larance, M. et al., 2005. Characterization of the role of the Rab GTPase-activating protein AS160 in insulin-regulated GLUT4 trafficking. *The Journal of biological chemistry*, 280(45), pp.37803-13.
- Latham, C.F. et al., 2006. Molecular dissection of the Munc18c/syntaxin4 interaction: implications for regulation of membrane trafficking. *Traffic (Copenhagen, Denmark)*, 7(10), pp.1408-19.
- Laufman, O., Hong, W. & Lev, S., 2011. The COG complex interacts directly with Syntaxin 6 and positively regulates endosome-to-TGN retrograde transport. *The Journal of cell biology*, 194(3), pp.459-72.
- Leto, D. & Saltiel, A.R., 2012. Regulation of glucose transport by insulin: traffic control of GLUT4. *Nature reviews. Molecular cell biology*, 13(6), pp.383-96.
- Li, F. et al., 2014. A half-zippered SNARE complex represents a functional intermediate in membrane fusion. *Journal of the American Chemical Society*, 136(9), pp.3456-64.
- Li, F. et al., 2007. Energetics and dynamics of SNAREpin folding across lipid bilayers. *Nature structural & molecular biology*, 14(10), pp.890-6.

- Li, J. et al., 2007. An ACAP1-containing clathrin coat complex for endocytic recycling. *The Journal of cell biology*, 178(3), pp.453-64.
- Li, L. V & Kandror, K. V, 2005. Golgi-localized, gamma-ear-containing, Arf-binding protein adaptors mediate insulin-responsive trafficking of glucose transporter 4 in 3T3-L1 adipocytes. *Molecular endocrinology (Baltimore, Md.)*, 19(8), pp.2145-53.
- Livingstone, C. et al., 1996. Compartment ablation analysis of the insulin-responsive glucose transporter (GLUT4) in 3T3-L1 adipocytes. *The Biochemical journal*, 315 (Pt 2, pp.487-95.
- Lizunov, V. a et al., 2013. Insulin regulates Glut4 confinement in plasma membrane clusters in adipose cells. *PloS one*, 8(3), p.e57559.
- Lizunov, V. a et al., 2005. Insulin stimulates the halting, tethering, and fusion of mobile GLUT4 vesicles in rat adipose cells. *The Journal of cell biology*, 169(3), pp.481-9.
- Low, S.H. et al., 2006. Syntaxins 3 and 4 are concentrated in separate clusters on the plasma membrane before the establishment of cell polarity. *Molecular biology of the cell*, 17(2), pp.977-89.
- Maianu, L., Keller, S.R. & Garvey, W.T., 2001. Adipocytes exhibit abnormal subcellular distribution and translocation of vesicles containing glucose transporter 4 and insulin-regulated aminopeptidase in type 2 diabetes mellitus: implications regarding defects in vesicle trafficking. *The Journal of clinical endocrinology and metabolism*, 86(11), pp.5450-6.
- Maier, V.H. & Gould, G.W., 2000. Long-term insulin treatment of 3T3-L1 adipocytes results in mis-targeting of GLUT4: implications for insulin-stimulated glucose transport. *Diabetologia*, 43(10), pp.1273-81.
- Maier, V.H. et al., 2000. v- and t-SNARE protein expression in models of insulin resistance: normalization of glycemia by rosiglitazone treatment corrects overexpression of cellubrevin, vesicle-associated membrane protein-2, and syntaxin 4 in skeletal muscle of Zucker diabetic fat. *Diabetes*, 49(4), pp.618-25.
- Mallard, F. et al., 2002. Early/recycling endosomes-to-TGN transport involves two SNARE complexes and a Rab6 isoform. *Journal of Cell Biology*, 156(4), pp.653-664.
- Martin, L.B. et al., 1998. Vesicle-associated membrane protein 2 plays a specific role in the insulin-dependent trafficking of the facilitative glucose transporter GLUT4 in 3T3-L1 adipocytes. *The Journal of biological chemistry*, 273(3), pp.1444-52.
- Martin, O.J., Lee, A. & McGraw, T.E., 2006. GLUT4 distribution between the plasma membrane and the intracellular compartments is maintained by an insulin-modulated bipartite dynamic mechanism. *The Journal of biological chemistry*, 281(1), pp.484-90.

- Martin, S. et al., 1994. Analysis of the co-localization of the insulin-responsive glucose transporter (GLUT4) and the trans Golgi network marker TGN38 within 3T3-L1 adipocytes. *The Biochemical journal*, 300 (Pt 3, pp.743-9.
- Martin, S. et al., 2000. Effects of insulin on intracellular GLUT4 vesicles in adipocytes: evidence for a secretory mode of regulation. *Journal of cell science*, 113 Pt 19, pp.3427-38.
- Martin, S. et al., 1996. The glucose transporter (GLUT-4) and vesicle-associated membrane protein-2 (VAMP-2) are segregated from recycling endosomes in insulin-sensitive cells. *Journal of Cell Biology*, 134(3), pp.625-635.
- Martinez-Arca, S. et al., 2000. Role of tetanus neurotoxin insensitive vesicle-associated membrane protein (TI-VAMP) in vesicular transport mediating neurite outgrowth. *The Journal of cell biology*, 149(4), pp.889-900.
- McMahon, H.T. et al., 1993. Cellubrevin is a ubiquitous tetanus-toxin substrate homologous to a putative synaptic vesicle fusion protein. *Nature*, 364, pp.346-349.
- McNew, J.A. et al., 2000. Compartmental specificity of cellular membrane fusion encoded in SNARE proteins. *Nature*, 407(6801), pp.153-9.
- Millar, C. a et al., 2000. Adipsin and the glucose transporter GLUT4 traffic to the cell surface via independent pathways in adipocytes. *Traffic (Copenhagen, Denmark)*, 1(2), pp.141-51.
- Millar, C. a et al., 1999. Differential regulation of secretory compartments containing the insulin-responsive glucose transporter 4 in 3T3-L1 adipocytes. *Molecular biology of the cell*, 10(11), pp.3675-88.
- Misura, K.M., Scheller, R.H. & Weis, W.I., 2000. Three-dimensional structure of the neuronal-Sec1-syntaxin 1a complex. *Nature*, 404(6776), pp.355-62.
- Mohrmann, R. et al., 2010. Fast vesicle fusion in living cells requires at least three SNARE complexes. *Science (New York, N.Y.)*, 330(6003), pp.502-5.
- Montecucco, C., Schiavo, G. & Pantano, S., 2005. SNARE complexes and neuroexocytosis: how many, how close? *Trends in biochemical sciences*, 30(7), pp.367-72.
- Mueckler, M., 1994. Facilitative glucose transporters. *European journal of biochemistry / FEBS*, 219(3), pp.713-25.
- Newell-Litwa, K. et al., 2009. Roles of BLOC-1 and adaptor protein-3 complexes in cargo sorting to synaptic vesicles. *Molecular biology of the cell*, 20(5), pp.1441-53.
- Nielsen, M.S. et al., 2001. The sortilin cytoplasmic tail conveys Golgi-endosome transport and binds the VHS domain of the GGA2 sorting protein. *The EMBO journal*, 20(9), pp.2180-90.

- Olson, a L., Knight, J.B. & Pessin, J.E., 1997. Syntaxin 4, VAMP2, and/or VAMP3/cellubrevin are functional target membrane and vesicle SNAP receptors for insulin-stimulated GLUT4 translocation in adipocytes. *Molecular and cellular biology*, 17(5), pp.2425-35.
- Palacios, S. et al., 2001. Recycling of the insulin-sensitive glucose transporter GLUT4. Access of surface internalized GLUT4 molecules to the perinuclear storage compartment is mediated by the Phe5-Gln6-Gln7-Ile8 motif. *The Journal of biological chemistry*, 276(5), pp.3371-83.
- Parlati, F. et al., 2002. Distinct SNARE complexes mediating membrane fusion in Golgi transport based on combinatorial specificity. *Proceedings of the National Academy of Sciences of the United States of America*, 99(8), pp.5424-9.
- Paumet, F., Rahimian, V. & Rothman, J.E., 2004. The specificity of SNARE-dependent fusion is encoded in the SNARE motif. *Proceedings of the National Academy of Sciences of the United States of America*, 101(10), pp.3376-80.
- Perera, H.K.I. et al., 2003. Syntaxin 6 regulates Glut4 trafficking in 3T3-L1 adipocytes. *Molecular biology of the cell*, 14(7), pp.2946-58.
- Pessin, J.E. & Bell, G.I., 1992. Mammalian facilitative glucose transporter family: structure and molecular regulation. *Annual review of physiology*, 54(39), pp.911-30.
- Piper, R.C. et al., 1991. Differential sorting of two glucose transporters expressed in insulin-sensitive cells. *Am J Physiol.*, 260(3), pp.570-580.
- Piper, R.C. et al., 1993. GLUT-4 NH2 terminus contains a phenylalanine-based targeting motif that regulates intracellular sequestration. *The Journal of cell biology*, 121(6), pp.1221-32.
- Piper, R.C., Whitters, E.A. & Stevens, T.H., 1994. Yeast Vps45p is a Sec1p-like protein required for the consumption of vacuole-targeted, post-Golgi transport vesicles. *European journal of cell biology*, 65(2), pp.305-18.
- Polgár, J., Chung, S. & Reed, G.L., 2002. Vesicle-associated membrane protein 3 (VAMP-3) and VAMP-8 are present in human platelets and are required for granule secretion. *Blood*, 100(3), pp.1081-3.
- Predescu, S. a et al., 2005. Cholesterol-dependent syntaxin-4 and SNAP-23 clustering regulates caveolar fusion with the endothelial plasma membrane. *The Journal of biological chemistry*, 280(44), pp.37130-8.
- Prekeris, R. et al., 1998. Syntaxin 13 mediates cycling of plasma membrane proteins via tubulovesicular recycling endosomes. *The Journal of cell biology*, 143(4), pp.957-71.

- Proctor, K.M. et al., 2006. Syntaxin 16 controls the intracellular sequestration of GLUT4 in 3T3-L1 adipocytes. *Biochemical and biophysical research communications*, 347(2), pp.433-8.
- Puertollano, R. et al., 2001. The GGAs promote ARF-dependent recruitment of clathrin to the TGN. *Cell*, 105(1), pp.93-102.
- Ramm, G. et al., 2000. Insulin recruits GLUT4 from specialized VAMP2-carrying vesicles as well as from the dynamic endosomal/trans-Golgi network in rat adipocytes. *Molecular biology of the cell*, 11(12), pp.4079-91.
- Randhawa, V.K. et al., 2004. Insulin and hypertonicity recruit GLUT4 to the plasma membrane of muscle cells by using N-ethylmaleimide-sensitive factor-dependent SNARE mechanisms but different v-SNAREs: role of TI-VAMP. *Molecular biology of the cell*, 15(12), pp.5565-73.
- Randhawa, V.K. et al., 2000. VAMP2, but not VAMP3/cellubrevin, mediates insulin-dependent incorporation of GLUT4 into the plasma membrane of L6 myoblasts. *Molecular biology of the cell*, 11(7), pp.2403-17.
- Rea, S. et al., 1998. Syndet, an adipocyte target SNARE involved in the insulin-induced translocation of GLUT4 to the cell surface. *The Journal of biological chemistry*, 273(30), pp.18784-92.
- Riggs, K. a et al., 2012. Regulation of integrin endocytic recycling and chemotactic cell migration by syntaxin 6 and VAMP3 interaction. *Journal of cell science*, 125(Pt 16), pp.3827-39.
- Roccisana, J. et al., 2013. Sorting of GLUT4 into its insulin-sensitive store requires the Sec1/Munc18 protein mVps45. *Molecular biology of the cell*, 24(15), pp.2389-97.
- Roccisana, J. (University of G., 2010. *The role of mVps45 in regulating GLUT4 trafficking in 3T3 L1 adipocytes*. University of Glasgow, Glasgow.
- Ros-Baro, A. et al., 2001. Lipid rafts are required for GLUT4 internalization in adipose cells. *Proceedings of the National Academy of Sciences of the United States of America*, 98(21), pp.12050-5.
- Rose, A.J. et al., 2009. Effects of contraction on localization of GLUT4 and v-SNARE isoforms in rat skeletal muscle. *American journal of physiology. Regulatory, integrative and comparative physiology*, 297(5), pp.R1228-37.
- Ross, S. a. et al., 1996. Characterization of the Insulin-regulated Membrane Aminopeptidase in 3T3-L1 Adipocytes. *Journal of Biological Chemistry*, 271(6), pp.3328-3332.
- Rossetto, O. et al., 1996. VAMP/synaptobrevin isoforms 1 and 2 are widely and differentially expressed in nonneuronal tissues. *The Journal of cell biology*, 132(1-2), pp.167-79.

- Rothman, J.E., 1994. Mechanisms of intracellular protein transport. *Nature*, 372(6501), pp.55-63. Available at: <http://www.ncbi.nlm.nih.gov/pubmed/7969419> [Accessed September 25, 2014].
- Sano, H. et al., 2007. Rab10, a target of the AS160 Rab GAP, is required for insulin-stimulated translocation of GLUT4 to the adipocyte plasma membrane. *Cell metabolism*, 5(4), pp.293-303.
- Scales, S.J. et al., 2000. SNAREs contribute to the specificity of membrane fusion. *Neuron*, 26(2), pp.457-64.
- Schäfer, I.B. et al., 2012. The binding of Varp to VAMP7 traps VAMP7 in a closed, fusogenically inactive conformation. *Nature structural & molecular biology*, 19(12), pp.1300-9.
- Schlaepfer, I.R. et al., 2003. Increased expression of the SNARE accessory protein Munc18c in lipid-mediated insulin resistance. *Journal of lipid research*, 44(6), pp.1174-81.
- Schwenk, R.W. et al., 2010. Requirement for distinct vesicle-associated membrane proteins in insulin- and AMP-activated protein kinase (AMPK)-induced translocation of GLUT4 and CD36 in cultured cardiomyocytes. *Diabetologia*, 53(10), pp.2209-19.
- Shanks, S.G. et al., 2012. The Sec1/Munc18 protein Vps45 regulates cellular levels of its SNARE binding partners Tlg2 and Snc2 in *Saccharomyces cerevisiae*. *PloS one*, 7(11), p.e49628.
- Sherman, F., 1991. Getting started with yeast. *Methods Enzymol*, 41(2002), pp.3-41.
- Shewan, A.M. et al., 2003. GLUT4 Recycles via a trans -Golgi Network (TGN) Subdomain Enriched in Syntaxins 6 and 16 But Not TGN38 : Involvement of an Acidic Targeting Motif. *Mol Biol Cell*, 14(March 2003), pp.973-986.
- Shewan, A.M. et al., 2000. The cytosolic C-terminus of the glucose transporter GLUT4 contains an acidic cluster endosomal targeting motif distal to the dileucine signal. *The Biochemical journal*, 350 Pt 1, pp.99-107.
- Shi, J., Huang, G. & Kandror, K. V, 2008. Self-assembly of Glut4 storage vesicles during differentiation of 3T3-L1 adipocytes. *The Journal of biological chemistry*, 283(44), pp.30311-21.
- Shi, J. & Kandror, K. V, 2005. Sortilin is essential and sufficient for the formation of Glut4 storage vesicles in 3T3-L1 adipocytes. *Developmental cell*, 9(1), pp.99-108.
- Shi, L. et al., 2013. Preparation and characterization of SNARE-containing nanodiscs and direct study of cargo release through fusion pores. *Nature protocols*, 8(5), pp.935-48.

- Shigematsu, S. et al., 2003. The adipocyte plasma membrane caveolin functional/structural organization is necessary for the efficient endocytosis of GLUT4. *The Journal of biological chemistry*, 278(12), pp.10683-90.
- Shin, K.-J. et al., 2006. A single lentiviral vector platform for microRNA-based conditional RNA interference and coordinated transgene expression. *Proceedings of the National Academy of Sciences of the United States of America*, 103(37), pp.13759-64.
- Shitara, A. et al., 2013. VAMP4 is required to maintain the ribbon structure of the Golgi apparatus. *Molecular and cellular biochemistry*, 380(1-2), pp.11-21.
- Sieber, J.J. et al., 2006. The SNARE motif is essential for the formation of syntaxin clusters in the plasma membrane. *Biophysical journal*, 90(8), pp.2843-51.
- Simpson, I.A. et al., 1983. Insulin-stimulated translocation of glucose transporters in the isolated rat adipose cells: characterization of subcellular fractions. *Biochimica et biophysica acta*, 763(4), pp.393-407.
- Sinha, R. et al., 2011. Two synaptobrevin molecules are sufficient for vesicle fusion in central nervous system synapses. *Proceedings of the National Academy of Sciences of the United States of America*, 108(34), pp.14318-23.
- Slot, J.W. et al., 1991. Immuno-localization of the insulin regulatable glucose transporter in brown adipose tissue of the rat. *The Journal of cell biology*, 113(1), pp.123-35.
- Söllner, T., Bennett, M.K., et al., 1993. A protein assembly-disassembly pathway in vitro that may correspond to sequential steps of synaptic vesicle docking, activation, and fusion. *Cell*, 75(3), pp.409-18.
- Söllner, T., Whiteheart, S.W., et al., 1993. SNAP receptors implicated in vesicle targeting and fusion. *Nature*, 362(6418), pp.318-24.
- Song, X.M., Hresko, R.C. & Mueckler, M., 2008. Identification of amino acid residues within the C terminus of the Glut4 glucose transporter that are essential for insulin-stimulated redistribution to the plasma membrane. *The Journal of biological chemistry*, 283(18), pp.12571-85.
- Steggmaier, M. et al., 1999. Vesicle-associated membrane protein 4 is implicated in trans-Golgi network vesicle trafficking. *Mol Biol Cell*, 10(6), pp.1957-1972.
- Stenkula, K.G. et al., 2010. Insulin controls the spatial distribution of GLUT4 on the cell surface through regulation of its postfusion dispersal. *Cell metabolism*, 12(3), pp.250-9.
- Struthers, M.S. et al., 2009. Functional homology of mammalian syntaxin 16 and yeast Tlg2p reveals a conserved regulatory mechanism. *Journal of cell science*, 122(Pt 13), pp.2292-9.

- Sutton, R.B. et al., 1998. Crystal structure of a SNARE complex involved in synaptic exocytosis at 2.4 Å resolution. *Nature*, 395(6700), pp.347-53.
- Takahashi, M. et al., 2013. The localization of VAMP5 in skeletal and cardiac muscle. *Histochemistry and cell biology*, 139(4), pp.573-82.
- Takamori, S. et al., 2006. Molecular anatomy of a trafficking organelle. *Cell*, 127(4), pp.831-46.
- Tanner, L.I. & Lienhard, G.E., 1987. Insulin elicits a redistribution of transferrin receptors in 3T3-L1 adipocytes through an increase in the rate constant for receptor externalization. *The Journal of biological chemistry*, 262(19), pp.8975-80.
- Tellam, J.T. et al., 1997. Identification of a Mammalian Golgi Sec1p-like Protein, mVps45. *Journal of Biological Chemistry*, 272(10), pp.6187-6193.
- Thurmond, D.C. et al., 2000. Munc18c function is required for insulin-stimulated plasma membrane fusion of GLUT4 and insulin-responsive amino peptidase storage vesicles. *Molecular and cellular biology*, 20(1), pp.379-88.
- Toonen, R.F.G. & Verhage, M., 2003. Vesicle trafficking: pleasure and pain from SM genes. *Trends in Cell Biology*, 13(4), pp.177-186.
- Tsui, M.M. & Banfield, D.K., 2000. Yeast Golgi SNARE interactions are promiscuous. *Journal of cell science*, 113 (Pt 1, pp.145-52.
- Vassilopoulos, S. et al., 2009. A role for the CHC22 clathrin heavy-chain isoform in human glucose metabolism. *Science (New York, N.Y.)*, 324(5931), pp.1192-6.
- Verderio, C. et al., 1999. Tetanus toxin blocks the exocytosis of synaptic vesicles clustered at synapses but not of synaptic vesicles in isolated axons. *The Journal of neuroscience : the official journal of the Society for Neuroscience*, 19(16), pp.6723-32.
- Verhey, K.J. & Birnbaum, M.J., 1994. A Leu-Leu sequence is essential for COOH-terminal targeting signal of GLUT4 glucose transporter in fibroblasts. *The Journal of biological chemistry*, 269(4), pp.2353-6.
- Vogel, K. & Roche, P.A., 1999. SNAP-23 and SNAP-25 are palmitoylated in vivo. *Biochemical and biophysical research communications*, 258(2), pp.407-10.
- Volchuk, a et al., 1994. Expression of vesicle-associated membrane protein 2 (VAMP-2)/synaptobrevin II and cellubrevin in rat skeletal muscle and in a muscle cell line. *The Biochemical journal*, 304 (Pt 1, pp.139-45.
- Volchuk, A. et al., 1995. Cellubrevin is a resident protein of insulin-sensitive GLUT4 glucose transporter vesicles in 3T3-L1 adipocytes. *J Biol Chem*, 270(14), pp.8233-8240.

- Watson, R.T. et al., 2004. Entry of newly synthesized GLUT4 into the insulin-responsive storage compartment is GGA dependent. *The EMBO journal*, 23(10), pp.2059-70.
- Weber, T. et al., 1998. SNAREpins: minimal machinery for membrane fusion. *Cell*, 92(6), pp.759-72.
- Wei, M.L. et al., 1998. GLUT4 and transferrin receptor are differentially sorted along the endocytic pathway in CHO cells. *The Journal of cell biology*, 140(3), pp.565-75.
- Wendler, F. & Tooze, S., 2001. Syntaxin 6: the promiscuous behaviour of a SNARE protein. *Traffic (Copenhagen, Denmark)*, 2(9), pp.606-11.
- Williams, D. et al., 2009. Evidence that electrostatic interactions between vesicle-associated membrane protein 2 and acidic phospholipids may modulate the fusion of transport vesicles with the plasma membrane. *Molecular biology of the cell*, 20(23), pp.4910-9.
- Williams, D. et al., 2006. Golgin-160 is required for the Golgi membrane sorting of the insulin-responsive glucose transporter GLUT4 in adipocytes. *Molecular biology of the cell*, 17(12), pp.5346-55.
- Williams, D. & Pessin, J.E., 2008. Mapping of R-SNARE function at distinct intracellular GLUT4 trafficking steps in adipocytes. *The Journal of cell biology*, 180(2), pp.375-87.
- Wong, S.H. et al., 1998. Endobrevin, a novel synaptobrevin/VAMP-like protein preferentially associated with the early endosome. *Molecular biology of the cell*, 9(6), pp.1549-63.
- Xu, Y. et al., 2011. Dual-mode of insulin action controls GLUT4 vesicle exocytosis. *The Journal of cell biology*, 193(4), pp.643-53.
- Yang, B. et al., 1999. SNARE interactions are not selective. Implications for membrane fusion specificity. *The Journal of biological chemistry*, 274(9), pp.5649-53.
- Yang, J. & Holman, G.D., 1993. Comparison of GLUT4 and GLUT1 subcellular trafficking in basal and insulin-stimulated 3T3-L1 cells. *The Journal of biological chemistry*, 268(7), pp.4600-3.
- Yeh, J.I., Verhey, K.J. & Birnbaum, M.J., 1995. Kinetic analysis of glucose transporter trafficking in fibroblasts and adipocytes. *Biochemistry*, 34(47), pp.15523-31.
- Yu, C. et al., 2007. The glucose transporter 4-regulating protein TUG is essential for highly insulin-responsive glucose uptake in 3T3-L1 adipocytes. *The Journal of biological chemistry*, 282(10), pp.7710-22.

- Zeigerer, A. et al., 2002. GLUT4 retention in adipocytes requires two intracellular insulin-regulated transport steps. *Molecular biology of the cell*, 13(7), pp.2421-35.
- Zeigerer, A., McBrayer, M.K. & McGraw, T.E., 2004. Insulin stimulation of GLUT4 exocytosis, but not its inhibition of endocytosis, is dependent on RabGAP AS160. *Molecular biology of the cell*, 15(10), pp.4406-15.
- Zeng, Q. et al., 1998. A novel synaptobrevin/VAMP homologous protein (VAMP5) is increased during in vitro myogenesis and present in the plasma membrane. *Molecular biology of the cell*, 9(9), pp.2423-37.
- Zeng, Q. et al., 2003. The cytoplasmic domain of Vamp4 and Vamp5 is responsible for their correct subcellular targeting: the N-terminal extension of VAMP4 contains a dominant autonomous targeting signal for the trans-Golgi network. *The Journal of biological chemistry*, 278(25), pp.23046-54.
- Zhao, P. et al., 2009. Variations in the requirement for v-SNAREs in GLUT4 trafficking in adipocytes. *Journal of cell science*, 122(Pt 19), pp.3472-80.